



HAL
open science

Epigenomic and 3D-genomic changes in Mantle Cell Lymphoma

Anna Karpukhina Schwager

► **To cite this version:**

Anna Karpukhina Schwager. Epigenomic and 3D-genomic changes in Mantle Cell Lymphoma. Cancer. Université Paris-Saclay, 2024. English. NNT : 2024UPASL061 . tel-04766220

HAL Id: tel-04766220

<https://theses.hal.science/tel-04766220v1>

Submitted on 4 Nov 2024

HAL is a multi-disciplinary open access archive for the deposit and dissemination of scientific research documents, whether they are published or not. The documents may come from teaching and research institutions in France or abroad, or from public or private research centers.

L'archive ouverte pluridisciplinaire **HAL**, est destinée au dépôt et à la diffusion de documents scientifiques de niveau recherche, publiés ou non, émanant des établissements d'enseignement et de recherche français ou étrangers, des laboratoires publics ou privés.

Epigenomic and 3D-genomic changes in Mantle Cell Lymphoma

*Changements épigénomiques et 3D-génomiques dans le lymphome à
cellules du manteau*

Thèse de doctorat de l'université Paris-Saclay

École doctorale n°582 : oncologie : biologie, médecine, santé (CBMS)
Spécialité de doctorat : Sciences du Cancer
Graduate School : Life Sciences and Health. Référent : Faculté de médecine

Thèse préparée dans l'unité de recherche **Aspects métaboliques et systémiques de l'oncogénèse pour de nouvelles approches thérapeutiques (Université Paris-Saclay, CNRS, Institut Gustave Roussy)**, sous la direction de **Yegor VASSETZKY**, DR1 CNRS, directeur de thèse

Thèse soutenue à Paris-Saclay, le 11 Octobre 2024, par

Anna SCHWAGER KARPUKHINA

Composition du Jury

Membres du jury avec voix délibérative

Marie-Hélène DELFAU-LARUE Professeure, Université Paris-Est, Créteil	Présidente
Christophe ESCUDE CRHC CNRS, HDR, Muséum d'Histoire Naturelle,	Rapporteur & Examineur
Alexander ISHOV Professeur, University of Florida, USA	Rapporteur & Examineur
Julie SOUTOURINA DR CNRS, Université Paris Saclay	Examinatrice

ACKNOWLEDGEMENTS

I would like to express my gratitude to my supervisor, Dr. Yegor VASSETZKY, who guided me throughout this project with unwavering support. I am grateful for his style of supervision which develops an independent and open mindset, curiosity and scientific courage. His mentorship has been a source of inspiration, and I am fortunate to have had the opportunity to work under his guidance.

I would also like to thank the members of my dissertation committee, Pr. Marie-Hélène DELFAU-LARUE, Dr. Christophe ESCUDE, D. Julie SOUTOURINA, Dr. Guillaume ANDRIEU and Pr. Alexander ISHOV, for their thoughtful feedback and constructive criticism. Their expertise in the field has been a valuable resource in shaping my research questions and methodology.

I am deeply grateful to the entire research unit UMR 9018, led by the remarkable Dr. Catherine BRENNER and Pr. Karim BENIHOUD, and the invaluable assistance of Isabelle CROQUISON, Joelle HERBAUT and Anne TAN, I extend my heartfelt appreciation. I would like to thank the members of the unit who provided me with scientific guidance and served for me as inspiring examples: Dr. Joelle WIELS, Dr. Nazanine MODJTAHEDI and Dr. Louis MIR. I appreciate the invaluable participation of my colleagues who helped me to master various methods and techniques, assisted with experiments, discussed with me the results I obtained and supported me throughout the years of my thesis: Dr. Diego GERMINI, Dr. Anna SHMAKOVA, Dr. Ivan TSIMAILO, Dr. Yana KOZHEVNIKOVA, Dr. Reynand CANOY, Dr. Yahir Alberto LOISSEL BALTAZAR, Dr. Fatimata BINTOU SALL, Dr. Carla DIB, Dr. Yinxing MA, Dr. Zhenrui PAN, Junyi FENG, Victoria GINESTET and Yelena GRISHINA. Their competence and collaboration have been instrumental in the successful and timely conduct of our research projects. I am forever indebted to each one of you for your dedication and support. I am also grateful to Dr. Svetlana DOKUDOVSKEYA for her unforgettable input into my PhD journey and her constant struggle to make me stronger.

I would like to thank our scientific collaborators who contributed significantly to this work by conducting key experiments, providing expert guidance, technical support and study participants: Dr. Vincent RIBRAG, Dr. Oleg DEMIDOV, Dr. Sergey ULIANOV, Eugenia TIUKACHIOVA.

I am grateful to Paris-Saclay University for providing me with the resources and facilities necessary to conduct my research. The help and opportunities for intellectual growth and professional development afforded by CBMS Cancerology, Biology, Medicine, Health with Professor Eric DEUTSCH as a director and Léa POISOT as an administrative and pedagogical assistant have

been invaluable. I would like to express my sincere gratitude to the members of my mid-term thesis committees, Dr. Vittore SCOLARI, Dr. Ken OULASSEN, Dr. Vincent RIBRAG, whose guidance and insights have been invaluable throughout the development of this research.

I owe a debt of gratitude to my family and my friends (Anastasia TEPLOVA, Zaira SEFERBEKOVA, Sergei ISAEV, Vlada ZAKHAROVA), who have provided me with unwavering love and support throughout my graduate studies. Their encouragement, understanding, and patience have been a constant source of inspiration and motivation.

Finally, I would like to thank my former scientific supervisors and colleagues, Dr. Olga PLJETIUSHKINA, Dr. Ekaterina POPOVA and Dr. Ivan GALKIN, for their guidance and support during my early research career that cultivated my passion for science. Their patience, insights and encouragement were invaluable, and I am grateful for their mentorship.

CONTENTS

Acknowledgements.....	2
Contents.....	4
List of abbreviations.....	6
List of figures.....	11
List of tables.....	11
Summary.....	12
Synthèse.....	13
1. Introduction.....	14
1.1. Mantle Cell Lymphoma.....	14
1.1.1. Epidemiology.....	14
1.1.2. Mechanisms/pathophysiology.....	14
1.1.2.1. Cellular origins of the tumor.....	14
1.1.2.2. Subtypes of MCL.....	16
1.1.2.3. CCND1 expression and cell cycle deregulation in MCL.....	17
1.1.2.4. Genomic instability in MCL.....	20
1.1.2.5. SOX11 expression.....	28
1.1.2.6. B cell receptor signaling.....	32
1.1.2.7. Epigenetic deregulation and genome architecture.....	36
1.1.2.8. Metabolic reprogramming.....	38
1.1.2.9. Tumor microenvironment.....	40
1.1.3. Diagnosis, screening and prevention.....	49
1.1.3.1. Diagnosis.....	49
1.1.3.2. Screening and prevention.....	49
1.1.4. Management.....	50
1.1.4.1. Front-line treatment.....	50
1.1.4.2. Relapse and refractory disease treatment.....	51
1.1.4.3. New targets and emerging therapies.....	53
1.1.5. Outlook.....	55
1.2. Enhancers and superenhancers.....	56
1.2.1. Composition of superenhancers.....	57
1.2.2. Identification of superenhancers.....	57
1.2.3. Superenhancers in normal gene regulation.....	57
1.2.4. Superenhancers in disease.....	58
1.2.5. Superenhancer-targeting drugs.....	59
1.3. 3D-genome architecture.....	60
1.3.1. General principles of the 3D-genome architecture.....	60
1.3.2. 3D-genome alterations and editing in pathology.....	61
1.3.3. Interchromosomal contacts.....	72
2. Objectives of the study.....	74
3. Results.....	75
3.1. Der14 relocates to the nuclear center in MCL cells.....	75

3.2. Active epigenetic signature is globally altered in MCL cells.....	76
3.3. MCL cells develop a novel superenhancer in the translocation breakpoint region....	79
3.4. Chromosome 19 is enriched for active promoters and deregulated genes in MCL....	79
3.5. A superenhancer in the translocation breakpoint region interacts with chromosome 19.....	81
3.6. The chr19-SE contact colocalizes with the upregulated genes and active RNAPol II.....	83
3.7. Minnelide modifies the chromatin landscape and transcription profile of MCL cells.....	85
3.8. Minnelide is effective against MCL cells in vitro and in vivo.....	90
4. Discussion.....	93
5. Conclusions and Perspectives.....	96
6. Materials and Methods.....	97
6.1. Cells.....	97
6.2. Patients.....	97
6.3. Blood collection and primary B cell isolation.....	97
6.4. FISH probe preparation.....	97
6.5. FISH and ImmunoFISH.....	98
6.6. Analysis of the FISH images.....	99
6.7. MTT cell viability assay.....	100
6.8. Annexin V - propidium iodide apoptosis test.....	100
6.9. CFSE proliferation test.....	101
6.10. Xenograft studies in NSG mice.....	101
6.11. RNA-seq library preparation and sequencing.....	102
6.12. ATAC-seq library preparation and sequencing.....	102
6.13. ChIP-seq library preparation and sequencing.....	102
6.14. HiC library preparation and sequencing.....	103
6.15. RNA-seq analysis.....	103
6.16. ATAC-seq analysis.....	104
6.17. ChIP-seq analysis.....	105
6.18. Identification of enhancers and their targets.....	106
6.19. Super-enhancer identification.....	106
6.20. HiC analysis.....	107
6.21. Statistical analysis.....	107
6.22. Code availability.....	107
Major publications related to the topic of PhD thesis.....	108
Participations in conferences.....	109
Annexes.....	110
Supplementary figures.....	110
Articles.....	115
References.....	149

LIST OF ABBREVIATIONS

3D-FISH - Three-Dimensional Fluorescence In Situ Hybridization
ABC - Activity by Contact
AEBP1 - AE Binding Protein 1
AHR - Aryl Hydrocarbon Receptor
ARID1A - AT-Rich Interaction Domain 1A
ARID2 - AT-rich Interaction Domain 2
ASCT - Autologous Stem Cell Transplant
ATM - Ataxia Telangiectasia Mutated
ATR - Ataxia Telangiectasia and Rad3-Related
ATX - Autotaxin
ATAC-seq - Assay for Transposase-Accessible Chromatin with High-throughput Sequencing
BCR - B Cell Receptor
BAFF - B-Cell Activating Factor
BMI1 - B Lymphoma Mo-MLV Insertion Region 1 Homolog
BCL2 - B-Cell Lymphoma 2
BCL3 - B-Cell Lymphoma 3
BCL7A - B-Cell Lymphoma 7A
BCOR - BCL6 Corepressor
BCORL1 - BCL6 Corepressor Like 1
BFB - Breakage-Fusion-Bridge
BET - Bromodomain and Extra-Terminal domain
BIRC3 - Baculoviral IAP Repeat Containing 3
BLK - B Lymphocyte Kinase
BLNK - B Cell Linker Protein
BTK - Bruton's Tyrosine Kinase
BTLA - B- and T-Lymphocyte Attenuator
CAR-T - Chimeric Antigen Receptor T-cell
CARD11 - Caspase Recruitment Domain Family Member 11
CARD9 - Caspase Recruitment Domain Family Member 9
CARM1 - Coactivator Associated Arginine Methyltransferase 1
CCND1 - Cyclin D1
CCND2 - Cyclin D2
CCND3 - Cyclin D3
CCL3 - C-C Motif Chemokine Ligand 3
CENPP - Centromere Protein P
CHD2 - Chromodomain Helicase DNA Binding Protein 2
ChIP - Chromatin Immunoprecipitation
ChIP-seq - Chromatin Immunoprecipitation Sequencing
CLL - Chronic Lymphocytic Leukemia
CPT1A - Carnitine Palmitoyltransferase 1A

CR - Complete Remission
CT - Computed Tomography
CTPS1 - CTP Synthase 1
CXCL12 - C-X-C Motif Chemokine Ligand 12
CXCL13 - C-X-C Motif Chemokine Ligand 13
CXCR4 - C-X-C Chemokine Receptor Type 4
CXCR5 - C-X-C Chemokine Receptor Type 5
DAG - Diacylglycerol
DEGs - Differentially Expressed Genes
DNA - Deoxyribonucleic Acid
DNA2 - DNA Replication Helicase/Nuclease 2
DNMT - DNA Methyltransferases
DNMT3A - DNA Methyltransferase 3 Alpha
DUSP2 - Dual Specificity Phosphatase 2
ECOG - Eastern Cooperative Oncology Group
ETV6 - Ets Variant 6
FDA - Food and Drug Administration
FDR - False Discovery Rate
FGF9 - Fibroblast Growth Factor 9
FDCs - Follicular Dendritic Cells
FAT3 - FAT Atypical Cadherin 3
FAT4 - FAT Atypical Cadherin 4
FOXP1 - Forkhead Box P1
FOXO1 - Forkhead Box O1
G1 phase - Gap 1 phase (of the cell cycle)
G1/S - Gap 1/ Synthesis phase of the cell cycle
GC - Germinal Center
GNAQ - G Protein Subunit Alpha Q
GO - Gene Ontology
GRIN2A - Glutamate Ionotropic Receptor NMDA Type Subunit 2A
HDAC - Histone Deacetylases
HDAC9 - Histone Deacetylase 9
HIF1A - Hypoxia-Inducible Factor 1-Alpha
HLA-DOA - Human Leukocyte Antigen DOA
HLA-DPB1 - Human Leukocyte Antigen DP Beta 1
HIST1H1C - Histone Cluster 1 H1 Family Member C
HIST1H1E - Histone Cluster 1 H1 Family Member E
HIST1H2BJ - Histone Cluster 1 H2 Family Member J
H3K27Ac - Histone H3 Lysine 27 Acetylation
H3K27me3 - Histone H3 Lysine 27 Trimethylation
H3K4me1 - Histone H3 Lysine 4 Monomethylation
H3K4me3 - Histone H3 Lysine 4 Trimethylation
H3K9Ac - Histone H3 Lysine 9 Acetylation
H3K9/14Ac - Histone 3 Lysine 9 and 14 Acetylation

H3K9me2 - Histone 3 Lysine 9 Dimethylation
HiC - High-throughput Chromosome Conformation Capture
IGF1R - Insulin-like Growth Factor 1 Receptor
IGF2 - Insulin-like Growth Factor 2
IGH - Immunoglobulin Heavy Chain
IGHV - Immunoglobulin Heavy Chain Variable Region
IGK - Immunoglobulin Kappa Light Chain
IGL - Immunoglobulin Lambda Light Chain
IGLL5 - Immunoglobulin Lambda-Like Polypeptide 5
IL-10 - Interleukin 10
IL-10R α - Interleukin 10 Receptor Alpha
IL-13 - Interleukin 13
IL-4 - Interleukin 4
IL7 - Interleukin 7
IL7R - Interleukin 7 Receptor
ING1 - Inhibitor of Growth Tumor Suppressor
IRS2 - Insulin Receptor Substrate
ISMCN - In Situ Mantle Cell Neoplasm
JAK2 - Janus Kinase 2
JNK - c-Jun N-terminal Kinase
KEGG - Kyoto Encyclopedia of Genes and Genomes
KMT2D - Lysine Methyltransferase 2D
LCK - Lymphocyte-Specific Protein Tyrosine Kinase
LDH - Lactate Dehydrogenase
LPA - Lysophosphatidic Acid
MALT1 - Mucosa Associated Lymphoid Tissue Lymphoma Translocation Protein 1
MAP3K1 - Mitogen-Activated Protein Kinase Kinase Kinase 1
MAP3K14 - Mitogen-Activated Protein Kinase Kinase Kinase 14
MAPK - Mitogen-Activated Protein Kinase
MCM - Mini Chromosome Maintenance
MECOM - MDS1 and EVI1 Complex
MCL - Mantle Cell Lymphoma
MIPI - Mantle Cell Lymphoma International Prognostic Index
MIR155 - MicroRNA 155
MIR17HG - MIR17 Host Gene
miRNA - MicroRNA
MYC - Myelocytomatosis Oncogene
MYCN - Myelocytomatosis Viral Oncogene Neuroblastoma
NF- κ B - Nuclear Factor Kappa B
NFKB2 - Nuclear Factor Kappa B Subunit 2
NFKBIZ - Nuclear Factor of Kappa Light Polypeptide Gene Enhancer in B-Cells Inhibitor, Zeta
NR4A1 - Nuclear Receptor Subfamily 4 Group A Member 1

NRIP1 - Nuclear Receptor Interacting Protein 1
NSG mice - NOD SCID Gamma mice
NCT - National Clinical Trial (number)
NOTCH1 - Neurogenic Locus Notch Homolog Protein 1
NOTCH2 - Neurogenic Locus Notch Homolog Protein 2
NOTCH3 - Neurogenic Locus Notch Homolog Protein 3
NOTCH4 - Neurogenic Locus Notch Homolog Protein 4
N-MCL2/3 - Nordic Mantle Cell Lymphoma 2/3
O-GlcNAc - O-Linked N-Acetylglucosamine
OS - Overall Survival
PCR - Polymerase Chain Reaction
PD-1 - Programmed Cell Death 1
PD-L1 - Programmed Cell Death Ligand 1
PDX - Patient-Derived Xenograft
PHF6 - PHD Finger Protein 6
PI3K - Phosphoinositide 3-Kinase
PIK3CA - Phosphoinositide 3-Kinase Catalytic Subunit Alpha
PRDM1 - PR/SET Domain 1
PTEN - Phosphatase and Tensin Homolog
PTPN11 - Protein Tyrosine Phosphatase Non-Receptor Type 11
RAD21 - RAD21 Cohesin Complex Component
RB1 - Retinoblastoma 1
RCB - Residual Disease Following Consolidation
REL - Reticuloendotheliosis Viral Oncogene Homolog
REPT - Recurrent Disease Following Transplant
RHOA - Ras Homolog Family Member A
ROR γ - Retinoic Acid Receptor-Related Orphan Receptor Gamma
RUNX1 - Runt-Related Transcription Factor 1
RUVBL1 - RuvB-Like 1
SAH - S-Adenosyl Homocysteine
SAMHD1 - SAM Domain and HD Domain 1
SCF - Stem Cell Factor
SCLC - Small Cell Lung Cancer
SF3B1 - Splicing Factor 3B Subunit 1
SMARCA4 - SWI/SNF Related, Matrix Associated, Actin Dependent Regulator Of Chromatin, Subfamily A, Member 4
SMO - Smoothed
SOX11 - SRY-Box Transcription Factor 11
STAT3 - Signal Transducer and Activator of Transcription 3
STK11 - Serine/Threonine Kinase 11
SYK - Spleen Tyrosine Kinase
TET2 - Ten-Eleven Translocation 2
TGF β - Transforming Growth Factor Beta
TNF - Tumor Necrosis Factor

Treg - Regulatory T Cell

U2AF1 - U2 Small Nuclear RNA Auxiliary Factor 1

UBC - Ubiquitin C

VAMP - Vesicle-Associated Membrane Protein

WNT - Wingless-Int

ZAP70 - Zeta-Chain Associated Protein Kinase 70

LIST OF FIGURES

- Figure 1. MCL oncogenesis alongside B cell differentiation.
- Figure 2. MCL histological variants.
- Figure 3. Cell cycle deregulation in MCL.
- Figure 4. Impaired DNA damage response in MCL.
- Figure 5. SOX11 expression in MCL oncogenesis.
- Figure 6. Abnormal BCR signaling in MCL.
- Figure 7. Nuclear positioning of the translocated loci.
- Figure 8. Epigenetic deregulation in MCL cells.
- Figure 9. Chromosome 19 is enriched for overexpressed genes and active promoters in MCL.
- Figure 10. Interchromosomal contacts in MCL cells.
- Figure 11. Transcriptional and epigenetic state of the chromatin around the der14-chr19 contact sites.
- Figure 12. Minnelide reprograms the epigenetic landscape of MCL cells.
- Figure 13. Transcriptomic changes following Minnelide and Abemaciclib treatment.
- Figure 14. The effect of Abemaciclib and Minnelide on the viability, apoptosis and proliferation of MCL cells.
- Supplementary Figure 1. Functional enrichment analysis of superenhancer-associated genes.
- Supplementary Figure 2. Per-chromosome distributions of the upregulated genes, up H3K27Ac peaks, overactive enhancers and unique super-enhancers in MCL cells.
- Supplementary Figure 3. Minnelide and Abemaciclib titration.
- Supplementary Figure 4. Molecular function enrichment and per-chromosome distributions of the genes downregulated by Minnelide and Abemaciclib.

LIST OF TABLES

- Table 1. Common genetic alterations in MCL
- Table 2. Epigenetic therapies for MCL

SUMMARY

Mantle cell lymphoma is an aggressive B cell malignancy with poor prognosis. More than 90% of MCL cases are associated with a recurrent chromosomal translocation t(11;14) that results in the overexpression of cyclin D1 (*CCND1*), a potent cell-cycle regulator. Nevertheless, *CCND1* overexpression alone does not lead to malignancies in animal models. Thus, the development of MCL should be triggered by additional factors, which may guide the development of new therapies once discovered.

A chromosomal translocation can trigger large-scale changes in the 3D genome organization, as well as the transcriptional and epigenetic changes in the translocated loci. Here we demonstrated that the translocated *CCND1* locus on derivative chr14 is relocated to the nuclear center in MCL cells. This is accompanied by the appearance of a new super-enhancer (SE) inside this locus. Surprisingly, the region around the novel SE was not significantly enriched for the genes overexpressed in MCL. Instead, most of the differentially expressed genes were located on chr19 in both the MCL cell lines and the B cells from MCL patients. Among these genes, there were many related to lymphoma or other cancers. Using HiC, we detected the presence of an interchromosomal contact between chr11 and chr19, which was further confirmed by 3D-FISH. The contact colocalized with the active RNAPolII and formed predominantly with the derivative *CCND1* locus.

We hypothesize that the deregulated chr19 genes contribute to the MCL oncogenesis, and their upregulation is at least partially explained by the action of an MCL-specific SE inside the *CCND1* locus. Thus, inhibiting super-enhancer activity may represent a new treatment strategy for MCL. We tested two substances with such properties, Abemaciclib and Minnelide, in MCL cell lines and the B cells from MCL patients. Minnelide had a strong inhibitory effect on the chromatin landscape of MCL cells, including the novel SE, and was effective against mantle cell lymphoma cells *in vitro* and *in vivo*. Our results provide valuable preclinical data and novel insights into the mechanisms of MCL pathogenesis.

Keywords: MCL, chromosomal translocations, 3D genome, epigenome.

SYNTHÈSE

Le lymphome à cellules du manteau (LM) est une tumeur maligne agressive des cellules B, caractérisée par un pronostic défavorable. Plus de 90 % des cas de LM sont associés à une translocation chromosomique récurrente t(11;14), entraînant la surexpression de la cycline D1 (*CCND1*), un puissant régulateur du cycle cellulaire. Néanmoins, la surexpression de la *CCND1* seule ne suffit pas à provoquer des tumeurs malignes dans les modèles animaux. Par conséquent, le développement du LM doit être déclenché par d'autres facteurs, dont la découverte pourrait orienter le développement de nouvelles thérapies.

Une translocation chromosomique peut entraîner des modifications à grande échelle de l'organisation 3D du génome, ainsi que des changements transcriptionnels et épigénétiques dans les loci transloqués. Nous avons démontré que le locus *CCND1* transloqué sur le chromosome 14 dérivé se déplace vers le centre nucléaire dans les cellules de LM. Cela s'accompagne de l'apparition d'un nouveau super-enhancer (SE) à l'intérieur de ce locus. De manière surprenante, la région autour du nouveau SE n'était pas significativement enrichie en gènes surexprimés dans les cellules de LM. En revanche, la plupart des gènes surexprimés étaient situés sur le chromosome 19, aussi bien dans les lignées cellulaires de LM que dans les cellules B de patients atteints de LM. Parmi ces gènes, nombreux sont ceux liés au lymphome ou à d'autres cancers. En utilisant la technique Hi-C, nous avons détecté la présence d'un contact interchromosomique entre les chromosomes 11 et 19, confirmé par 3D-FISH. Ce contact se colocalise avec l'ARN polymérase II active et se forme principalement avec le locus *CCND1* dérivé.

Nous émettons l'hypothèse que les gènes dérégulés sur le chr19 contribuent à l'oncogenèse du LM et que leur régulation est influencée par l'action d'un SE spécifique au LM à l'intérieur du locus *CCND1*. Ainsi, l'inhibition de l'activité de ce SE pourrait représenter une nouvelle stratégie thérapeutique pour le LM. Nous avons testé deux substances présentant de telles propriétés, l'Abemaciclib et le Minnelide, sur des lignées cellulaires de LM et sur les cellules B de patients atteints de LM. Le Minnelide a montré un fort effet inhibiteur sur la chromatine des cellules de LM, y compris sur le nouveau SE, et s'est révélé efficace contre les cellules de lymphome à cellules du manteau *in vitro* et *in vivo*. Nos résultats fournissent des données précliniques importantes et offrent de nouvelles perspectives sur les mécanismes de la pathogenèse du LM.

Mots-clés : Lymphome à cellules du manteau, translocations chromosomiques, génome 3D, épigénome.

1. INTRODUCTION

1.1. Mantle Cell Lymphoma

Mantle cell lymphoma (MCL) is a rare and aggressive form of non-Hodgkin's lymphoma characterized by the abnormal proliferation of mature B lymphocytes in the mantle zone of a lymph node. MCL comprises 3-10% of adult NHLs (Jain & Wang 2019; Teras et al. 2016) and is usually diagnosed at an advanced Ann Arbor stage (III, IV) with generalized lymphadenopathy, splenomegaly and symptomatic extra-nodal involvement (Bosch et al. 1998; Teras et al. 2016). The median age of diagnosis is 68 years old with a 1.6-3/1 male to female ratio in different populations (Leux et al. 2014; Velders et al. 1996). Despite significant advances in treatment and diagnosis, the survival rate for this malignancy is still poor, especially for the relapsed cases (Bhatt et al. 2016), and a limited progress has been made recently in deciphering the mechanisms underlying the disease. Below, I attempt to systematize the existing information on the pathogenic mechanisms and treatment modalities of mantle cell lymphoma and draw the perspectives for future treatments development.

1.1.1. Epidemiology

MCL has an annual incidence around one case per 200 000 people (Teras et al. 2016), comprising around 3-10% of adult-onset non-Hodgkin's lymphomas. The median age at diagnosis is 68 years old (range 18-85 years) (Abrahamsson et al. 2014; Dreyling et al. 2024; Fu et al. 2017; Leux et al. 2014; Velders et al. 1996) with the incidence increasing with age (Fu et al. 2017; Lee et al. 2017). Males are more frequently affected with a 1.6-3/1 male to female ratio in different populations (Leux et al. 2014; Velders et al. 1996). The incidence rates also vary depending on ethnicity and the geographic region. Non-hispanic whites are most frequently affected (Wang & Ma 2014) and the reported rates are higher in Western ((Abrahamsson et al. 2014; Epperla et al. 2018; Fu et al. 2017)) compared to Asian (Lee et al. 2017; Meng et al. 2018) countries. Median overall survival ranges from 28.8 (years 2004-2017; Europe) to 52.0 months (years 1999-2013; US) (Yang et al. 2019). Although the MCL prognosis has dramatically improved during the last decades, especially for the younger patients, MCL is still considered not curable with standard therapies, highlighting the need for further related research.

1.1.2. Mechanisms/pathophysiology

1.1.2.1. Cellular origins of the tumor

The major genetic hallmark of MCL is the translocation of the *CCND1* gene to the immunoglobulin (IG) genes locus (Campo et al. 2022). More than 95% of the tumors bear the t(11;14)(q13;q32) translocation that juxtaposes the *CCND1* gene at 11q13 to the immunoglobulin heavy chain complex (IGH) at chromosome 14q32 (Li et al. 1999; Vandenberghe et al. 1991). In rare cases, tumors with the MCL phenotype lack t(11;14), but present the rearrangements involving other combinations of *CCND1*, *CCND2* (12p13) or *CCND3* (6p21) with the *IGH*, *IGK* (2p11) or *IGL* (22q11) loci. In any

case, the translocation is considered an initial oncogenic event driving subsequent transformation.

The translocation is thought to occur predominantly at the pro-B stage of B cell differentiation, during the V(D)J recombination of the IGH variable region (IGHV) in the bone marrow, as most of the IG breaks have evidence of being mediated by RAG enzymes (Hummel et al. 1994; Kienle et al. 2003; Küppers et al. 1999; Nadeu et al. 2020) (**Figure 1**). Furthermore, spatial proximity between the CCND1 and IGH loci, a prerequisite for a chromosomal translocation, was observed in pro/pre B-cells and not in mature B cells (Sklyar et al. 2016). Nevertheless, the tumor consists of *mature* B cells that already express BCR and have passed the antigen-dependent negative selection, suggesting that the full neoplastic potential post-translocation is reached at a later stage of B cell differentiation and is probably dependent on the lymph node microenvironment, where the tumor starts to develop. As evident from its name, mantle cell lymphoma arises from the B cells residing in the mantle zone - an outer rim of the lymph node follicle consisting of *naive* B lymphocytes that are pushed away to the outer edge of the follicle following the appearance and growth of the germinal center (GC). In the germinal center, mature antigen-activated B cells undergo somatic hypermutation of their assembled variable regions of IgH and IgL genes to increase the BCR affinity to the encountered antigen. Most (>90%) of mantle cell lymphomas have their IGHV genes non-hypermutated and express IgM/IgD and CD5, typical for naive B cells. Nevertheless, with an increase in testing sensitivity, up to 36% of cases classified as MCLs are found to have significant levels of IGHV hypermutation (Navarro et al. 2012), suggesting a more complex subtype repertoire of the tumor-founding cells, with some tumors likely influenced by the antigen-driven selection. Additionally, around 10% of MCL tumors express stereotypic BCR (identical BCR clonotypes between different patients) (Messmer et al. 2004; Stamatopoulos et al. 2007). Such stereotypicity generally implies some kind of antigen-driven selection during the clonogenic expansion of the founding tumor cells. Some B cell populations with characteristics intermediate between that of naive and germinal center B cells were also proposed to be the normal counterparts of MCL cells. These may include a specific (IgD+CD38-CD23-FSChiCD71+) population discovered in tonsils (Kolar et al. 2007) with modest somatic hypermutations and the expression of AID, an enzyme critical for somatic hypermutation and class-switch recombination (Muramatsu et al. 2000). Consistently, in rare MCL cases the t(11;14) translocation breakpoint has characteristics of AID involvement (Nadeu et al. 2020), suggesting its origin in the already mature cells during the class switch recombination. All together, the data indicate that the founding mantle cell lymphoma cells are likely heterogenous from case to case and cover a spectrum of cells ranging from completely naive to GC-influenced to antigen-stimulated B lymphocytes.

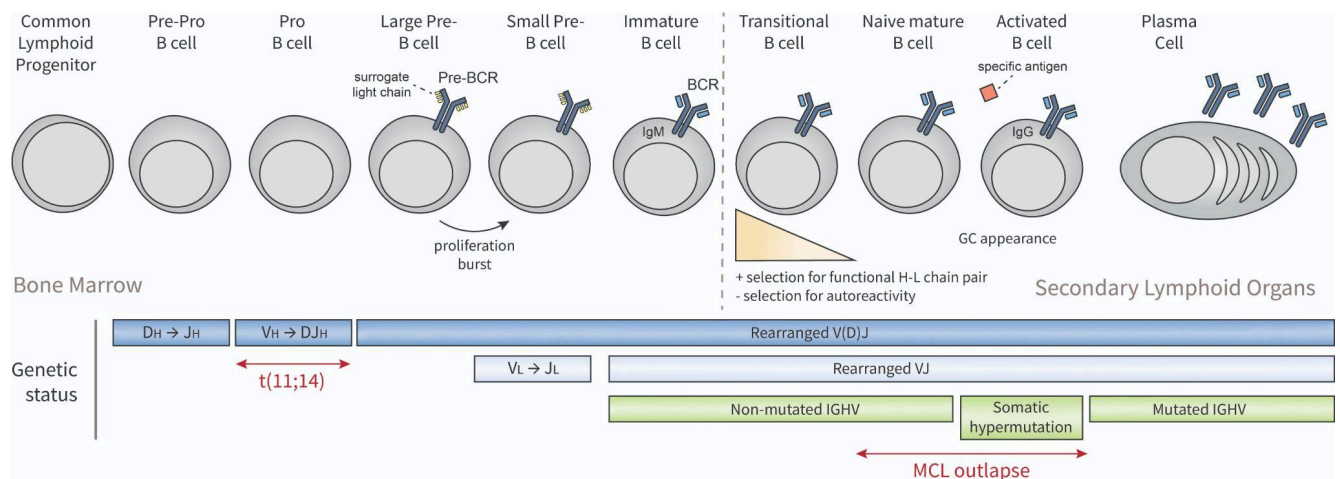


Figure 1. MCL oncogenesis alongside B cell differentiation.

1.1.2.2. Subtypes of MCL

In the ICC/WHO 2022 update of lymphoid malignancies, MCL was subdivided in two distinct categories: nodal, or conventional, MCL (cMCL) and non-nodal MCL (nnMCL), manifesting in a leukemic form (Alaggio et al. 2022; Campo et al. 2022). Conventional MCL is much more frequent representing 80-90% of the cases. It typically bears no or minimal IGHV hypermutations (Hummel et al. 1994; Del Giudice et al. 2012), suggesting the origin from naive B cells, and has a high genomic instability with a tendency to accumulate additional genomic aberrations overtime. Expression of *SOX11*, one of the MCL markers, is another feature distinguishing the conventional MCL from its non-nodal form. In contrast, nnMCL develops from the cells with already mutated IGHV (Orchard et al. 2003; Del Giudice et al. 2012; Royo et al. 2012), does not express *SOX11* and rarely acquires additional chromosomal aberrations.

Clinically, conventional MCL tends to be aggressive. Patients with cMCL typically present with nonlocalized, palpable lymphadenopathy. Other symptoms include fever, weight loss, fatigue, night sweats and splenomegaly-related discomfort (Argatoff et al. 1997). Approximately 25% of the patients may have bulky lymphadenopathy with the tumor masses $\geq 10\text{cm}$ in the largest diameter. Lactate dehydrogenase levels are elevated in around half of the cases. At the time of diagnosis, the tumor is typically widespread, with more than 80% of the patients diagnosed at Ann Harbour stages III-IV. Extranodal involvement, especially that involving the gastrointestinal tract, spleen and bone marrow, is common. Some cases are present with leukemic involvement, which is generally associated with bad prognosis (Ferrer et al. 2007).

Non-nodal MCL is rare and usually presents with splenomegaly, without lymphadenopathy or systemic symptoms. Some patients may have slowly progressing, non-bulky adenopathy (Nodit et al. 2003; Thieblemont et al. 2008). nnMCL is often indolent and may be observed without immediate treatment. It can, however, progress into symptomatic forms requiring intervention overtime.

The WHO-HAEM5 currently distinguishes the third rare MCL “subtype”, in situ mantle cell neoplasm (ISM CN), which represents colonization of the mantle zones of lymphoid follicles with the B cells carrying the *IG::CCND1* fusion (Alaggio et al. 2022). ISMCN is characterized by an indolent course (Carvajal-Cuenca et al. 2012) and is typically an incidental finding. The risk of progression of ISMCN to overt MCL is typically low (<10%) (Swerdlow et al. 2016).

Histologically, MCL is presented in three major variants: classical, blastoid and pleomorphic (**Figure 2**) (Alaggio et al. 2022). Classical MCL consists of monomorphic small to medium-sized lymphocytes with scant cytoplasm, irregular nuclei, condensed chromatin and poor-distinguishable nucleoli. Blastoid tumors are also characterized by the proliferation of homogenous lymphocytes with scant cytoplasm, irregular nuclei and inconspicuous nucleoli, but the cells tend to be medium-sized and have finely dispersed chromatin appearance. Finally, pleomorphic tumors are composed of heterogeneous atypical cells with irregular nuclei, vesicular chromatin and distinct nucleoli. Blastoid and pleomorphic tumors are associated with complex karyotypes, higher proliferation rates and aggressive clinical courses (Sarkozy et al. 2014; Dreyling, Klapper, and Rule 2018). Thus, blastoid or pleomorphic cytomorphology is a biomarker of high-risk MCL (Alaggio et al. 2022).

MCL histological variants

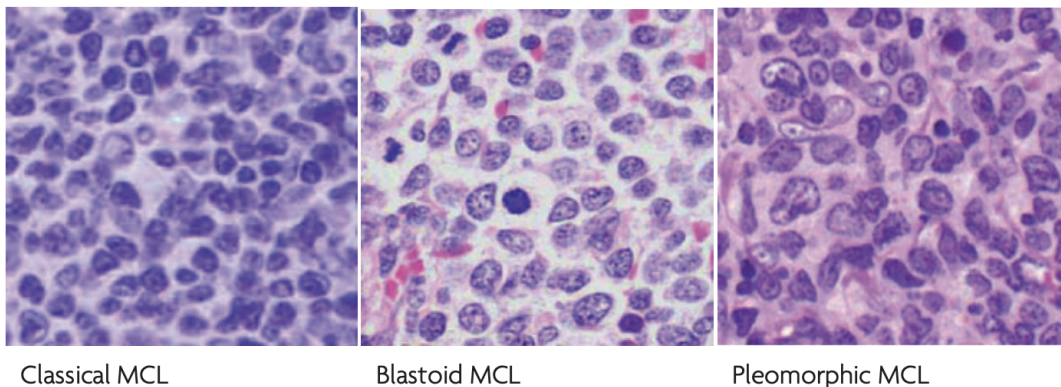


Figure 2. MCL histological variants.
(reproduced from PMID: 23023712)

1.1.2.3. *CCND1* expression and cell cycle deregulation in MCL

The juxtaposition of the *CCND1* gene to the *IGH* gene locus post t(11;14) translocation brings *CCND1* into a relative proximity of a highly-active *IGH* enhancer, leading to constitutive *CCND1* overexpression. *CCND1* encodes for the Cyclin D1 protein. In healthy mature B cells, its expression is low (Gladkikh et al. 2010; Lam et al. 2010) and is likely present only upon growth stimulation (Scharer et al. 2018). Together with its two homologues, Cyclin D2 and Cyclin D3, it regulates the G1 to S transition during the cell cycle (**Figure 3**). In the absence of stimuli, this transition is blocked by the retinoblastoma protein (pRb), which binds the E2F transcription factors essential for the DNA synthesis. Entry to the S phase requires subsequent activation of cyclin dependent kinases (CDKs) 4/6 and 2, which are activated by binding to Cyclin D and

Cyclin E, respectively. Upon Cyclin D binding, CDK4 phosphorylates and partially inactivates pRB, causing the release of the pRb-bound E2F factors that activate the expression of pro-proliferative genes, including *CCNE1* and 2 (encoding for Cyclins E). Cyclin E activates CDK2, which further hyperphosphorylates the Rb causing the full E2F release.

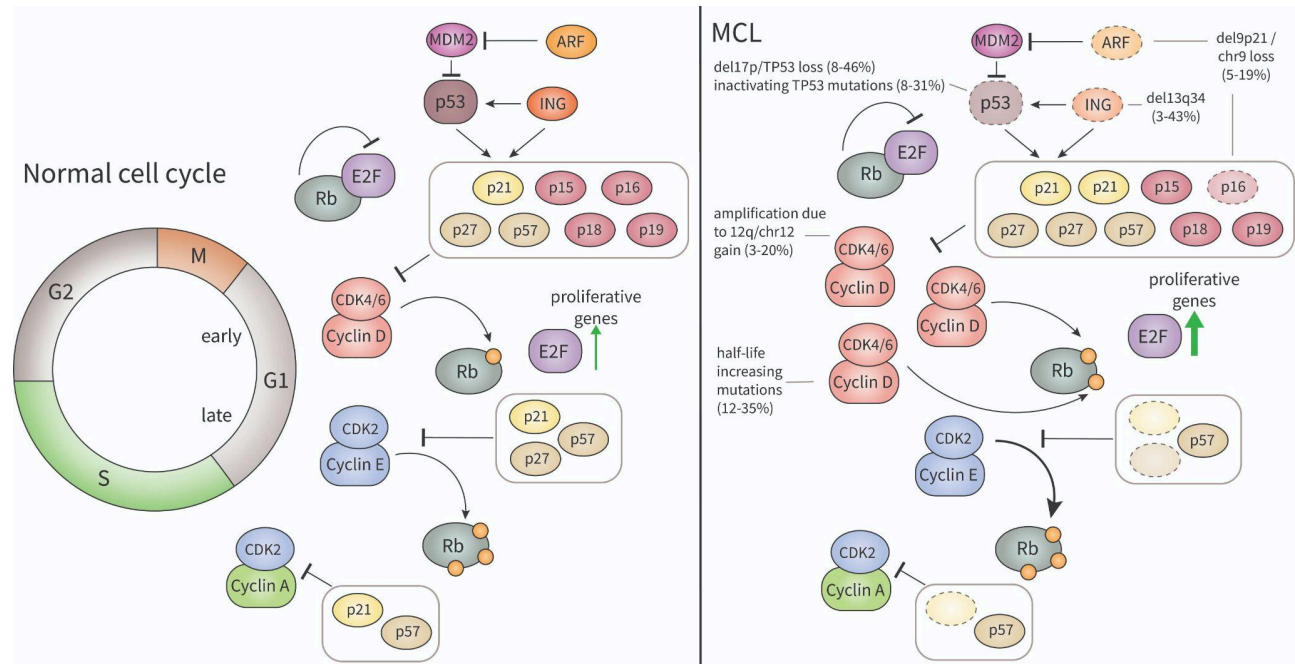


Figure 3. Cell cycle deregulation in MCL.

Constitutive *CCND1* overexpression in MCL leads to an increased concentration of activated Cyclin D1 - CDK4/6 complexes, possibly resulting in accelerated pRb phosphorylation (**Figure 3**). Excessive Cyclin D1 - CDK4/6 complexes may also sequester the cyclin-dependent kinase inhibitors (CDKI) p27 and p21, which bind cyclin-CDK complexes to prevent their activation. Indeed, in MCL cells most of the p27 protein was shown to be sequestered by Cyclin D1-CDK4/6 as demonstrated by exhaustive immunoprecipitation (Quintanilla-Martinez et al. 2003). All these potentially facilitate cell cycle progression following *CCND1* upregulation post-translocation. A direct relationship between the expression of *CCND1* and proliferation signature genes was demonstrated in MCL (Rosenwald et al. 2003). Nevertheless, contradictory results were obtained concerning the correlation between *CCND1* expression and the positivity for the proliferation marker Ki-67 in different tumors, with some studies confirming the association (Kurozumi et al. 2019; Shevra, Ghosh, and Kumar 2015; Ortiz et al. 2017) and others showing no or negative correlation between *CCND1* presence and Ki-67 index (Shoker et al. 2001; Oyama et al. 1998; Tut et al. 2001; Kodet 2009). Another study found no evidence of early cell cycle phases shortening in 18 MCL biopsy specimens (Vogt et al. 2015). This is in line with the fact that the *CCND1* overexpression is not enough for the oncogenic transformation. Transgenic mice with the *CCND1* overexpression alone do not develop tumors and have a quasi-normal phenotype (Lovec et al. 1994; Bodrug et al. 1994). Moreover, t(11;14)-positive B cells can sometimes be detected in the peripheral blood of healthy individuals (Lecluse et al. 2009), suggesting that

additional factors should be present to onset the hyper-proliferation and oncogenic transformation of MCL cell.

A number of events acquired in the course of tumor evolution may contribute to MCL cell cycle deregulation independent of *CCND1* overexpression. These are mostly chromosomal aberrations or mutations involving relevant genes. In 3-20% of the cases an additional *CDK4* gene copy may be acquired due to 12q (Sílvia Beà et al. 1999; Hernández et al. 2005; Au et al. 2002; Wlodarska et al. 1999) or whole chromosome 12 (Au et al. 2002; Wlodarska et al. 1999) gains. Loss of a copy of the *CDKN2A* gene due to 9p21 deletion (Salaverria et al. 2007; Au et al. 2002) or chromosome 9 loss (Salaverria et al. 2007; Au et al. 2002; Wlodarska et al. 1999) occurs in 5-19% of MCL cases (see **Table 1**). *CDKN2A* encodes for a CDK4/6 inhibitor protein p16 (*INK4A*) and an alternate reading frame protein p14 (*ARF*). Reduced p16 concentration weakens the inhibition of the CCND-CDK4/6 complexes, leading to more consistent pRb phosphorylation. p14 protein interacts and sequesters the E3 ubiquitin-protein ligase MDM2, responsible for the degradation of the p53 tumor-suppressor protein, which arrests the cell cycle on DNA damage recognition. p14 loss thus contributes to reduced p53 stability. p53 itself is also frequently lost (8-46% of the cases) (Salaverria et al. 2007; Au et al. 2002; Streich et al. 2020; Malarikova et al. 2020) or mutated (8-34% of the cases) (Ferrero et al. 2020; Jeong et al. 2020; Malarikova et al. 2020; T. Greiner et al. 1996; The AACR Project GENIE Consortium et al. 2017) in MCL. Most of the works report inactivating (P. Yang et al. 2018; Ferrero et al. 2020) missense or nonsense *TP53* mutations (P. Yang et al. 2018; Ferrero et al. 2020; Jeong et al. 2020), though *TP53* was also shown to be overexpressed in mutated vs wild-type *TP53* in one study (T. Greiner et al. 1996) and is found overexpressed in many MCL tumors independent of the mutation status (Aukema et al. 2018). In any case, *TP53* mutations or overexpression are significant prognostic factors for reduced overall survival (P. Yang et al. 2018; Ferrero et al. 2020; Jeong et al. 2020; Malarikova et al. 2020; T. Greiner et al. 1996; Delfau-Larue et al. 2015; Eskelund et al. 2017). The same is true for the tumors with the *CDKN2A* deletion (Delfau-Larue et al. 2015; Gaudio et al. 2023) or *CDK4* amplification (Hernández et al. 2005). All three alterations were correlated with an increased proliferation phenotype as assessed by Ki-67 staining (Hernández et al. 2005) and were especially prevalent in the aggressive blastoid MCL variants (Derby et al. 2010; Streich et al. 2020; Hernández et al. 2005). In 3-43% of MCLs (see **Table 1**), 13q14 deletion leads to a copy loss and reduced expression of the inhibitor of growth tumor suppressor ING1 (Hartmann et al. 2010). ING1 interacts with p53 preventing its degradation and promoting activation of p21 by p53. It can also activate p21 independently of p53, in a complex with miSin3a, thus negatively regulating the cell cycle (Archambeau, Blondel, and Pedoux 2019).

Less frequent alterations include the amplifications of *BMI1* gene, encoding for a repressor of CDKIs p16 and p19 (Sílvia Beà et al. 1999) and inactivating intragenic deletions of *RB1* gene encoding for the Rb protein (Pinyol et al. 2007). *MYC* oncogene

rearrangements or amplifications can be found in some aggressive advanced stage cases (Choe et al. 2016; Z. Hu et al. 2017; Sílvia Beà et al. 1999). In one study with 110 MCL cases, p27 protein levels were shown to be reduced in MCL due to increased proteasomal degradation by the ubiquitin proteasome pathway (Chiarle et al. 2000).

All together, cell cycle is frequently deregulated in MCL favoring increased tumor proliferation. Proliferation gene expression signature is a strong survival predictor in MCL (Rosenwald et al. 2003) and multiple MCL treatment strategies are targeted at cell cycle inhibition (see *Management*). Nevertheless, it is by far not the only oncogenic hallmark of MCL tumors.

1.1.2.4. Genomic instability in MCL

T(11;14)(q13;q32) translocation, or, in rare cases, other translocations involving the cyclin D and IGH genes (see above), are considered to be the initial oncogenic event in MCL. Nonetheless, MCL, specifically its conventional form, has one of the highest rates of genomic instability among B-cell malignancies. More than 90% of mantle cell lymphomas accumulate additional genomic aberrations overtime, with losses being slightly more common than gains (Wlodarska et al. 1999; Au et al. 2002; Salaverria et al. 2007). Chromothripsis and chromoplexia occur occasionally in both the conventional and non-nodal MCL, while recombination via breakage-fusion-bridge (BFB) cycles seems to be unique to cMCL (Nadeu et al. 2020). High number of copy number variations, structural variations, the presence of BFB or chromothripsis all confer a poor prognosis in terms of overall survival (Nadeu et al. 2020). Most of the secondary aberrations in MCL are not highly recurrent, though the structural variation breaks tend to occur in open chromatin regions, such as promoters, enhancers and transcription-elongation-associated chromatin (Nadeu et al. 2020). Common heterozygous/homozygous losses and gains, as well as single genes most frequently mutated in MCL are summarized in **Table 1**.

Table 1. Common genetic alterations in MCL

Losses		
Location	% (number of patients)	Relevant genes inside
13q	37% (46) (Yi et al. 2022); 13q14 - 23% (19) 13q33-q34 - 33% (27) (Nadeu et al. 2020); 13q14-q34 - 43% (33), 13q11-q13 - 18% (14) (Salaverria et al. 2007); 13q12-14 (6) - (43%), 13q31-33 (6) - (43%) (Schraders et al. 2005); 27% (21) (Hartmann et al. 2010); 6% (13) (Au et al. 2002); 3% (1) (Wlodarska et al. 1999). Across all studies (any site): 30%	<i>IRS2, DIS3, BRCA2, ERCC5, FLT3, CUL4A, ING1, RB1</i>

1p21-p32	29% (36) (Yi et al. 2022); 1p21-p23 - 29% (24) 1p32 - 6% (5) (Nadeu et al. 2020); 51% (39) (Salaverria et al. 2007); 47% (36) (Hartmann et al. 2010); 50% (7) (Schraders et al. 2005); 11% (24) (Au et al. 2002); 10% (4) (Wlodarska et al. 1999); 24% (11) (Beà et al. 1999). Across all studies: 26%	<i>BCL10, CDKN2C</i>
11q21-23	28% (34) (Yi et al. 2022); 30% (23) (Salaverria et al. 2007); 50% (38) (Hartmann et al. 2010); 57% (8) (Schraders et al. 2005); 11% (23) (Au et al. 2002); 8% (3) (Wlodarska et al. 1999). Across all studies: 24%	<i>ATM, SDHD, BIRC3, KMT2A, MRE11,</i>
17p	35% (43) (Yi et al. 2022); 13% (9) (Salaverria et al. 2007); 8% (17) (Au et al. 2002); 46% (6) (Streich et al. 2020); 32% (36) (Malarikova et al. 2020); 23% (18) (Hartmann et al. 2010); 16% (7) (Beà et al. 1999). Across all studies: 21%	<i>TP53</i>
8p21-pter	22% (27) (Yi et al. 2022); 14% (11) (Salaverria et al. 2007); 21% (16) (Hartmann et al. 2010). Across all studies: 19%	<i>PPP2R2A</i>
9p21-(24)pter	38% (47) (Yi et al. 2022); 21% (17) (Nadeu et al. 2020); 19% (15) (Salaverria et al. 2007); 27% (21) (Hartmann et al. 2010); 5% (10) (Au et al. 2002); 16% (7) (Beà et al. 1999). Across all studies: 19%	<i>CDKN2A, JAK2</i>
6q21-(25)qter	11% (14) (Yi et al. 2022); 22% (16) (Salaverria et al. 2007); 36% (5) (Schraders et al. 2005); 21% (16) (Hartmann et al. 2010); 19% (40) (Au et al. 2002); 15% (6) (Wlodarska et al. 1999). Across all studies: 18%	<i>ARID1B, HDAC2</i>

6q15-q21	11% (13) (Yi et al. 2022); 27% (22) (Nadeu et al. 2020); 18% (13) (Salaverria et al. 2007); 3% (1) (Wlodarska et al. 1999); 27% (12) (Beà et al. 1999). Across all studies: 18%	<i>HDAC2</i>
9q21-qter	9q22-q31 - 18% (15) (Nadeu et al. 2020); 21% (16) (Salaverria et al. 2007); 3% (1) (Wlodarska et al. 1999). Across all studies: 17%	<i>ABL1, FANCC, NUP214</i>
10p15-p13	15% (12) (Nadeu et al. 2020);	<i>KLF6</i>
19p	15% (12) (Nadeu et al. 2020);	<i>KEAP1, SMARCA4, CDKN2D</i>
-13	13% (27) (Au et al. 2002); 28% (11) (Wlodarska et al. 1999). 44% (20) (Beà et al. 1999); 27% (21) (Hartmann et al. 2010). Across all studies: 21%	<i>IRS2, DIS3, FLT3, CUL4A, ING1</i>
-9	5% (4) (Salaverria et al. 2007); 8% (18) (Au et al. 2002); 13% (5) (Wlodarska et al. 1999); 13% (17) (Yi et al. 2022). Across all studies: 9%	<i>CDKN2A, ABL1, FANCC, NOTCH1, FANCC, FANCG, JAK2, NUP214, SMARCA2, FBXO10, TOR1B</i>
-Y	10% (21) (Au et al. 2002); 15% (6) (Wlodarska et al. 1999). Across all studies: 11%	<i>CRLF2</i>
-14	6% (12) (Au et al. 2002); 18% (7) (Wlodarska et al. 1999). Across all studies: 8%	<i>FANCM, MLH3, PARP2, RAD51B</i>
-15	6% (12) (Au et al. 2002); 8% (3) (Wlodarska et al. 1999). Across all studies: 6%	<i>FANCI, RAD51, PML</i>
-20	6% (12) (Au et al. 2002); 5% (2) (Wlodarska et al. 1999). Across all studies: 6%	<i>SAMHD1, ASXL1</i>
-21	6% (12) (Au et al. 2002); 3% (1) (Wlodarska et al. 1999). Across all studies: 6%	<i>RUNX1</i>
-18	6% (12) (Au et al. 2002); 3% (1) (Wlodarska et al. 1999);	<i>BCL2</i>

	Across all studies: 6%	
Gains		
3q	3q21-29 - 38% (47) (Yi et al. 2022); 3q25-q29 - 43% (35) (Nadeu et al. 2020); 3q21-qter - 32% (25) (Salaverria et al. 2007); 6% (12) (Au et al. 2002); 3% (1) (Wlodarska et al. 1999); 49% (18) (Beà et al. 1999); 31% (24) (Hartmann et al. 2010). Across all studies: 26%	<i>ATR, BCL6, MECOM, MLF1, POLQ, RPN1</i>
8q21-qter	20% (25) (Yi et al. 2022); 8q24 - 15% (12) (Nadeu et al. 2020); 13% (10) (Salaverria et al. 2007); 22% (10) (Beà et al. 1999); 13% (10) (Hartmann et al. 2010). Across all studies: 17%	<i>UBR5, MYC, NBN, RUNX1N1</i>
7p	15% (12) (Nadeu et al. 2020); 13% (10) (Hartmann et al. 2010). Across all studies: 14%	<i>IGF2BP3</i>
18q21-q(22)2 3	11% (13) (Yi et al. 2022); 13% (11) (Nadeu et al. 2020); 10% (8) (Salaverria et al. 2007); 18% (8) (Beà et al. 1999). Across all studies: 12%	<i>BCL2</i>
15q21-qter	11% (13) (Yi et al. 2022); 13% (10) (Salaverria et al. 2007); 5% (2) (Wlodarska et al. 1999). Across all studies: 11%	<i>FANCI</i>
10p12	11% (9) (Nadeu et al. 2020).	<i>BMI1</i>
13q31	10% (8) (Nadeu et al. 2020).	<i>MIR17HG</i>
11q	11% (13) (Yi et al. 2022); 6% (13) (Au et al. 2002); 15% (6) (Wlodarska et al. 1999). Across all studies: 9%	<i>FGF19, FGF4, FGF3, CHEK1, KMT2A</i>
12q	14% (17) (Yi et al. 2022); 20% (9) (Beà et al. 1999); 6% (4) (Hernández et al. 2005) 4% (9) (Au et al. 2002); 8% (3) (Wlodarska et al. 1999). Across all studies: 8%	<i>CDK4, ARID2, MDM2</i>

+3	6% (13) (Au et al. 2002); 10% (4) (Wlodarska et al. 1999). Across all studies: 7%	<i>ROBO1, BAP1, BCL6, FANCD2, MECOM, MLF1, MLH1, MYD88, RPN1</i>
+12	4% (9) (Au et al. 2002); 3% (1) (Wlodarska et al. 1999). Across all studies: 4%	<i>CDK4, ARID2, MDM2</i>
Mutated genes (excluding cases of losses and gains)		
Gene name	% (number of patients)	Description
<i>ATM</i>	59% (24) (Jain et al. 2023); 32% (8) (Karolová et al. 2023); 34% (42) (Yi et al. 2022); 48% (39) (Nadeu et al. 2020); 42% (78) (Ferrero et al. 2020); 34% (18) (Jeong et al. 2020); 37.5% (6) (Yang et al. 2018); 18% (3) (Khodadoust et al. 2017); 42% (24) (Zhang et al. 2014); 42% (69) (The AACR Project GENIE Consortium et al. 2017); 41% (12) (Beà et al. 2013); 58% (7) (Schaffner et al. 2000). Average: 41%	mainly truncating or missense mutations involving the PI-3K domain (Camacho et al. 2002; Jeong et al. 2020; Karolová et al. 2023; Khodadoust et al. 2017); associated with lack of protein expression (Camacho et al. 2002) and inferior survival in TP53-WT cases (Koff et al. 2022).
<i>TP53</i>	41% (17) (Jain et al. 2023); 48% (12) (Karolová et al. 2023); 31% (38) (Yi et al. 2022); 26% (21) (Nadeu et al. 2020); 21% (15) (Rodrigues et al. 2020); 8% (15) (Ferrero et al. 2020); 17% (9) (Jeong et al. 2020); 38% (43) (Malarikova et al. 2020); 31% (5) (Yang et al. 2018); 41% (7) (Khodadoust et al. 2017); 26% (46) (The AACR Project GENIE Consortium et al. 2017); 19% (11) (Zhang et al. 2014); 15% (8) (Greiner et al. 1996). Average: 24%	mainly missense or nonsense mutations (Greiner et al. 1996; Jeong et al. 2020; Ferrero et al. 2020; Rodrigues et al. 2020; Karolová et al. 2023; Khodadoust et al. 2017; Jain et al. 2023) associated with poor prognosis (Greiner et al. 1996; Jeong et al. 2020; Ferrero et al. 2020; Rodrigues et al. 2020; Karolová et al. 2023; Khodadoust et al. 2017; Jain et al. 2023).
<i>KMT2D</i>	15% (6) (Jain et al. 2023); 28% (7) (Karolová et al. 2023); 23% (19) (Nadeu et al. 2020); 12% (23) (Ferrero et al. 2020); 32% (17) (Jeong et al. 2020); 18% (33) (The AACR Project GENIE	missense, frameshift and nonsense mutations (Jeong et al. 2020; Karolová et al. 2023; Jain et al. 2023); associated with poor clinical outcome (Ferrero et

	Consortium et al. 2017). Average: 18%	al. 2020).
<i>CCND1</i>	15% (6) (Jain et al. 2023); 20% (5) (Karolová et al. 2023); 44% (36) (Nadeu et al. 2020); 12% (15) (Yi et al. 2022); 12% (22) (Ferrero et al. 2020); 19% (3) (Yang et al. 2018); 29% (5) (Khodadoust et al. 2017); 13% (24) (The AACR Project GENIE Consortium et al. 2017); 14% (9) (Zhang et al. 2014); 35% (10) (Beà et al. 2013). Average: 18%	deletions or point mutations leading to truncation of the destabilization elements in the 3'UTR of the transcript and expression of the truncated protein with longer half-life (Wiestner et al. 2007; Nadeu et al. 2020); mutations in exon 1 (Beà et al. 2013) leading to increased protein stability (Mohanty et al. 2016); missense mutations (Zhang et al. 2014; Karolová et al. 2023; Jain et al. 2023).
<i>WHSC1</i>	15% (29) (Ferrero et al. 2020); 31% (5) (Yang et al. 2018); 12% (2) (Khodadoust et al. 2017); 10% (18) (The AACR Project GENIE Consortium et al. 2017); 10% (13) (Beà et al. 2013); 7% (4) (Zhang et al. 2014). Average: 12%	missense mutations (Ferrero et al. 2020; Zhang et al. 2014; Khodadoust et al. 2017); correlate with poor prognosis (Yang et al. 2018)
<i>SP140</i>	20% (5) (Karolová et al. 2023); 8% (10) (Yi et al. 2022); 13% (11) (Nadeu et al. 2020); 12% (2) (Khodadoust et al. 2017). Average: 11%	mainly nonsense and frameshift mutations (Karolová et al. 2023; Khodadoust et al. 2017) resulting in a truncated protein form; associated with inferior survival (Yi et al. 2022).
<i>SMARCA4</i>	15% (6) (Jain et al. 2023); 12% (3) (Karolová et al. 2023); 7% (9) (Yi et al. 2022); 9% (7) (Nadeu et al. 2020); 12% (2) (Khodadoust et al. 2017); 9% (16) (The AACR Project GENIE Consortium et al. 2017); 12.5% (7) (Zhang et al. 2014). Average: 10%	mainly missense (Zhang et al. 2014; Yi et al. 2022; Karolová et al. 2023; Khodadoust et al. 2017); predictor of poor progression-free survival (Yi et al. 2022).

<i>BIRC3</i>	7% (3) (Jain et al. 2023); 22% (18) (Nadeu et al. 2020); 5% (6) (Yi et al. 2022); 6% (11) (Ferrero et al. 2020); 12% (22) (The AACR Project GENIE Consortium et al. 2017); 9% (5) (Zhang et al. 2014); 6% (11) (Beà et al. 2013). Average: 9%	truncating or missense mutations in the zinc finger ring domain (Ferrero et al. 2020); frameshift mutations (Yi et al. 2022; Jain et al. 2023).
<i>NOTCH1</i>	12% (5) (Jain et al. 2023); 12% (3) (Karolová et al. 2023); 7% (9) (Yi et al. 2022); 5% (4) (Nadeu et al. 2020); 12% (13) (Kridel et al. 2012); 12% (2) (Khodadoust et al. 2017); 5% (9) (The AACR Project GENIE Consortium et al. 2017); 14% (8) (Zhang et al. 2014); 5% (8) (Beà et al. 2013); 8% (14) (Ferrero et al. 2020). Average: 8%	mainly truncating mutations in the C-terminal domain; frameshift mutations (Yi et al. 2022); associated with shorter overall patient survival (Kridel et al. 2012; Ferrero et al. 2020; Beà et al. 2013).

**As not all studies provide the precise genomic locations of gains and deletions and those locations also vary across patients, as an approximation, the total percentages for losses and gains are calculated for the smallest deleted/gained region common for all the described gains/losses. For example, the total percentage for the 13q loss takes into account both the 13q14 and the 13q33-q34 losses, as well as the general reports of the del(13q) without further specifications. When available, more precise loss/gain locations are specified for the particular studies cited in the table.*

Increased genomic instability is likely related to the alterations in the key DNA damage response genes, *ATM* and *TP53*, which are the two most frequently deleted and/or mutated genes in MCL (see **Table 1**). *ATM* is a serine/threonine kinase recruited to the sites of double strand breaks (DSBs) where it phosphorylates the key proteins initiating the DNA damage response (J.-H. Lee and Paull 2021). It is mutated predominantly in cMCL (Nadeu et al. 2020). *ATM*-mutant cells have impaired DNA double strand break repair and impaired apoptosis (Weston et al. 2010). In mouse models, *ATM* deficiency leads to persistent DNA damage, increased rate of chromosomal aberrations and development of lymphomas (Y et al. 2017; Yamamoto et al. 2012; Hathcock et al. 2015; Y. Xu et al. 1996). WGS studies of MCL tumors also show that MCL cells with mutated *ATM* have decreased telomere length (Nadeu et al. 2020), which may facilitate genomic aberrations *via* breakage-fusion-bridge cycles. Accordingly, MCLs with *ATM* inactivation bear more chromosomal imbalances than MCLs with the wild-type gene, while bi-allelic *ATM* alterations are further associated with frequent extranodal involvement (Camacho et al. 2002). Occasionally, *ATM* mutations are present in the germline of MCL patients (Fang et al. 2003; Nadeu et al.

2020), suggesting a possible genetic predisposition. Importantly, throughout normal B cell differentiation, ATM is weakly expressed or absent in the bone marrow and germinal center B lymphocytes, while the highest ATM levels are present in the B lymphocytes of the mantle zone and in plasma cells (Starczynski et al. 2003).

Nevertheless, the direct role of ATM in MCL pathogenesis is debatable. Although very frequent, *ATM* loss was not correlated with the overall survival of MCL patients (T. C. Greiner et al. 2006). In another study, the correlation of ATM deficiency with inferior survival was observed in the sub-group of patients with the wild-type *P53*, but not in the group with mutated *P53*, while *P53* mutation was a negative survival predictor either alone or in combination with mutated ATM (Koff et al. 2022). This likely suggests that p53 serves as a converging hub for both aberrations, as it is one of the main DNA-damage response proteins activated by ATM phosphorylation.

p53 is involved in both double- (DSB) and single- (SSB) strand break responses (**Figure 4**), acting as a DNA damage sensor during the G1/S and G2/M checkpoints. Depending on the nature of the damage, DNA damage signaling coordinated by ATM (DSB) or ATR (SSB) produces a spectrum of p53 post-translational modifications (mainly phosphorylation), which tailor the appropriate and proportional p53 activation. Activated p53 relocates to the nucleus and induces transcription of genes involved in repair and cell cycle arrest, which allows the cell to repair the damage before replicating or enter apoptosis in case of failure. *TP53* is thus one of the major tumor suppressors and also the most commonly mutated gene across all human cancers (Levine 2020). *TP53* knockout mice develop early spontaneous tumors, predominantly T cell lymphomas (Donehower et al. 1992; Dudgeon et al. 2014; Palanichamy et al. 2023), while the mice with specific *TP53* deletion in the B cell lineage exhibit a spectrum of phenotypes ranging from marginal zone expansion to marginal zone lymphoma to diffuse large/mixed B-cell lymphomas of the spleen (Palanichamy et al. 2023). In almost half of Mantle cell lymphoma cases *TP53* is either lost or bears a missense, nonsense or frameshift mutation compromising the p53 protein function (see **Table 1**). In MCL, *TP53* alteration is a secondary mutation, though its high frequency and the survival advantage it confers to the bearing cells (D. H. Kim et al. 2024) suggests it might be an early event in the oncogenesis of *TP53*-altered MCL tumors. *TP53* alterations in MCL are associated with poor prognosis (T. Greiner et al. 1996; E et al. 2019; Ferrero et al. 2020; Jeong et al. 2020; Rodrigues, Hassan, et al. 2020; Scheubeck et al. 2023; Elhassadi et al. 2021), aggressive clinical course (Eskelund et al. 2017) and blastoid morphology (Eskelund et al. 2017; Derby et al. 2010), and identify younger mantle cell lymphoma patients who do not benefit from intensive chemoimmunotherapy (Eskelund et al. 2017). Of note, non-loss *TP53* mutations frequently translate into elevated p53 protein levels in immunohistochemistry studies (Rodrigues, Hassan, et al. 2020), though the overexpressed p53 is likely dysfunctional; thus, p53 overexpression is an equally significant criteria for patient inclusion into a high-risk group (Alaggio et al. 2022).

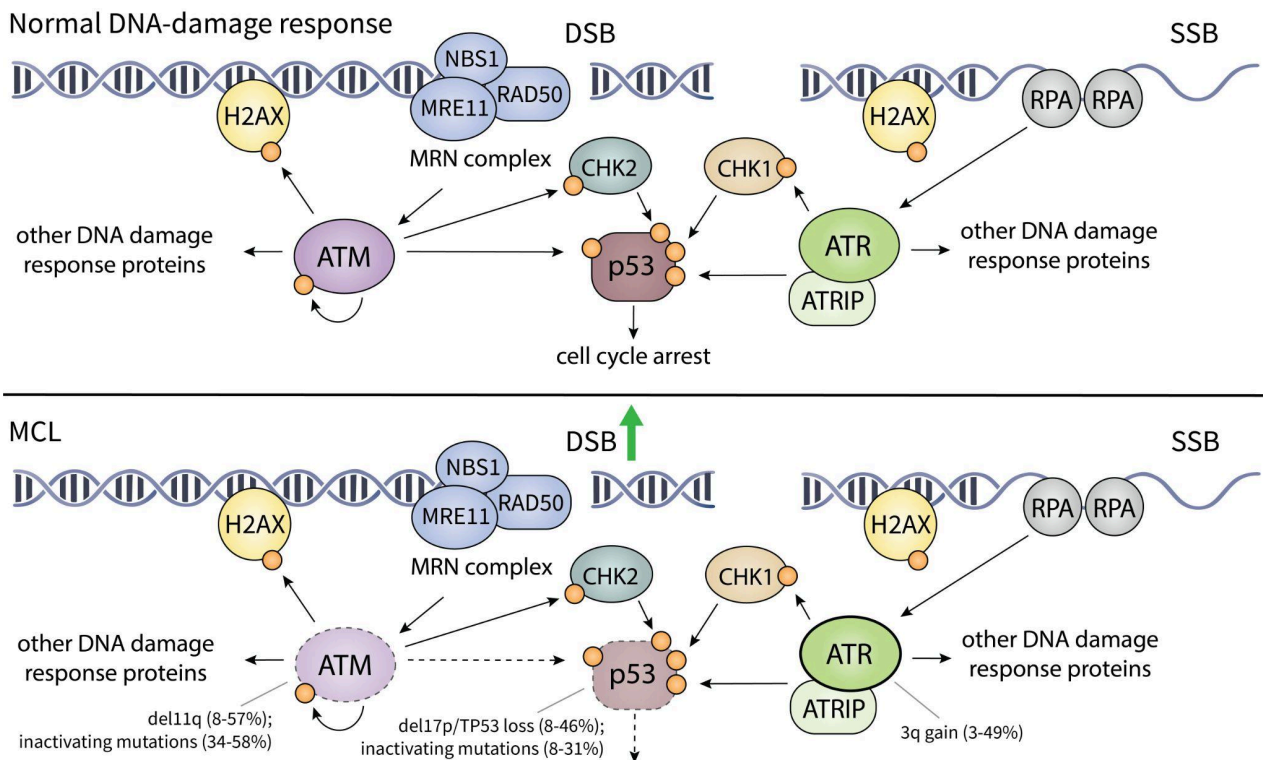


Figure 4. Impaired DNA damage response in MCL.

Other proteins of the DNA damage pathway are rarely altered in MCL. Decreased expression of checkpoint kinases CHK2 and CHK1, acting downstream of ATM and ATR (**Figure 4**), was reported in occasional aggressive cases (F. Tort et al. 2005; Frederic Tort et al. 2002; Nadeu et al. 2020). Moreover, similarly to *ATM1*, *CHK2* mutations were sometimes observed in the germline of the MCL patients (Hangaishi et al. 2002; Frederic Tort et al. 2002), though not systematically.

Interestingly, overexpressed *CCND1* was proposed to counterbalance the high rates of genomic instability in MCL helping to maintain the pool of viable tumor cells (S. Mohanty et al. 2013). *CCND1* depletion exhibited a toxic effect on MCL xenotransplants and was associated with the DNA damage manifested by increased histone H2AX phosphorylation (S. Mohanty et al. 2017). Moreover, *CCND1* silencing rendered MCL cells more sensitive to conventional chemotherapeutic agents (Tiemann et al. 2011) and replication inhibitors which induce DNA damage through relocation stress (S. Mohanty et al. 2017).

1.1.2.5. SOX11 expression

SOX11 is another specific marker of MCL. Its nuclear expression is detected in almost all MCL cases except for the non-nodal forms and unequivocally distinguishes conventional MCLs from benign lymphoid tissues (Ek et al. 2008; Mozos et al. 2009). SOX11 staining is equally valuable for differential MCL diagnostics: nuclear SOX11 is absent in chronic lymphocytic leukemia and diffuse large B cell lymphoma, most frequently confused with MCL, as well as in many other lymphoid neoplasms, including follicular lymphoma, marginal zone lymphoma, and primary bone marrow

lymphoma (Mozos et al. 2009); up to 50% of Burkitt lymphomas (Dictor et al. 2009; Mozos et al. 2009), most B and T-lymphoblastic leukemia/lymphomas and some hairy cell leukemias (Dictor et al. 2009) can be SOX11-positive, but those tumors are usually not mistaken for MCL. Importantly, nuclear SOX11 is also detected in CCND1-negative MCLs (Mozos et al. 2009), which further increases its diagnostic value.

SOX11 is a neurogenic transcription factor mainly known for promoting neural fate, neural differentiation, and neuron maturation in the developing nervous system, together with the two other SOXC family transcription factors, SOX4 and SOX12 (Uy et al. 2015; Tsang, Oliemuller, and Howard 2020). It is equally reported to have a broader function as a general regulator of progenitor and stem cells behavior; at varying levels, *SOX11* expression is present in non-neural embryonic tissues, including the epithelium and the mesenchyme of lung, gut, pancreas and mammary glands (Dy et al. 2008). In adult tissues, *SOX11* is normally silent, while its ectopic expression is associated with cancer and genetic disorders (Tsang, Oliemuller, and Howard 2020). Although SOX11 is normally not detected in the cells of the lymphocyte ontogeny at any developmental stage, it is highly homologous to SOX4, which is crucial for B lymphopoiesis (Sun et al. 2009) and pro-B cells survival in particular (Sun et al. 2013). The specificity of the Sox proteins' DNA-binding domain is low by itself and is thought to be achieved through protein partners and post-translational modifications (reviewed in (Bernard and Harley 2010)); thus SOX11 likely gains some functional properties similar to that of SOX4 when ectopically expressed in the B cell context. Functional redundancy of SOX4 and SOX11 has been demonstrated in multiple processes, e.g. spinal cord development (Thein et al. 2010), retina development (Jiang et al. 2013) and wound repair (Miao et al. 2019). Interestingly, the t(11;14) translocation is thought to occur in the pro-B cell stage (Hummel et al. 1994; Küppers et al. 1999; Kienle et al. 2003; Nadeu et al. 2020), the critical period of *SOX4* expression (Sun et al. 2013).

In mantle cell lymphoma, SOX11 likely blocks the tumor cells in the mature B-cell stage, preventing their terminal differentiation. It directly upregulates PAX5, a transcription factor committing lymphoid progenitors to the B-lymphocyte lineage (Cobaleda, Jochum, and Busslinger 2007) and driving the transition to the mature B-lymphocyte stage afterwards (Hill et al. 2020). Pax5 loss in B cells promotes plasma cell differentiation (Nera et al. 2006). Similarly, *SOX11* silencing in MCL cells produces a shift from the mature B cell expression signature to that of early plasmacytic differentiation, although it is not sufficient to induce a complete plasma cell phenotype (Vegliante et al. 2013). Accordingly, plasmacytic differentiation is not characteristic for mantle cell lymphoma, while the occasional MCL cases with focal areas of plasma cell presence tend to be SOX11-negative (Ribera-Cortada et al. 2015). SOX11 also represses the expression of *BCL6* through direct binding to the regulatory region within its intron 1 sequence (J. Palomero et al. 2016). *BCL6* is a transcription factor critical for the germinal center formation. It prevents premature

activation and differentiation of GC B cells allowing for their proliferation, and also promotes B cell tolerance to DNA breaks required for somatic hypermutation (Basso and Dalla-Favera 2012). BCL6 downregulation by SOX11 likely blocks the entrance of the t(11;14) B cell to the GC, preventing SHM and further differentiation stages. This is in line with the non-mutated IGHV status of most MCL tumors (Pighi et al. 2013). Consistently, low or absent SOX11 expression is also more generally characteristic for the rare subset of MCL tumors with mutated IGHV (Yi et al. 2022). Finally, SOX11 may contribute to MCL oncogenicity by stimulating tumor angiogenesis. It directly upregulates the proangiogenic platelet-derived growth factor A (PDGFA), which was shown to be secreted by MCL cells *in vitro* promoting endothelial cell proliferation, migration and tube formation (Jara Palomero et al. 2014). SOX11+ MCL tumors overexpress angiogenic gene signature, including *PDGFA* (Jara Palomero et al. 2014), and present higher microvascular development (Petrakis et al. 2019; Annese et al. 2020), which contributes to their aggressive phenotype.

Paradoxically, SOX11 seems to decrease tumor proliferation in MCL (Gustavsson et al. 2010; R. Yang et al. 2020; Conrotto et al. 2011) as well as in gastric and prostate cancer, glioma and nasopharyngeal carcinoma (Hide et al. 2009; Song Zhang, Li, and Gao 2013; X. Xu et al. 2015; Pugongchai, Bychkov, and Sampatanukul 2017). This may be partially due to the suppression of the WNT/ β -Catenin pathway, as in MCL cells, SOX11 was shown to directly upregulate the expression of NLK, a negative WNT-signaling regulator, and downregulate the expression of SMAD3, a protein protecting β -catenin from ubiquitin-proteasome-dependent degradation (P.-Y. Kuo et al. 2015). Other proliferation-related effects of SOX11 have been deduced in several overexpression/knockdown experiments. Knock-down of lipid storage regulating protein HIG2, another direct transcriptional target of SOX11 (Xiao Wang et al. 2010; Kuci et al. 2016), reciprocally reduced SOX11 expression and increased cellular proliferation in MCL cells (Kuci et al. 2016). Forced overexpression of *SOX11* in MCL cells led to the upregulation of the cell cycle suppressing *CDKN2A* locus and transforming growth factor- β (TGF- β), which blocks the progression through the G1 phase (Gustavsson et al. 2010), while *SOX11* knock down resulted in more aggressive tumor growth *in vivo* and increased *ATX* expression (Conrotto et al. 2011). *ATX* encodes for autotaxin, a secreted lysophospholipase D which produces lysophosphatidic acid (LPA), a lipid mediator stimulating multiple cellular processes, including the G0/G1- to S-phase transition (Jones and Kazlauskas 2001). All together, experimental results argue that SOX11 should rather restrict MCL growth and its pathogenic effect, if any, should be mediated otherwise. Accordingly, most clinical studies associate SOX11 positivity with better patient outcome. Two studies involving 53 (Xiao Wang et al. 2008) and 127 (Nordström et al. 2014) patients reported the absence of nuclear SOX11 to be associated with shorter overall survival; in another study of 186 patients, SOX11 negativity was equally associated with reduced overall survival, as well as higher frequency of lymphocytosis, elevated lactate dehydrogenase (LDH) level and p53 positivity (Nygren et al. 2012). Finally, in the largest study available up to date (365 patients), patients with low SOX11 expression

also had shorter OS, though time to treatment failure (TTF) was not affected (Aukema et al. 2018). On the other hand, one study has reported contradicting data, associating SOX11 expression with shorter overall survival (Fernández et al. 2010). An attempt to resolve this controversy has come from a recent study, which demonstrated that SOX11 inhibited tumor proliferation *via* CD43 dependent manner (R. Yang et al. 2020). While both CD43 and SOX11 positivity were separately associated with low Ki-67 index, only double positive SOX11+ CD43+ and single positive CD43+ cases had a significantly improved overall survival in a 37 patients cohort. Whether this finding will enhance the clinical significance of SOX11 as a prognostic indicator remains to be established.

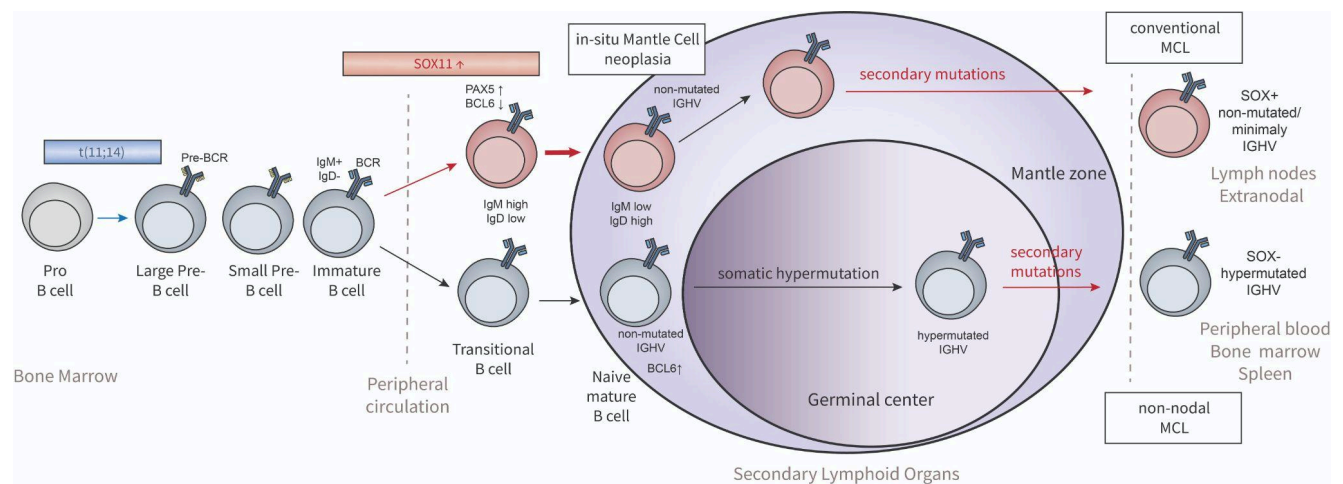


Figure 5. SOX11 expression in MCL oncogenesis.

As *SOX11* gene is not targeted by any genetic alteration in MCL (Nadeu et al. 2020), it is impossible to infer the precise time point of its deregulation from the clonal studies of developed tumors. Nevertheless, the high rate of SOX11-positivity (90% of total cases) implies that it should be a relatively early event in the evolution of conventional MCL. This is partially confirmed by the single-cell studies, which reveal that most of the *SOX11*-expressing MCL B cells are positive for IgM (90.5%) and negative for IgD (82.2%) (Valentin Hansen et al. 2021), which is characteristic for immature B lymphocytes of the bone marrow. In serial biopsies of the lymph nodes of MCL patients, SOX11 is already detected in yet indolent in situ MCL cells (Carvajal-Cuenca et al. 2012). Moreover, *IGHV* genes of the SOX11+ positive tumors are almost always non mutated. It is thus tempting to speculate that *SOX11* deregulation occurs at the immature B lymphocyte stage, and the subsequent *PAX5* upregulation drives the acquisition of the mature B cell phenotype by the majority of the tumor cells (**Figure 5**).

The reasons for SOX11 upregulation in MCL are equally elusive. *SOX11* expression is epigenetically controlled. *SOX11* promoter is hypomethylated in both healthy hematopoietic system and SOX11-positive lymphoid neoplasms (Vegliante et al. 2011; Wasik et al. 2013), but in healthy cells, it is heavily silenced due to the presence of inactivating histone marks H3K9me2 and H3K27me3 (Vegliante et al. 2011); this

silencing can be reversed by a histone deacetylase inhibitor, but not a methyltransferase inhibitor (Vegliante et al. 2011).

In contrast, in lymphoid neoplasms that express *SOX11* (MCL, a subset of B-ALLs, a subset of BLs), its promoter is marked by the activating histone modifications H3K9/14Ac and H3K4me3 (Vegliante et al. 2011). *SOX11* expression is also influenced by a distal super-enhancer located 624-653 Kb downstream of the gene (Queirós et al. 2016). This enhancer region is hypomethylated only in *SOX11*+ MCL cases and presents high contact frequencies with the *SOX11* gene in a bi-allelic fashion (Queirós et al. 2016; Vilarrasa-Blasi et al. 2022). Although this interaction is not translated into a large-scale disruption of topologically associated domains (TADs) in the region, there is a significant increase in the density of 3D interactions within the existing TAD in *SOX11*+ MCL cells (Vilarrasa-Blasi et al. 2022).

In summary, while *SOX11* stands out as one of the most specific markers for MCL, there is limited understanding regarding the reasons and timing of its upregulation. Moreover, its role in MCL progression is controversial, as it promotes certain aggressive clinical characteristics while also constraining tumor proliferation. Further investigation is necessary to shed light on the consequences of *SOX11* expression in MCL pathology and the clinical relevance of *SOX11* as a prognostic and stratification marker.

1.1.2.6. B cell receptor signaling

B cell receptor (BCR), a transmembrane receptor on the B cell surface, is crucial for normal B cell development and adaptive immunity. The survival of pre-B cells is highly dependent on the presence of a functional pre-BCR, while B cell maturation relies on the selection of the B cells with the functional non-autoreactive BCRs (**Figure 1**). Upon recognition of a specific antigen, mature B cells receive strong proliferation signals and differentiate into antibody-secreting plasma cells or memory cells. In malignant cells, BCR signaling functions in a manner similar to that of a healthy B cell at a corresponding differentiation stage, and is usually co-opted to promote cell survival and proliferation.

Normally, BCR generates two types of signal: an antigen-independent continuous signal of low strength, known as 'tonic', required for cell maintenance and survival, and an antigen-dependent 'activated' signal inducing intense proliferation and differentiation. All BCR signal transduction is mediated through the heterodimer of Ig α and Ig β proteins (CD79A and CD79B) that is non-covalently associated with the membrane part of the BCR (**Figure 6**). The cytoplasmic tails of Ig α and Ig β contain immunoreceptor tyrosine-based activation motifs (ITAMs), that can be activated through phosphorylation by SRC-family protein tyrosine kinases (SFKs) - LYN, FYN and BLK (Saijo et al. 2003), LYN kinase being the most highly expressed in B cells (Yamanashi et al. 1991). Upon antigen binding, LYN phosphorylates the ITAMs of Ig α and Ig β . In the absence of the antigen, transient ITAMs phosphorylation is still

possible due to the sensitive balance between the constitutively active PTKs and protein-tyrosine phosphatases ('tonic' signaling). Phosphorylated ITAMs become the docking site for the spleen tyrosine kinase (SYK), which is then activated by local SRC-family kinases and by autophosphorylation (Rowley et al. 1995). Activated SYK recruits B cell linker protein (BLNK), which coordinates the activation of phospholipase Cy2 (PLCy2) and Bruton tyrosine kinase (BTK) (Baba et al. 2001). Recruited BTK, also phosphorylated directly by LYN (Baba et al. 2001), phosphorylates PLCy2 on its Y753 and Y759 residues, significantly boosting its lipase activity (Y. J. Kim et al. 2004). Active PLCy2 catalyzes phosphatidylinositol-4,5-bisphosphate (PIP2) hydrolysis into diacylglycerol (DAG) and inositol trisphosphate (IP3), the latter inducing the influx of calcium into the cell. Together with increased calcium levels, DAG activates protein kinase C (PKC) isoforms that phosphorylate multiple downstream substances, leading to the activation of NF- κ B and RAS-MAPK-ERC pathways, both contributing to the survival and proliferation of mature B cells. LYN also phosphorylates the positive BCR-coreceptor CD19, that recruits phosphoinositide 3-kinase (PI3K) generating phosphatidylinositol-3,4,5-trisphosphate (PIP3) from PIP2. PIP3 acts as a second messenger to recruit the serine/threonine protein kinase AKT and BTK to the plasma membrane *via* their pleckstrin homology (PH) domains. AKT signaling fosters cell survival and growth, while BTK recruited to the membrane further amplifies the BCR signaling through extended PLCy2 phosphorylation. BCR activation is counterbalanced by the negative B-cell coreceptors CD5 and CD22, that contain the immunoreceptor tyrosine-based inhibitory motifs (ITIMs) or ITIM-like sequences (in case of CD5). ITIMs recruit cytosolic phosphatases, such as tyrosine phosphatase SHP1 and the inositol phosphatases SHIP1 and SHIP2, that attenuate the signaling through ITAMs and PI3K respectively.

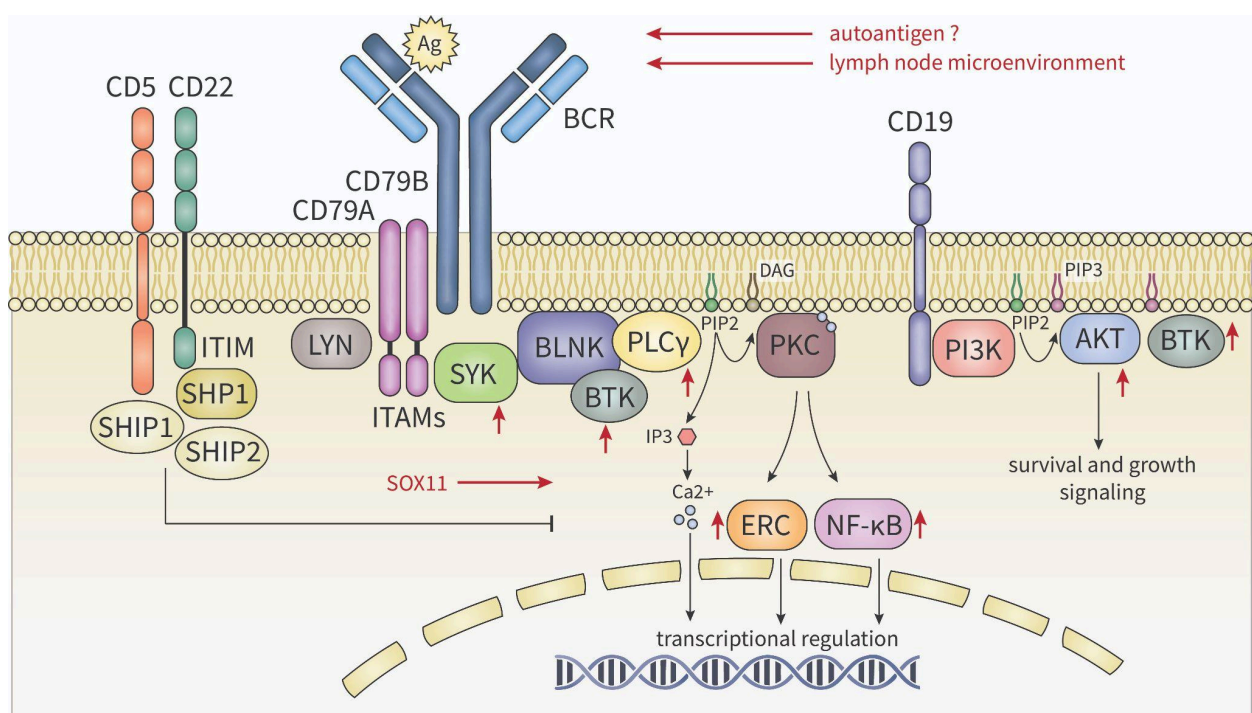


Figure 6. Abnormal BCR signaling in MCL.

Mutations in the elements of the BCR signaling pathway are not common for MCL. Still, phosphoproteomics studies identify B-cell receptor signaling as the most activated pathway in MCL cell lines (Pighi et al. 2011). Many BCR-pathway kinases, including SYK, LYN, BTK and PKC δ , were found among the most represented phospho-peptides in MCL cells (Pighi et al. 2011). Compared to the PBMCs from healthy donors, B cells from MCL patients demonstrated highly potentiated α -BCR-induced signaling, elevated basal levels of p-AKT, p-SYK, p-PLC γ (Myklebust et al. 2017) and p-BTK (Ma et al. 2014). Blastoid MCL variants were also reported to have constitutive PI3K-dependent phosphorylation of Akt (Rudelius et al. 2006), and elevated association of the active PKC β with the plasma membrane was reported for leukemic MCL (Boyd et al. 2009). Highly active BCR signaling was directly correlated with increased tumor proliferation (Ki67 index and the expression of proliferation signature genes) and was a strong predictor for poor OS after cytotoxic therapy (Saba et al. 2016). High basal levels of particular members of the BCR pathway, p-AKT, p-ERK and p-p38 MAPK, were also significantly associated with shorter OS of MCL patients independent of their MIPI index (Myklebust et al. 2017).

Importantly, increased activation of the BCR pathway in MCL seems to be dependent on the lymph-node microenvironment, at least in a large subset of cases. Within the same patients, BCR and Nf-Kb gene signatures were expressed at higher levels in the lymph-node biopsies compared to the peripheral blood in 59% (10/17) of samples (Saba et al. 2016). Some data also suggest the implication of SOX11 in the BCR signaling upregulation in MCL. In transgenic mice, B-cell-specific overexpression of SOX11 promoted clonal B cell expansion and augmented the signaling through the BCR pathway, specifically by increasing the baseline levels of phosphorylated BTK and PLC γ , and the levels of phosphorylated BTK, PLC, ERK1/2, p38, and MAPKAP2 upon IgM stimulation (Pei-Yu Kuo et al. 2018). In ChIP-seq and ChIP studies, SOX11 was shown to bind upstream of the *MIR17HG* locus (P.-Y. Kuo et al. 2015; Kawaji-Kanayama et al. 2023), encoding for the Mir-17-92 microRNA cluster overexpressed in MCL (Navarro et al. 2013; Kawaji-Kanayama et al. 2023) and other lymphoproliferative disorders (Dal Bo et al. 2015). Mir-17-92 inhibitors reduced the cellular response to the BCR-stimulation and decreased the levels of activated SYK, BTK, and AKT, suggesting the presence of miRNA-mediated activation of the BCR pathway by SOX11 (Kawaji-Kanayama et al. 2023). Finally, although MCL is generally thought to arise from the antigen-naive B cells, one can not completely exclude the pathogenic role of antigen in the abnormal BCR activation and related cellular proliferation of MCL cells. Around 10% of MCL tumors express stereotype BCR (identical BCR clonotypes between different patients) (Messmer et al. 2004; Stamatopoulos et al. 2007), suggesting the cell expansion was triggered by a specific antigen. While it has not been clearly demonstrated for MCL tumors, the pathological role of antigens, in particular autoantigens, such as apoptotic cell proteins or structural elements of the immunoglobulin heavy chain, have been shown for other lymphomas, notably CLL (Catera et al. 2008; Chu et al. 2010; Minden et al. 2012) and

DLBCL (Young et al. 2015). Further research might shed light on the origins of the BCR stereotypy and its interplay with the abnormal BCR pathway activation in MCL.

Extensive attempts have been taken to target the elements of the BCR pathway for treatment purposes. Several inhibitors of Syk, Akt and PI3K induced dose/time-dependent apoptosis in MCL cell lines *in vitro* (Pighi et al. 2011; Rinaldi et al. 2006; Rudelius et al. 2006; Dal Col et al. 2008). Nevertheless, not all of them proved equally successful in clinical trials. In a phase 1/2 trial, a Syk inhibitor fostamatinib exhibited some effect only in 1 out of 9 MCL patients (Friedberg et al. 2010), while PI3K δ inhibitor idelalisib achieved the overall response rate of 40% (16/40 patients), with the complete response in only 2 out of 40 patients (5%) (Kahl et al. 2014). A recent study demonstrated that MCL lymph nodes expressed high levels of PI3K γ isoform compared to other lymphomas (Till et al. 2023). A dual PI3K- δ and PI3K- γ inhibitor duvelisib might offer a favorable efficacy in MCL patients (Z. Wang et al. 2023).

A breakthrough came along with an accidental discovery of the effectiveness of the BTK inhibition against MCL tumors, first demonstrated in a phase I clinical trial in NHL patients (Advani et al. 2013). The effect was subsequently confirmed in a disease-specific phase II trial, where a BTK inhibitor ibrutinib showed a response rate of 68% (75 MCL patients), including 21% of patients with complete response (M. L. Wang et al. 2013). The mechanisms of ibrutinib action are likely multifaceted. As expected, ibrutinib prohibited the phosphorylation of BTK and downstream signaling proteins PLC γ 2, MAP kinases ERK, JNK and AKT following the stimulation of MCL cells by anti-IgM and CXCL12/13 chemokines (Chang et al. 2013). Interestingly though, only the inhibition of ERK and AKT, but not the BTK phosphorylation *per se* correlated with the cellular response to ibrutinib in MCL cell lines and primarily tumors (Ma et al. 2014). In another *in-vitro* study, ibrutinib induced concentration-dependent apoptosis and decreased the levels of anti-apoptotic Bcl-2, Bcl-xL and Mcl-1 proteins (Cinar et al. 2013). Furthermore, ibrutinib likely disrupts the homing of the MCL cells in the lymphoid tissues and promotes the egress of MCL cells into peripheral blood, where they die devoid of the survival signals and microenvironment protection (Chang et al. 2013). This is supported by the clinical observation that ibrutinib induces transient escalation of the absolute lymphocyte count (ALC) due to an increase in circulating MCL cells shortly after treatment (Chang et al. 2013). These cells have decreased Ki67 and pERK proliferation markers and decreased surface expression of CXCR4, a chemokine receptor critical for B cell homing and chemotaxis. As opposed to disease progression, the ALC increase following ibrutinib treatment is accompanied by a substantial tumor volume and lymphadenopathy reduction (Chang et al. 2013). In co-culture experiments, ibrutinib blocked the migration of MCL cells beneath stromal cells and suppressed the stromal cell-induced chemokine and cytokine secretion, which further proved the importance of BTK-signaling for the migration and adhesion of MCL cells (Chang et al. 2013).

In summary, potentiated BCR pathway is one of the key factors sustaining cell survival and proliferation in MCL, similarly to other lymphomas. Heightened BCR signaling correlates with aggressive tumor behavior and poor prognosis (Gambino et al. 2024). All this, together with the therapeutic success of the BTK inhibitors, highlights the potential of targeting the components of the BCR pathway for MCL treatment, motivating further research on the BCR axis in the MCL context.

1.1.2.7. Epigenetic deregulation and genome architecture

Gene expression profiles of MCL tumors are highly correlated with the epigenetically-defined regions of open chromatin observed in naive mature B cells (J. Zhang et al. 2014), suggesting that MCL cells are epigenetically similar to their presumed normal counterparts. In terms of the 3D-genome architecture, MCLs also resemble naive B lymphocytes (Vilarrasa-Blasi et al. 2021). Nevertheless, multiple evidence suggests that MCL cells acquire a number of tumor-specific epigenetic and 3D-genome features.

The t(11;14) translocation was shown to affect the radial positioning of the derivative chromosome 14 in the 3D nuclear space by bringing the der14 closer to the nuclear center and the nucleoli (Allinne et al. 2014). Such relocalization may translate into affected chromatin state of the translocated loci, as the center of the nucleus is generally enriched with active chromatin compartments (Chen et al. 2018; Su et al. 2020; Mota et al. 2022). Indeed, the euchromatic marker H3K9Ac was elevated around the t(11;14) breakpoint as compared to the average genome acetylation level (Markozashvili et al. 2016). Consistently, the region spanning the most frequent translocation breakpoints on chr11 is decorated with the H3K4me1 enhancer marks in normal naive and memory cells, but not the germinal cells, and those marks tend to extend following the translocation in MCL (Nadeu et al. 2020), suggesting that the t(4;10) translocation may foster the development of novel enhancers or promoters. The gain of activating regulatory marks in MCL has also been observed genomewide. 27% of stably active (A), inactive (B) or intermediate (I) chromatin compartments present during normal B cell differentiation were shown to change their state in mantle cell lymphoma cells, with the tendency (57%) towards compartment activation (B to I or I to A transitions) (Vilarrasa-Blasi et al. 2021). The newly activated compartments were enriched for the active chromatin functional states (e.g. active enhancers and promoters) and exhibited an increase in accessibility and transcription. Interestingly, the gain in compartment activity was not restricted to der14; instead, it was most frequently observed on chromosomes 2, 10, 12, 13, 14, 15, 16, 19 and 20 (Vilarrasa-Blasi et al. 2021). Significant changes in the 3D genome structure were also observed between the conventional and non-nodal MCL subtypes. In particular, cMCL was characterized by *de novo* gains of A and I compartments in the 6.1 Mb region around the *SOX11* locus, consistent with the *SOX11*-positive status of most cMCL tumors. Apart from *SOX11*, 43% of the genes in this region were overexpressed in cMCL vs nnMCL in at least one MCL cohort (Vilarrasa-Blasi et al. 2021).

Several works explored the mechanisms of epigenetic gene repression in the context of MCL. EZH2, a key component of the polycomb repressive complex 2, was shown to be overexpressed in proliferating MCL cell lines (Visser et al. 2001; Demosthenous et al. 2020), while the negative regulator of EZH2, miR-26A1, was found uniformly silenced in the MCL patient samples (Kopparapu et al. 2016). EZH2 was proposed to contribute to mantle cell lymphoma growth by depositing the repressive H3K27me3 histone marks on the CDKN2B promoter (Demosthenous et al. 2020). One study also established the role of EZH2 in the silencing of the HOX genes in MCL (Kanduri et al. 2013), although without a clear link with the MCL pathogenesis.

DNA-hypermethylation of *CDKN2A*, encoding for the CDK4/6 inhibitor p16, was detected in 82% of the MCL samples, though the links with the gene expression or patient prognosis were not investigated (Chim et al. 2007). Five other genes, *SOX9*, *HOXA9*, *AHR*, *NR2F2*, and *ROBO*, were also found frequently methylated in MCL, and the hypermethylation of two or more of these genes was associated with aggressive clinicopathological features and shorter patient survival (Enjuanes et al. 2011). Nonetheless, it is unclear whether this association reveals a direct causal relationship or is simply due to the confounding variables such as advanced tumor stage and patient age, as DNA methylation changes tend to gradually accumulate during rounds of cell division, especially in cancer (Beerman et al. 2013; Siegmund et al. 2009; Aran et al. 2011; Landan et al. 2012; Nadeu et al. 2020). Supporting the latter, recent works showed that the main source of DNA-methylation variability between MCL tumors comes from the presumed cells of origin, ie, germinal center-inexperienced and germinal center-experienced B lymphocytes, followed by their proliferative history (Queirós et al. 2016; Nadeu et al. 2020).

Finally, up to 20% of MCL tumors bear mutations or deletions involving the genes coding for the components of the SWI-SNF complex, notably *SMARCA4* (most often) and *ARID2* (Agarwal et al. 2019). SWI/SNF are a family of chromatin remodeling complexes that hydrolyse ATP to slide or eject the nucleosomes (Kwon et al. 1994). They are enriched at enhancers and promoters and are essential to modulate enhancer accessibility necessary for the transcription factors to activate gene expression (Xiaofeng Wang et al. 2017; Nakayama et al. 2017). SWI/SNF also actively participate in DNA damage repair by modifying the chromatin structure around the damaged sites and recruiting the DNA damage response proteins (Ogiwara et al. 2011; Qi et al. 2015; Chen et al. 2019). Mutations in the components of SWI-SNF are found in up to 25% of known cancers, and both their role in DNA damage response and transcription regulation may be compromised in different malignancies (reviewed in (Mittal and Roberts 2020)). In MCL, losses or mutations in *SMARCA4* and *ARID2* convey primary resistance to the combination therapy with the BTK inhibitor ibrutinib and BCL-2 inhibitor venetoclax (Agarwal et al. 2019), likely by priming the cells to survive the therapeutic challenge. MCL cells with the *SMARCA4* loss increase the expression of Bcl-xL, another anti-apoptotic protein from the BCL-2 family, and are positively selected for during the ibrutinib-venetoclax treatment (Agarwal et al.

2019). Conversely, addition of the Bcl-xL inhibitor is effective to overcome the ibrutinib-venetoclax resistant phenotype (Agarwal et al. 2019). Although the mechanistic link between the SWI-SNF complex and the described effect is not entirely clear, it likely has an epigenetic component. While SMARCA4 loss did not affect the chromatin state of the loci showing increased expression in *SMARCA4* knockdown cells, significant decrease in accessibility was observed for the repressed genes, suggesting that the direct effect of the SWI-SNF impairment in MCL is rather the loss of activity of relevant genes than any specific target upregulation. In particular, increased *Bcl-xL* expression was explained by the decrease in chromatin accessibility and transcription in the *ATF3* locus (Agarwal et al. 2019), encoding for the *Bcl-xL* direct transcriptional repressor (Chüeh et al. 2017).

All together, despite the significant potential for exploration, there is currently a limited number of studies investigating the epigenetic landscape in mantle cell lymphoma, resulting in few robust conclusions. Further research into MCL-specific epigenetic alterations behind the oncogenic transformation is essential to translate the latest advances in epigenetic therapies to mantle cell lymphoma treatment.

1.1.2.8. Metabolic reprogramming

Although not at the origins of MCL pathogenesis, metabolic reprogramming has been described as a predictor of poor prognosis and/or treatment response in MCL. Altered thermogenesis, fatty acid degradation and oxidative phosphorylation were reported in patients with poor response to the Nordic MCL 2 and 3 (N-MCL2/3) clinical trials protocol, which included first-line R-CHOP (rituximab, cyclophosphamide, doxorubicin vincristine, and prednisone), high-dose cytarabine cycles and autologous stem cell transplantation. Overexpression of the CPT1A protein, a key enzyme in the carnitine-dependent transport which initiates mitochondrial oxidation of long-chain fatty acids, was a predictor of short time to progression (TPP) and reduced OS in this cohort (Gerdtsson et al. 2023). A recent study also highlighted the role of aberrant nucleotide metabolism in MCL. The authors were able to stratify MCL patients based on the nucleotide metabolism expression score, that included the expression levels of six genes related to nucleotide biosynthesis (*CTPS1*, *DTYMK*, *NUDT1*, *PDE3B*, *TK1* and *TYMS*); the patients with high score had significantly worse OS ($p < 0.0001$) (Liang et al. 2023).

The expression of *CTSP1*, encoding for a key enzyme in cytidine triphosphate (CTP) synthesis, was the strongest OS predictor, associated with decreased OS independently of the other nucleotide metabolism genes. Of note though, the same study demonstrated that the *CTSP1* expression is likely upregulated by MYC (Liang et al. 2023), which is itself a predictor of poor outcome (Choe et al. 2016; Rodrigues, Hollander, et al. 2020; Nadeu et al. 2020).

Constitutive activation of the PI3K/Akt signaling in aggressive blastoid MCL variants (Dal Col et al. 2008; Rudelius et al. 2006) led to the exploration of one of its major

downstream targets, the mammalian target of rapamycin (mTOR), in the context of MCL. mTOR is a central regulator of cell metabolism, growth and survival, which in B cells promotes pro-survival signaling. It exists in two functionally and structurally distinct complexes, mTOR complex 1 (mTORC1) and mTORC2, the former being mostly sensitive to nutrients and the latter mostly responsive to the signaling via PI3K and growth factors. mTORC1 inhibitors exhibited anti-proliferative activity against MCL cells (Hipp et al. 2005; Haritunians et al. 2007; Dal Col et al. 2008). Nevertheless, mTORC1 inhibition did not prove effective in clinics, at least as a single therapy, the main issue being the very short-lived response (Hess et al. 2009; Ansell et al. 2008; Renner et al. 2012; Witzig et al. 2005). One of the reasons behind this short effect duration is the fact that selective mTORC1 inhibitors suppress the mTORC1-dependent negative feedback loop and paradoxically increase Akt signaling, thus shifting the balance to increased mTORC2 activity (Shi et al. 2005; Gupta et al. 2009). Second generation mTOR inhibitors targeting both the mTORC1 and mTORC2, overcome this issue, but have not been extensively tested in MCL. In one *in-vitro* study, mTORC1/2 inhibitor exhibited only a slight cytostatic and cytotoxic effect in MCL cell lines and primary MCL cells; nonetheless, it also decreased the levels of the Krebs cycle metabolites and partially reversed the upregulation of the glycolysis by-product lactic acid induced by a selective nuclear export inhibitor (Sekihara et al. 2017). This suggests the potential utility of the second generation mTOR inhibitors in combination therapies to suppress the energy metabolism through glycolysis, typical for cancer cells (Warburg, Wind, and Negelein 1927).

Finally, metabolism has been extensively studied as a means to overcome MCL drug resistance. Metabolic reprogramming towards oxidative phosphorylation (OXPHOS) (L. Zhang et al. 2019; Y. Liu et al. 2023) was associated with resistance to the BTK-inhibitor ibrutinib. MCL cells from the ibrutinib resistant patients had elevated levels of the mitochondrial OXPHOS pathway components (L. Zhang et al. 2019) and the transcription factor early growth response gene 1 (ERG1) (Y. Liu et al. 2023). ERG1 contributes to the transcriptional activation of PDP1, which activates the E1 component of the large pyruvate dehydrogenase complex, leading to increased intracellular ATP production (Y. Liu et al. 2023). Small molecule inhibition of the ETC Complex I resulted in substantial growth reduction of the ibrutinib-resistant MCL cells *in-vitro* and in patient-derived *in-vivo* models (L. Zhang et al. 2019), while a derivative of an anti-diabetic drug metformin synergized with ibrutinib in killing MCL cell lines and primary samples from MCL patients (Y. Liu et al. 2023). Ibrutinib resistance was equally associated with the metabolic shift towards glutaminolysis (L. Zhang et al. 2019; S.-C. Lee et al. 2019). Glutaminolysis accounted for up to 50% of the ATP production in MCL cell lines, independently of the ibrutinib response status (S.-C. Lee et al. 2019), but glutamine uptake was upregulated in the ibrutinib-resistant MCL cells (L. Zhang et al. 2019). Ibrutinib treatment suppressed glutaminolysis and TCA cycle in the ibrutinib-responsive, but not resistant MCL cells (S.-C. Lee et al. 2019), while blockage of glutamine metabolism with glutaminolysis inhibitors resulted in oxidative stress, energy stress (L. Zhang et al. 2019) and growth

restriction (S.-C. Lee et al. 2019) in the ibrutinib-resistant MCL cell lines. All together, these results point to the potential of targeting the OXPHOS and glutamine metabolism pathways to overcome ibrutinib resistance in relapsed/refractory MCL. The safety of some oxidative phosphorylation inhibitors in lymphoma patients is currently being explored in a phase 1 clinical trial (NCT03291938).

Alterations in hexosamine metabolism may be implicated in the resistance to a proteasome inhibitor bortezomib, approved for the treatment of relapsed and refractory MCL. Bortezomib induces apoptosis and cell cycle arrest in MCL cells (Pham et al. 2003; Pérez-Galán et al. 2006), primarily by decreasing the proteasomal degradation of I κ B and subsequent inhibition of the NF κ B pathway. Additionally, bortezomib was shown to exhibit its cytotoxic effect through the activation of the mitochondrial apoptotic pathway dependent on the generation of reactive oxygen species (ROS) (Pérez-Galán et al. 2006) and the induction of a proapoptotic protein Noxa independent of NF κ B activation (Pérez-Galán et al. 2006; Rizzatti et al. 2008). Unfortunately, up to 60% of patients have intrinsic bortezomib resistance (Fisher et al. 2006; Goy et al. 2005; O'Connor et al. 2005). O-GlcNAcylation is a dynamic post-translational modification effectuated by the O-GlcNAc transferase (OGT), that attaches O-linked N-acetylglucosamine (O-GlcNAc) moieties to cytoplasmic, nuclear and mitochondrial proteins. It is thought to function as a nutrient and stress sensor, regulating a variety of processes from transcription and epigenetic regulation to signal transduction and metabolism (reviewed in (X. Yang and Qian 2017)). A drug-like inhibitor of O-GlcNAcase (OGA), an enzyme removing the O-GlcNAc residues, was shown to sensitize MCL cells to bortezomib-induced apoptosis through prolonged O-GlcNAcylation of the proapoptotic protein tBid, that interfered with its proteasomal degradation (Luanpitpong et al. 2018). These results suggest the potential utility of OGA-inhibitors to combat bortezomib resistance, as well as the relevance of the hexosamine metabolic pathway, a major source of O-GlcNAc, in the response of MCL tumors to chemotherapy.

In conclusion, metabolic reprogramming plays a non-negligible role in mantle cell lymphoma pathogenesis, impacting treatment response and drug resistance. Efforts to target the metabolic pathways overexploited by MCL cells hold promise for improving MCL outcomes. Nevertheless, MCL metabolism still remains a largely unexplored area and further research is needed to translate the existing findings into meaningful clinical interventions.

1.1.2.9. Tumor microenvironment

Interactions between malignant cells and components of the tumor microenvironment (TME), such as stromal cells, immune cells, and extracellular matrix, are pivotal factors underlying the tumor behavior and treatment response. Depending on the location, the components of the microenvironment may provide migration and homing signals, thus facilitating the tumor spread and metastasis,

promote survival and proliferation of tumor cells, and even serve as a protective layer against anti-tumor therapies.

Migration and homing of MCL cells

Trafficking and homing of normal and lymphoma B cells to the secondary lymphoid tissues relies on the coordinated expression of chemokines, their receptors and adhesion molecules on both the migrating cells and the cells of the microenvironment. B cells express surface G-protein coupled chemokine receptors, such as CXCR4 and CXCR5, while stromal cells in the lymphatic tissues constitutively express chemokines, such as CXCL12 and CXCL13, which form the concentration gradients and guide the B-cell positioning and homing at distinct compartments (Bajénoff et al. 2006; Allen et al. 2004; Reif et al. 2002). Chemokine binding to the G protein coupled receptors, together with other stimuli, such as BCR activation (Spaargaren et al. 2003), activates the B cell surface integrins (e.g. ITGAL and VLA-4), that bind to the molecules of the extracellular matrix and to adhesion molecules expressed on the other surrounding cells (S. Liu et al. 1999; W. Shen et al. 2001). Besides mediating the mechanical adhesion to the matrix, integrins transmit pro-survival signals upon adhesion and also govern the cell polarity and cytoskeletal remodeling when the cells migrate in response to cytokines (W. Guo and Giancotti 2004). In most integrins, this signaling is mediated through the recruitment of focal adhesion kinase (FAK) (Lipfert et al. 1992), which cooperates with the SRC-family kinases (SFKs) (Xing et al. 1994) and paxillin (Bellis, Miller, and Turner 1995; Y.-L. Hu et al. 2014) to recruit multiple downstream effectors and activate the pro-survival and pro-migratory pathways.

Mantle cell lymphoma (MCL) is characterized by an early, widespread dissemination, most common secondary locations being the lymph nodes, bone marrow and digestive system (Veloza, Ribera-Cortada, and Campo 2019). In line with their high motility and metastatic potential, MCL cells express high levels of CXCR4, CXCR5 and integrin VLA-4 (Kurtova et al. 2009; Y.-R. Kim and Eom 2014). MCL cell lines also exhibit high expression of FAK and pFAK (Rudelius et al. 2018) and 64% of MCL tumors are FAK-positive on immunohistochemistry sections (Ozkal et al. 2009). Importantly, this percentage reaches 100% for the bone marrow MCL infiltrates (Rudelius et al. 2018), reflecting both the importance of FAK for tumor dissemination and the sustained integrin and extracellular matrix signaling in the bone marrow microenvironment. In-vitro, MCL cells are highly motile and migrate spontaneously beneath mesenchymal stem cells in co-culture systems (Kurtova et al. 2009; Y.-R. Kim and Eom 2014). This migration largely depends on the CXCL12/CXCR4 axis (Y.-R. Kim and Eom 2014). Stimulation by CXCL12 and CXCL13 induced actin polymerization, an early requirement for the migratory response, and chemotaxis in MCL cells, while both of these effects could be blocked by a CXCR4 antagonist (Kurtova et al. 2009). CXCL12- and CXCL13-dependent chemotaxis of MCL cells is further enhanced by the B-cell activating factor (BAFF) abundantly secreted by mesenchymal stromal cells, which likely navigate the MCL cells to migrate to a certain niche (Medina et al. 2012).

High invasion potential of MCL tumors may be additionally stimulated by SOX11. ChIP data revealed *CXCR4* and *PTK2* (encoding for FAK) to be direct SOX11 transcriptional targets (Balsas et al. 2017). SOX11-positive MCL cells exhibited a stronger chemotaxis response to CXCL12 stimulation and also migrated more actively beneath the CXCL12-secreting bone marrow stromal cells compared to their SOX11-negative counterparts (Balsas et al. 2017). SOX11+ cells also engrafted better in an intravenous xenograft mouse model compared to the same cells with a SOX11 knockdown, while treatment with the FAK- and CXCR4-specific inhibitors reduced the dissemination and growth of the SOX11+ tumors to the level of the SOX11-negative ones (Balsas et al. 2017). In a subset of MCL cell lines, the adhesion of the cells to the micro environment seems to be boosted by BCR signaling (Sadeghi et al. 2020; W. Wu et al. 2021). These cells increased the expression of the BCR signature genes and the genes of the downstream NfKb pathway upon adhesion to the stromal cells in co-culture (Sadeghi et al. 2020), while the treatment with ibrutinib reduced their adhesion rates (Sadeghi et al. 2020; W. Wu et al. 2021). Such cells also happen to be sensitive to ibrutinib-induced cell death, suggesting that adhesion impairment is one of the mechanisms of ibrutinib action - a hypothesis supported by clinical evidence (Chang et al. 2013) (see *BCR signaling*).

Stromal support

Once in the lymphoid tissues, lymphoma cells may receive multiple proliferation and survival signals from the surrounding cells. In physiological settings, adhesion-activated FAK was shown to contribute to cell cycle progression through direct regulation of the *CCND1* promoter (Zhao, Pestell, and Guan 2001). However, in MCL this effect may be negligible, as the *CCND1* promoter is already constantly active. CXCL12, either added externally or secreted from the stromal cells in a co-culture setting, was shown to induce FAK phosphorylation and downstream activation of PI3K/AKT (Balsas et al. 2017; Rudelius et al. 2018), ERK1/2 (Kurtova et al. 2009; Balsas et al. 2017; Rudelius et al. 2018) and Nf-κB pathways, leading to increased proliferation of MCL cells (Balsas et al. 2017). Another study demonstrated that interactions with the stromal cells supported long-term expansion of MCL cells *in-vitro*, inhibiting spontaneous apoptosis and activating the canonical and non-canonical Nf-κB signaling (Medina et al. 2012). This activation was dependent on the B-cell activation factor (BAFF) secreted by the mesenchymal cells, as addition of the decoy BAFFR-Fc receptor to the system abrogated the effect (Medina et al. 2012). Finally, adhesion may produce long lasting pro-survival effects through epigenetic reprogramming. In MCL cell lines, adhesion to stromal cells induced the expression of histone demethylase KDM6B, which was accompanied by the reduction in the repressive H3K27me3 marks and the increase in the activating H3K27me3 marks at the promoters of the NF-κB encoding genes (Sadeghi and Wright 2023).

Pro-survival and anti-apoptotic signaling activated upon adhesion, as well as possible mechanical protection, contribute to the widespread phenomenon of cell

adhesion-mediated drug resistance (CAM-DR), described for many tumors, including MCL. Co-culture with the stromal cells reduced the sensitivity of MCL cell lines and primary cells to doxorubicin, bortezomib or fludarabine (Medina et al. 2012; Balsas et al. 2017). Adherent MCL cells demonstrated very low to no response to chemotherapeutic agents, while the non-adherent MCL cells in the same co-culture had an intermediate resistance phenotype (Medina et al. 2012). This suggested that while both soluble and adhesion-dependent factors contributed to the drug resistance, a dominant role belonged to the adhesion-mediated signals. In line with this data, another study was able to overcome the chemotherapy resistance of MCL cells *in-vitro* by simultaneous blockage of CXCR4 and VLA-4, but this blockage was no longer effective once the MCL cells adhered to the stroma (Y.-R. Kim and Eom 2014), highlighting the importance of the early prevention of MCL cell migration and dissemination and the necessity to target the downstream effectors in the already adherent cells. For example, inhibition of FAK helped overcome ibrutinib (Rudelius et al. 2018) and bortezomib (Balsas et al. 2017) resistance in the MCL cells co-cultured with the bone marrow stem cells. Of note, CAM-DR was shown to be more pronounced in SOX11+ MCL cells due to the direct upregulation of CXCR4 and FAK expression by SOX11 and subsequent activation of the FAK/PI3K/AKT pathway (Balsas et al. 2017). SOX11 knockdown reduced the adhesion rates of MCL cell lines and counterbalanced the protective effect of the bone marrow stromal cells upon doxorubicin treatment (R. Yang et al. 2020).

Immune cells in the MCL microenvironment

A pivotal role in the tumor-microenvironment interactions belongs to the immune cells, which not only orchestrate the anti-tumor immunity through surveillance and cytotoxic activity but also, in certain cases, can paradoxically exert pro-tumorigenic signaling, fostering tumor growth and progression.

CD4+ and CD8+ T-cells play a central role in the cell-mediated anti-tumor immune response. CD8+ T cells recognize the antigens on the MHC-I class molecules of the tumor cells and exert a direct cytotoxic effect against the tumor. Meanwhile, CD4+ cells recognize the MHC-II-associated antigens on the antigen-presenting cells and can either stimulate or suppress the activity of the effector cells, e.g. CD8+ T, NK and macrophages, depending on the microenvironmental signals. Moreover, CD4+ T cells can serve as antitumor effector cells on their own, either through a direct cytotoxic activity against the MHC-II-positive tumors or by emitting the effector cytokines (e.g. IFN γ and TNF), that negatively affect both the tumor and the stromal compartments (reviewed in (Speiser et al. 2023)).

MCL cells express high levels of both class I and II MHC molecules (Khodadoust et al. 2017), and can thus be targeted by both CD8+ and CD4+ T-cells. High counts of CD4+ (Nygren et al. 2014; X.-Y. Zhang et al. 2016) and CD8+ (Nygren et al. 2014) T cells in the tumor infiltrate and peripheral blood of MCL patients predict positive outcomes (Nygren et al. 2014; X.-Y. Zhang et al. 2016), while reduced expression of the

transcripts related to T-cell costimulation and receptor signaling is associated with poor overall survival (Balsas et al. 2021). Of note, high CD4⁺ count is a more significant predictor of favorable OS than CD8⁺ count, and high CD4:CD8 ratio is associated with good prognosis independent of other risk-defining prognostic factors (Nygren et al. 2014; X.-Y. Zhang et al. 2016), suggesting a prevalent role of the CD4⁺ T lymphocytes in anti-tumor immunity. A possible explanation for this phenomenon comes from the genomic and proteomic MHC-profiling of MCL cells (Khodadoust et al. 2017). This study revealed that the lymphoma-specific neoantigens detected in MCL patients were presented almost exclusively on MHC-II (Khodadoust et al. 2017). Remarkably, all of those neoantigen peptides came from the somatically mutated variable regions of 13 immunoglobulin genes (Khodadoust et al. 2017). Among all the other genes bearing somatic coding mutations, 46% were represented by at least one peptide on either MHC-I or MHC-II molecule, but all of those peptides were derived from the non-mutated gene regions (Khodadoust et al. 2017). Low presentation of the mutated antigens as MHC epitopes was described for other hematological malignancies (Berlin et al. 2015; Kowalewski et al. 2015) and may represent one of the mechanisms of tumor immune-escape; nevertheless, one can not exclude that their absence is due to the technical limitations of the methods that are yet unable to detect the rare epitopes. Similarly, it is not clear whether the confinement of the MCL-specific epitopes to the Ig genes reveals the true biology or a methodological constraint. Regardless, Ig-derived neoantigens bear potential for MCL immunotherapy, as isolated circulating CD4⁺ cells specific for the Ig-derived neoantigens were capable of killing the autologous lymphoma cells (Khodadoust et al. 2017).

Unfortunately, certain CD4⁺ T cell subtypes have also been found to promote tumor persistence and growth. One example is regulatory T cells (T_{Regs}), which are essential for maintaining peripheral tolerance and preventing autoimmunity, but, on the other hand, are known to limit the antitumor immune response through cytotoxic T cell, NK and dendritic cell inhibition (Togashi, Shitara, and Nishikawa 2019). In mantle cell lymphoma, the balance between different CD4⁺ T cell populations was shown to be affected by the SOX11 status of the tumors. While the expression of SOX11 was positively correlated with both the CD4⁺ and CD8⁺ inflammatory infiltrate (Annese et al. 2020), SOX11-positive tumors exhibited reduced expression of the genes involved in T-cell related antitumor activity compared to their SOX11-negative counterparts (Balsas et al. 2021). On the contrary, SOX11⁺ tumors were characterized by an increased proportion of intratumoral T_{Reg} cells with an immunosuppressive role (Balsas et al. 2021). Such imbalance in the SOX11⁺ MCL microenvironment may be linked to the overactive CD70-CD27 co-stimulatory pathway that promotes T_{Reg} proliferation. SOX11 was shown to bind upstream of the *CD70* TSS and SOX11-positivity was strongly associated with high CD70 expression. In turn, high CD70, was associated with reduced overall patient survival independently of the other high-risk features (Balsas et al. 2021). Of note though, the effect of SOX11 on the overall T-cell counts in the MCL TME are conflicting, one study reporting a

positive correlation between the SOX11 expression and T-lymphocytes infiltration (Annese et al. 2020), and another one showing the lower T cell counts in the SOX+ vs SOX11- MCL tumors (Balsas et al. 2021).

Another type of CD4+ T cells with a potential pro-lymphomagenic effect are follicular helper T cells (T_{FH}). These cells provide co-stimulation to the B cells in the germinal center *via* the co-stimulatory molecule CD40 interacting with CD40-ligand (CD40-L) on the B cell, and are crucial for the germinal center formation. While this cross-talk is necessary for an effective antibody-mediated immune response, it may have a flip-side function, providing proliferation signals for B-cell lymphomas, notably those arising from the germinal center, e.g. follicular lymphoma (Epron et al. 2012) and GC B cell-diffuse large B cell lymphoma (GC-DLBCL) (Suzuki, Nozawa, and Abe 2004). *In vitro*, mantle cell lymphoma cells proliferate in response to externally added CD40L (Castillo et al. 2000; Andersen et al. 2000). Nevertheless, it is unlikely that such stimulation is prevalent *in vivo*, as CD40L only activates the B cells presenting the antigen recognised by a corresponding activated CD4+T cell, and most of the MCL cells are considered antigen naive. Also, except for the non-nodal MCL forms, MCL are thought not to enter the GC (**Figure 4**).

Apart from the cytotoxic T cells, other effector cells have been studied in the context of the MCL TME. *Natural Killer (NK) cells* recognize stressed cells, such as infected or tumor cells, and exhibit their cytotoxic activity through the release of cytolytic granules and cytotoxic cytokines (Prager and Watzl 2019). NK activation depends on the integrated signal from their germline-encoded activating and inhibitory receptors. Activating receptors recognize antibody-coated cells or host gene-encoded ligands induced by the cell stress pathways, while inhibitory receptors recognize MHC-I molecules and protect the potentially normal cells from killing, though the inhibition may be overcome by strong activation (Wolf, Kissiov, and Raulet 2023). Among others, NK cells can be activated in response to lipid-based antigens presented in the context of an MHC-I-like molecule CD1d (Rossjohn et al. 2012). MCL tumors were shown to have elevated levels of sphingosine-1-phosphate (S1P) (M. S. Lee, Sun, and Webb 2020), a signaling lipid regulating multiple processes in the vascular and immune system best known for its role in T-cell trafficking (Mandala et al. 2002). S1P was shown to interfere with the CD1d-mediated NK cell activation by target cells, while blocking either S1P production or signaling could restore the NK response to MCL cells *in vitro* (M. S. Lee, Sun, and Webb 2020). Of note, pharmacological inhibition of S1P receptors also resulted in the time- and dose-dependent cytotoxicity in MCL cells (Q. Liu et al. 2010), though the effect was only demonstrated *in vitro* and in an immunodeficient xenograft model, and was thus independent of NK activity.

Though in one study the numbers and repertoire of the NK cells in MCL patients were shown to be similar to that of healthy donors (Flinsenbergh et al. 2020), low absolute counts of NK cells in peripheral blood of MCL patients were associated with

inferior survival (Zhou et al. 2019). Thus, mobilizing NK in the MCL therapeutic context might be a plausible strategy. Phase 1 clinical trial exploring the effects of an *ex vivo*-expanded allogeneic natural killer cell MG4101 combined with rituximab in relapsed/refractory B Cell Non-Hodgkin Lymphoma, including two MCL patients, demonstrated a very favorable safety profile and a potentially synergistic action of the combination, though only one MCL patient achieved partial response (Yoon et al. 2023). Some of the already approved drugs were shown to modulate the NK activity in the MCL context. Lenalidomide, a drug demonstrating clinical benefit for patients with relapsed and refractory MCL (Goy et al. 2013), caused a 10-fold increase in NK cells in MCL-bearing SCID mice (L. Zhang et al. 2009); similarly, a significant increase in NK cells relative to total lymphocyte count was observed in MCL patients who responded to lenalidomide if compared to non-responders (Hagner et al. 2017). Preclinical experiments with MCL cell lines revealed that lenalidomide increased lytic immunological synapse formation and secretion of granzyme by NKs, thus enhancing their cytotoxicity against MCL cells (Hagner et al. 2017). On the other hand, one of the most widely used anti-MCL drugs ibrutinib was shown to negatively affect the NK effector functions (Flinsenberget al. 2020). NK-cell activation and target cell killing were suppressed by ibrutinib *in-vitro* and in the cells from MCL patients examined before and after ibrutinib treatment, while the repertoire and numbers of NK cells were not affected following therapy (Flinsenberget al. 2020). This effect was likely due to the off-target inhibitory activity of ibrutinib against IL-2-inducible kinase (ITK) (Dubovsky et al. 2013) positively regulates the effector activity of NK cells, stimulating their degranulation (Khurana et al. 2007; Flinsenberget al. 2020).

Tumor-associated macrophages (TAMs) are another cell type found in MCL lymph-nodes (Song et al. 2013; Pham et al. 2015; Le et al. 2021). Macrophages circulate in the blood in the form of monocytes and differentiate into mature forms following extravasation. Both monocytes and macrophages express high levels of chemokine receptor CCR1 and migrate in response to its ligand CCL3 (Le et al. 2023). The serum of untreated MCL patients, as well as conditioned mediums from MCL cells, have increased soluble CCL3 levels (Sonbol et al. 2014; Le et al. 2023), which favors monocyte/macrophages migration towards MCL TME (Le et al. 2023). Depending on the signals emitted by the host tissue microenvironment, macrophages can adopt one of the two polarization states known as M1 ("classically activated") and M2 ("alternatively activated"). M1 macrophages are typically activated by IFN- γ or lipopolysaccharide (LPS) and play a classic pro-inflammatory role, producing cytokines and microbicidal agents, phagocytizing microbes and initiating immune response. In contrast, M2 macrophages are mainly involved in tissue repair and wound healing. They are activated following exposure to certain cytokines, e.g. (TGF)- β , IL-4, IL-10, or IL-13, and produce prolines and polyamines that induce collagen production and cellular proliferation. M2 macrophages inhibit inflammation and promote angiogenesis. While those functions are essential for repairing tissues, within the tumor microenvironment, they can be hijacked to promote tumor nutrition, growth and immune evasion. MCL cells were shown to shift the

macrophages polarization towards the M2 phenotype in both co-culture and xenograft systems (Le et al. 2021; 2023). This shift was dependent on the CCL3/CCR1 axis, as CCR1^{-/-} macrophages did not exhibit a similar response under the same conditions (Le et al. 2023). Macrophages affected by MCL cells increased their secretion of IL-10, a cytokine associated with an M2 phenotype (Le et al. 2023). In turn, IL-10 stimulated the proliferation of MCL cells *via* IL-10R α - STAT1 pathway (Le et al. 2021). Moreover, increased STAT1 binding to the CCL3 promoter region further upregulated the CCL3 expression by MCL cells, initiating a vicious positive-feedback loop attracting more macrophages to the site (Le et al. 2023).

Increased number of TAMs were associated with high Ki67 index (Philippa Li et al. 2021) and inferior OS of MCL patients (Philippa Li et al. 2021; Rodrigues et al. 2021) and was also negatively correlated with high SOX11 expression (Annese et al. 2020). Nevertheless, in the studies where both M1 and M2 macrophages were tracked, there was no clear association between the OS and macrophage polarization state, both M1 and M2 type macrophages being increased in high-proliferative tumors (Philippa Li et al. 2021). Consistently, in a syngeneic mouse model of MCL, M1 and M2 macrophages were roughly equally present in the dissected tumors (Le et al. 2021), while in clinical samples M1 macrophages were prevailing with an M1:M2 ratio close to 3:1 (Philippa Li et al. 2021). Thus, though high TAM infiltration is clearly an indicator of poor prognosis, no strong conclusions can be yet made regarding the contribution of each macrophage type to the tumor microenvironment. It is yet promising to target the macrophage population in MCL TME to counterbalance some of the known pro-tumorigenic effects of TAMs. Attempts have been made to target TAM accumulation in the MCL context. In a syngeneic mouse model of MCL, blockade of CCR1 significantly reduced the levels of M2-TAMs and the overall tumor burden (Le et al. 2023). Similar effect was achieved by macrophage depletion with Clodrosome in a xenograft mouse model of MCL. Tumors established following the injection of MCL cells together with human CD14⁺ monocytes were reduced after Clodrosome treatment, and the reduction in both the total and M2-type macrophages was observed within the tumor sections (Le et al. 2021).

Follicular dendritic cells (FDCs) are antigen-presenting cells of stromal origin that reside in primary follicles and germinal centers of secondary and tertiary lymphoid organs. With their long intermingled dendrites, FDCs form tight networks throughout the follicle. They also retain and concentrate the antigens and produce the factors controlling B cell survival, allowing for an efficient germinal center reaction : antigen-activated B cells are retained in the FDC nets and undergo clonal expansion (Heesters, Myers, and Carroll 2014). A clinicopathological study revealed two distinct FDC patterns in the MCL lymph node biopsies: a diffuse pattern (17 cases) and the nodular pattern, resembling that of the normal primary follicles (72 cases) or that of a colonized germinal center (1 case) (Schrader et al. 2006). The patients with the primary follicle- like pattern had a significantly better outcome than those with the two other patterns (Schrader et al. 2006). Another study explored the degree of

overlap of lymphoma cells, defined as the percentage of the total number of lymphoma cells found in the FDC meshwork (Hou et al. 2018). The patients with the higher degree of overlap had a better clinical prognosis (Hou et al. 2018). All together, these data suggest that the FDC histological patterns may be used as a prognostic factor for patient stratification.

TME composition and treatment response

The composition of the TME may significantly affect the response of MCL to treatment. A recent transcriptomic profiling of the MCL tissue biopsies revealed four distinct subtypes of the MCL TME (Jain et al. 2023). The lymph-node like subtype was enriched for the components of the normal lymph node, e.g. CD4+ T-cells, follicular dendritic cells (FDC), T-follicular helper cells (TFH) cells, and lymphatic endothelium. The immune-enriched subtype was characterized by high-level expression of the immune and checkpoint molecules and low stromal expression. Mesenchymal subtype showed increased stromal signature and tumor-promoting cytokines. Finally, the immune-depleted subtype presented with the lowest expression of the immune cell signatures and possessed the highest content of malignant B cells. This immune-depleted subtype was associated with poor patient outcomes and resistance to BTK inhibitors, such as ibrutinib (Jain et al. 2023). Inversely, the patients with the immune-enriched TME subtype tended to be sensitive to the inhibitors of BTK (Jain et al. 2023). Longitudinal single-cell profiling of ibrutinib-responsive and non-responsive MCL patients at baseline, during treatment and/or at disease remission/progression provided further evidence in favor of immune depletion-associated ibrutinib resistance (Shaojun Zhang et al. 2021). This study demonstrated a substantial reduction in the proportion of effector CD8+ T cells in the peripheral blood of non-responders, whereas there was a dynamic increase in the proportion of these cells in responsive patients throughout the therapy. On the other hand, the non-responders exhibited increased communication between the MCL cells and certain cells of the microenvironment, including CD4+, CD8+ T cells and monocytes, *via* the galectin-1->CXCR4/CD69, and TGF- β 1->CXCR4 ligand receptor-based interactions (Shaojun Zhang et al. 2021). CXCR4 axis is known to promote tumor invasion, metastasis and therapeutic resistance (Shunshun Bao et al. 2023). CD69 is expressed on activated T cells, and its interaction with galectin suppresses their differentiation towards the T helper 17 (Th17) phenotype, representing an anti-inflammatory mechanism critical for T cell homeostasis and peripheral tolerance (de la Fuente et al. 2014). Nevertheless, the same mechanism may hamper the anti-tumor immune response in the pathological context.

All together, the tumor microenvironment is a critical determinant of lymphoma progression, behavior and therapeutic response. Understanding the complex interactions within the MCL TME is essential for developing targeted therapies that disrupt supportive signals within the tumor microenvironment and improve treatment outcomes for MCL patients.

1.1.3. Diagnosis, screening and prevention

1.1.3.1. Diagnosis

Mantle cell lymphoma is clinically and biologically heterogeneous, ranging from indolent cases that do not require therapy for years to highly proliferative blastoid variants with very limited prognosis (Jain and Wang 2019; Silkenstedt and Dreyling 2023). In $\frac{2}{3}$ of cases, it is diagnosed at an advanced stage, and typically manifests with lymphadenopathy, splenomegaly and extranodal localization with the bone marrow infiltration. Extra-nodal involvement is observed in 90% of the cases and can involve bone marrow (53-82%) or digestive tract (20-60%) (Silkenstedt and Dreyling 2023). The presence of polypous lymphomatosis highly suggests the disease. Constitutional symptoms such as fever and night sweats are not frequent at diagnosis (approximately 30% of cases) (Jain and Wang 2019). The spleen is enlarged in 40% of patients, which is generally associated with a leukemic manifestation and indolent course of the disease (Silkenstedt and Dreyling 2023).

Diagnosis and staging of MCL involves a combination of clinical evaluation, imaging (CT and PET scan) and laboratory analysis. Imaging evaluates the lymph node structures and the size of the spleen. The definitive diagnosis of MCL is given based on cytological, cytogenetic and histopathology laboratory analyzes from the biopsy of tumor tissue (nodal MCL) and/or circulating tumor cells in the blood (non-nodal leukemic MCL). MCL cells are typically positive for the general B-cell markers (CD20, CD19, CD22), negative for CD23 and CD10, and frequently express some specific abnormal markers suggesting of lymphoma, such as CD5 and FMC7 (Alaggio et al. 2022; Silkenstedt and Dreyling 2023). The presence of the t(11;14)(q13;q32) translocation or, in rare cases, other translocations involving the recombination of CCND1, CCND2 (12p13) or CCND3 (6p21) loci with the IGH, IGK (2p11) or IGL (22q11) loci, is the strongest indicator of the disease (Alaggio et al. 2022). Histologically, nodal mantle cell lymphoma (MCL) is characterized by disrupted nodal architecture and abnormal cellular proliferation within the mantle zone of lymph node follicles.

Following diagnosis, a patient is usually given a prognostic index to assess the appropriate treatment strategies. MIPI (Mantle Cell Lymphoma International Prognostic Index) is the most commonly used prognostic index for MCL. It integrates four clinical parameters: age, Eastern Cooperative Oncology Group (ECOG) performance status, lactate dehydrogenase (LDH) level, and leukocyte count (Hoster et al. 2008). An enhanced version of MIPI - MIPIb (biological MIPI) - additionally takes into account the Ki-67 proliferation index obtained from the lymphoma-rich areas on tissue biopsies not involving the bone marrow (biological MIPI) (Hoster et al. 2008).

1.1.3.2. Screening and prevention

Unlike some other cancers, there is currently no recommended screening test for MCL in the general population. The disease is infrequent and this is rare for patients to present early symptoms that could justify earlier therapeutic intervention and screening efforts. Some studies demonstrated association between lymphoma and

exposure to certain toxic agents including herbicides (Hardell et al. 2023). Prevention and protection measures against toxic agents are essential in exposed populations. Research on screening efforts in these at-risk populations could be useful for further screening considerations.

A family history of hematopoietic malignancies has been associated with a 2-fold increased risk of NHL, including MCL (S. S. Wang et al. 2007). Several factors may contribute to the observed familial aggregation, including inherited genetic susceptibility and shared environmental exposures among family members. Since individuals with a family history of lymphoma may have an increased risk of developing the disease, more vigilant monitoring or further evaluation in the event of symptoms among related individuals may be recommended (Y. Wang and Ma 2014b).

1.1.4. Management

MCL has long been considered an incurable disease with an unsatisfactory response to R-CHOP treatment. Nevertheless, this perception is now being revised with the significant and successive therapeutic advances since the 2000s. The introduction of anti-CD20 immunotherapy, autologous peripheral stem cell transplantation, cell therapies, BTK and BCL-targeted therapies and effective intensive chemotherapies based on cytarabine and platinum salts (Mcl-younger trial, LyMa or Nordic regimens) has significantly improved the survival and prognosis of MCL patients (Geisler et al. 2008; Advani et al. 2013; Hermine et al. 2016; Le Gouill Steven et al. 2017; Tessoulin et al. 2021). In young subjects treated with curative intent, prolonged and event-free remissions with follow-up of more than 10 years are now observed, setting a goal towards full curability of the disease in this patient group.

1.1.4.1. Front-line treatment

The first step is to determine whether to treat the patient and when to begin treatment. For patients with indolent MCL (10 to 15% of cases), therapeutic abstention or monitoring may be appropriate. Localized MCL may be effectively treated with radiotherapy, although this type of MCL is extremely rare and the identification of this disease group remains debatable. For the rest of MCL patients with a typical non-indolent disease, first-line treatment is tailored based on the patient's age and the presence of comorbidities (Jain and Wang 2019; Silkenstedt and Dreyling 2023; Zelenetz et al. 2023). Standard initial treatment usually involves immunochemotherapy combining anti-CD20 antibodies (e.g. rituximab) with the chemotherapeutic agents. The dose intensity of the chemotherapy is adjusted according to the patient's age and health conditions.

For young patients (under 65 years old) eligible for intensive regimens, the treatment is based on aggressive induction therapy regimen alternating anthracycline-based and platinum/aracytin-based immunochemotherapy such as LyMA regimen (Le

Gouill Steven et al. 2017; Hermine et al. 2016) or Nordic trial regimen (Geisler et al. 2008). If the disease is chemosensitive, treatment is intensified with high-dose chemotherapy and autologous stem cell transplant (ASCT), followed by anti-CD20 maintenance therapy for three years (Le Gouill Steven et al. 2017; Hermine et al. 2016). Additionally, the recent results of the TRIANGLE trial in patients aged 18-65 y.o. demonstrated the beneficial effect of adding a BTK inhibitor ibrutinib to the induction and maintenance therapy with rituximab (Dreyling et al. 2024). This option is now being considered as a variant of first line therapy in the NCCN US guidelines.

For elderly patients (> 65 years old) or patients otherwise unfit for high-dose chemotherapy, the treatment is based on the less aggressive induction therapy such as R-CHOP (rituximab, cyclophosphamide, doxorubicin, vincristine, prednisone) immunochemotherapy followed by maintenance treatment with rituximab (H. C. Kluin-Nelemans et al. 2012). Rituximab with bendamustine could be an alternative option in fragile patients for whom chemotherapy with R-CHOP is deemed to be toxic (Silkenstedt and Dreyling 2023; Jain and Wang 2019). Other regimens such as VR-CAP (bortezomib, rituximab, cyclophosphamide, doxorubicin, and prednisone) (Robak et al. 2018) or R-GemOx (rituximab, gemcitabine, oxaliplatin) (Obrador-Hevia et al. 2016) could be proposed, especially when anthracycline is contraindicated. Even less aggressive therapy options without chemotherapy include rituximab-lenalidomide (Ruan et al. 2018) or rituximab-acalabrutinib (Zelenetz et al. 2023). Rituximab maintenance after R-CHOP was shown to be beneficial and superior to the interferon alfa maintenance in the European MCL elderly trial (H. C. Kluin-Nelemans et al. 2012), with the demonstrated safety of prolonged rituximab usage until progression (Hanneke C. Kluin-Nelemans et al. 2020). The feasibility of rituximab maintenance after bendamustine-rituximab treatment has also been validated in the SHINE trial (M. Wang et al. 2022) with a good safety profile. Nevertheless, although the experimental arm of this trial combining bendamustine, rituximab and ibrutinib (BRI) reached its primary objective (benefit in PFS of BRI compared to bendamustine rituximab alone), it did not convert to a benefit in OS and the results were judged not convincing enough to consider the BRI a first-line therapeutic option for elderly patients.

1.1.4.2. Relapse and refractory disease treatment

BTK inhibitors

Covalent BTK inhibitors (ibrutinib, acalabrutinib, zanubrutinib) are generally used in cases of relapse or refractory MCL (Silkenstedt and Dreyling 2023; Zelenetz et al. 2023). Their safety profile is now well known and the cardiac toxicity has to be tightly monitored, especially in elderly population. Apart from experiencing the dose-limiting toxicity, many patients ultimately cease to respond, frequently due to mutation in the C481 residue of BTK, which is currently targeted by all of the covalent BTK inhibitors available in clinics.

Noncovalent BTK inhibitors have been developed with the aim to limit the off-target

toxicity and preserve the efficacy in the patients with the C481 mutation. In 2023, A highly-selective non-covalent BTK inhibitor pirtobrutinib has gained accelerated FDA approval for use in patients with relapsed/refractory MCL following the subset analysis of the phase I/II BRUIN study (Mato et al. 2021; Telaraja et al. 2024). Currently, pirtobrutinib is considered for use after the failure of covalent BTK inhibitors (M. L. Wang et al. 2023), and the existing NCCN guidelines on the up-front BTK inhibitor usage are likely to change in the coming years to suggest an earlier introduction of pirtobrutinib in the treatment strategy.

Alternative agents targeted at BTK proteolytic degradation rather than its kinase activity are now being developed and may increase the benefit-risk ratios of targeting BTK in MCL in the years to come (Nawaratne et al. 2024).

BCL2 inhibitors

The oral BCL-2 inhibitor venetoclax produces prolonged antitumor responses in MCL relapse or refractory patients (Davids et al. 2021) and can be combined with ibrutinib. The potential benefit of venetoclax combined with ibrutinib is currently being examined in a phase-3 SYMPATICO study (NCT03112174) in relapsed MCL (M. Wang et al. 2021). Other BCL-2 inhibitors are also being assessed in MCL in combination with BTK inhibitors (L.-L. Lee et al. 2023; Guangzhou Lupeng Pharmaceutical Company LTD. 2023).

Cellular therapies

CAR T-cells directed against CD19, e.g. brexucabtagene autoleucl (M. Wang et al. 2020), and lisocabtagene maraleucl (M. Wang et al. 2024), showed promising efficacies in relapsed or refractory mantle cell lymphoma. Updates of the long-term follow-up of patients treated with CAR-T for relapse or refractory MCL are awaited to know the durability of the responses.

Immunomodulatory agents

Lenalidomide, an immunomodulatory drug with antiproliferative and immunological effects, showed meaningful activity in relapsed or refractory mantle cell lymphoma (Trněný et al. 2016).

PI3K – mTOR pathway inhibitors

The first targeted therapy approved in mantle lymphoma was an mTORC1 inhibitor temsirolimus, though in the current therapeutic landscape the benefit risk ratio of the drug has to be updated (Freeman et al. 2022). Several other targeted therapies addressing the PI3K/AKT pathway have been developed, including piasclisib. Parasclisib specifically targets the PI3K delta subunit, which potentially reduces the off-target effects associated with PI3K/AKT targeting drugs (Zinzani et al. 2023). However, blocking the PI3K/AKT pathway is still associated with various toxicities, particularly infections. Therefore, the risk/benefit ratio of using treatments targeting the PI3K/AKT pathway in MCL remains unclear.

1.1.4.3. New targets and emerging therapies

Bispecific CD20 x CD3 immunotherapies

CD20XCD3 bispecific antibodies bind to both the CD20 marker present on B cells and the CD3 marker present on T cells, bringing those cells into close proximity and thus facilitating the T-cell mediated killing of malignant B cells. Bispecific antibodies, including glofitamab, mosunetuzumab, epcoritamab, and odronextamab, demonstrated clinical benefit for the patients with several types of relapsed or refractory B cell lymphomas, e.g. follicular lymphoma (Bannerji et al. 2022; Nierengarten 2023) and diffuse large B cell lymphoma (Bannerji et al. 2022; Karimi et al. 2023; Shirley 2023). For mantle cell lymphoma, the benefit of bispecific CD20 x CD3 is currently being explored and demonstrates promising preliminary results with the objective response rate of 50% (Bannerji et al. 2022).

CDK4/6 inhibitors

CCND1 overexpression ultimately leads to the hyperactivation of the CDK4/6 pathway. Thus, some CDK4 and CDK6 inhibitors, such as palbociclib and abemaciclib, have emerged as therapeutic options for relapse or refractory MCL (Morschhauser et al. 2021; Leonard et al. 2012). Notably though, despite a seemingly direct link with the MCL pathogenesis, the objective response rates to CDK4/6 inhibitors as single-agent therapy in MCL patients have been modest (0-23%) (C. Lee et al. 2020).

Receptor orphan tyrosine kinase-like receptor (ROR1)

Zilovetamab vedotin (ZV) is an antibody-drug conjugate that specifically binds to the orphan receptor tyrosine kinase-like receptor (ROR-1), an oncoprotein pathologically expressed in tumor tissues, including mantle cell lymphoma cells (Choi et al. 2015). In a phase 1 study, ZV induced objective tumor responses in 7 of 15 patients with MCL (M. L. Wang et al. 2022).

ATR inhibitors

Ataxia telangiectasia and Rad3-related protein (ATR) is one of the key kinases in the DNA-damage response. Though ATR is not generally altered in MCL, its inhibition was shown to be synthetically lethal in cells with the ATM deficiency (Reaper et al. 2011). *ATM* is the gene most frequently mutated in MCL. Single-agent ATR inhibitors have therapeutic utility in the treatment of cancers, like MCL, in which ATM function has been compromised or lost (Menezes et al. 2015).

Epigenetic modifiers

As both genetic (chromosomal aberrations, CNV, mutations) and epigenetic (modification of DNA methylation, histone modification distribution pattern, changes in 3D genome organization) changes are present in MCL, epigenetic drugs can be potentially used in treatment. Recently developed epigenetic drugs include those targeting DNA and protein methyltransferases, histone deacetylases, and chromatin modifiers (Rosenthal, Munoz, and Villasboas 2023) (**Table 2**).

Table 2. Epigenetic therapies for MCL

Inhibitor class	Molecules	Monotherapy	Combination therapy
DNMT	azacitidine decitabine	no results	<i>no published results</i> MGCD0103+azacitidine (NCT00543582)
			<i>no published results</i> decitabine+valproic acid (NCT00109824)
EZH2	XNW5004 tazemetostat	<i>Ongoing phase I trial</i> XNW5004	
		<i>Ongoing phase I trial</i> tazemetostat (NCT03010982; NCT03028103)	
HDAC	vorinostat; abexinostat	<i>no clinical response</i> vorinostat (Ogura et al. 2014)	<i>no clinical response</i> cladribine, rituximab +vorinostat (Spurgeon et al. 2019)
		<i>no clinical response</i> vorinostat (Kirschbaum et al. 2011)	<i>significant toxicity</i> fludarabine, mitoxantrone, dexamethasone + vorinostat (Shin et al. 2016)
		<i>modest activity</i> abexinostat (Evens et al. 2016)	<i>modest activity</i> bortezomib + vorinostat (Yazbeck et al. 2018)

DNA methyltransferases (DNMT) are enzymes that establish the methylation of the CpG dinucleotides and inhibit gene transcription by blocking accessibility to transcriptional activators. Although DNMT inhibitors (azacitidine and decitabine) are approved for treatment for some malignancies, no published record of an effect of these drugs in individuals with MCL exists. Clinical trials involving azacitidine and decitabine in MCL did not provide any results (NCT00543582; NCT00109824).

Enhancer of zeste homolog 2 (EZH2) is a histone-lysine N-methyltransferase that participates in histone H3 methylation at lysine 27, a modification leading to transcriptional repression. EZH2 is expressed in ~40% of primary MCLs; its expression is associated with the aggressive histological variants, high Ki-67 index

and inferior overall survival of MCL patients (Martinez-Baquero et al. 2021). Phase I clinical study of EZH2 inhibitor (XNW5004) in B cell lymphoma, including MCL is under way (Weiwei et al. 2022). An oral EZH2 inhibitor tazemetostat (EZM6438) is also in phase I trial for MCL (NCT03010982; NCT03028103). Another EZH2 inhibitor OR-S1 shows activity in an MCL xenograft model (Kagiyama et al. 2021). Combination of EZH2 inhibitor tazemetostat with ibrutinib or zanubrutinib showed synergistic activity in the drug-resistant MCL xenograft model (Keats et al. 2021).

Histone deacetylases (HDACs) catalyze the removal of the activatory acetyl groups from histones and other protein regulatory factors. Vorinostat, a first-generation HDAC inhibitor, was not efficient in monotherapy for MCL patients (Kirschbaum et al. 2011; Ogura et al. 2014) and showed a modest clinical activity (bortezomib+ vorinostat) (Yazbeck et al. 2018) or high toxicity (fludarabine, mitoxantrone, dexamethasone + vorinostat) (Shin et al. 2016) when used in combination therapy. Another pan-HDAC inhibitor Abexinostat showed modest activity as a monotherapy (Evens et al. 2016) and is now being studied in combination with ibrutinib (NCT03939182). Fimepinostat, romidepsin and belinostat also demonstrate promising results in a xenograft model of MCL alone or in combination with other drugs (Paoluzzi et al. 2010; H. Guo et al. 2019).

Other potential targets of epigenetic drugs in MCL include protein arginine methyltransferase 5 (PRMT5) that plays a role in the epigenetic and post-translational modification of cell cycle regulators and is overexpressed in MCL (Che et al. 2023; Sloan et al. 2023). An oral PRMT5 inhibitor PRT343 is currently being tested in a phase 1 clinical trial (NCT03886831) on relapsed patients with MCL and other malignancies. Targeting PRMT5 with GSK3326595 in xenografts derived from patients with MCL provided a therapeutic benefit (Sloan et al. 2023). At the same time, the use of PRMT5 inhibitors in MCL may lead to acquired resistance (Long et al. 2023).

1.1.5. Outlook

Toward personalized treatment: stratified at-risk disease approaches

Prognostic indices, both at baseline and minimal residual disease (MRD) status during or after induction therapy, are expected to guide therapeutic decisions, facilitating personalized treatment strategies based on individual risk profiles. Currently, the primary factor influencing the choice between intensive and non-intensive chemotherapy for initial treatment is the patient's age and comorbidities. However, more personalized therapeutic approaches should be developed, stratified based on baseline prognostic risk factors or molecular abnormalities. For instance, patients with *TP53* mutations might benefit most from therapies targeting BTK and BCL2, as well as CAR-T cell therapy, though this hypothesis needs validation through large clinical trials. Preliminary results from the TRIANGLE trial (Dreyling et al. 2024) suggest that ibrutinib, in combination with chemoimmunotherapy and maintenance therapy, could significantly impact treatment outcomes, particularly in younger patients. It is crucial to assess this

impact within the TP53-mutated subgroup. Consequently, the role of high-dose therapy (HDT) may need to be reevaluated for this patient population.

Clarifying the molecular origins of the disease

Understanding the genetic and epigenetic alterations that underlie the development and/or proliferation of mantle cell lymphoma (MCL) remains a major challenge. Clarifying the pathophysiological mechanisms of the disease remains crucial for advancing drug research and improving patient care. The epigenetic field, in particular, holds significant promise for innovative research and new MCL treatments. Nonetheless, the epigenetics of MCL remains poorly studied and there are currently no epigenetic modifier treatments available for MCL.

Reducing the global burden of disease and therapy toxicity

The burden of MCL is primarily driven by disease symptoms and secondarily by the toxicity of treatments, both short- and long-term. Reducing therapy toxicity while maintaining or improving disease control is an ongoing challenge. Introducing BTK-targeted treatments in front-line MCL therapy could potentially reduce the toxicity associated with intensive chemotherapies, for example if the ASCT could be omitted when the BTK-inhibitors are added. This question is currently being investigated in the TRIANGLE trial (Dreyling et al. 2024). Notably, the treatments that do not involve chemotherapy, e.g. targeted therapies and immunotherapies, are also not devoid of short- and long-term toxicities. Quality of life and patient-reported outcome (PRO) studies will be essential for capturing data on these toxicities from the patient's perspective, providing a more comprehensive understanding of the impact of these treatments on patient well-being.

1.2. Enhancers and superenhancers

Establishment of unique patterns of gene expression during development and differentiation is orchestrated by enhancers, DNA regulatory elements that distantly activate gene transcription. The first enhancer was identified in 1981 in the SV40 genome (Banerji, Rusconi, and Schaffner 1981; Benoist and Chambon 1981) and since then, enhancers have been found in all higher eukaryotes. Enhancers are modular elements characterized by their lack of a consensus sequence and variable distance from the transcription start sites of genes. Most enhancers activate transcription regardless of their orientation and position relative to the target gene (reviewed in (Erokhin et al. 2015)).

Superenhancers (SE), regulatory regions of the genome that play a crucial role in controlling gene expression, are formed by clustered enhancers and can span over tens and even hundreds of kilobases. They are characterized by a large size, high density of transcription factors, and specific epigenetic marks. A term “superhancer” was coined in 2013 by Richard Young and co-authors (Whyte et al. 2013) for large enhancer domains that controlled the pluripotent state of cells. Further studies established that SE acted as major amplifiers of gene expression,

often controlling master developmental genes and those involved in specific cell identity. Therefore, they are essential for maintaining cell state and function and are of particular interest in biomedical research for their potential role in gene therapies and disease treatments (reviewed in (Ishov, Gurumurthy, and Bungert 2020)).

1.2.1. Composition of superenhancers

Superenhancers are composed of several key components that contribute to their unique properties and powerful regulatory functions. SEs are formed by the clustering of multiple traditional enhancers. These individual enhancers, when grouped together, create a region with enhanced regulatory capacity compared to single enhancers. Similarly to enhancers, SEs contain a high density of binding sites for transcription factors. These proteins bind to specific DNA sequences within an SE and are critical for initiating and regulating the transcription of target genes. They also include the mediator complex that functions as a bridge between SE-bound transcription factors and the promoters of the target genes. Structural proteins such as CTCF (CCCTC-binding factor) and cohesin that contribute to the three-dimensional organization of the genome are also present at SEs; this helps to bring distant genomic regions into close contact, facilitating the interaction between enhancers and promoters.

Specific histone modifications are hallmarks of active SEs. These include the H3K27ac mark associated with active enhancers and highly enriched at SEs and H3K4me1 often found at SEs (Whyte et al. 2013). SEs are also associated with regions of high transcriptional activity. They facilitate the production of non-coding RNAs, including enhancer RNAs (eRNAs) (Ørom et al. 2010), which can contribute to the regulation of gene expression by various mechanisms, such as altering chromatin structure or recruiting additional regulatory proteins.

1.2.2. Identification of superenhancers

Superenhancers are identified by their elevated enrichment for binding of transcriptional factors and cofactors, such as the bromodomain and extra-terminal domain (BET) family protein BRD4 and Mediator complex subunit 1 (MED1), and/or the presence of the active chromatin marks H3K27ac, H3K4Me1 (Whyte et al. 2013) and H4Ac (Das et al. 2023). The most widely used computational method is the ROSE algorithm (Rank Ordering of Super-Enhancers). This computational tool is widely used to rank enhancers based on ChIP-Seq data (Whyte et al. 2013). The algorithm identifies clusters of enhancers and ranks them by the density of transcription factor binding and histone marks. The highest-ranking clusters are designated as SE.

1.2.3. Superenhancers in normal gene regulation

Superenhancers are instrumental in establishing and maintaining the specific gene expression programs that define different cell types. They control the expression of genes critical for cell type-specific functions, such as insulin production in pancreatic β -cells (Jian and Felsenfeld 2018) or hemoglobin production in erythroid cells (Hay et

al. 2016; Gurumurthy et al. 2021). SEs also participate in lineage specification driving the expression of lineage-specific genes, and thus aiding in the differentiation process from progenitor cells to fully specialized cells (C. Wang et al. 2022). SE may play a role in enabling cells to respond to external signals and changes in their environment, eg. some superenhancers are activated in response to mechanical stress (J. Li et al. 2024). SEs also contribute to the higher-order organization of chromatin as they frequently interact with promoters of target genes in a three-dimensional chromatin space, facilitating efficient transcription. These interactions help form chromatin loops that bring distant regulatory elements into close proximity with their target genes, enhancing transcriptional efficiency (Grubert et al. 2020).

1.2.4. Superenhancers in disease

Cancer

Superenhancers frequently become dysregulated in cancer cells, leading to the sustained activation of oncogenes or other genes promoting tumor survival. For example, in many types of cancer, including lymphoma, superenhancers are found near the *MYC* oncogene, leading to its overexpression (Chapuy et al. 2013) and uncontrolled cell proliferation (reviewed in (Lancho and Herranz 2018)).

Superenhancers can drive the expression of genes that help cancer cells evade immune detection, such as PD-L1 (C. Shi et al. 2023); some of them also regulate angiogenesis (Mushimiyimana et al. 2021), supplying the tumor with necessary nutrients and oxygen. SE play a critical role in maintaining the properties of cancer stem cells, which are a subpopulation of cells within a tumor that have the ability to self-renew and drive tumor growth by controlling the expression of stemness-related genes, maintaining the stem cell-like characteristics of these cells and contributing to cancer progression and resistance to therapy (Dong et al. 2021). In MCL, SEs contribute to cell survival through activation of B cell receptor (BCR) signaling and the IKZF-MYC axis. Inhibiting SEs may help overcome MCL resistance to ibrutinib or lenalidomide (Tsukamoto et al. 2020).

Other diseases

Superenhancers play significant roles in various diseases beyond cancer, primarily through the modulation of gene expression.

In Rheumatoid Arthritis (RA), SEs are involved in the regulation of genes that govern inflammatory responses. For instance, genetic loci linked to RA are often located within or near SE active in immune cells (Vahedi et al. 2015). These regions can enhance the production of pro-inflammatory cytokines and other factors driving the disease. In diabetes, SEs regulate the genes vital for pancreatic β -cell function and insulin production (Jian and Felsenfeld 2018). Malfunctions in these superenhancers can result in reduced insulin secretion and β -cell dysfunction, which are key factors in diabetes development. SEs impact the expression of genes associated with amyloid processing, tau pathology, or neuroinflammation (Peipei Li et al. 2019). Genetic variants within these regions have been linked to an increased risk of

Alzheimer's Disease (Nott et al. 2019). By controlling genes related to lipid metabolism, inflammation, and vascular function, SEs can affect endothelial function, chronic inflammation, and lipid accumulation, all of which are involved in atherosclerosis and congenital heart conditions (J. Li et al. 2024). Finally, SEs regulate some of the genes essential for brain development and synaptic function. Disruptions here can alter neuronal connectivity and signaling, contributing to schizophrenia (Casella, Colantuoni, and Ament 2022).

1.2.5. Superenhancer-targeting drugs

Due to their crucial role in regulating key cancer-related genes, superenhancers represent potential therapeutic targets. SE-targeting drugs typically interfere with the components that bind to SE, disrupting their activity and thereby affecting the expression of the SE-regulated associated genes.

BET inhibitors target bromodomain-containing proteins like BRD4, which bind to acetylated histones within SEs. By preventing BRD4 from binding to these regions, BET inhibitors reduce the expression of SE-driven genes. JQ1 is a small molecule inhibitor that binds to the bromodomains of BET proteins, displacing them from chromatin and downregulating oncogenes like MYC (Lovén et al. 2013). Another BET inhibitor OTX015 (Birabresib) is currently being tested in clinical trials for hematologic malignancies and solid tumors (Lewin et al. 2018). BET proteins can also be targeted by Proteolysis Targeting Chimeras (PROTACs) designed to target specific proteins for degradation by linking them to an E3 ubiquitin ligase. PROTACs targeting BET proteins (such as BRD4) can lead to their degradation and a subsequent decrease in SE activity. ARV-771, a PROTAC that targets BET proteins for degradation, shows promising results in preclinical cancer models (Fiskus et al. 2021).

Cyclin-dependent kinase 7 (CDK7) is involved in the transcription initiation and elongation of SE-associated genes (Chipumuro et al. 2014). CDK7 inhibitors reduce the phosphorylation of RNA polymerase II, leading to a decrease in transcription of SE-driven genes. THZ1, a selective CDK7 inhibitor, has shown efficacy in several cancer cell lines (Chipumuro et al. 2014).

Cyclin-dependent kinase 9 (CDK9) regulates transcription elongation by phosphorylating the carboxyl-terminal domain of RNA polymerase II. CDK9 inhibitors can disrupt the transcription of SE-associated genes by reducing RNA polymerase II phosphorylation. For example, Flavopiridol and Dinaciclib have demonstrated activity against different cancers including hematologic malignancies (reviewed in (Toure and Koehler 2023)).

Abemaciclib, a CDK4/6 inhibitor primarily used in the treatment of breast cancer, has recently been found to affect SEs by increasing the level of the Activator Protein-1 (AP-1) transcription implicated in the SE activity (Watt et al. 2021). Despite its activity in preclinical models (Gelbert et al. 2014), Abemaciclib did not have any

significant effect as a second-line therapy for relapsed MCL (Morschhauser et al. 2021).

Minnelide, a water-soluble derivative of the compound triptolide found in the thunder god vine (*Tripterygium wilfordii*), is a general transcriptional inhibitor and a potent antitumor agent that has shown promising results in targeting SEs in cancer cells (Noel et al. 2020). Triptolide was shown to inhibit CDK7 and XPB subunits of the TFIIH complex (Titov et al. 2011; Manzo et al. 2012) thus disrupting the SE activity. It has passed phase I clinical trial in patients with advanced gastrointestinal cancers (Borazanci et al. 2024) and is now undergoing Phase II in patients with advanced adenocarcinoma of the pancreas (Skorupan et al. 2022).

All these drugs offer a promising avenue for cancer therapy by specifically targeting the regulatory mechanisms that drive the expression of critical genes involved in disease progression by disrupting the function of SE.

1.3. 3D-genome architecture

1.3.1. General principles of the 3D-genome architecture

Chromatin organization within the nucleus is not random. In the 3D nuclear space, chromosomes occupy defined territories conserved across multiple species and taxons (T. Cremer et al. 1982; Zink et al. 1998; A. E. Visser and Aten 1999; Abranches et al. 2000; Parada et al. 2002; Bolzer et al. 2005; Branco and Pombo 2006; Noma et al. 2006; Sehgal et al. 2016). Chromosomes are further organized into active (A) and non-active (B) compartments, with A-compartments being more accessible, gene-dense, transcriptionally active and earlier replicated (Lieberman-Aiden et al. 2009; Pope et al. 2014; C. Y et al. 2018). Active and accessible compartments protrude further into the nuclear interior (C. Y et al. 2018; Su et al. 2020b; Mota et al. 2022b), while inactive compartments are more often localized at the nuclear periphery, close to the nuclear lamina (Kind et al. 2015; Su et al. 2020b). Compartment A and compartment B loci tend to spatially segregate in single cells (S. Wang et al. 2016; Su et al. 2020b), and active compartments also tend to be proximal to the nuclear condensates, such as nuclear speckles (C. Y et al. 2018; Su et al. 2020b), which may represent the driving force for nuclear condensate formation through phase-separation (Schede et al. 2023). At higher resolution, chromosomes are organized into topologically associated domains (TADs) defined by increased intra-domain chromatin contacts (Dixon et al. 2012) and believed to coordinate the interactions between promoters and their *cis*-regulatory elements (Lupiáñez et al. 2015). Highly transcribed gene-dense regions can also extrude from their chromosome territories to form *interchromosomal* contacts (ICCs) (Mahy, Perry, and Bickmore 2002; Su et al. 2020b), which are though much less studied, mainly due to the fact that they are less readily detectable by HiC, a standard method to explore the 3D genome in a population of cells. Finally, centromeres occupy specific positions in the chromosome territories distinct from that of other regions (Ollion et

al. 2015).

1.3.2. 3D-genome alterations and editing in pathology

The 3D organization of the cell nucleus is crucial for both normal cellular function and the development of pathological conditions. 3D organization of the genome is altered in many pathological processes. Disruptions in this architecture are linked to various pathological conditions, including cancer, developmental disorders, neurological diseases, and immune system dysfunctions. Understanding the complexities of nuclear organization can provide insights into the mechanisms underlying these diseases and inform potential therapeutic strategies. The review of which I am a co-author (Tiukacheva et al., *Mol. Ther.*, 2023) discusses these alterations in detail. My role in writing this review was to describe and discuss 3D genome alterations associated with cancer and facioscapulohumeral dystrophy (FSHD).

3D genome alterations and editing in pathology

Eugenia A. Tiukacheva,^{1,2,3,4,5} Sergey V. Ulianov,^{2,4} Anna Karpukhina,^{1,5} Sergey V. Razin,^{2,4} and Yegor Vassetzky^{1,5}

¹CNRS UMR9018, Institut Gustave Roussy, 94805 Villejuif, France; ²Institute of Gene Biology, Moscow 119334, Russia; ³Moscow Institute of Physics and Technology, Moscow 141700, Russia; ⁴Faculty of Biology, Lomonosov Moscow State University, Moscow 119991, Russia; ⁵Koltzov Institute of Developmental Biology, Moscow 119334, Russia

The human genome is folded into a multi-level 3D structure that controls many nuclear functions including gene expression. Recently, alterations in 3D genome organization were associated with several genetic diseases and cancer. As a consequence, experimental approaches are now being developed to modify the global 3D genome organization and that of specific loci. Here, we discuss emerging experimental approaches of 3D genome editing that may prove useful in biomedicine.

INTRODUCTION

The interphase genome is folded in a highly ordered manner, essential both for DNA compaction and for the regulation of various intranuclear processes. Each chromosome occupies a restricted volume in the nucleus, a chromosome territory (CT). In mammals, large chromosomes and chromosomes with low gene density tend to localize at the nuclear periphery, whereas smaller chromosomes with high gene density are located more centrally.^{1,2} CTs have a spongy internal structure and are composed of bulk chromatin masses penetrated by the channels of the “interchromatin compartment,” a dynamically organized system of cavities serving for the diffusion of nucleoplasm components.³

Within CTs, active and repressed genomic regions are spatially segregated into A and B compartments formed by local *cis* as well as distant *cis* and *trans* interactions (Figure 1A).⁴ A compartments are early-replicating gene-rich and typically highly transcribed regions enriched in active histone marks such as H3K36me3, H3K27ac, and H3K4me1–3. In contrast, B compartments contain late-replicating transcriptionally silenced regions enriched with nucleolus- and lamina-associated domains (NADs and LADs, respectively) marked with H3K9me2 and H3K9me3.^{5–8} Compartment partitioning strongly correlates with the transcription profile and thus is highly cell-type specific,^{9,10} whereas the degree of compartmentalization might vary significantly within a cell population.^{11,12}

The compartments are further divided into subcompartments, distinguished by the patterns of different histone modifications, and further into topologically associated domains (TADs) with a high CCCTC-binding factor (CTCF)/cohesin occupancy at their borders^{13,14} and representing globular structures with a remarkable cell-to-cell variability in their 3D shape and folding density.^{15,16} TADs serve as “warehouses” for genes, gene loci, and their regulatory systems,¹⁷ delimiting the areas of enhancer action (Figure 1B).^{18,19} Consequently, genes within a TAD are often co-regulated²⁰; this is achieved by looping between enhancers/locus control regions and promoters.^{21,22} Mo-

lecular details of the loop formation mechanisms are still not fully understood, but cohesin-driven extrusion^{23,24} and liquid-liquid phase separation^{25,26} are the most consistent models. The CTCF-cohesin complex preferentially determines strong long-range interactions including contacts between TAD borders,⁸ while the short-range enhancer-promoter and promoter-promoter interactions are also maintained through the Mediator complex and various transcription factors (TFs)²⁷ in cooperation with transcription machinery.²⁸ Complex contact patterns within TADs are manifested in non-structured hierarchical nucleosome assemblies such as clutches²⁹ and nanodomains.³⁰ Clutches are relatively small nucleosome agglomerates (about 2–20 nucleosomes/clutch) whose density and size strongly depend on the level of histone acetylation. This implies that clutches are formed by weak transient electrostatic interactions between nucleosomes. A group of clutches constitutes a nanodomain. Nanodomains are distributed throughout the nucleus, but their concentration increases near the nuclear periphery. Nanodomain structures are preserved upon CTCF and cohesin degradation, and they seem to be formed through liquid-liquid phase separation.^{30,31}

In sum, TADs represent cornerstone structural and functional units of the 3D genome. These units contribute to multiple cellular processes including stem cell differentiation, limb growth and development, epidermal-mesenchymal transition, and cellular senescence.^{9,19,32–34} Changes in the normal profile of TADs can lead to pathologies. Below, we highlight the role of TAD rearrangement and disruption of TAD borders in the development of severe pathologies and discuss 3D genome editing techniques.

3D ORGANIZATION OF THE GENOME AND PATHOLOGIES

Over the past several years, a number of diseases have been associated with 3D genome structure abnormalities (Figure 2). Pathological changes in loop and TAD profiles are caused by structural variations (SVs; rearrangements of 50 nucleotides or more in length: insertions, duplications, deletions, etc.), single-nucleotide polymorphisms (SNPs), large chromosomal rearrangements, viral/transposon DNA integrations, and epigenetic factors. These genome and epigenome perturbations could affect or eliminate TAD boundaries and violate

<https://doi.org/10.1016/j.ymthe.2023.02.005>.

Correspondence: Yegor Vassetzky, CNRS UMR9018, Institut Gustave Roussy, 94805 Villejuif, France.

E-mail: yegor.vassetzky@cnr.fr

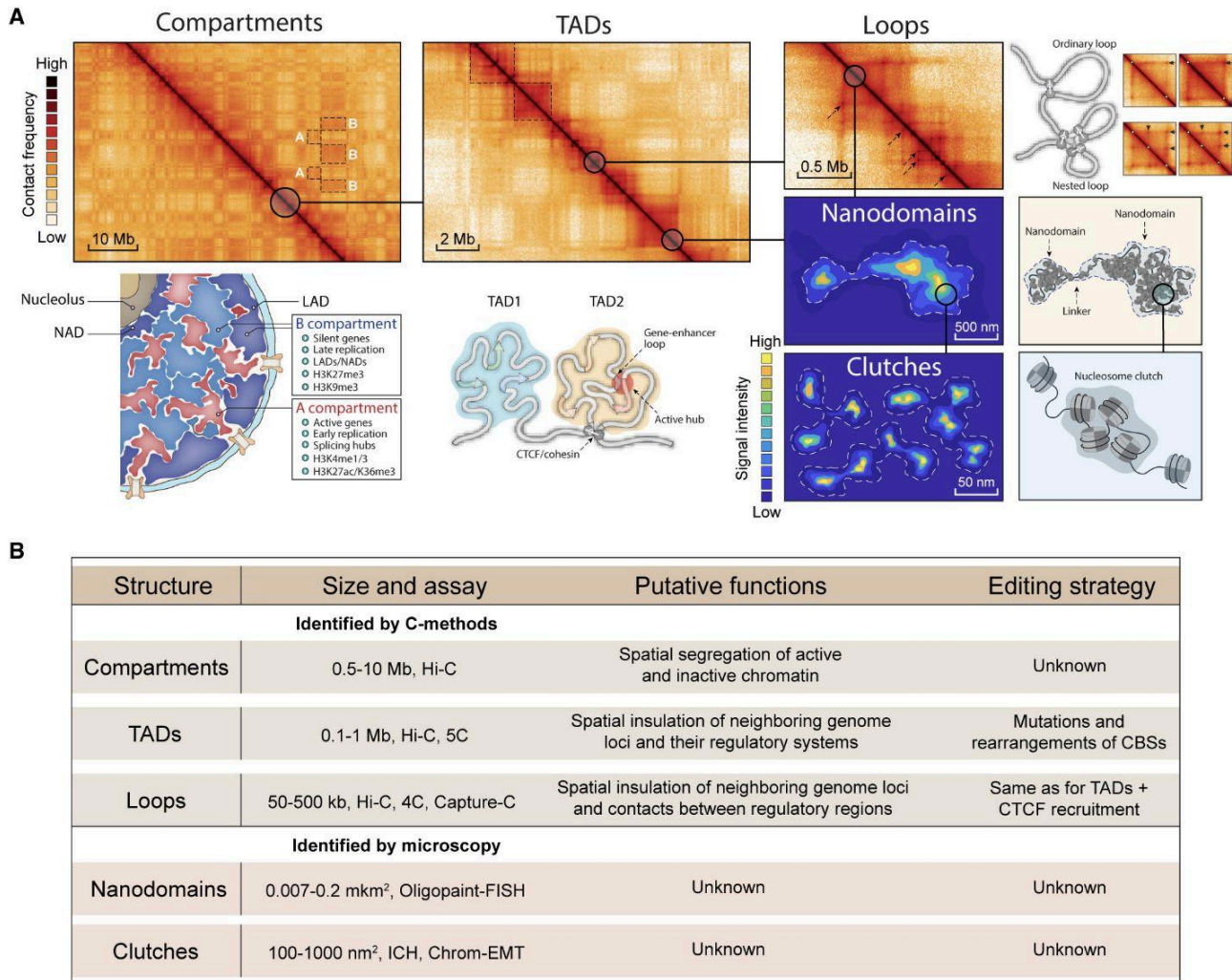


Figure 1. Different levels of 3D genome organization

(A) Top panel: contact maps of 3D genome structures; bottom panel: graphical representation of the corresponding structures. (B) Summary of different levels of 3D genome organization.

distant regulatory interactions that result in transcription dysregulation and manifest in development of pathologies.

Deletions

Deletions are among the most frequent SVs in the human genome.³⁵ Extended deletions eliminating CTCF-marked TAD boundaries result in aberrant activation of proto-oncogenes *TAL1* and *LMO2* by distal enhancers in T cell acute lymphoid leukemia (T-ALL).³⁶ A 600-kb deletion eliminating a TAD boundary results in interactions between unrelated strong enhancers and the *LMNB1* promoter, causing *LMNB1* overexpression and myelin degeneration in autosomal-dominant adult-onset demyelinating leukodystrophy (ADLD).³⁷ In the developing human limb bud, deletion of an entire TAD including boundaries within the 6p22.3 locus correlates with activation of the *ID4* gene by enhancers from the neighboring

TAD. This results in the development of mesomelic dysplasia with hypoplastic tibia and fibula.³⁸

Deletions also cause the Liebenberg syndrome, a limb malformation due to dysregulation of the *PITX1* expression: the forelimbs develop into the hindlimbs. *PITX1* controls the normal development of the hindlimbs where its expression is governed by the interaction with the *Pen* enhancer. In the forelimb buds, *PITX1* is not expressed due to spatial isolation from the *Pen* by a nearby insulator. In Liebenberg syndrome, multiple deletions eliminate this insulator, allowing the *Pen* enhancer to activate *PITX1* and leading to abnormal formation of the forelimb bones and the kneecap near the elbow.^{32,39}

An SV-affecting CTCF binding site (CBS) is associated with facioscapulohumeral muscular dystrophy (FSHD). This disease is caused by

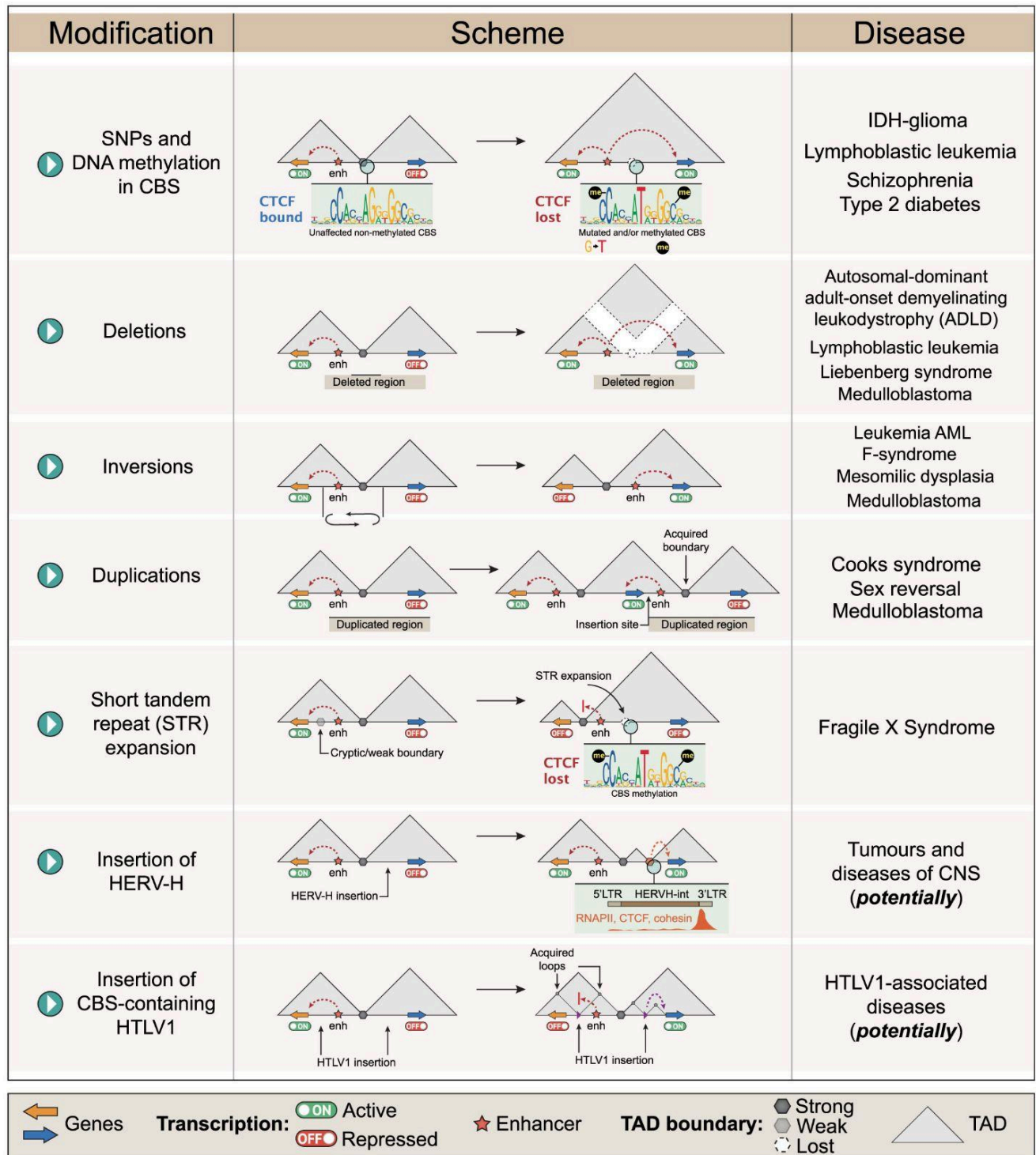


Figure 2. TAD-centric view on the 3D genome organization and disease

Note that some disorders may be causing different rearrangements: autosomal-dominant retinitis pigmentosa, F-syndrome (acropectorovertebral dysgenesis), acute myeloid leukemia, medulloblastoma, brachydactyly, polydactyly.

abnormal expression of the *DUX4* gene and potentially some other genes, including *FRG1*. In healthy muscles, enhancers regulating *DUX4* and *FRG1* are physically separated from their target genes by an FR-MAR insulator.^{40–42} Massive deletion, including several copies of the *DUX4* gene and/or hypomethylation of the locus, cause redistribution of loop contacts. A decrease in the FR-MAR insulator activity leads to *FRG1* and *DUX4* upregulation and muscle pathology.⁴³

Duplications

Duplications also affect the TAD profile and/or intra-TAD spatial interactions. The *SOX9/KCNJ2/KCNJ16* locus contains genes coding for the developmental regulator *SOX9* and potassium channels *KCNJ2/KCNJ16*, located in adjacent TADs. Duplications within the *SOX9* TAD result in female-to-male sex reversal. In the same locus, duplications encompassing the TAD boundary and the entire *KCNJ2* gene result in the formation of a new TAD, where *KCNJ2* is upregulated by *SOX2*-specific enhancers. This leads to the limb malformations with aplasia of nails and short digits known as Cooks syndrome.⁴⁴ In addition to duplications, a translocation involving the *SOX9/KCNJ2/KCNJ16* locus leads to the Snijders Blok-Campeau syndrome, which is characterized by intellectual disability, speech problems, and distinctive facial features.⁴⁵

Inversions

Large-scale inversions lead to branchiooculofacial syndrome (BOFS), which is characterized by skin, face, and eye defects of varying severity. This pathology occurs when the normal expression of the neural crest regulator *TFAP2A* is impaired. Usually, it is a result of a partial gene deletion; however, a recent study⁴⁶ describes a patient with an 89-Mb inversion that does not affect *TFAP2A*, per se, but compromises its expression. This inversion disrupts the *TFAP2A*-containing TADs and the interaction between the *TFAP2A* gene and a group of its enhancers.

Multiple rearrangements

Numerous SVs lead to the emergence of new TADs within the *YPEL2/LINC01476* locus leading to dysregulation of gene expression in autosomal-dominant retinitis pigmentosa (adRP).⁴⁷ In some loci, large-scale SVs cause a variety of distinct pathologies. The canonical example is the *WNT6/IHH/EPHA4/PAX3* locus, where different deletions, inversions, and duplications result in limb malformation. Some of the intergenic SVs induce F syndrome (acropectorovertebral dysgenesis), a rare inherited skeletal disorder characterized by the fusion of the thumb and index finger. In particular, F syndrome is caused by an inversion, which leaves the TAD boundary intact but relocates an enhancer from the neighboring TAD to a close vicinity of the *WNT6* gene, promoting its overexpression. Other duplications and deletions affecting TAD structure within the regions cause brachydactyly and polydactyly.^{48,49}

Different SVs affecting the 3D genome can lead to a phenomenon called “enhancer hijacking” where enhancers activate genes that are not their normal targets. For example, an SV in the vicinity of the *GFIIB* gene leads to *GFIIB* interaction with distal superenhancers and overexpression in medulloblastoma.⁵⁰ In acute myeloid leukemia

(AML), multiple rearrangements affect more than 40 cancer-related loci.⁵¹ These mutations are represented by translocations, deletions, and inversions; SVs lead to the formation of new loops with “hijacking” of an enhancer or a silencer in 27 of these loci.

SNPs

SNPs affect the genome topology by mutations in the binding sites of architectural proteins or tissue-specific TFs.

In the human 3p21.2 locus, the SNP rs2535629 has a strong association with schizophrenia. rs2535629 (A/G) is located within the CBS, which resides in a repressor element in the seventh intron of the *ITIH3* gene. The presence of this SV prevents CTCF binding to CBS and also changes the expression profiles of nearby genes: it downregulates *GLT8D1* and *SFMBT1* and upregulates *NEK4*. The *SFMBT1* gene product is involved in the regulation of proliferation and differentiation of nerve stem cells, the formation of dendritic spines, and the proper functioning of neural synapse. Its downregulation is associated with schizophrenia development.⁵²

SNP rs7903146 (CT/TT) is present in the enhancer of the *TCF7L2* locus and promotes the formation of the gene-enhancer contact.⁵³ This interaction leads to an increase in the *TCF7L2* expression with a subsequent decrease in insulin secretion, possibly contributing to the development of type 2 diabetes.⁵⁴

STR expansion and viral DNA integration

Expansion of DNA repeats and viral DNA integration can also affect the profile of spatial interactions between remote genomic elements. Short tandem repeats (STRs) alter TAD boundaries by modulating CTCF binding.⁵⁵ In several pathological models, STRs accumulate at TAD boundaries, increasing the density of CpG islands, which are often hypermethylated in pathologies. One example is the *FMRI* gene, whose repression leads to fragile X chromosome syndrome (Martin-Bell syndrome). STR accumulation at the boundary of encompassing TADs promotes DNA hypermethylation followed by a decrease of CTCF binding and significant alteration in the enhancer landscape of the locus. These lead to the loss of the TAD boundary and *FMRI* repression.⁵⁶

Integration of a primate-specific human endogenous retrovirus subfamily H (HERV-H) transposon establishes TAD boundaries in the genome of human pluripotent stem cells.⁵⁷ In this case, active viral transcription creates a TAD boundary at the site of the HERV-H integration. This is in line with recent observations showing that active transcription constitutes a barrier for the cohesin-driven extrusion.⁵⁸ In contrast to HERV-H, insertion of the human T-lymphotropic virus HTLV-1 establishes *de novo* loops due to the presence of a CBS within the viral genome. This results in abnormal host gene transcription not only in loci proximal to the integration site but also more than 300-kb away.⁵⁹ The same was observed for the bovine leukemia virus (BLV) carrying several CBSs involved in the formation of new chromatin loops with the host chromosome loci after the provirus integration.⁶⁰

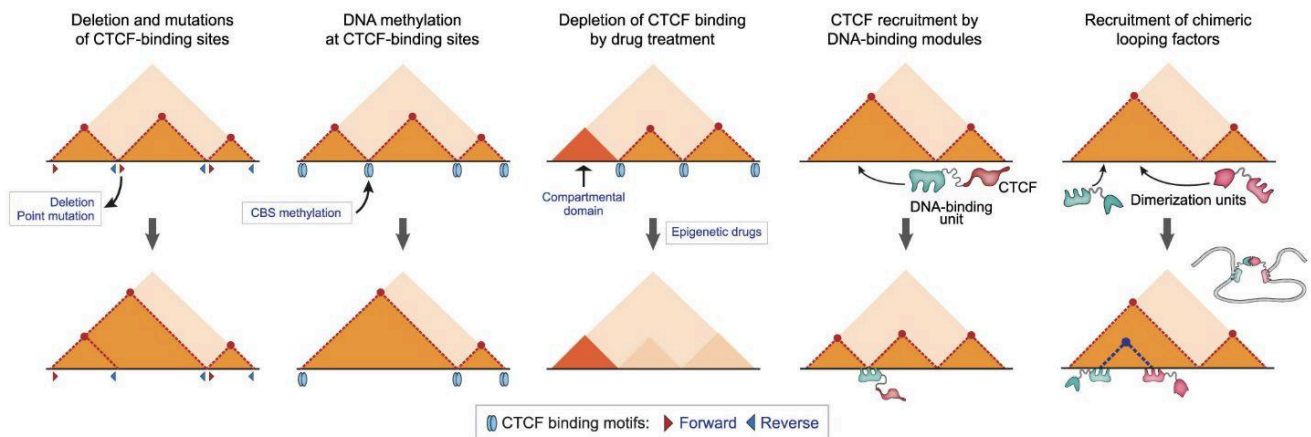


Figure 3. Strategies for 3D genome editing

Epigenetic factors

Abnormal DNA methylation is also involved in violation of the 3D genome via suppression of CTCF binding. This decreases insulation at TAD boundaries, allowing aberrant enhancer-promoter interactions that may affect disease-related genes. In human glioma, mutations in the *IDH* gene result in an increased genome-wide DNA methylation including that in the *PDGFRA* oncogene locus. Methylation of the 5'-flanking insulator serving as a TAD boundary in this locus results in a loss of CTCF binding and perturbs local interaction patterns; this drives an abnormal activation of the *PDGFRA* gene by a distal enhancer.⁶¹ In some cases, abnormal methylation at CBSs could be driven by external factors, such as drug use. For example, cocaine addiction results in a pathogenic looping within the *IRXA* locus in brain neurons due to DNA hypomethylation at a set of CBSs.⁶² Recent studies reveal that besides abnormal methylation and CBS mutations, some other mechanisms could impact chromatin looping. In T-ALL, disappearance of the TAD boundary between *MYC* and a group of enhancers in the neighbor TAD leads to *MYC* overexpression.⁶³ Interestingly, in this case, a loss of CTCF binding is not caused by CBS mutations or methylation and is accompanied by decreased chromatin accessibility. Thus some additional factors may influence CTCF binding. One potential candidate is *Jpx* non-coding RNA, which regulates CTCF binding at a subset of developmentally sensitive loci by competitive inhibition.⁶⁴

Finally, at a whole-nucleus scale, contacts between non-homologous chromosomes can also lead to oncogenic chromosomal translocations. This disrupts local regulatory 3D interaction networks and alters cellular transcription programs. A few examples include interactions of chromosomes 8 and 14 or 11 and 14 in B lymphocytes leading to Burkitt or mantle cell lymphomas, respectively; chromosomes 12 and 16 in adipocytes leading to liposarcoma; and chromosomes 5 and 6 in hepatocytes leading to hepatocarcinoma.^{65–69}

Together, alterations in the genome 3D organization are quite common in cancer and developmental disorders. Screening revealed that 7.3% of balanced chromosomal abnormalities disrupt TADs at known syn-

dromic loci⁷⁰; 14% of SVs affect TAD boundaries and lead to remarkable changes in expression of nearby genes in cancers.⁷¹ The ability of naturally occurring SVs to affect 3D genome and cause socially significant diseases imposes the development and further clinical validation of 3D genome editing technologies applicable for treating patients.

3D GENOME EDITING

Since alterations in the chromatin contact profiles are associated with many pathologies, development of 3D genome editing methods is on the frontlines of biomedicine. The existing approaches largely rely on the use of either native architectural proteins such as CTCF or artificial looping proteins (Figure 3).

As highlighted above, CTCF is a master regulator of the mammalian interphase genome folding⁷² and thus is a predominant target for 3D genome engineering. CBS deletion/insertion/inversion and point mutations are streamlined paths for the precise control of CTCF binding within genome regulatory elements and TAD boundaries/loop anchors.^{73,74} In several loci, such manipulations alter loop profile and result in changes of gene expression that could be potentially used as a strategy for the cell-type-specific transcription reprogramming in patients.⁷⁵ However, genomic DNA editing possesses risks of chromosome rearrangements that should be considered while designing clinically relevant applications.⁷⁶

In the case of *de novo* TAD formation or excessive CTCF binding, depletion of CTCF from particular sites in chromatin can be accomplished through epigenetic modifications of CBS to inhibit CTCF binding without changes in the primary DNA sequence. In this case, chimeric proteins consisting of catalytically deficient (“dead” Cas9 [dCas9]) fused with the Krüppel-associated box (KRAB), an H3K9me3-catalyzing repressor (dCas9-KRAB), or DNA-methyltransferases DNMT3A and DNMT3A3L were shown to be effective inhibitors of CTCF binding when precisely targeted to the CBS.^{77,78}

Another approach being developed for clinical applications is the usage of small molecules interfering with the CTCF binding. Treatment

of cells with the anti-cancer agent curaxin (CBL0137) leads to a partial depletion of CTCF from chromatin and compromises enhancer-promoter contacts.⁷⁹ On the other hand, DNA methylation interfering with the CTCF binding could be eliminated by cell treatment with 5-aminosalicylic acid (5-ASA). In the case of AML cells, treatment with 5-ASA restores a normal pattern of CTCF-dependent insulation in chromatin and effectively suppresses the interactions between a set of enhancers and oncogenes.⁵¹

Other perspective molecules for the 3D genome manipulations are bromodomain and extra-terminal motif inhibitors (BETis). BET proteins are widespread transcription regulators often associated with architectural proteins. For instance, BET protein bromodomain-containing protein 4 (BRD4) binds to CTCF-associated Yin Yang 1 (YY1) factor throughout the genome including at TAD boundaries. Pan-BETi (Apa20, JQ1, IBET762) treatment weakens BRD4-YY1 binding, removes BRD4 from chromatin, and causes chromatin decondensation.⁸⁰ BETi JQ1 treatment suppresses cohesin and CTCF binding to the Kaposi's sarcoma-associated herpesvirus (KSHV) genome. This results in the loss of looping between latent and lytic control regions of the viral chromosome and virus transition to a lytic state.⁸¹

Together, this opens an avenue for the rational *in silico* design of inhibitors of DNA binding and competitors for the protein-protein interactions for the factors involved in the 3D genome maintenance.

Since some diseases are associated with the decrease of CTCF occupancy at particular CBSs,⁸² stabilization of CTCF binding at such loci is a strategy to be considered. Several post-translational modifications are essential for the CTCF insulator and barrier activities.⁸³ Indeed, mutations in the CTCF region subjected to poly(ADP-ribosylation) by poly(ADP-ribose) polymerase 1 (PARP1) compromise cohesin enrichment at CBSs, e.g., interfere with cohesion-/CTCF-dependent loop formation.⁸⁴ In the Epstein-Barr virus genome, PARP1 acts to stabilize CTCF binding at particular sites.⁸⁵ Thus, inducible recruitment of PARP1 to certain CBSs could be a tool for the stabilization of selective CTCF binding to these sites. Other post-translational modifications of CTCF such as SUMOylation and phosphorylation^{86,87} are also of interest for 3D genome manipulation in both genome-wide and locus-specific manners. Together, these examples illustrate that epigenome targeting and inducible CTCF post-translational modifications could potentially serve as a proxy for 3D genome editing.

A number of diseases are characterized by a complete loss of CBSs at critical regulatory elements due to deletions and other SVs.⁸⁸⁻⁹⁰ In such cases, recruitment of CTCF by an unrelated DNA-binding module and restoration of the original loop profile might be a potential treatment strategy. One example is a dCas9-mediated CTCF recruitment enforced by the coupling with SunTag technology, allowing recruitment of multiple CTCF molecules to the same binding site.⁹¹ This method has been tested in the *TFE* locus associated with breast, lung, and colon cancers⁹² and demonstrated a potential utility for 3D genome engineering in multi-gene disease-associated loci.

Some pathologies are accompanied by a total loss of *CTCF* expression followed by genome-wide alterations of chromatin 3D structure. Consequently, insertion of a functional *CTCF* gene could restore an original loop pattern of the affected loci. For example, breast cancer could be inhibited by the increased *CTCF* expression; the *CTCF* gene is frequently deleted in this type of cancer, and this negatively affects the survival rate of patients at late stages.⁹³ *CTCF* gene insertion by pseudoviruses also slows down the cancer cell division and/or migration, as well as metastasis in the lungs and brain, and affects the expression of almost 130 genes.

An alternative approach for manipulation of the 3D genome architecture relies on the expression of chimeric proteins containing DNA-binding modules (zinc finger [ZF]), transcription activator-like effector [TALE], dCas9) fused with units forming homo- or heterodimers, such as dimerization domains of mammalian TFs, e.g., the self-associating domain of the Ldb1 protein.⁹⁴ These chimeric proteins form relatively stable dimers and are suitable for the formation of constant distant interactions in chromatin. These contacts can be made reversible via inducible polymerization. One example is the chromatin loop reorganization using CRISPR-dCas9 (CLOuD9) system, where PYL1 and ABI1 fused with two different dCas9 modules interact with each other in the presence of abscisic acid (ABA). Application of the CLOuD9 system to the *Oct4* locus associated with various types of cancers demonstrated that recruitment of these fusion proteins to the *Oct4* promoter and its distal enhancer induced loop formation and upregulation of *Oct4* after ABA addition.⁹⁵ A similar approach, light-activated dynamic looping (LADL), utilizes co-expression of cryptochrome 2 (CRY2) and N-truncated CRY-interacting basic-helix-loop-helix protein 1 (CIBN) fused to dCas9. Exposure of cells to 470-nm blue light induces dimerization of CRY2 and heteromerization of CRY2 and CIBN. As a result, loci targeted by dCas9-CIBN form a transient loop. In a proof-of-concept study, LADL-induced looping between *Zfp462* and the *Klf4* superenhancer was successfully used to increase the *Zfp462* expression in mouse embryonic stem cells.⁹⁶

CONCLUDING REMARKS

Genome-wide association studies revealed a number of genomic SVs associated with the development of various diseases. Most of these SVs are located outside genes and their regulatory modules. Consequently, the mechanical links between disease-associated SVs and regulation of genome activity remained obscure. Recent results discussed here argue that many of the disease-associated SVs affect 3D genome organization. This raises the issue of the need for 3D genome editing. Several approaches for such editing have been proposed and tested on cell cultures. The question is whether any of the developed strategies have the prospect of practical application. In the case of cancer, the straightforward strategy is to kill a cancer cell if it can be recognized and targeted rather than to try to correct anything in this cell. The only possible application here is to use low-molecular-weight agents (e.g., curaxins) that affect all cells with some preference to cancer cells. More interesting opportunities for practical applications of 3D genome editing arise in cases where it is necessary to

deliver to the organism its own normal cells, which will exist alongside corrupted ones or replace them. This strategy assumes that damaged cells are taken from the patient, manipulated in the laboratory, and returned to the patient's body. In the future, this approach could be useful for the treatment of a number of diseases of the hematopoietic and endocrine organs, as well as some types of muscular dystrophies.

However, similarly to genome editing, 3D genome manipulations could have off-target effects. In particular, targeted recruitment of the full-length CTCF or any other natural architectural protein to an ectopic site requires its overexpression in a cell. This could increase the abundance of the overexpressed factor at endogenous binding sites affecting their contact profile genome-wide. Usage of truncated forms of architectural proteins lacking natural DNA-binding domains and/or weak promoters for the expression cassettes potentially solve this problem. Further, binding by an artificial module such as dCas9 may change the chromatin residence time of the recruited protein, which, in turn, may affect the looping strength and nucleosome/epigenetic profiles in a vicinity of the binding site.⁹⁷ Thus, a sophisticated design of chimeric proteins and comprehensive analysis of epigenetic and transcription profiles within the edited locus and in its neighborhood are prerequisites for the development of clinically relevant applications.

ACKNOWLEDGMENTS

This work was supported by the Russian Science Foundation (21-64-00001) and by the Russian Ministry of Science and Higher Education (075-15-2021-1062) to S.V.U. and S.V.R. and from the AFM (CTCFSHD) and the IDB RAS Government basic research programs (0088-2022-0007 and 0088-2022-0016) to Y.V.

AUTHOR CONTRIBUTIONS

S.V.R. and Y.V. conceptualized the manuscript. E.A.T., S.V.U., and A.K. wrote the draft. S.V.U. prepared the figures. All authors made corrections to the final version of the manuscript. All authors have read and agreed to the published version of the manuscript.

DECLARATION OF INTERESTS

The authors declare no competing interests.

REFERENCES

- Boyle, S., Gilchrist, S., Bridger, J.M., Mahy, N.L., Ellis, J.A., and Bickmore, W.A. (2001). The spatial organization of human chromosomes within the nuclei of normal and emerin-mutant cells. *Hum. Mol. Genet.* *10*, 211–219.
- Crosetto, N., and Bienko, M. (2020). Radial organization in the mammalian nucleus. *Front. Genet.* *11*, 33. <https://doi.org/10.3389/fgene.2020.00033>.
- Albiez, H., Cremer, M., Tiberi, C., Vecchio, L., Schermelleh, L., Dittrich, S., Küpper, K., Joffe, B., Thormeyer, T., von Hase, J., et al. (2006). Chromatin domains and the interchromatin compartment form structurally defined and functionally interacting nuclear networks. *Chromosome Res.* *14*, 707–733. <https://doi.org/10.1007/s10577-006-1086-x>.
- Lieberman-Aiden, E., van Berkum, N.L., Williams, L., Imakaev, M., Ragoczy, T., Telling, A., Amit, I., Lajoie, B.R., Sabo, P.J., Dorschner, M.O., et al. (2009). Comprehensive mapping of long range interactions reveals folding principles of the human genome. *Science* *326*, 289–293. <https://doi.org/10.1126/science.1181369>.
- Dillinger, S., Straub, T., and Németh, A. (2017). Nucleolus association of chromosomal domains is largely maintained in cellular senescence despite massive nuclear reorganization. *PLoS ONE* *12*, e0178821. <https://doi.org/10.1371/journal.pone.0178821>.
- Guelen, L., Pagie, L., Brasset, E., Meuleman, W., Faza, M.B., Talhout, W., Eussen, B.H., de Klein, A., Wessels, L., de Laat, W., and van Steensel, B. (2008). Domain organization of human chromosomes revealed by mapping of nuclear lamina interactions. *Nature* *453*, 948–951. <https://doi.org/10.1038/nature06947>.
- Nichols, M.H., and Corces, V.G. (2021). Principles of 3D compartmentalization of the human genome. *Cell Rep.* *35*, 109330. <https://doi.org/10.1016/j.celrep.2021.109330>.
- Rao, S.S.P., Huntley, M.H., Durand, N.C., Stamenova, E.K., Bochkov, I.D., Robinson, J.T., Sanborn, A.L., Machol, I., Omer, A.D., Lander, E.S., and Aiden, E.L. (2014). A three-dimensional map of the human genome at kilobase resolution reveals principles of chromatin looping. *Cell* *159*, 1665–1680. <https://doi.org/10.1016/j.cell.2014.11.021>.
- Dixon, J.R., Jung, I., Selvaraj, S., Shen, Y., Antosiewicz-Bourget, J.E., Lee, A.Y., Ye, Z., Kim, A., Rajagopal, N., Xie, W., et al. (2015). Chromatin architecture reorganization during stem cell differentiation. *Nature* *518*, 331–336. <https://doi.org/10.1038/nature14222>.
- Winick-Ng, W., Kukalev, A., Harabula, I., Zea-Redondo, L., Szabó, D., Meijer, M., Serebreni, L., Zhang, Y., Bianco, S., Chiariello, A.M., et al. (2021). Cell-type specialization is encoded by specific chromatin topologies. *Nature* *599*, 684–691. <https://doi.org/10.1038/s41586-021-04081-2>.
- Bintu, B., Mateo, L.J., Su, J.-H., Sinnott-Armstrong, N.A., Parker, M., Kinrot, S., Yamaya, K., Boettiger, A.N., and Zhuang, X. (2018). Super-resolution chromatin tracing reveals domains and cooperative interactions in single cells. *Science* *362*, eaau1783. <https://doi.org/10.1126/science.aau1783>.
- Kim, H.-J., Yardımcı, G.G., Bonora, G., Ramani, V., Liu, J., Qiu, R., Lee, C., Hesson, J., Ware, C.B., Shendure, J., et al. (2020). Capturing cell type-specific chromatin compartment patterns by applying topic modeling to single-cell Hi-C data. *Plos Comput. Biol.* *16*, e1008173. <https://doi.org/10.1371/journal.pcbi.1008173>.
- Gómez-Marín, C., Tena, J.J., Acemel, R.D., López-Mayorga, M., Naranjo, S., de la Calle-Mustienes, E., Maeso, I., Beccari, L., Aneas, I., Vielmas, E., et al. (2015). Evolutionary comparison reveals that diverging CTCF sites are signatures of ancestral topological associating domains borders. *Proc. Natl. Acad. Sci. USA* *112*, 7542–7547. <https://doi.org/10.1073/pnas.1505463112>.
- Merkenschlager, M., and Nora, E.P. (2016). CTCF and cohesin in genome folding and transcriptional gene regulation. *Annu. Rev. Genomics Hum. Genet.* *17*, 17–43. <https://doi.org/10.1146/annurev-genom-083115-022339>.
- Stevens, T.J., Lando, D., Basu, S., Atkinson, L.P., Cao, Y., Lee, S.F., Leeb, M., Wohlfahrt, K.J., Boucher, W., O'Shaughnessy-Kirwan, A., et al. (2017). 3D structure of individual mammalian genomes studied by single cell Hi-C. *Nature* *544*, 59–64. <https://doi.org/10.1038/nature21429>.
- Ulianov, S.V., Zakharaeva, V.V., Galitsyna, A.A., Kos, P.I., Polovnikov, K.E., Flyamer, I.M., Mikhaleva, E.A., Khrameeva, E.E., Germini, D., Logacheva, M.D., et al. (2021). Order and stochasticity in the folding of individual *Drosophila* genomes. *Nat. Commun.* *12*, 41. <https://doi.org/10.1038/s41467-020-20292-z>.
- Razin, S.V., Gavrillov, A.A., Vassetzky, Y.S., and Ulianov, S.V. (2016). Topologically-associating domains: gene warehouses adapted to serve transcriptional regulation. *Transcription* *7*, 84–90. <https://doi.org/10.1080/21541264.2016.1181489>.
- Nora, E.P., Goloborodko, A., Valton, A.-L., Gibcus, J.H., Ueberohrn, A., Abdennur, N., Dekker, J., Mirny, L.A., and Bruneau, B.G. (2017). Targeted degradation of CTCF decouples local insulation of chromosome domains from genomic compartmentalization. *Cell* *169*, 930–944.e22. <https://doi.org/10.1016/j.cell.2017.05.004>.
- Pang, Q.Y., Tan, T.Z., Sundararajan, V., Chiu, Y.-C., Chee, E.Y.W., Chung, V.Y., Choolani, M.A., and Huang, R.Y.-J. (2022). 3D genome organization in the epithelial-mesenchymal transition spectrum. *Genome Biol.* *23*, 121. <https://doi.org/10.1186/s13059-022-02687-x>.
- Dixon, J.R., Gorkin, D.U., and Ren, B. (2016). Chromatin domains: the unit of chromosome organization. *Mol. Cell* *62*, 668–680. <https://doi.org/10.1016/j.molcel.2016.05.018>.

21. Amândio, A.R., Lopez-Delisle, L., Bolt, C.C., Mascrez, B., and Duboule, D. (2020). A complex regulatory landscape involved in the development of mammalian external genitals. *eLife* 9, e52962. <https://doi.org/10.7554/eLife.52962>.
22. Bonev, B., Mendelson Cohen, N., Szabo, Q., Fritsch, L., Papadopoulos, G.L., Lubling, Y., Xu, X., Lv, X., Hugnot, J.-P., Tanay, A., and Cavalli, G. (2017). Multiscale 3D genome rewiring during mouse neural development. *Cell* 171, 557–572.e24. <https://doi.org/10.1016/j.cell.2017.09.043>.
23. Bauer, B.W., Davidson, I.F., Canena, D., Wutz, G., Tang, W., Litos, G., Horn, S., Hinterdorfer, P., and Peters, J.-M. (2021). Cohesin mediates DNA loop extrusion by a “swing and clamp” mechanism. *Cell* 184, 5448–5464.e22. <https://doi.org/10.1016/j.cell.2021.09.016>.
24. Davidson, I.F., Bauer, B., Goetz, D., Tang, W., Wutz, G., and Peters, J.-M. (2019). DNA loop extrusion by human cohesin. *Science* 366, 1338–1345. <https://doi.org/10.1126/science.aaz3418>.
25. Hnisz, D., Shrinivas, K., Young, R.A., Chakraborty, A.K., and Sharp, P.A. (2017). A phase separation model predicts key features of transcriptional control. *Cell* 169, 13–23. <https://doi.org/10.1016/j.cell.2017.02.007>.
26. Razin, S.V., and Gavrilov, A.A. (2020). The role of liquid-liquid phase separation in the compartmentalization of cell nucleus and spatial genome organization. *Biochemistry* 85, 643–650. <https://doi.org/10.1134/S0006297920060012>.
27. Krietenstein, N., Abraham, S., Venev, S.V., Abdennur, N., Gibcus, J., Hsieh, T.-H.S., Parsi, K.M., Yang, L., Maehr, R., Mirny, L.A., et al. (2020). Ultrastructural details of mammalian chromosome architecture. *Mol. Cell* 78, 554–565.e7. <https://doi.org/10.1016/j.molcel.2020.03.003>.
28. Hsieh, T.-H.S., Cattoglio, C., Slobodyanyuk, E., Hansen, A.S., Rando, O.J., Tjian, R., and Darzacq, X. (2020). Resolving the 3D landscape of transcription-linked mammalian chromatin folding. *Mol. Cell* 78, 539–553.e8. <https://doi.org/10.1016/j.molcel.2020.03.002>.
29. Ricci, M.A., Manzo, C., García-Parajo, M.F., Lakadamyali, M., and Cosma, M.P. (2015). Chromatin fibers are formed by heterogeneous groups of nucleosomes in vivo. *Cell* 160, 1145–1158. <https://doi.org/10.1016/j.cell.2015.01.054>.
30. Szabo, Q., Donjon, A., Jerković, I., Papadopoulos, G.L., Cheutin, T., Bonev, B., Nora, E.P., Bruneau, B.G., Bantignies, F., and Cavalli, G. (2020). Regulation of single-cell genome organization into TADs and chromatin nanodomains. *Nat. Genet.* 52, 1151–1157. <https://doi.org/10.1038/s41588-020-00716-8>.
31. Ulianov, S.V., Velichko, A.K., Magnitov, M.D., Luzhin, A.V., Golov, A.K., Ovsyannikova, N., Kireev, I.I., Gavrikov, A.S., Mishin, A.S., Garaev, A.K., et al. (2021). Suppression of liquid-liquid phase separation by 1,6-hexanediol partially compromises the 3D genome organization in living cells. *Nucleic Acids Res.* 49, 10524–10541. <https://doi.org/10.1093/nar/gkab249>.
32. Kragestein, B.K., Spielmann, M., Paliou, C., Heinrich, V., Schöpflin, R., Esposito, A., Annunziatella, C., Bianco, S., Chiariello, A.M., Jerković, I., et al. (2018). Dynamic 3D chromatin architecture contributes to enhancer specificity and limb morphogenesis. *Nat. Genet.* 50, 1463–1473. <https://doi.org/10.1038/s41588-018-0221-x>.
33. Rodríguez-Carballo, E., Lopez-Delisle, L., Willemin, A., Beccari, L., Gitto, S., Mascrez, B., and Duboule, D. (2020). Chromatin topology and the timing of enhancer function at the HoxD locus. *Proc. Natl. Acad. Sci. USA* 117, 31231–31241. <https://doi.org/10.1073/pnas.2015083117>.
34. Criscione, S.W., Teo, Y.V., and Neretti, N. (2016). The chromatin landscape of cellular senescence. *Trends Genet.* 32, 751–761. <https://doi.org/10.1016/j.tig.2016.09.005>.
35. Sudmant, P.H., Rausch, T., Gardner, E.J., Handsaker, R.E., Abyzov, A., Huddleston, J., Zhang, Y., Ye, K., Jun, G., Fritz, M.H.Y., et al. (2015). An integrated map of structural variation in 2,504 human genomes. *Nature* 526, 75–81. <https://doi.org/10.1038/nature15394>.
36. Hnisz, D., Weintraub, A.S., Day, D.S., Valton, A.-L., Bak, R.O., Li, C.H., Goldmann, J., Lajoie, B.R., Fan, Z.P., Sigova, A.A., et al. (2016). Activation of proto-oncogenes by disruption of chromosome neighborhoods. *Science* 351, 1454–1458. <https://doi.org/10.1126/science.aad9024>.
37. Giorgio, E., Robyr, D., Spielmann, M., Ferrero, E., Di Gregorio, E., Imperiale, D., Vaula, G., Stamoulis, G., Santoni, F., Atzori, C., et al. (2015). A large genomic deletion leads to enhancer adoption by the lamin B1 gene: a second path to autosomal dominant adult-onset demyelinating leukodystrophy (ADLD). *Hum. Mol. Genet.* 24, 3143–3154. <https://doi.org/10.1093/hmg/ddv065>.
38. Flöttmann, R., Wagner, J., Kobus, K., Curry, C.J., Savarirayan, R., Nishimura, G., Yasui, N., Spranger, J., Van Esch, H., Lyons, M.J., et al. (2015). Microdeletions on 6p22.3 are associated with mesomelic dysplasia Savarirayan type. *J. Med. Genet.* 52, 476–483. <https://doi.org/10.1136/jmedgenet-2015-103108>.
39. Kragestein, B.K., Brancati, F., Digilio, M.C., Mundlos, S., and Spielmann, M. (2019). H2AFY promoter deletion causes PITX1 endoactivation and Liebenberg syndrome. *J. Med. Genet.* 56, 246–251. <https://doi.org/10.1136/jmedgenet-2018-105793>.
40. Himeda, C.L., Jones, T.I., and Jones, P.L. (2015). Facioscapulohumeral muscular dystrophy as a model for epigenetic regulation and disease. *Antioxid. Redox Signal.* 22, 1463–1482. <https://doi.org/10.1089/ars.2014.6090>.
41. Petrov, A., Pirozhkova, I., Carnac, G., Laoudj, D., Lipinski, M., and Vassetzky, Y.S. (2006). Chromatin loop domain organization within the 4q35 locus in facioscapulohumeral dystrophy patients versus normal human myoblasts. *Proc. Natl. Acad. Sci. USA* 103, 6982–6987. <https://doi.org/10.1073/pnas.0511235103>.
42. Petrov, A., Allinne, J., Pirozhkova, I., Laoudj, D., Lipinski, M., and Vassetzky, Y.S. (2008). A nuclear matrix attachment site in the 4q35 locus has an enhancer-blocking activity in vivo: implications for the facio-scapulo-humeral dystrophy. *Genome Res.* 18, 39–45. <https://doi.org/10.1101/gr.6620908>.
43. Karpukhina, A., Tiukacheva, E., Dib, C., and Vassetzky, Y.S. (2021). Control of DUX4 expression in facioscapulohumeral muscular dystrophy and cancer. *Trends Mol. Med.* 27, 588–601. <https://doi.org/10.1016/j.molmed.2021.03.008>.
44. Franke, M., Ibrahim, D.M., Andrey, G., Schwarzer, W., Heinrich, V., Schöpflin, R., Kraft, K., Kempfer, R., Jerković, I., Chan, W.-L., et al. (2016). Formation of new chromatin domains determines pathogenicity of genomic duplications. *Nature* 538, 265–269. <https://doi.org/10.1038/nature19800>.
45. Melo, U.S., Schöpflin, R., Acuna-Hidalgo, R., Mensah, M.A., Fischer-Zirnsak, B., Holtgrewe, M., Klever, M.-K., Türkmen, S., Heinrich, V., Pluym, I.D., et al. (2020). Hi-C identifies complex genomic rearrangements and TAD-shuffling in developmental diseases. *Am. J. Hum. Genet.* 106, 872–884. <https://doi.org/10.1016/j.ajhg.2020.04.016>.
46. Lausch, M., Bartusel, M., Rehimi, R., Alirzayeva, H., Karaolidou, A., Crispatsu, G., Zentis, P., Nikolic, M., Bleckwehl, T., Kolovos, P., et al. (2019). Modeling the pathological long-range regulatory effects of human structural variation with patient-specific hiPSCs. *Cell Stem Cell* 24, 736–752.e12. <https://doi.org/10.1016/j.stem.2019.03.004>.
47. de Bruijn, S.E., Fiorentino, A., Ottaviani, D., Fanucchi, S., Melo, U.S., Corral-Serrano, J.C., Mulders, T., Georgiou, M., Rivolta, C., Pontikos, N., et al. (2020). Structural variants create new topological-associated domains and ectopic retinal enhancer-gene contact in dominant retinitis pigmentosa. *Am. J. Hum. Genet.* 107, 802–814. <https://doi.org/10.1016/j.ajhg.2020.09.002>.
48. Lupiáñez, D.G., Kraft, K., Heinrich, V., Krawitz, P., Brancati, F., Klopocki, E., Horn, D., Kayserili, H., Opitz, J.M., Laxova, R., et al. (2015). Disruptions of topological chromatin domains cause pathogenic rewiring of gene-enhancer interactions. *Cell* 161, 1012–1025. <https://doi.org/10.1016/j.cell.2015.04.004>.
49. Lupiáñez, D.G., Spielmann, M., and Mundlos, S. (2016). Breaking TADs: how alterations of chromatin domains result in disease. *Trends Genet.* 32, 225–237. <https://doi.org/10.1016/j.tig.2016.01.003>.
50. Northcott, P.A., Lee, C., Zichner, T., Stütz, A.M., Erkek, S., Kawauchi, D., Shih, D.J.H., Hovestadt, V., Zapatka, M., Sturm, D., et al. (2014). Enhancer hijacking activates GFII family oncogenes in medulloblastoma. *Nature* 511, 428–434. <https://doi.org/10.1038/nature13379>.
51. Xu, J., Song, F., Lyu, H., Kobayashi, M., Zhang, B., Zhao, Z., Hou, Y., Wang, X., Luan, Y., Jia, B., et al. (2022). Subtype-specific 3D genome alteration in acute myeloid leukaemia. *Nature* 611, 387–398. <https://doi.org/10.1038/s41586-022-05365-x>.
52. Li, Y., Ma, C., Li, S., Wang, J., Li, W., Yang, Y., Li, X., Liu, J., Yang, J., Liu, Y., et al. (2022). Regulatory variant rs2535629 in ITIH3 intron confers schizophrenia risk by regulating CTCF binding and SFMBT1 expression. *Adv. Sci.* 9, e2104786. <https://doi.org/10.1002/adv.202104786>.
53. Miguel-Escalada, I., Bonàs-Guarch, S., Cebola, I., Ponsa-Cobas, J., Mendieta-Esteban, J., Atla, G., Janvier, B.M., Rolando, D.M.Y., Farabella, I., Morgan, C.C., et al. (2019). Human pancreatic islet three-dimensional chromatin architecture provides insights

- into the genetics of type 2 diabetes. *Nat. Genet.* 51, 1137–1148. <https://doi.org/10.1038/s41588-019-0457-0>.
54. Lyssenko, V., Lupi, R., Marchetti, P., Del Guerra, S., Orho-Melander, M., Almgren, P., Sjögren, M., Ling, C., Eriksson, K.-F., Lethagen, A.L., et al. (2007). Mechanisms by which common variants in the TCF7L2 gene increase risk of type 2 diabetes. *J. Clin. Invest.* 117, 2155–2163. <https://doi.org/10.1172/JCI30706>.
 55. Ibrahim, D.M., and Mundlos, S. (2020). Three-dimensional chromatin in disease: what holds us together and what drives us apart? *Curr. Opin. Cell Biol.* 64, 1–9. <https://doi.org/10.1016/j.cob.2020.01.003>.
 56. Sun, J.H., Zhou, L., Emerson, D.J., Phyto, S.A., Titus, K.R., Gong, W., Gilgenast, T.G., Beagan, J.A., Davidson, B.L., Tassone, F., and Phillips-Cremins, J.E. (2018). Disease-associated short tandem repeats co-localize with chromatin domain boundaries. *Cell* 175, 224–238.e15. <https://doi.org/10.1016/j.cell.2018.08.005>.
 57. Zhang, Y., Li, T., Preissl, S., Amaral, M.L., Grinstein, J.D., Farah, E.N., Destici, E., Qiu, Y., Hu, R., Lee, A.Y., et al. (2019). Transcriptionally active HERV-H retrotransposons demarcate topologically associating domains in human pluripotent stem cells. *Nat. Genet.* 51, 1380–1388. <https://doi.org/10.1038/s41588-019-0479-7>.
 58. Brandão, H.B., Paul, P., van den Berg, A.A., Rudner, D.Z., Wang, X., and Mirny, L.A. (2019). RNA polymerases as moving barriers to condensin loop extrusion. *Proc. Natl. Acad. Sci. USA* 116, 20489–20499. <https://doi.org/10.1073/pnas.1907009116>.
 59. Melamed, A., Yaguchi, H., Miura, M., Witkover, A., Fitzgerald, T.W., Birney, E., and Bangham, C.R. (2018). The human leukemia virus HTLV-1 alters the structure and transcription of host chromatin in cis. *eLife* 7, e36245. <https://doi.org/10.7554/eLife.36245>.
 60. Bellefroid, M., Rodari, A., Galais, M., Krijger, P.H.L., Tjalsma, S.J.D., Nestola, L., Plant, E., Vos, E.S.M., Cristinelli, S., Van Driessche, B., et al. (2022). Role of the cellular factor CTCF in the regulation of bovine leukemia virus latency and three-dimensional chromatin organization. *Nucleic Acids Res.* 50, 3190–3202. <https://doi.org/10.1093/nar/gkac107>.
 61. Flavahan, W.A., Drier, Y., Liau, B.B., Gillespie, S.M., Venteicher, A.S., Stemmer-Rachamimov, A.O., Suvà, M.L., and Bernstein, B.E. (2016). Insulator dysfunction and oncogene activation in IDH mutant gliomas. *Nature* 529, 110–114. <https://doi.org/10.1038/nature16490>.
 62. Vaillancourt, K., Yang, J., Chen, G.G., Yerko, V., Théroux, J.F., Aouabed, Z., Lopez, A., Thibeault, K.C., Calipari, E.S., Labonté, B., et al. (2021). Cocaine-related DNA methylation in caudate neurons alters 3D chromatin structure of the IRXA gene cluster. *Mol. Psychiatry* 26, 3134–3151. <https://doi.org/10.1038/s41380-020-00909-x>.
 63. Kloetgen, A., Thandapani, P., Ntziachristos, P., Ghebrechristos, Y., Nomikou, S., Lazaris, C., Chen, X., Hu, H., Bakogianni, S., Wang, J., et al. (2020). Three-dimensional chromatin landscapes in T cell acute lymphoblastic leukemia. *Nat. Genet.* 52, 388–400. <https://doi.org/10.1038/s41588-020-0602-9>.
 64. Oh, H.J., Agular, R., Kesner, B., Lee, H.-G., Kriz, A.J., Chu, H.-P., and Lee, J.T. (2021). Jpx RNA regulates CTCF anchor site selection and formation of chromosome loops. *Cell* 184, 6157–6173.e24. <https://doi.org/10.1016/j.cell.2021.11.012>.
 65. Allinne, J., Pichugin, A., Iarovaia, O., Klibi, M., Barat, A., Zlotek-Zlotkiewicz, E., Markozashvili, D., Petrova, N., Camara-Clayette, V., Ioudinkova, E., et al. (2014). Perinuclear relocalization and nucleolin as crucial events in the transcriptional activation of key genes in mantle cell lymphoma. *Blood* 123, 2044–2053. <https://doi.org/10.1182/blood-2013-06-510511>.
 66. Germini, D., Tsfasman, T., Klibi, M., El-Amine, R., Pichugin, A., Iarovaia, O.V., Bilhou-Nabera, C., Subra, F., Bou Saada, Y., Sukhanova, A., et al. (2017). HIV Tat induces a prolonged MYC relocalization next to IGH in circulating B-cells. *Leukemia* 31, 2515–2522. <https://doi.org/10.1038/leu.2017.106>.
 67. Kuroda, M., Tanabe, H., Yoshida, K., Oikawa, K., Saito, A., Kiyuna, T., Mizusawa, H., and Mukai, K. (2004). Alteration of chromosome positioning during adipocyte differentiation. *J. Cell Sci.* 117, 5897–5903. <https://doi.org/10.1242/jcs.01508>.
 68. Parada, L.A., McQueen, P.G., and Misteli, T. (2004). Tissue-specific spatial organization of genomes. *Genome Biol.* 5, R44. <https://doi.org/10.1186/gb-2004-5-7-r44>.
 69. Roix, J.J., McQueen, P.G., Munson, P.J., Parada, L.A., and Misteli, T. (2003). Spatial proximity of translocation-prone gene loci in human lymphomas. *Nat. Genet.* 34, 287–291. <https://doi.org/10.1038/ng1177>.
 70. Redin, C., Brand, H., Collins, R.L., Kammin, T., Mitchell, E., Hodge, J.C., Hanscom, C., Pillalamarri, V., Seabra, C.M., Abbott, M.-A., et al. (2017). The genomic landscape of balanced cytogenetic abnormalities associated with human congenital anomalies. *Nat. Genet.* 49, 36–45. <https://doi.org/10.1038/ng.3720>.
 71. Akdemir, K.C., Le, V.T., Chandran, S., Li, Y., Verhaak, R.G., Beroukhim, R., Campbell, P.J., Chin, L., Dixon, J.R., Futreal, P.A., et al. (2020). Disruption of chromatin folding domains by somatic genomic rearrangements in human cancer. *Nat. Genet.* 52, 294–305. <https://doi.org/10.1038/s41588-019-0564-y>.
 72. van Ruiten, M.S., and Rowland, B.D. (2021). On the choreography of genome folding: a grand pas de deux of cohesin and CTCF. *Curr. Opin. Cell Biol.* 70, 84–90. <https://doi.org/10.1016/j.cob.2020.12.001>.
 73. Narendra, V., Bulajić, M., Dekker, J., Mazzoni, E.O., and Reinberg, D. (2016). CTCF-mediated topological boundaries during development foster appropriate gene regulation. *Genes Dev.* 30, 2657–2662. <https://doi.org/10.1101/gad.288324.116>.
 74. Willemijn, A., Lopez-Delisle, L., Bolt, C.C., Gadolini, M.-L., Duboule, D., and Rodriguez-Carballo, E. (2021). Induction of a chromatin boundary in vivo upon insertion of a TAD border. *Plos Genet.* 17, e1009691. <https://doi.org/10.1371/journal.pgen.1009691>.
 75. Gong, W., Liu, Y., Qu, H., Liu, A., Sun, P., and Wang, X. (2019). The effect of CTCF binding sites destruction by CRISPR/Cas9 on transcription of metallothionein gene family in liver hepatocellular carcinoma. *Biochem. Biophys. Res. Commun.* 510, 530–538. <https://doi.org/10.1016/j.bbrc.2019.01.107>.
 76. Samuelson, C., Radtke, S., Zhu, H., Llewellyn, M., Fields, E., Cook, S., Huang, M.-L.W., Jerome, K.R., Kiem, H.-P., and Humbert, O. (2021). Multiplex CRISPR/Cas9 genome editing in hematopoietic stem cells for fetal hemoglobin reinduction generates chromosomal translocations. *Mol. Ther. Methods Clin. Dev.* 23, 507–523. <https://doi.org/10.1016/j.omtn.2021.01.008>.
 77. Liu, X.S., Wu, H., Ji, X., Stelzer, Y., Wu, X., Czauderna, S., Shu, J., Dadon, D., Young, R.A., and Jaenisch, R. (2016). Editing DNA methylation in the mammalian genome. *Cell* 167, 233–247.e17. <https://doi.org/10.1016/j.cell.2016.08.056>.
 78. Tarjan, D.R., Flavahan, W.A., and Bernstein, B.E. (2019). Epigenome editing strategies for the functional annotation of CTCF insulators. *Nat. Commun.* 10, 4258. <https://doi.org/10.1038/s41467-019-12166-w>.
 79. Kantidze, O.L., Luzhin, A.V., Nizovtseva, E.V., Safina, A., Valieva, M.E., Golov, A.K., Velichko, A.K., Lyubitelev, A.V., Feofanov, A.V., Gurova, K.V., et al. (2019). The anti-cancer drugs curaxins target spatial genome organization. *Nat. Commun.* 10, 1441. <https://doi.org/10.1038/s41467-019-09500-7>.
 80. Tsujikawa, L.M., Kharenko, O.A., Stotz, S.C., Rakai, B.D., Sarsons, C.D., Gilham, D., Wasiak, S., Fu, L., Sweeney, M., Johansson, J.O., et al. (2022). Breaking boundaries: Pan BETi disrupt 3D chromatin structure, BD2-selective BETi are strictly epigenetic transcriptional regulators. *Biomed. Pharmacother.* 152, 113230. <https://doi.org/10.1016/j.biopha.2022.113230>.
 81. Chen, H.-S., De Leo, A., Wang, Z., Kerekovic, A., Hills, R., and Lieberman, P.M. (2017). BET-inhibitors disrupt Rad21-dependent conformational control of KSHV latency. *PLoS Pathog.* 13, e1006100. <https://doi.org/10.1371/journal.ppat.1006100>.
 82. Miyata, K., Imai, Y., Hori, S., Nishio, M., Loo, T.M., Okada, R., Yang, L., Nakadai, T., Maruyama, R., Fujii, R., et al. (2021). Pericentromeric noncoding RNA changes DNA binding of CTCF and inflammatory gene expression in senescence and cancer. *Proc. Natl. Acad. Sci. USA* 118, e2025647118. <https://doi.org/10.1073/pnas.2025647118>.
 83. Pavlaki, I., Docquier, F., Chernukhin, I., Kita, G., Gretton, S., Clarkson, C.T., Teif, V.B., and Klenova, E. (2018). Poly(ADP-ribosylation) associated changes in CTCF-chromatin binding and gene expression in breast cells. *Biochim. Biophys. Acta Gen. Regul. Mech.* 1861, 718–730. <https://doi.org/10.1016/j.bbarm.2018.06.010>.
 84. Pugacheva, E.M., Kubo, N., Loukinov, D., Tajmul, M., Kang, S., Kovalchuk, A.L., Strunnikov, A.V., Zentner, G.E., Ren, B., and Lobanov, V.V. (2020). CTCF mediates chromatin looping via N-terminal domain-dependent cohesin retention. *Proc. Natl. Acad. Sci. USA* 117, 2020–2031. <https://doi.org/10.1073/pnas.1911708117>.
 85. Lupey-Green, L.N., Caruso, L.B., Madzo, J., Martin, K.A., Tan, Y., Hulse, M., and Tempera, I. (2018). PARP1 stabilizes CTCF binding and chromatin structure to maintain Epstein-Barr virus latency type. *J. Virol.* 92, 007555–18–e818. <https://doi.org/10.1128/JVI.00755-18>.
 86. Kitchen, N.S., and Schoenherr, C.J. (2010). Sumoylation modulates a domain in CTCF that activates transcription and decondenses chromatin. *J. Cell. Biochem.* 111, 665–675. <https://doi.org/10.1002/jcb.22751>.

87. Luo, H., Yu, Q., Liu, Y., Tang, M., Liang, M., Zhang, D., Xiao, T.S., Wu, L., Tan, M., Ruan, Y., et al. (2020). LATS kinase-mediated CTCF phosphorylation and selective loss of genomic binding. *Sci. Adv.* 6, eaaw4651. <https://doi.org/10.1126/sciadv.aaw4651>.
88. Dahlqvist, J., Fulco, C.P., Ray, J.P., Liechi, T., de Boer, C.G., Lieb, D.J., Eisenhaure, T.M., Engreitz, J.M., Roederer, M., and Hacohen, N. (2022). Systematic identification of genomic elements that regulate FCGR2A expression and harbor variants linked with autoimmune disease. *Hum. Mol. Genet.* 31, 1946–1961. <https://doi.org/10.1093/hmg/ddab372>.
89. Guo, Y.A., Chang, M.M., Huang, W., Ooi, W.F., Xing, M., Tan, P., and Skanderup, A.J. (2018). Mutation hotspots at CTCF binding sites coupled to chromosomal instability in gastrointestinal cancers. *Nat. Commun.* 9, 1520. <https://doi.org/10.1038/s41467-018-03828-2>.
90. Ushiki, A., Zhang, Y., Xiong, C., Zhao, J., Georgakopoulos-Soares, I., Kane, L., Jamieson, K., Bamshad, M.J., Nickerson, D.A., University of Washington Center for Mendelian Genomics, et al. (2021). Deletion of CTCF sites in the SHH locus alters enhancer-promoter interactions and leads to acheiropodia. *Nat. Commun.* 12, 2282. <https://doi.org/10.1038/s41467-021-22470-z>.
91. Oh, S., Shao, J., Mitra, J., Xiong, F., D'Antonio, M., Wang, R., Garcia-Bassets, I., Ma, Q., Zhu, X., Lee, J.-H., et al. (2021). Enhancer release and retargeting activates disease-susceptibility genes. *Nature* 595, 735–740. <https://doi.org/10.1038/s41586-021-03577-1>.
92. Xu, Q., Chen, M.Y., He, C.Y., Sun, L.P., and Yuan, Y. (2013). Promoter polymorphisms in trefoil factor 2 and trefoil factor 3 genes and susceptibility to gastric cancer and atrophic gastritis among Chinese population. *Gene* 529, 104–112. <https://doi.org/10.1016/j.gene.2013.07.070>.
93. Duan, J., Bao, C., Xie, Y., Guo, H., Liu, Y., Li, J., Liu, R., Li, P., Bai, J., Yan, Y., et al. (2022). Targeted core-shell nanoparticles for precise CTCF gene insert in treatment of metastatic breast cancer. *Bioact. Mater.* 11, 1–14. <https://doi.org/10.1016/j.bioactmat.2021.10.007>.
94. Deng, W., Rupon, J.W., Krivega, I., Breda, L., Motta, I., Jahn, K.S., Reik, A., Gregory, P.D., Rivella, S., Dean, A., and Blobel, G.A. (2014). Reactivation of developmentally silenced Globin genes by forced chromatin looping. *Cell* 158, 849–860. <https://doi.org/10.1016/j.cell.2014.05.050>.
95. Morgan, S.L., Mariano, N.C., Bermudez, A., Arruda, N.L., Wu, F., Luo, Y., Shankar, G., Jia, L., Chen, H., Hu, J.-F., et al. (2017). Manipulation of nuclear architecture through CRISPR-mediated chromosomal looping. *Nat. Commun.* 8, 15993. <https://doi.org/10.1038/ncomms15993>.
96. Kim, J.H., Rege, M., Valeri, J., Dunagin, M.C., Metzger, A., Titus, K.R., Gilgenast, T.G., Gong, W., Beagan, J.A., Raj, A., and Phillips-Cremmins, J.E. (2019). LADL: light-activated dynamic looping for endogenous gene expression control. *Nat. Methods* 16, 633–639. <https://doi.org/10.1038/s41592-019-0436-5>.
97. Soochit, W., Sleutels, F., Stik, G., Bartkuhn, M., Basu, S., Hernandez, S.C., Merzouk, S., Vidal, E., Boers, R., Boers, J., et al. (2021). CTCF chromatin residence time controls three-dimensional genome organization, gene expression and DNA methylation in pluripotent cells. *Nat. Cell Biol.* 23, 881–893. <https://doi.org/10.1038/s41556-021-00722-w>.

1.3.3. Interchromosomal contacts

Increasing evidence suggests that interchromosomal contacts represent an important regulatory and structural layer of the genome. The most well-known and widely-conserved ICC is the nucleolus, where the ribosomal genes from five different acrocentric chromosomes coalesce within a defined nucleolar compartment for ribosome biogenesis. Multiple interchromosomal contacts have been reported to play a regulatory or fate-defining role, frequently in a stochastic manner (Spilianakis et al. 2005; Lomvardas et al. 2006; Horta et al. 2018; Apostolou and Thanos 2008; Johnston and Desplan 2014; Harada et al. 2015; Fitz-James et al. 2023; Tchurikov et al. 2023). For example, the choice of one out of a thousand of olfactory receptor genes in a single olfactory neuron is determined by a stochastic interchromosomal contact with a *trans*-acting enhancer on chr 14 (Lomvardas et al. 2006; Horta et al. 2018). The subset of cells that express *IFN- β* in response to viral infection was shown to be stochastically determined by the presence of ICCs with three distinct genetic loci that could mediate binding of the limiting transcription factor NF- κ B to the *IFN- β* enhancer (Apostolou and Thanos 2008). The developmental pathway followed by a CD4+ T-cell is also influenced by an interchromosomal interaction between the promoter region of the *IFN- γ* gene on chromosome 10 and the regulatory regions of the TH2 cytokine locus on chromosome 11 (Spilianakis et al. 2005). The loci from different chromosomes may also come into contact following recruitment to the same transcription sites (Jackson et al. 1993; Osborne et al. 2004; Razin et al. 2011). This is the case for the active globin genes (Schoenfelder et al. 2010; Simonis et al. 2006), plasma cell identity genes (Bortnick et al. 2018), immediate early genes in B cells upon stimulation of the B cell receptor signaling pathway (Osborne et al. 2007) and the heat shock response genes in yeast (Chowdhary et al. 2019). In general, ICCs were shown to form predominantly between transcriptionally active and accessible loci rather than between the silent ones (Kalhor et al. 2012). Being a more stochastic process than an intrachromosomal contact, partially predefined by the 2D distance between the loci, a particular ICC is likely present in a fraction of cells in a population (Noordermeer et al. 2011), and an increase in transcriptional activity and accessibility of a locus might favor its participation in an ICC.

Transcription activity and chromatin accessibility are generally inversely correlated with the proximity of the loci to the nuclear periphery (Sadoni et al. 1999; M. Cremer et al. 2001; Kind et al. 2015; C. Y et al. 2018; Mota et al. 2022b) and experimental repositioning of chromosomes in the nuclear space leads to gene expression changes (Finlan et al. 2008). Chromosomal translocations inevitably lead to the repositioning of at least one of the translocated loci. Inversely, the frequency of a certain translocation may be influenced by the temporal spatial proximity of the potential translocation partners (Canoy et al. 2023; Engreitz, Agarwala, and Mirny 2012). For example, *MYC* and *IGH*, the genes involved in one of the most frequent oncogenic translocations causing Burkitt lymphoma, were shown to be preferentially recruited to the same transcription factory upon induction of the B cell receptor signaling pathway, which may explain the high rate of this translocation in B

lymphocytes (Osborne et al. 2007). An inverse, yet similar phenomenon, was observed in Mantle Cell Lymphoma, where the translocated *CCND1* allele relocated closer to the nucleolus, to the vicinity of active Pol II sites (Allinne et al. 2014b). Interchromosomal contacts likely follow a similar dependency, where an increase in loci proximity leads to an increase in the probability of an ICC formation. Simultaneous increase in accessibility and transcription further escalates the ICC chance (Kalhor et al. 2012), as the transcriptional machinery and co-factors associated with the actively transcribing chromatin can form condensates thus prompting the interaction (Cho et al. 2018; Chong et al. 2018; Gibson et al. 2019; H. Lu et al. 2018; Sabari et al. 2018). This is in line with the observation that A compartments have a stronger predisposition to form ICCs with the likelihood to interact in *trans*- decreasing sequentially from A-A > A-B \approx B-B (Branco and Pombo 2006; Rao et al. 2014; Yaffe and Tanay 2011; Su et al. 2020b), as well as with the tendency of A-compartments to be speckle-associated (C. Y et al. 2018; Su et al. 2020b).

A and B compartments can be relatively well-predicted using epigenetic data (Fortin and Hansen 2015). The loss of cohesin, one of the proteins responsible for the formation of chromatin loops, causes the pattern of long-range contacts to match that of the histone marks (Rao et al. 2017); notably, it results in the colocalization of super-enhancers (SEs) (Rao et al. 2017) - large stretches of enhancer elements marked by high levels of H3K27 acetylation (Parker et al. 2013), which suggest the involvement of SEs in the formation of long-range chromatin interactions. This process might be facilitated by condensate formation through phase-separation, as acetylated chromatin was shown to phase separate *in vitro* upon binding of the multi-bromodomain proteins, such as BRD4 (Gibson et al. 2019), which is typically present at SEs (Chapuy et al. 2013). Interestingly, ICCs associated with nuclear speckles, ubiquitous nuclear condensates, were found enriched for the common super-enhancer domains (Joo et al. 2023) (SEs showing persistent and ubiquitous H3K27ac signals across different cell and tissue types (Ryu et al. 2019)), allowing to speculate that the rearrangement of super-enhancer landscape, common for multiple cancers (Betancur et al. 2017; Ke et al. 2017; Wong et al. 2017; Y.-Y. Jiang et al. 2017; Cohen et al. 2017; Yohe et al. 2018), might induce aberrant ICC formation in certain circumstances.

2. OBJECTIVES OF THE STUDY

T(11;14) translocation is the most specific characteristic of Mantle Cell Lymphoma present in the vast majority of patients. Among the consequences of this translocation, *CCND1* upregulation is the most studied. Nevertheless, data from animal models argue that *CCND1* overexpression alone is not enough to cause MCL (Lovec et al. 1994; Bodrug et al. 1994). Efforts have been made to uncover other molecular mechanisms and pathways deregulated in MCL, but, with the exception of BTK inhibitors, the therapeutic agents targeting those pathways exhibited limited clinical success. The therapeutic response and life expectancy of MCL patients remain modest, making MCL a B cell lymphoma with one of the worst prognosis. Thus, further insights into the pathogenesis of the disease bringing up new treatment strategies are urgently needed.

Chromosomal translocation inevitably alters the 3D-genome of the cell, which, in turn, may alter its epigenetic and transcriptional landscape, potentially affecting cancer-related genes and pathways. Still, the 3D-genome and the epigenome of MCL are largely underexplored. In this work, we aimed to study the 3D-genomic, epigenomic and associated transcriptomic changes happening in MCL cells to uncover some previously unknown mechanisms driving MCL oncogenesis after the t(11;14), other than *CCND1* upregulation. Through this study, we aimed to contribute to the advancement of knowledge in the field and provide a basis for future therapy development, specifically in the rapidly growing field of epigenetic drugs.

3. RESULTS

3.1. Der14 relocates to the nuclear center in MCL cells

Chr11-chr14 translocation is a major hallmark of MCL cells, and its effect on the *CCND1* gene expression is well-studied. Meanwhile, chromosomal translocation also alters the 3D-organization of the genome and inevitably affects the nuclear positioning of one or both of the translocated loci. To explore the changes in the nuclear positioning of the t(11;14) translocation partners, we performed 3D-FISH with the fluorescent probes allowing us to distinguish the intact chromosomes 11 and 14, and the derivative chromosome 14, resulting from the chr14-chr11 fusion (**Figure 7a**). The red probe was complementary to the region downstream of the translocation breakpoint and encompassed the *CCND1* locus, while the green probe was complementary to the region upstream of the translocation breakpoint and encompassed the locus immediately upstream of the variable IGH region; in this set-up, the derivative chromosome 14 could be distinguished by the overlap of the green and red signals (**Figure 7ab**).

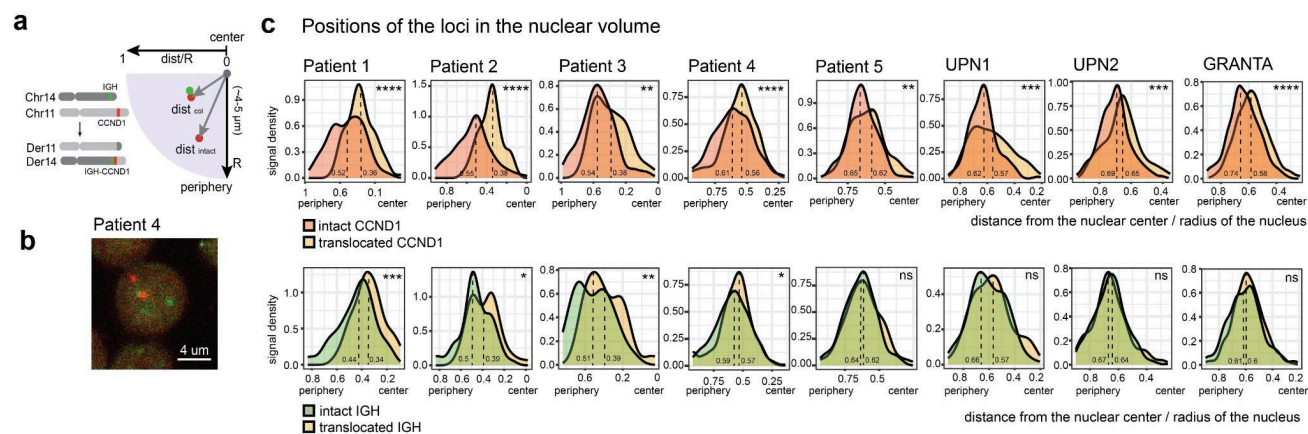


Figure 7. Nuclear positioning of the translocated loci.

a, Schematic representation of the fluorescent probes used for the detection of the intact *CCND1* and *IGH* loci and the derivative chromosome 14, and the approach used for the signal quantification. Briefly, for each cell, the distances from the intact and translocated signals to the nuclear center were measured and normalized to the nuclear radius. The resulting values for all quantified cells were then plotted to show the distributions of the signals in a population of cells. **b**, Representative image of a B cell with the t(11;14) translocation; maximum projection z-stack of three 0.5 μm confocal slices. **c**, Density plots showing the distributions of the intact (red or green) and translocated (yellow) *CCND1* and *IGH* loci in the nuclear volume in the B cells from five MCL patients and three MCL cell lines (UPN1, UPN2 and GRANTA). Statistical significance is determined using the Kolmogorov-Smirnov test for the equity of distributions; pval <0.05*, <0.01**, <0.001***, 0.0001****.

The 3D-FISH experiment was performed in the B cells from five MCL patients and three MCL cell lines (GRANTA-519, UPN1, UPN2), and the distance of each signal to the nuclear center was measured and normalized to the nuclear radius (**Figure 7a**). In all patients and most of the MCL cell lines, the intact *IGH* locus was more centrally located than the intact *CCND1* locus, consistent with their reported chromosome territories (Bolzer et al. 2005). Nevertheless, while the position of the translocated *IGH* locus was almost unaffected by the translocation, the distribution of the translocated *CCND1* allele was shifted to the nuclear center when compared to the intact *CCND1* copy (**Figure 7c**). Thus, in MCL cells, the translocated *CCND1* allele relocated to the nuclear center, closer to the translocation partner locus.

3.2. Active epigenetic signature is globally altered in MCL cells

Relocalisation of the loci in the nuclear space may bring about the changes in their epigenetic and transcription profiles. Notably, centrally located genomic regions are generally characterized by being epigenetically accessible and transcriptionally active. To explore the changes in the epigenetic and transcriptional landscape of mantle cell lymphoma cells, we analyzed the profiles of transcription and chromatin accessibility, as well as the distribution of the activating H3K27Ac mark, known to label active enhancers and promoters, in the B cells from MCL patients and control naive B cells from healthy donors.

More than 1000 sites with increased chromatin accessibility and more than 13000 sites with increased H3K27Ac binding were identified in MCL cells compared to the control naive B cells (**Figure 8a**). The genes nearest to the upregulated ATAC and H3K27Ac sites were functionally enriched for a number of categories relevant for lymphoma, including B cell activation, positive activation of cytokine production and cell adhesion, as well as for some categories indicating epigenetic reprogramming, e.g. histone modification (**Figure 8b**). Consistent with the increased transcriptional activity of many genes in MCL vs control B cells (**Figure 8d**), most (80%) of the sites with increased H3K27Ac binding were located in gene promoters, while approximately 20% of those sites mapped to other locations (**Figure 8c**) and likely represented the newly active enhancers.

To further explore the deregulation of the enhancer landscape in MCL cells, we applied the activity by contact (ABC) model (Fulco et al. 2019) that infers the enhancer-gene interactions from the ATAC-seq, H3K27Ac ChIP-seq, HiC and expression data (*see Materials and Methods*). We identified 939 enhancers that were novel or more active in MCL cells compared to the control B cells, as determined by the increased H3K27Ac binding. Those overactive enhancers were predicted to regulate more than 370 genes that were highly upregulated in MCL (**Figure 8d**), including the *MYCN* oncogene, *MECOM* and *SRC* proto-oncogenes, and several proliferation or growth-stimulating genes, such as *CCNE1*, *RASGRF1* and *PIK3R2*. *CCND1* gene was also predicted to be regulated by an overactive enhancer on

chromosome 11, though in MCL context such interaction could only occur for the intact *CCND1* copy, as the translocated one is found in a different genomic context.

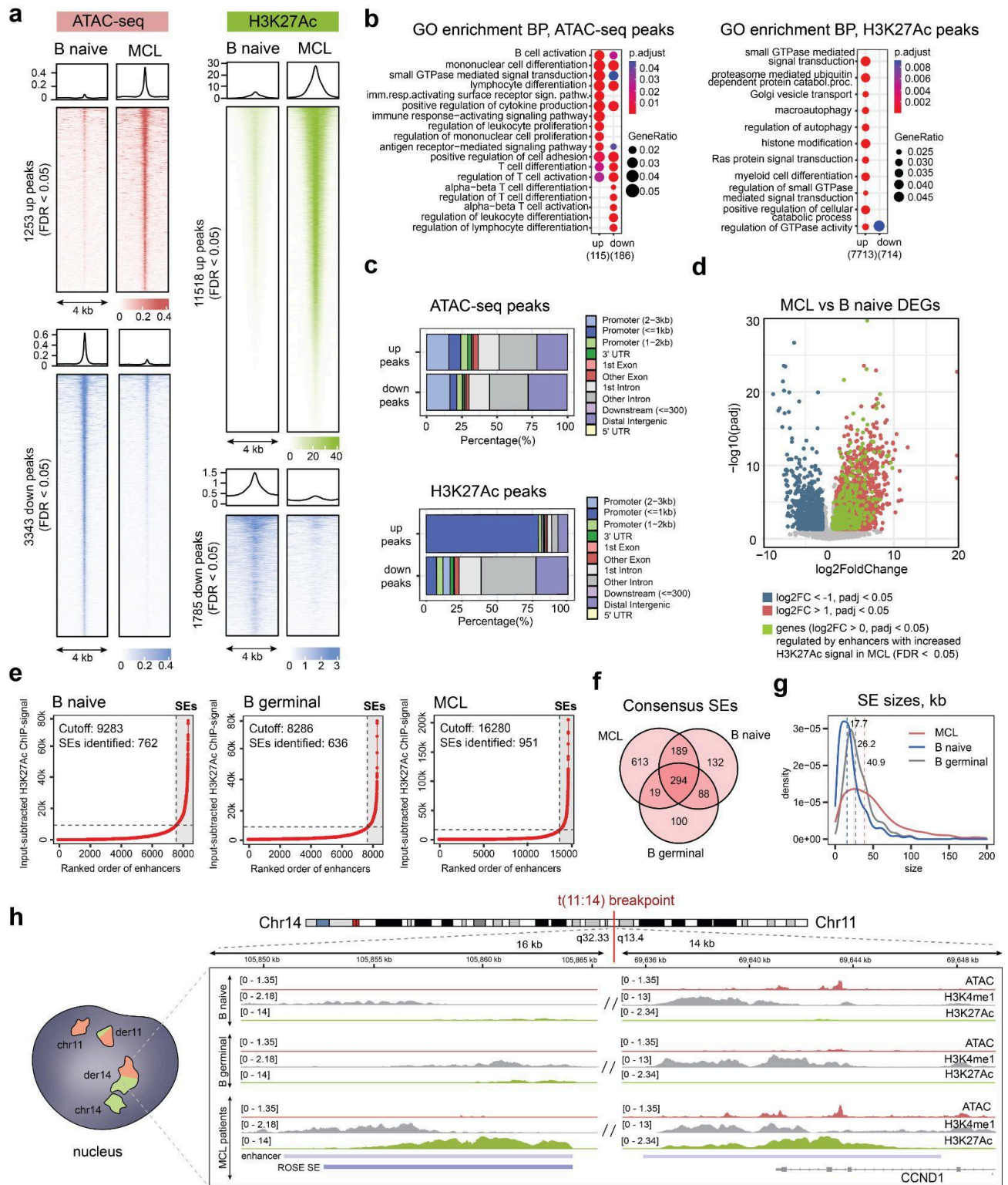


Figure 8. Epigenetic deregulation in MCL cells.

a, ChIP-seq/ATAC-seq profiles for the H3K27Ac and ATAC peaks with the significantly different H3K27Ac/ATAC signal in the MCL patients vs control naive B cells from healthy

donors (FDR < 0.05). **b**, Gene Ontology enrichment analysis for the ATAC/ H3K27Ac peaks with the significantly different ATAC/H3K27Ac signal in the MCL patients vs control naive B cells from healthy donors (FDR < 0.05). Top 10 enriched categories. **c**, Distributions of the up/down ATAC/H3K27Ac peaks relative to genomic features. **d**, Differentially expressed genes (DEGs) in the MCL patients B cells vs control naive B cells from healthy donors. Upregulated genes ($\log_2FC > 1$, $p_{adj} < 0.05$) are colored red, downregulated genes ($\log_2FC > 1$, $p_{adj} < 0.05$) are colored blue. The genes predicted to be regulated by an enhancer with the significantly increased (FDR < 0.05) H3K27Ac signal in MCL patients vs control naive B cells are colored green. The gene-enhancer pairs were inferred using the ABC model (see Materials and methods). **e**, Rank Ordering of Super Enhancers (ROSE) graphs for the MCL patients and control naive or germinal B cells (representative graphs for one biological replicate). Each dot represents an enhancer region ranked by increasing cumulative H3K27Ac signal. The dashed line demarcating the shaded region to the right represents the threshold of calling a region a super-enhancer. **f**, Venn diagram showing the numbers of SEs consensus between the biological replicates for each condition (MCL, control naive B cells, control germinal B cells) and the overlap of those consensus SEs between the conditions. **g**, Size distributions of the consensus SEs in the MCL patients and control naive or germinal B cells from healthy donors. The dashed lines indicate the median values. **h**, A novel MCL-specific super-enhancer formed due to the extension of the IGH enhancer into the CCND1 locus. Representative tracks for the ATAC-seq, H3K27Ac and H3K4me1 ChIP-seq signal scaled to one million mapped reads are shown. The blue bars indicate that an H3K27Ac peak (“enhancer”) or a ROSE super-enhancer were detected in the region.

Considering a large number of overactive enhancers in MCL cells, we also explored their super-enhancer landscape. Using the rank-ordering of super-enhancers (ROSE) algorithm on the H3K27Ac ChIP data, we detected 1121 superenhancers to be active in at least two MCL patient samples, compared to 752 and 520 for control naive and germinal B cells respectively (**Figure 8e**, **Supplementary figure 1a**). 26% (294) of MCL SEs were shared between all the three groups (**Figure 8f**) and represented the SEs defining the core B cell identity. Those SEs were associated with the genes encoding the components of the MHC II complex (e.g. *HLA-DOA*, *HLA-DPB1*), Ig proteins (*IgL*, *IGK*, *IGH*) and the core genes of the BCR signaling pathway (e.g. *SYK*) (**Supplementary figure 8c**). Consistent with the presumed origin of MCL from naive B cells, 17% (189) of MCL SEs were shared exclusively with the naive B cells group, while for the germinal B cells this overlap was only 1.7% (19) (**Figure 8f**). The genes associated with the SEs unique for MCL were mainly involved in immune-response signaling and lymphocyte activation (**Supplementary figure 1d**) and were also enriched for lymphoma-related genes (**Supplementary figure 1b**). Several of them have been previously described in the context of MCL, including *CD5*, *WEE1* and *IL2RA* (Alaggio et al. 2022; Chilà et al. 2014; Bassam et al. 2013). Others included known oncogenes (*PIM1*), pro-survival genes (*MAP4K1*, *PIM1*, *IL2RA*) or have been linked to other relevant processes, such as chromatin remodeling and transcription regulation (*PRDM8*, *ETV6*). We have also observed an increase in the size of super-enhancers in MCL cells: the median SE size of the control or germinal B cells was 17.7 - 26.2 kb, while in MCL this value was approximately twice as large (40.9 kb) (**Figure 8g**). All together, this data suggested the large-scale remodeling of the active enhancer

landscape in MCL cells.

3.3. MCL cells develop a novel superenhancer in the translocation breakpoint region

We next explored the local epigenetic changes in the breakpoint adjacent region on the derivative chromosome 14. Consistent with the known involvement of the IGH enhancer in the *CCND1* upregulation, we detected high levels of the H3K27Ac and H3K4me1 signal in the IGH locus (**Figure 8h**). This locus was classified as a super-enhancer in both the control and the MCL B cells. Importantly though, the level of the activating H3K27Ac mark in the region was more than twice as high in MCL compared to the control naive B cells. Moreover, in MCL cells, the enhancer-characteristic marks were largely extended into the adjacent region on chr11, including the *CCND1* locus, and this phenomenon was unique for MCL cells (**Figure 8h**). Thus, MCL cells formed a novel *IGH-CCND1* super-enhancer spanning the translocation breakpoint region.

3.4. Chromosome 19 is enriched for active promoters and deregulated genes in MCL

CCND1 overexpression is not sufficient for Mantle Cell Lymphoma development. Still, the t(11;14) translocation is a hallmark and likely the founding event of MCL. We have observed that, apart from the *CCND1* overexpression, the translocation induces the relocalisation of the *CCND1* locus on the derivative chromosome 14 to the nuclear center, which is accompanied by the formation of a novel MCL-specific super-enhancer in the breakpoint region. We thus searched for the genes other than *CCND1* that might be regulated by this novel SE using bulk RNA-seq data from a total of nine MCL patients and a cultured cell line GRANTA-519 (see *Materials and Methods*).

Contrary to what was expected, the largest number of upregulated genes in MCL samples was not located on chromosomes 11 or 14 (**Figure 9a**). Instead, it was chromosome 19 which was most enriched for the upregulated genes in MCL vs control cells (**Figure 9ab**). This phenomenon was reproducible between the patient samples and the MCL cell line (**Supplementary figure 2c**), and was evident with or without normalization of the upregulated gene numbers to chromosome size or to the number of genes per chromosome (**Figure 9a, Supplementary figure 2ac**). The genes upregulated on chromosome 19 were mostly enriched for the immune-response signaling pathways and leukocyte-mediated immunity, the categories relevant for MCL (**Figure 9b**). Many of those genes have been previously associated with mantle cell lymphoma, e.g. *BAX*, *CD70* (Beltran et al. 2011; Balsas et al. 2021), other lymphomas and leukemias, e.g. *BCL3*, *ELANE*, *MAP2K7* (Y. Shen et al.

2017; Manfroi et al. 2018; Seaton et al. 2024), or have been reported to have a pro-tumorigenic effect on the tumor microenvironment, e.g. *CD70*, *TYROBP* and *CEACAM1* (L. Guo et al. 2023; J. Lu et al. 2021; Gerstel et al. 2011; Balsas et al. 2021).

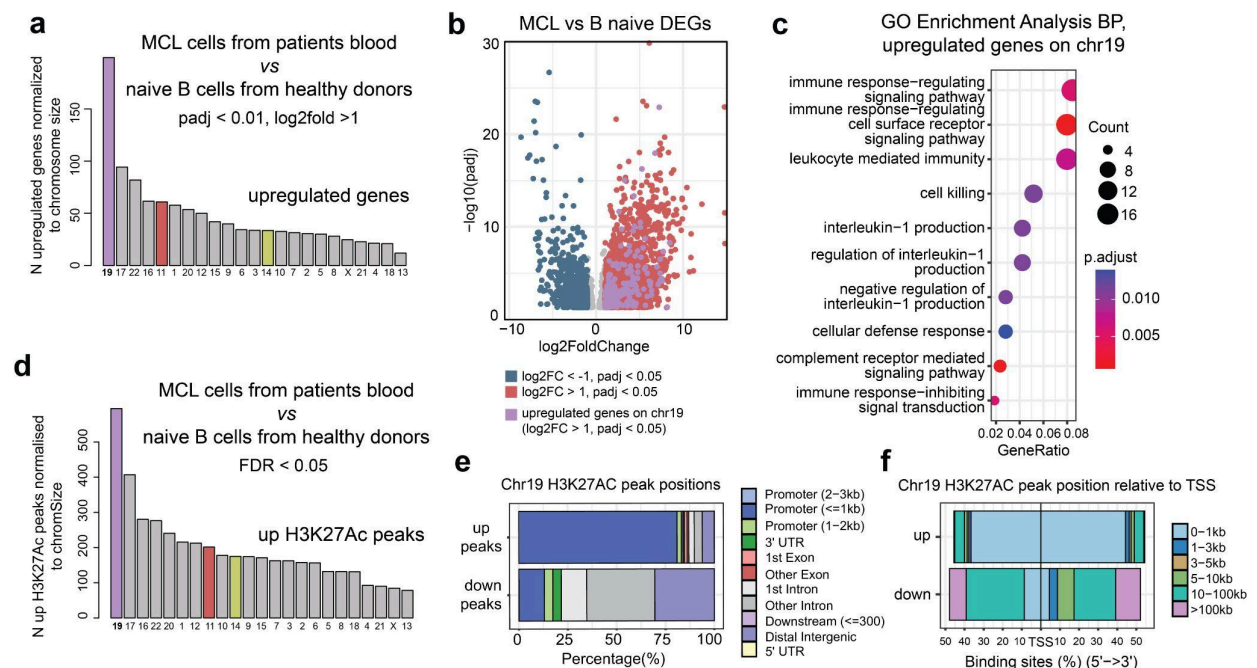


Figure 9. Chromosome 19 is enriched for overexpressed genes and active promoters in MCL.

a, The numbers of upregulated genes per chromosome in MCL patients B cells vs control naive B cells from healthy donors ($\text{padj} < 0.01$, $\log_2\text{FC} > 1$) normalized to chromosome sizes. **b**, Differentially expressed genes (DEGs) in the MCL patients B cells vs control naive B cells from healthy donors. Upregulated genes ($\log_2\text{FC} > 1$, $\text{padj} < 0.05$) are colored red, downregulated genes ($\log_2\text{FC} < -1$, $\text{padj} < 0.05$) are colored blue. The upregulated genes on chr19 are colored violet. **c**, Gene Ontology Biological Process enrichment for the genes upregulated on chr19 in the MCL patients B cells vs control naive B cells from healthy donors ($\text{padj} < 0.01$, $\log_2\text{FC} > 1$). Top 10 enriched categories. **d**, The numbers of up H3K27Ac per chromosome in MCL patients B cells vs control naive B cells from healthy donors ($\text{FDR} < 0.05$) normalized to chromosome sizes. **e**, Distribution of the H3K27Ac peaks differentially enriched in MCL on chr19 relative to genomic features. **f**, Positions of the H3K27Ac peaks differentially enriched in MCL on chr19 relative to the transcription start sites (TSS).

In line with the upregulated gene expression, chr19 also bore the largest number of up H3K27Ac peaks (**Figure 9d**, **Supplementary figure 2b**) and most of those peaks represented the overactivated promoters (**Figure 9ef**). The number of overactive enhancers was also relatively high on chr19, but this chromosome was not consistently at the top of the rank (ranked first, 12th or 13th depending on the method) (**Supplementary figure 9d**). Most of the up H3K27Ac peaks on chr19 were also not a part of SEs unique for MCL, and no prominent enrichment for the unique SEs was observed for chr19 (ranked first, 5th or 6th depending on the normalization) (**Supplementary figure 9e**). All together, chr19 was the most enriched for the overexpressed genes and overactivated promoters in MCL vs control B cells, but this

phenomenon was not directly correlated with a similar increase in the enhancer activity on this chromosome.

3.5. A superenhancer in the translocation breakpoint region interacts with chromosome 19

We found that chromosome 19 is most enriched for the overexpressed genes and overactive promoters in MCL. This was not directly related to the aberrant enhancer activity on this chromosome and no recurrent genetic aberrations are known to occur on chr19 in MCL. Meanwhile, chromosome 19 is known to occupy the territory in the nuclear center (Bolzer et al. 2005; Thomas Cremer and Cremer 2010). We observed the relocalisation of the breakpoint adjacent region of the derivative 14 to the nuclear center (**Figure 7c**) and the formation of an extended *IGH-CCND1* super-enhancer in this region (**Figure 8h**). We thus hypothesized that an interchromosomal contact might be present between this SE and some regions on chr19, which could explain the large-scale upregulation of gene expression in this chromosome.

To check this, we have performed HiC in the MCL cell line GRANTA and control lymphoblastoid cell line RPMI8866 without the t(11;14) translocation; we also explored the previously published HiC data from five MCL patients and three control samples of naive B cells from healthy donors (Vilarrasa-Blasi et al. 2021). We have observed that the contacts between the chr19 and the SE-containing locus on chr11 were indeed present in the MCL and control B cells (**Figure 10a**). Moreover, similar contacts were present on the other chromosomes enriched for the overexpressed genes, chr17 and chr22, potentially suggesting a grouped interchromosomal interaction. As all these chromosomes are relatively small and mobile, we had a look at another chromosome of a similar size, which was yet not enriched for the upregulated genes (chr21), and no contacts with the SE region were detected on this chromosome (**Figure 10a**). Chr21 was thus used as a negative control for further experiments. Apart from the contacts with the chr11 SE region, a drastic change in the chromatin compartments state on chr19 was observed in MCL patient cells. While in the control B cells from healthy donors most of the compartments on chr19 were classified as inactive, they switched to an active state in MCL cells (**Figure 10a**), indicating the large-scale chromatin activation on this chromosome and in line with the substantial upregulation of gene expression on chr19.

Although HiC is not a reliable quantitative method, the intensity of the chr19-chr11 interaction relative to the background seemed higher in MCL patient samples compared to the controls (**Figure 10a**). To further confirm the presence of the chr19-chr11 SE contact and quantify its prevalence in a population of cells, we performed 3D-FISH with the already described probes for the *IGH* and *CCND1* loci, and the probe overlapping the most intense chr19-chr11 contact hotspot on chr19

(site 1 in **Figure 10a**). The contact of interest was detected in 30-50% of MCL cells (depending on the patient or the cell line) (**Figure 10bc**), which was highly above the probability of random colocalization of two spheres of 1 μm diameter inside the 8 μm diameter nucleus ($\sim 2\%$). In accordance with the HiC results, the contact was also detected in the control B cells from healthy donors, but only in 15% of cells (**Figure 10c**). As an internal negative control, the contacts of the *CCND1* locus and chr21, for which no interaction was detected by HiC, were also quantified; as expected, the frequency of the chr11-chr21 interaction was equally low in all conditions (**Figure 10c**). Finally, in MCL cells, the contact formed predominantly with the derivative chromosome 14 and not the intact *CCND1* copy, suggesting that the interaction was facilitated by the presence of the *IGH-CCND1* super-enhancer.

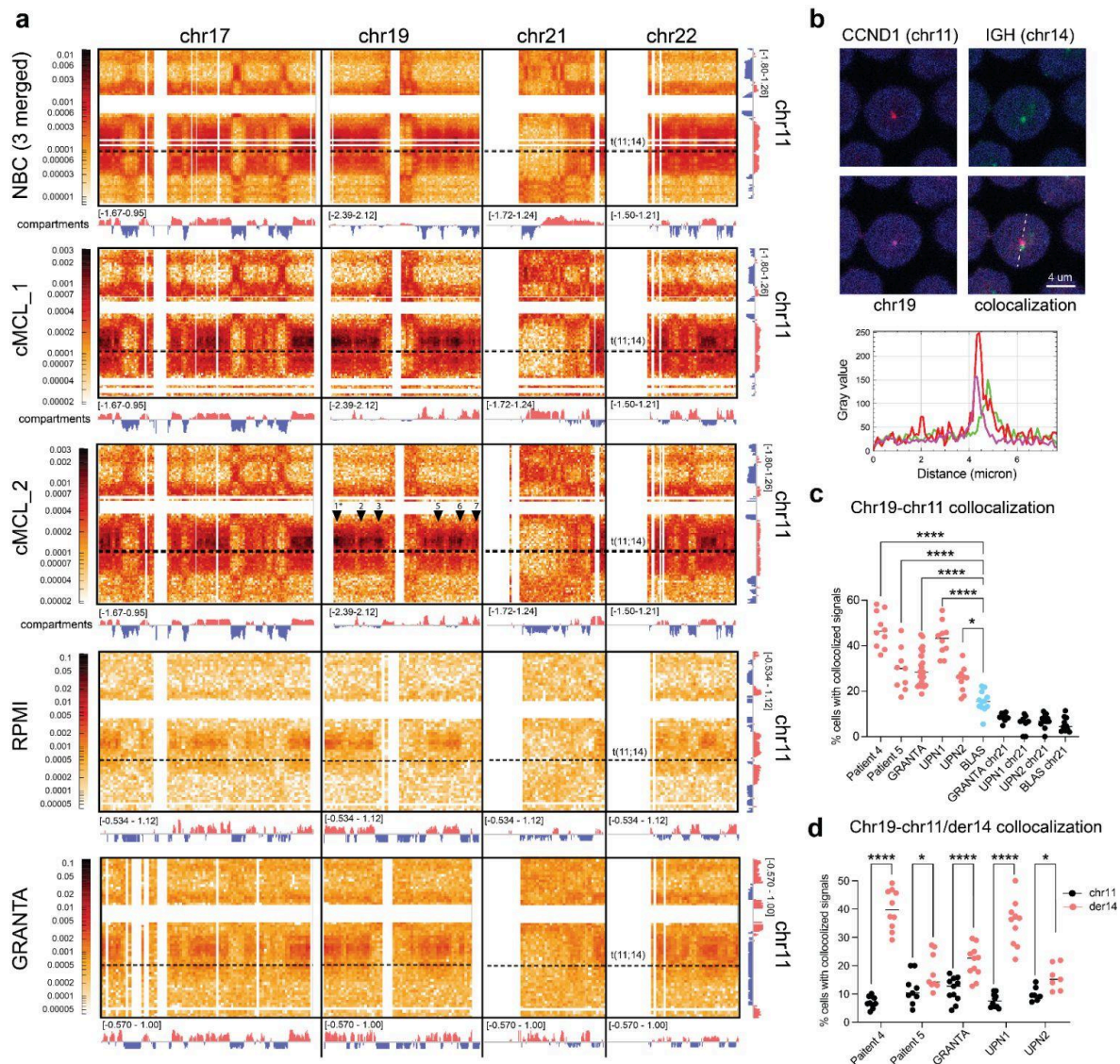


Figure 10. Interchromosomal contacts in MCL cells.

a, HiC maps of the regions of the interchromosomal contacts between the chr11 (*CCND1* locus) and the top 3 chromosomes by the number of upregulated genes - 19, 17 and 22. Chromosome 21, which is not enriched for the upregulated genes, is shown as negative control. For chromosome 11, only the region of interest is shown; *CCND1* locus is marked by

a dashed horizontal line. Black arrows demarcate the six contact hotspots referred to in the text. The arrow with the asterisk marks the contact region covered by the FISH probe in b-d. The tracks on the sides show the eigenvector values assigning the region to either active (positive scores, red) or inactive (negative scores, blue) compartments. N patients = 5 (representative maps for the two patients with conventional MCL are shown); N control B naive samples = 3 (merged replicates map is shown). **b**, The representative image of a contact between the derivative chromosome 14 and the locus on chr19 detected by 3D-FISH in the cells of an MCL patient. CCND1 locus is colored red, IGH locus is colored green and the chr19 locus is colored magenta. A maximum projection Z-stack of three 0.5 μm confocal slices is shown. The location of the chr19 FISH probe is marked by an arrow with the asterisk in a. **c**, The percentages of cells bearing the CCND1 - chr19 contact in a population of cells as detected by 3D-FISH in two MCL patients, three MCL cell lines (UPN1, UPN2, GRANTA) and a control lymphoblastoid cell line from a healthy donor (BLAS). The data is shown as median \pm SD, each dot represents a technical replica. Statistical significance is determined using ordinary one-way ANOVA with Dunnett's correction for multiple comparisons. The colocalization of chr11 with the chr21 for which no contact was detected by HiC is shown as negative control. **d**, The percentages of cells bearing the contact between chr19 and the intact (black) or translocated (red) CCND1 loci in two MCL patients and three MCL cell lines (UPN1, UPN2, GRANTA). The data is shown as median \pm SD, each dot represents a technical replica. Statistical significance is determined using paired t-test.

3.6. The chr19-SE contact colocalizes with the upregulated genes and active RNAPol II

Following the confirmation of the contact presence, we explored the epigenetic and transcriptional states of the detected interaction sites on chr19. The genome regions in the vicinity of the detected contacts were generally characterized by an increased chromatin accessibility and H3K27Ac levels in MCL patients vs control cells (**Figure 11a**; representative sites are shown). The genes overexpressed in MCL vs control naive B cells on chr19 also tended to cluster around the interaction hotspots (**Figure 11b**). Some of those genes have been previously associated with MCL or other malignancies. For example, the *ABCA7* gene (interaction site 1; >3 fold upregulation) encoding for the ATP-binding cassette transporter of the brain and immune system was found frequently mutated in the asian MCL patient population (Jeong et al. 2020) and its overexpression was associated with poor prognosis in ovarian carcinoma (Hedditch et al. 2014; Elsnerova et al. 2017). *ARID3A* (interaction site 1, >7 fold upregulation) encodes for a transcription factor involved in embryogenesis and B cell differentiation. It was shown to ensure the development and maintenance of the CD5+ B1a cells, and increased Arid3A levels supported the ability of those cells to develop B cell tumors with age (Hayakawa et al. 2019). CD5 is one of the most specific markers of MCL cells (Alaggio et al. 2022), and a subpopulation of the B1-derived B cells was reported to localize to the mantle zone and give rise to the MCL-like neoplasia in aged mice (Hayakawa et al. 2018). Some other genes included *KEAP1* (interaction site 2, >4.5 fold upregulation), one of the key oxidative stress sensors, whose expression was associated with the advanced stages in diffuse large

B cell lymphoma (X. Yi et al. 2018); *PIN1* (interaction site 2, >2 fold upregulation), encoding for the peptidyl-prolyl cis-trans isomerase highly expressed in the majority of cancers and negatively related to the clinical prognosis (Yang Chen et al. 2018) and the proto-oncogene *BCL3* (interaction site 5, > 4 fold upregulation) well-known for its role in lymphoma development (Seaton et al. 2024).

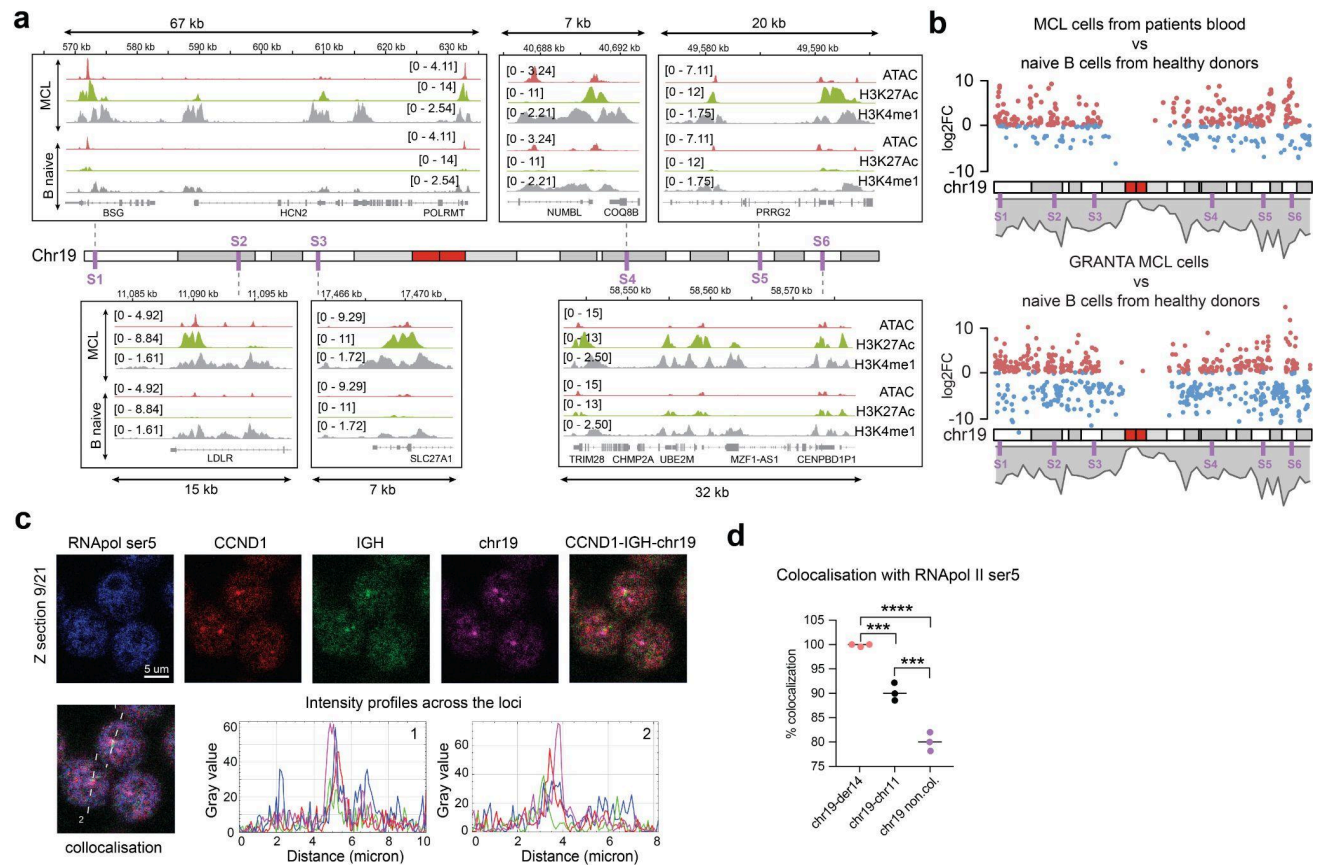


Figure 11. Transcriptional and epigenetic state of the chromatin around the der14-chr19 contact sites.

a, ATAC-seq, H3K27Ac and H3K4me1 ChIP-seq signals on chr19 around the chr19-chr11 contact hotspots in the MCL patients cells and the control naive B cells from healthy donors. Representative tracks scaled to one million mapped reads are shown. Chr19-chr11 contact hotspots identified by HiC are marked by violet bars. **b**, Differentially expressed genes (DEGs) on chr19 in the MCL patients B cells vs control naive B cells from healthy donors (up) or GRANTA-519 MCL cell line vs control naive B cells from healthy donors (down). Upregulated genes ($\log_2FC > 1$, $p_{adj} < 0.05$) are colored red, downregulated genes ($\log_2FC < -1$, $p_{adj} < 0.05$) are colored blue. Chr19-chr11 contact hotspots identified by HiC are marked by violet bars. **c**, Immuno-3D-FISH with the three hybridisation probes (CCND1 - red, IGH - green, chr19 - violet) and the antibodies against the RNAPolIII-ser5 (blue); representative images (one Z section) and the intensity profiles across the quadruple colocalization sites are shown. **d**, The frequencies of colocalization of the chr19-der14 contacts, chr19-intact chr11 contacts and non-colocalized chr19 with the RNAPolIII-ser5. The data is shown as median \pm SD, each dot represents a technical replica. Statistical significance is determined using ordinary one-way ANOVA with Dunnett's correction for multiple comparisons.

Given the large number of upregulated genes in the vicinity of the contacts, we next performed the immuno-3D-FISH with the *IGH*, *CCND1* and chr19-site1 probes and the antibodies against the RNA pol II CTD phospho Ser5, which is an activated form of RNAPol II confined to promoters and necessary for transcription initiation. Almost all of the chr19-der14 contacts (triple *IGH-CCND1*-chr19 colocalization events) also colocalized with the active RNAPol II staining (**Figure 11c**), suggesting the presence of the active transcription hub around the interaction. The intact *CCND1*-chr19 contacts also colocalized with the RNA-pol II, but with a lower frequency, and this frequency was even lower for the chr19 signals non colocalized with either of the chr11 probes (**Figure 11d**). All together, these data demonstrated that the der14-chr19 contacts were characterized by increased transcriptional activity, involving the genes relevant for lymphoma development.

3.7. Minnelide modifies the chromatin landscape and transcription profile of MCL cells

We have observed the general activation of the enhancer landscape in mantle cell lymphoma cells, both in the translocation breakpoint/ on chr19 and genome wide. Those newly active enhancers contributed to the upregulation of the genes potentially involved in lymphomagenesis. We thus tried to revert this pathological enhancer activation with the drugs reported to modify the enhancer landscape. We used Minnelide, a water-soluble pro-drug of a natural compound triptolide, which was shown to inhibit the super-enhancer activity in pancreatic cancer cells (Noel et al. 2020), likely by targeting the XPB subunits of the TFIIH complex (He et al. 2015; Noel et al. 2020). In parallel, we used a CDK4/6-dependent kinase inhibitor Abemaciclib reported to remodel the chromatin architecture in breast cancer cells (Watt et al. 2021). In this cells, Abemaciclib reduced chromatin accessibility over gene promoters regulating progression through G1, consistent with its cell cycle inhibitor function, but at the same time induced widespread enhancer activation at other regions, including the super-enhancers driving luminal differentiation and apoptotic evasion. As the MCL-specific super-enhancer at the translocation breakpoint overlaps the *CCND1* gene that drives the G1/S progression, and the cell cycle deregulation is present in MCL, Abemaciclib was considered a potential treatment candidate.

To assess the effect of Minnelide and Abemaciclib on the chromatin landscape of MCL cells, we performed ATAC-seq in the MCL (GRANTA-519) and control (BLAS) cells treated or not with 50 nM Minnelide and 500 nM Abemaciclib for 3 and 7 days respectively. The times of treatment were chosen based on the previous studies (Noel et al. 2020; Watt et al. 2021), while the concentrations were additionally optimized through titration on the cell lines used in this work (**Supplementary figure 3a**) and turned out to be similar to those previously reported for the

pancreatic (20-100 nM Minnelide) (Noel et al. 2020) or breast cancer cells (500 nM Abemaciclib) (Watt et al. 2021).

Minnelide induced widespread chromatin remodeling mostly characterized by the new regions of reduced chromatin accessibility (22742 down, 830 up peaks) (**Figure 12a**). In contrast, the effect of Abemaciclib was almost negligible with only 44 and 217 down and up ATAC peaks respectively (**Figure 12a**). In the PCA analysis, the cells treated with Abemaciclib were almost indistinguishable from the non-treated cells, while Minnelide treatment was a clear source of variation (**Figure 12b**).

The sites decreasing their accessibility following Minnelide treatment were located both in gene promoters and within distal intergenic regions or introns (**Figure 12c**), suggesting that Minnelide caused the reduction in the activity of both enhancers and their corresponding promoters. Those sites overlapped substantially with the sites over-accessible in GRANTA-519 (MCL) vs BLAS (control) cells and the MCL patient cells vs control naive B cells from healthy donors (**Figure 12de**), suggesting that Minnelide treatment counter-balanced some of the MCL-associated epigenetic deregulation. Importantly, Minnelide also reduced the accessibility of the super-enhancer region around the translocation breakpoint (**Figure 12f**), and the regions around the putative chr11 contact hotspots on chr19 (**Figure 12g**).

Functionally, the genes associated with the sites of decreased accessibility after Minnelide treatment were enriched for the processes related to transcriptional coactivator activation and RNAPolII-dependent transcription factor binding (**Figure 12h**), consistent with the Minnelide being an enhancer disruptor (Noel et al. 2020) and an inhibitor of RNA pol II-dependent transcription (Vispé et al. 2009). Those genes encoded for the subunits of the mediator complex (*MED13*, *MED14*, *MED16*, *MED24*, *MED25*, *MED30*, *MED4*), general transcription factors (*GTF2A1*, *GTF2A2*, *GTF2I*), lysine acetyltransferases (*KAT2B*, *KAT5*, *KAT6A*), as well as the transcription factors reported to facilitate the enhancer-promoter looping (*YY1*, *SP1*) (Weintraub et al. 2017; Mastrangelo et al. 1991). Biological processes associated with the down peaks included positive regulation of lymphocyte activation and cell-cell adhesion (**Figure 12h**), while the associated pathways included the Th17 differentiation, Rap1 signaling, regulating cell adhesion, and TNF signaling, known to promote inflammation and proliferation of lymphoma cells (**Figure 12h**).

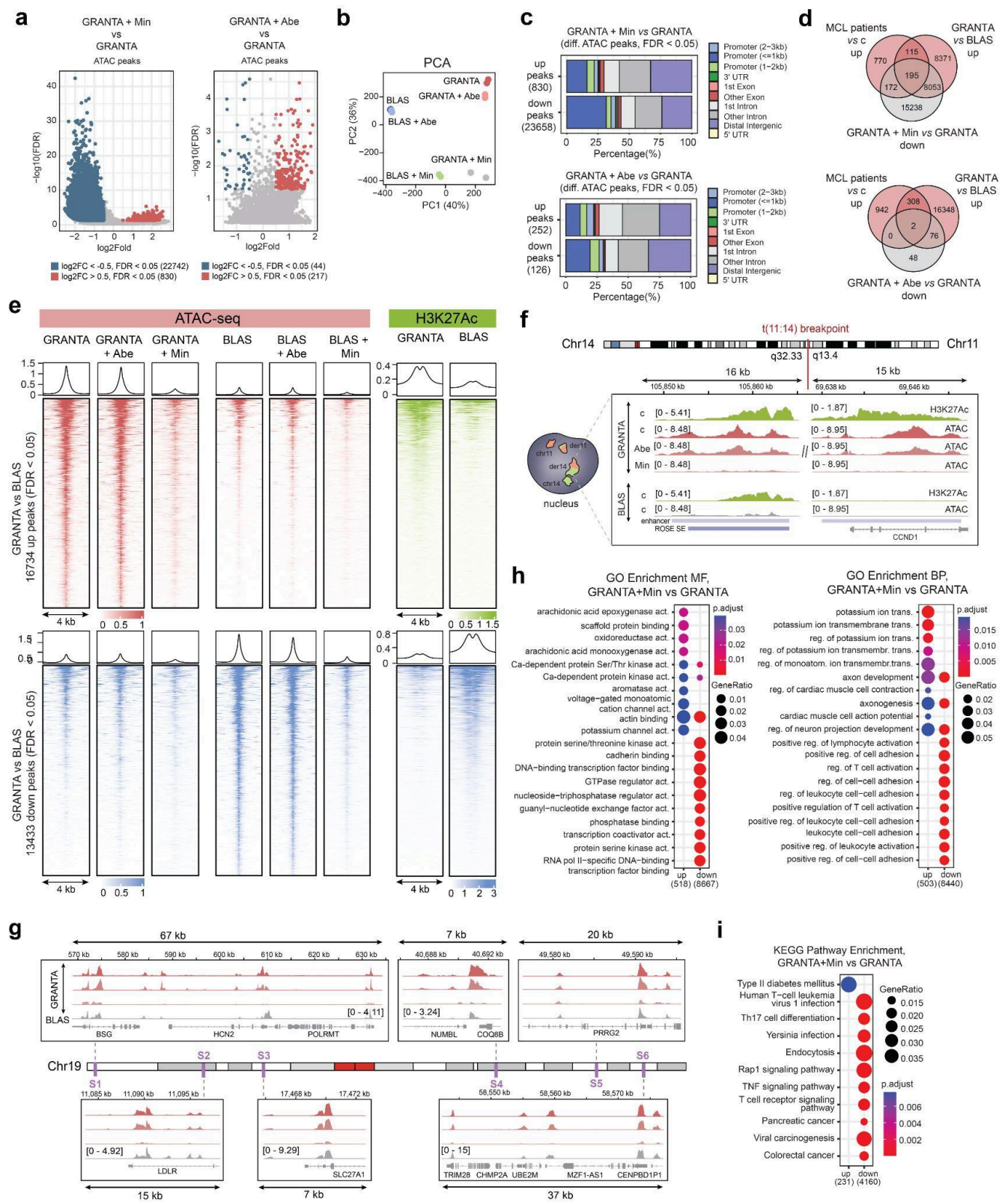


Figure 12. Minnelide reprograms the epigenetic landscape of MCL cells.

a, Differentially accessible ATAC peaks in GRANTA-519 MCL cells treated or not with Minnelide (left) or Abemaciclib (right); up peaks ($\log_2\text{FC} > 0.5, \text{FDR} < 0.05$) are colored red, down peaks ($\log_2\text{FC} < -0.5, \text{FDR} < 0.05$) are colored blue. **b**, Principal Component Analysis (PCA) for the treated and non-treated control (BLAS) and MCL (GRANTA-519) cells performed

on the ATAC-seq peaks. **c**, Distributions of the up/down ATAC peaks relative to genomic features in GRANTA-519 + Minnelide vs non-treated GRANTA-519 cells. **d**, Venn diagrams showing the intersections between the ATAC peaksets upregulated in the MCL patients' cells vs control naive B cells, GRANTA-519 MCL cells vs control BLAS cells comparison, and the peakset downregulated in the GRANTA-519 MCL cells treated with Minnelide or Abemaciclib. **e**, ATAC/ChIP-seq profiles within the sites of significantly increased chromatin accessibility in the GRANTA-519 MCL cells vs control BLAS cells; the H3K27Ac profiles are shown for the non-treated cells, the ATAC profiles are shown for the non-treated cells and the cells treated with 50nM Minnelide or 500nM of Abemaciclib. **f**, Representative tracks of the ATAC (red) and H3K27Ac (green) signal within the super-enhancer (SE) region in the t(11;14) translocation breakpoint in the cells treated or not with 50nM Minnelide or 500nM of Abemaciclib. The signals scaled to one million mapped reads are shown. **g**, Representative tracks of the ATAC-seq signal within the regions of the putative chr11-chr19 contacts on chr19 in the cells treated or not with 50nM Minnelide or 500nM of Abemaciclib. The approximate contact sites are indicated as S1-S6. The signals scaled to one million mapped reads are shown. **h,i**, Gene Ontology (h) or KEGG pathway (i) enrichment analysis for the ATAC peaks significantly increasing (up) or decreasing (down) their accessibility in GRANTA-519 MCL cells following Minnelide treatment (50nM, 3d), (FDR < 0.05). Top 10 enriched categories.

We next investigated the transcriptional changes associated with the Abemaciclib and Minnelide treatment in GRANTA-519 MCL cells, control lymphoblastoid cells BLAS and the PBMCs from an MCL patient in a leukemic phase. The immortalized cells were treated as described for the ATAC-seq; the patient PBMCs were treated with two concentrations of Minnelide, 25nM or 50nM, and the lower concentration was retained for the RNA-seq analysis due to high cellular mortality following the 50nM Minnelide treatment.

Minnelide caused pronounced changes in gene expression with a large number of both upregulated and downregulated genes (**Figure 13a**). Among the genes that were downregulated by Minnelide, approximately 40% were predicted to be regulated by enhancers active in the MCL patients' B cells, supporting the presence of an epigenetic component in the mechanism of action of the drug (**Figure 13b**). In the patient PBMCs, the downregulated genes were functionally enriched for the leukocyte migration and immune-response associated signaling pathways (**Figure 13c**). Some examples included the chemokines and their receptors (*CCL5*, *CCL18*, *CXCL16*, *CXCL3*, *CXCL10*, *CXCL9*, *CCR1*, *CCR2*, *CCR5*, *CXCR3*, *CX3CR1*), growth factors (*PDGFB*, *VEGFA*), the components and the downstream effectors of the BCR-signaling pathway (*HCK*, *YES1*, *TXK*, *SH2D1A*), as well as several known proto-oncogenes (*SRC*, *KIT*, *SPI1*, *YES1*). All of the above-mentioned genes were upregulated in the B cells from MCL patients compared to the naive B cells from healthy donors, and roughly 30% of the overall genes upregulated in MCL were reciprocally downregulated by Minnelide (**Figure 13b**). Thus, Minnelide decreased the expression of many immune-related genes highly relevant for MCL.

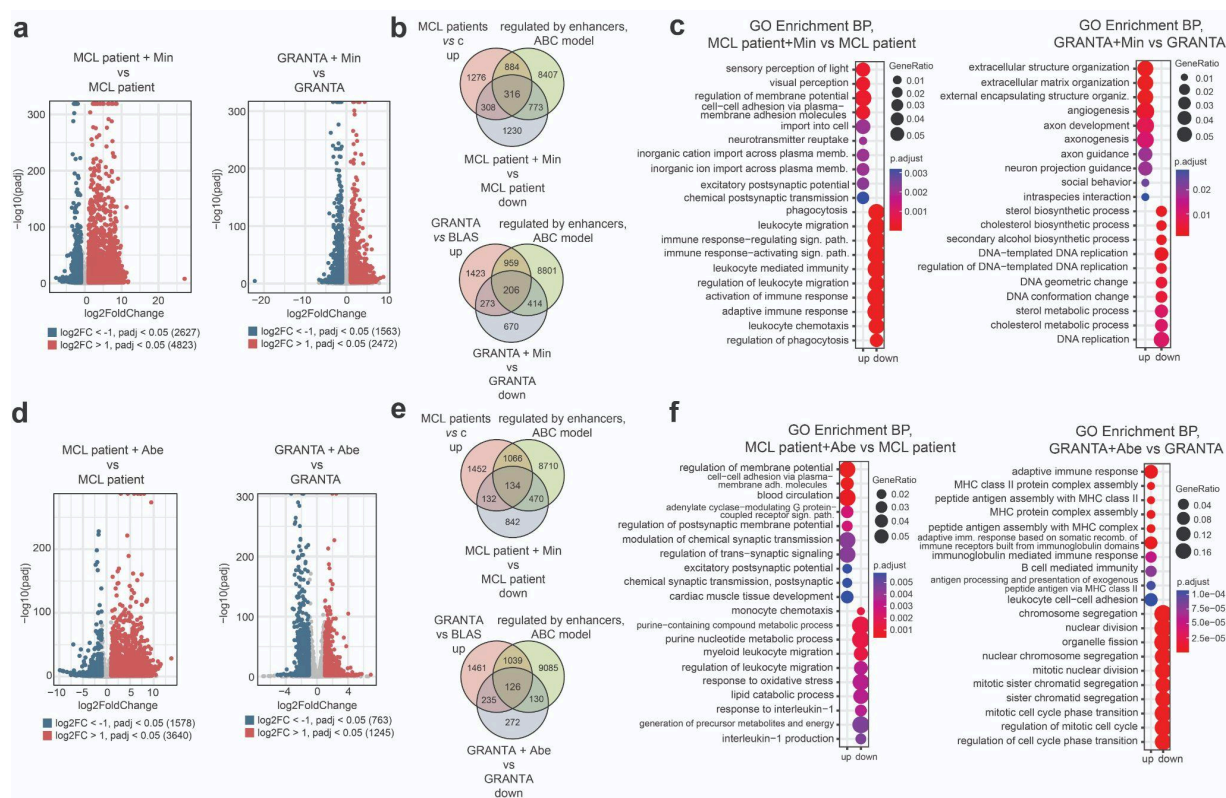


Figure 13. Transcriptomic changes following Minnelide and Abemaciclib treatment.

a, Differentially expressed genes (DEGs) in the MCL patient cells (left) / MCL cells GRANTA-519 (right) treated with Minnelide vs corresponding not-treated controls. Upregulated genes ($\log_2FC > 1$, $\text{padj} < 0.05$) are colored red, downregulated genes ($\log_2FC < -1$, $\text{padj} < 0.05$) are colored blue. **b**, The intersection between the genes upregulated in MCL patients vs control naive B cells/ GRANTA-519 MCL cells vs control lymphoblastoid cells BLAS, the genes predicted to be regulated by enhancers by the ABC model in MCL patients, and the genes downregulated by Minnelide in MCL patient/MCL cell line GRANTA-519. **c**, Gene Ontology enrichment analysis for the genes upregulated ($\log_2FC > 1$, $\text{padj} < 0.05$) or downregulated ($\log_2FC < -1$, $\text{padj} < 0.05$) following Minnelide treatment in the MCL patient (left) and the MCL cell line GRANTA-519 (right). **d**, Differentially expressed genes (DEGs) in the MCL patient cells (left) / MCL cells GRANTA-519 (right) treated with Abemaciclib vs corresponding not-treated controls. Upregulated genes ($\log_2FC > 1$, $\text{padj} < 0.05$) are colored red, downregulated genes ($\log_2FC < -1$, $\text{padj} < 0.05$) are colored blue. **e**, The intersection between the genes upregulated in MCL patients vs control naive B cells/ GRANTA-519 MCL cells vs control lymphoblastoid cells BLAS, the genes predicted to be regulated by enhancers by the ABC model in MCL patients, and the genes downregulated by Abemaciclib in MCL patient/MCL cell line GRANTA-519. **f**, Gene Ontology enrichment analysis for the genes upregulated ($\log_2FC > 1$, $\text{padj} < 0.05$) or downregulated ($\log_2FC < -1$, $\text{padj} < 0.05$) following Abemaciclib treatment in the MCL patient (left) and the MCL cell line GRANTA-519 (right).

The genes downregulated by Minnelide in the MCL cell line GRANTA-519 were less enriched for the immune-related categories, likely due to the lack of environmental stimulation in the monoculture. Instead, they provided insights into the mechanisms of action of the drug, with the most enriched biological processes being the DNA replication and DNA conformation change (**Figure 13c**) and one of the most

enriched molecular functions being the methyltransferase activity (**Supplementary figure 4a**). These downregulated genes included chromatin remodelers associated with transcription activation (*CARM1, HMGA1, INO80*), cancer-associated histone methyltransferases (*CARM1, SMYD2, SMYD5, PRMT2, PRMT3*), cell-cycle regulators (*CDK2, FBXO5, CCNE1*) and multiple genes essential for the initiation and maintenance of DNA replication and repair (*MCM3, MCM7, DDX11, POLD2, POLD1, LIG3, NBN, TIMELESS, GINS2, GINS3, RTEL1, CDC45, CDC6, CDC7, TRAIIP, DNA2, ZRANB3*). All together, Minnelide strongly affected the expression of epigenetic remodelers and the genes maintaining DNA replication and genome stability, consistent with its observed effect on the chromatin landscape and its reported anti-cancer properties.

Abemaciclib treatment also caused pronounced changes in the transcriptomic profile of MCL cells (**Figure 13d**). In patients' PBMCs, it downregulated the expression of the genes related to leukocyte migration (*CCL3, CCL4, CCL22, CX3CR1, CXCL13*), interleukin-1 production (*IL1R2, TNFAIP3, SPHK1*) and energy metabolism, e.g. (*PKM, ENO1, LDHA, HIF1A*), while in the MCL cell line GRANTA-519, the most enriched downregulated categories were related to the mitotic nuclear division (*TOP2A, PRC1, TPX2, KIFC1, BIRC5, CENPF, PLK1, AURKA, RAD21*) and cell cycle (*MKI67, CCNB1, CCNG1, CDC20, CDK1, CDK2, CDC25A, CKS2, GTSE1, KLF4*) (**Figure 13f**), as expected. Combined with the lack of effect on the chromatin landscape, these results allowed us to conclude that the effect of Abemaciclib on MCL cells was mostly not linked to epigenetic reprogramming and was rather explained by its known mechanism of action as a CDK4/6 inhibitor.

We also explored the per chromosome distribution of the genes downregulated by Minnelide and Abemaciclib. For Abemaciclib, no consistent enrichment for any chromosome was found (**Supplementary figure 4cd**). For Minnelide, enrichment was found for chromosome 19, which was top 1 chromosome by the number of downregulated genes in GRANTA-519 cells independent of the normalization method (**Supplementary figure 4e**). At the same time, the chr19 enrichment in patients' PBMCs was less consistent (top 1-8 depending on the normalization) (**Supplementary figure 4f**). This suggested that the effect of both substances was rather spread genomewide.

All together, these results demonstrated a strong inhibitory effect of Minnelide on the chromatin landscape of MCL cells and the expression of genes involved in epigenetic remodeling, DNA replication, genome stability and immune signaling. In contrast, Abemaciclib did not significantly affect the epigenetic state of the MCL cells and primarily downregulated the genes related to cell cycle and mitosis, suggesting that it could not be considered an epigenetic drug in the MCL context.

3.8. Minnelide is effective against MCL cells *in vitro* and *in vivo*

We next tested the effect of Abemaciclib and Minnelide on the viability, proliferation

and apoptosis rates of MCL cells *in-vitro*. Both Abemaciclib (500nM) and Minnelide (25, 50 or 100nM) were able to reduce the viability of MCL cells, as measured by the MTT assay (**Figure 14a**). Minnelide was more potent with the effect visible already from the second day of treatment with 25nM of the drug, while Abemaciclib had a milder effect with the IC50 achieved only on day 7 of the treatment. The viability of the control lymphoblastoid cell lines established from healthy donors (BLAS, BLIT, BLYaK) was also affected by Minnelide treatment, but the effect on MCL cells was more pronounced and occurred more rapidly across all tested MCL cell lines (GRANTA-519, UPN1, UPN2, Jeko, Mino, NCEB). Interestingly, neither of the drugs was effective against the chronic myelogenous leukemia cell line RPMI8866, suggesting the relative specificity of the effect.

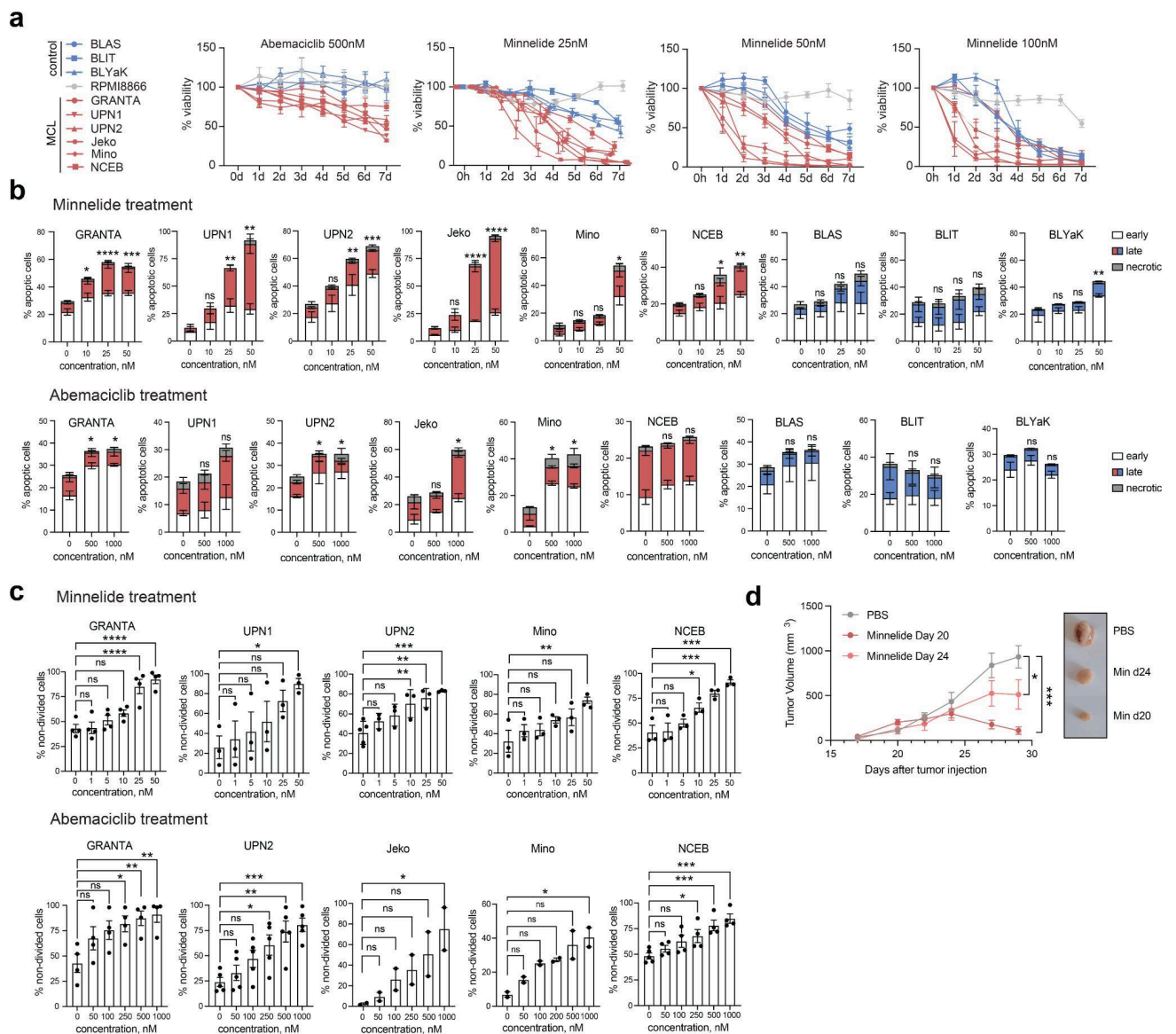


Figure 14. The effect of Abemaciclib and Minnelide on the viability, apoptosis and proliferation of MCL cells.

a, MTT assay of the viability of MCL and control cells treated with 500nM of Abemaciclib or 25-100nM Minnelide for 0-7 days. MCL cell lines are plotted in red, control lymphoblastoid

cell lines from healthy donors are plotted in blue, chronic myelogenous leukemia cell line RPMI8866 is plotted in gray. Data are shown as mean +/- SEM, N=3-9. **b**, Annexin V-PI apoptosis assay for the MCL (red) and control (blue) cells treated with 0-50nM of Minnelide for 3 days or 0-1000nM Abemaciclib for 7 days. Mean values of total apoptotic and necrotic cells +/- SEM are shown. The colors of the bars indicate the proportion of early apoptotic (Annexin+, PI-) cells in red, late apoptotic (Annexin+, PI+) cells in blue and necrotic (Annexin-, PI+) cells in gray. Statistical significance was determined by one-way ANOVA with Dunnett's correction for multiple comparisons. pval <0.05*, <0.01**, <0.001***, 0.0001****, N = 3-6. **c**, CFSE proliferation assay for the MCL cells treated with 0-50nM of Minnelide for 3 days or 0-1000nM of Abemaciclib for 7 days. The percentage of non-divided cells in the population at the end of the treatment is shown. The data are presented as means +/- SEM. Statistical significance was determined by one-way ANOVA with Dunnett's correction for multiple comparisons. pval <0.05*, <0.01**, <0.001***, 0.0001****, N = 2-5. **d**, Mice tumor volumes on days 15-29 following subcutaneous injections of GRANTA-519 MCL cells. The treatment groups (N = 5) received daily injections of 0.5 mg/kg of Minnelide starting from days 20 or 24 post tumor injection. Control group (N=6) received daily PBS injections starting from day 20. Data are shown as mean +/- SEM. Statistical significance was determined for the values at day 29 using one-way ANOVA with Dunnett's correction for multiple comparisons. pval <0.05*, <0.01**, <0.001***.

Minnelide also caused a dose-dependent increase in the apoptosis rates in all of the tested MCL cell lines (**Figure 14b**). Depending on the cell line, the percentage of apoptotic cells increased 2-6 fold following the treatment with 50nM of the drug (**Figure 14b**). The pro-apoptotic effect of Abemaciclib was milder and less consistent. At the highest tested concentration (1000nM), Abemaciclib affected the apoptosis rates of four out of six MCL cell lines with the size of the effect of 1.5-2.5 fold (**Figure 14b**).

Finally, both of the drugs reduced the proliferation of the MCL cells, as measured by the CFSE assay (**Figure 14c**). The effect was dose-dependent, with approximately 80% of the cellular population not dividing at maximum concentrations of any of the drugs (1000nM Abemaciclib, 50nM Minnelide).

We next proceeded with the testing of a more potent drug, Minnelide, *in-vivo* in xenografted NSG mice. MCL cells GRANTA-519 were injected subcutaneously into the right flanks of the mice and the treatment with Minnelide was started on day 20 or day 24 following the injection. In both set-ups, Minnelide was able to reduce or completely stop the tumor growth (**Figure 14d**).

All together, Minnelide exhibited a strong anti-tumor effect against mantle cell lymphoma cells both *in-vitro* and *in-vivo*.

4. DISCUSSION

Balanced chromosomal translocations, a main cause of lymphomas, lead to significant changes in gene expression although the gene dosage remains the same as in normal cells. This is partially caused by enhancer hijacking, a mechanism whereby a control element from one chromosome becomes juxtaposed with an oncogene from another chromosome following translocation (reviewed in (Canoy et al. 2023)). This is the case of mantle cell lymphoma where *CCND1* is overexpressed following the t(11;14) translocation. At the same time, *CCND1* overexpression alone can not induce the oncogenic transformation *in vitro* (Fiancette et al. 2010) or in animal models (Lovec et al. 1994; Bodrug et al. 1994). To gain insight into additional mechanisms of MCL lymphomagenesis, we explored other possible consequences of chromosomal translocations, e.g. changes in the genome architecture and epigenetic marks.

Indeed, the position of a gene or a gene locus within the nucleus plays a critical role in regulating its activity. Genes located in regions of euchromatin are generally more active because the DNA is more accessible to transcription machinery. Conversely, genes in heterochromatin are typically silenced or less active, as the dense packing restricts access to transcription factors and RNA polymerase. In the nucleus, euchromatin typically occupies a more interior position. The interior is generally more euchromatic and rich in transcription factors and machinery, which facilitates gene expression.

Therefore, we first examined whether the position of the 11q13 locus involved in the translocation changed in the MCL cell lines and MCL patients' cells. We observed that the position of the translocated IGH locus was almost unaffected by the translocation while the distribution of the translocated 11q13 allele was shifted to the nuclear center when compared to the intact 11q13 (**Figure 7**). Thus, in MCL cells, the translocated allele relocated to the nuclear center, closer to the 14q32 translocation partner locus, and not *vice versa*.

As centrally positioned euchromatic regions may have distinct transcription patterns, chromatin marks and chromatin accessibility, we next used RNA-seq, ATAC-seq and ChIP-seq to examine the potential changes after the t(11;14) translocation in B cells from MCL patients vs. the control naive B cells from healthy donors. We selected the activating H3K27Ac mark, known to label active enhancers and promoters as a landmark of epigenetic changes. More than 13000 sites with increased H3K27Ac binding were identified in MCL cells compared to the control. Most of these sites were located in gene promoters (**Figure 8**). We also identified over 1000 sites with altered chromatin accessibility as revealed by ATAC-seq (**Figure 8**). We next applied the activity by contact (ABC) model (Fulco et al. 2019) that infers the enhancer-gene interactions from the ATAC-seq, H3K27Ac ChIP-seq, HiC and expression data (see *Materials and Methods*). We identified almost 1000 enhancers that were more active

in MCL cells compared to the control B cells. These enhancers potentially regulated ~370 genes including the *MYCN* oncogene, *MECOM* and *SRC* proto-oncogenes, and several proliferation or growth-stimulating genes, such as *CCNE1*, *RASGRF1* and *PIK3R2* (**Figure 8**).

Using the rank-ordering of super-enhancers (ROSE) algorithm on the H3K27Ac ChIP data, we also identified 1121 superenhancers to be active in at least two MCL patient samples, compared to 752 and 520 for control naive and germinal B cells respectively. SEs unique for MCL were mainly involved in immune-response signaling and lymphocyte activation and also regulated many lymphoma-related genes including *CD5*, *WEE1* and *IL2RA* implicated in MCL pathogenesis. We have also observed an increase in the size of super-enhancers in MCL cells, suggesting the role of superenhancers in this lymphoma. Indeed, a superenhancer regulating *SOX11* oncogene expression was recently identified in MCL (Vilarrasa-Blasi et al. 2022).

We next focused our attention to local epigenetic changes in the translocation breakpoint region and found that a new superenhancer (SE) emerges upstream and inside of the *CCND1* locus after the t(11;14). We tried to search for the potential targets of this SE by mapping the genes differentially expressed in MCL vs. the controls to their corresponding chromosomal locations. To our surprise, chromosome 19, and not chromosomes 11 or 14, was most enriched in genes upregulated in MCL (**Figure 9**). These genes included those involved in immune-response signaling pathways and oncogenesis. Several of these genes were already known to be associated with MCL, e.g. *BAX* and *CD70* (Beltran et al. 2011; Balsas et al. 2021).

Chromosome 19 is preferentially located in the nuclear center. As the derivative chromosome 14 relocated to the nuclear center in MCL cells, we hypothesized that it could develop an interaction with chromosome 19 in *trans via* the novel SE in the 11q13 locus, which would explain the upregulation of gene expression on chromosome 19. To check this hypothesis, we carried out HiC in the control and MCL cell lines and observed an interaction between chromosomes 19 and 11 (**Figure 10**). This interaction was confirmed by the analysis of published HiC data from five MCL patients (Vilarrasa-Blasi et al. 2021) and by 3D-FISH experiments. It should be noted that although this interaction was observed both in normal and MCL cells, the superenhancer was presumably present only in the translocated 11q13 locus; thus transcriptional upregulation on chromosome 19 could occur only upon the interaction with the derivative chromosome 14 and not the intact chromosome 11. To ascertain this, we carried out immuno-FISH analysis with probes covering specific loci on chromosomes 11, 14 and 19 and the antibodies against the RNA pol II CTD phospho Ser5, an activated form of RNAPol II. We observed that in MCL cells the chr11-chr19 interchromosomal contact formed predominantly with the derivative 11q13 locus, and most of the chr19-der14 contacts also colocalized with the active RNAPol II staining (**Figure 11**), suggesting the presence of the active transcription hub around the interaction. The intact chr11-chr19 contacts also colocalized with the

RNA-pol II, but with a lower frequency, and this frequency was even lower for the chr19 signals non colocalized with either of the chr11 probes (**Figure 11**).

Superenhancer-targeting drugs emerge as a new class of anticancer compounds (see section 1.2 for details). Treatment with I-BET151, a drug targeting a superenhancer protein component BRD4, has already demonstrated an antiproliferative effect against MCL cell lines *in vitro* (Tsukamoto et al. 2020). We thus decided to test the effect of another SE-targeting drug, Minnelide, on the viability of MCL cells *in vitro* and *in vivo*. Minnelide inhibits SE by targeting the XPB subunit of the TFIIH complex (He et al. 2015; Noel et al. 2020) and has demonstrated cytotoxic activity in multiple cancer cell lines (reviewed in (Shiwei Bao et al. 2024)). We also used Abemaciclib, a CDK4/6-dependent kinase inhibitor reported to remodel the chromatin architecture in breast cancer cells (Watt et al. 2021). In *in vitro* experiments, Minnelide has shown a much higher cytotoxic activity against MCL cell lines vs. the controls (three lymphoblastoid cell lines) compared to Abemaciclib (**Figure 14**). We thus chose this drug for the subsequent *in vivo* experiment. In NSG mice xenografted with the GRANTA-519 MCL cells, Minnelide significantly diminished or completely stopped the tumor growth when injected at 0.5 mg/kg starting from day 24 or day 20 after tumor inoculation (**Figure 14**).

To gain insight into the mechanisms of action of Minnelide, we carried out ATAC-seq on the control and MCL cells treated with Minnelide and Abemaciclib. In contrast to Abemaciclib, Minnelid significantly reduced chromatin accessibility in treated cells, particularly in sites that were initially more accessible in MCL cells than in the controls. This included the novel superenhancer in the breakpoint region, which drastically reduced its accessibility following Minnelide treatment. We then used RNA-seq to analyze transcriptional changes induced by Abemaciclib and Minnelide in GRANTA-519 MCL cells, control lymphoblastoid cells and the PBMCs from an MCL patient. Approximately 40% genes downregulated by Minnelide, were predicted to be regulated by enhancers active in the MCL patients' B cells (**Figure 13**), and many of the downregulated genes were related to chromatin remodeling, DNA replication and stability, confirming the epigenetics-mediated mechanism of action of the drug. Importantly, Minnelide also decreased the expression of many immune-related genes and proto-oncogenes highly relevant for MCL. When per chromosome distribution of the genes downregulated by Minnelide and Abemaciclib was analyzed, no consistent enrichment for any chromosome was found in the case of Abemaciclib. For Minnelide, enrichment was found for chromosome 19, which was top 1 chromosome by the number of downregulated genes in GRANTA-519 MCL cells.

All together, our results demonstrated the role of a novel superenhancer on the derivative chromosome 14 in the MCL pathogenesis and the potential utility of the SE-targeting drugs as a new MCL treatment strategy.

5. CONCLUSIONS AND PERSPECTIVES

In this work, we have shown that t(11;14) translocation, a landmark of MCL, brings about large-scale changes in the 3D genome and the epigenome of MCL cells. In particular, it leads to the appearance of a novel superenhancer on derivative chromosome 14 that can activate the expression of lymphoma-related genes *in trans*. Targeting this and other superenhancers with an SE-inhibiting drug Minnelide significantly reduced the viability of MCL cells *in vitro* and *in vivo*, suggesting the potential utility of this drug for MCL treatment.

Our work stresses the importance of epigenetics and 3D genome organization in the oncogenesis of MCL and potentially other malignancies associated with large chromosomal aberrations. It also highlights the potential of epigenetic drugs as possible treatments for these malignancies.

In perspective, we will study other lymphomas (e.g. Burkitt lymphoma and follicular lymphoma) to assess their 3D organization and epigenetic landscape with a special focus on a potential *in trans* regulation of gene activity. Also, while demonstrating a potent pre-clinical activity in our data, Minnelide was reported to induce several side effects in clinics, including reversible leukopenia, neutropenia, and cerebellar toxicities (Borazanci et al. 2024). In collaboration with our colleagues from the Lviv Medical University, we are currently developing and testing less toxic Minnelide analogs for potential future clinical applications.

6. MATERIALS AND METHODS

6.1. Cells

MCL cell lines GRANTA-519, UPN1, UPN2, Jeko, Mino and NCEB, chronic myelogenous leukemia cell line RPMI8866 and control cell lines BLAS, BLIT and BLYaK were used in this study. BLAS, BLIT and BLYaK cells were freshly established from the B cells of healthy donors collected in the laboratory with the donors' informed consent; these cells were immortalized by the EBV (B95-8) transformation and characterized by Genethon (Evry, France). All cells were maintained at 37 °C and 5% CO₂ under high humidity and cultured in high-glucose RPMI-1640 medium supplemented with 10% fetal bovine serum (FBS), 2% glucose, 2 mM L-Glutamine, 1 mM Pyruvate, 1000 units/mL of penicillin and 1000 µg/mL of streptomycin (all from Gibco, Thermo Fisher Scientific).

6.2. Patients

Blood samples from hospitalized MCL patients who signed a written informed consent for the study were collected in Gustave Roussy Institute, Villejuif, in accordance with the French legislation. B cells from patients 1-4 were used in the FISH experiments (see *FISH* and *ImmunoFISH*) and the RNA-seq experiment without treatments (see *RNA-seq library preparation and sequencing*). B cells from patients 4-5 were used in the FISH experiments. B cells from patient 6 were used for the RNA-seq experiment with Minnelide and Abemaciclib treatments (see *RNA-seq library preparation and sequencing*).

6.3. Blood collection and primary B cell isolation

Peripheral blood mononuclear cells (PBMCs) were purified by Pancoll (PAN biotech) density gradient centrifugation. PBMCs derived from the MCL patients in a leukemic phase and containing >80% of B cells were used right away. Other samples were subjected to the B cell enrichment by negative cell selection with the MagniSort Human B cell Enrichment Kit (Thermo, cat. # 8804-6867-74) prior to downstream applications.

6.4. FISH probe preparation

The probes for the fluorescent in situ hybridisation (FISH) were prepared from the backmids ordered from BACPAC Genomics. The following backmids were used: RP11-1021J3 (chr11, CCND1 locus), RP11-346I20 (chr14, upstream of the IGH locus), CTD-2589F14 (chr19) and RP11-1056O16 (chr 21). The backmids were received as stab cultures, amplified in the DH5α E.coli and purified using the QIAGEN Large-Construct Kit (cat. no. 12462). After purification, the backmids were labeled with fluorophore-dUTPs using the Nick Translation DNA Labeling System 2.0 (Enzo, ENZ-GEN111) according to the manufacturer's instructions. SEEBRIGHT® Orange 552 dUTPs (ENZ-42842), SEEBRIGHT® Green 496 dUTPs (ENZ-42831) and SEEBRIGHT® Red 650 dUTPs (ENZ-42522) were used to label the chr11, chr14 and chr19/chr21 probes respectively.

6.5. FISH and ImmunoFISH

The cells were pelleted and resuspended in the FBS-free RPMI-1640 medium to a concentration of 8×10^6 cells/ml. 80 μ l of cell suspension was put onto the glass coverslips covered with 0.25mg/ml Poly-L-lysine hydrobromide (Mol. Wt.: 150000-300000) (Merck P1399) and the cells were left to attach at 37 °C for 30 minutes. The non-attached cells were washed with 0.3X PBS. The attached cells were then fixed in 4% PFA in 0.3X for (10 min, RT), washed three times with PBS, permeabilized in 2% Triton X-100 in PBS (10 min, RT) and left in 20% glycerol in PBS overnight at 4 °C . Next day, the coverslips with the cells were subjected to 3 freeze-defreeze cycles in liquid nitrogen, each cycle followed by incubation in the 20% glycerol. The coverslips were then washed 3 times with PBS, incubated in 0.1M HCL (20 min, RT), washed 2 times with 2X SSC and incubated with RNase (200 μ g/ml in 2X SSC) for 1h at 37 °C. Following the RNase treatment, the coverslips were washed 3 times in 2X SSC, equilibrated in 50% formamide/2X SSC and stored at 4 °C for up to 6 months before the hybridisation with the fluorescent probes.

For one hybridisation reaction (two coverslips), the nick-translated probes mixed with 3 μ g of COT Human DNA (Roche 11581074001) were purified using ethanol precipitation according to the instructions from the Nick Translation DNA Labeling System 2.0 (Enzo, ENZ-GEN111). The probes of different colors intended to be used in one hybridization reaction were mixed together at the precipitation step. The DNA pellet was then resuspended in 10 μ l of the in situ hybridisation buffer (Empire Genomics) to obtain the hybridisation mix.

For hybridisation, two coverslip with cells were put onto a glass slide into drops (50 μ l) of 70% formamide in 2X SSC, cells oriented towards the drop. The slide and the hybridisation mix were then incubated at 80 °C for 5 min on the appropriate warming plates. Immediately following the incubation, the hybridisation mix was transferred on ice. Next, the hybridisation sandwich was prepared: one of the coverslips was turned on the other side, so that the cells were facing up, 10 μ l of the hybridisation mix was put onto this coverslip, and the second coverslip was put onto the first one, so that the cells were between the coverslips, both touching the hybridisation mixture. The edges of the sandwich were sealed with the silicon glue and the sandwich was put into the humid chamber at 37 °C for three days.

Following this incubation, the glue was removed and the coverslips were detached from each other and put into the wells of a 6-well plate, cells facing up. The coverslips were then washed two times with 2X SSC for 5 min and three times with PBS for 5 min. In case of regular FISH, this was the last step before the mounting. In case of ImmunoFISH, the cells on the coverslips were further saturated in 0.5% BSA in PBS, washed with PBS two times for 5 min and incubated with the antibodies against RNA pol II CTD phospho Ser5 (Active Motif, 39233) diluted 1:2000 in 0.5% BSA for two hours at RT. The coverslips were then washed three times with PBS for 5 min, and incubated with the secondary Goat anti-Rabbit IgG (H+L) Cross-Adsorbed Secondary Antibody, Alexa Fluor™ 405 (ThermoFisher, A31556) for one hour at RT,

followed by three washes in PBS for 5 min. At this step, the ImmunoFISH coverslips were ready for mounting.

The prepared coverslips were mounted onto glass slides in the Vectashield mounting medium (Eurobio scientific, H-1000-10). For regular FISH, the mounting medium was pre-mixed with 1.5 µg/ml of DAPI (ThermoFisher, D1306) to stain the nuclei. For ImmunoFISH, the mounting medium was non-stained as the fluorescent secondary antibodies absorbing/emitting at the same wavelength as DAPI were used.

The FISH slides were observed on the Leica TCS SP8 Multiphoton Confocal Microscope (Leica Microsystems). Ten random 291 x 291 µm (lower magnification) or 185 x 185 µm (higher magnification) fields per slide were acquired for each sample. The Z-step size was set to 0.5 µm. All images within the experiment were captured with the same laser intensity, gain and exposure settings.

6.6. Analysis of the FISH images

The 3D images from the Leica TCS SP8 Multiphoton Confocal Microscope were analyzed in the Imaris software (Bitplane).

The colocalization of the FISH signals was analyzed as follows. The FISH signals in the corresponding channel were first detected using the "Create spots" function with the estimated spot diameter set to 1 µm. The debris wrongly classified as spots was manually deleted. The procedure was repeated for all channels of interest. For further analysis, only the "complete" cells with the two strong signals present in each channel of interest were retained. The colocalization between the spots was determined using the "Colocalize spots" function with the colocalization threshold set to 1 µm. The percentage of cells with a certain colocalization was calculated relative to all "complete" cells in the field. The procedure was performed separately for each of the ten acquired fields in each experiment, and the numbers obtained from one field were considered a technical replica if no less than 50 "complete" cells were present. The statistical significance was determined on technical replicates using ordinary one-way ANOVA with Dunnett's correction for multiple comparisons or paired t-test, depending on the comparisons performed (specified in Figure legends); pval <0.05*, <0.01**, <0.001***, 0.0001****.

The distribution of the signals relative to the nuclear center was analyzed as follows. The nuclei were detected in the DAPI channel using the "Add cells" function with the filter width of 2 µm and the estimated diameter for nuclei splitting of 8-12 µm depending on the cell line or patient sample. The FISH signals in the corresponding channel were detected as described above. The non-complete nuclei and the debris misclassified as nuclei or spots were manually deleted. The spots were next imported inside the nuclei using the "Import spots to vesicles" function. For each spot, the statistics "Distance to Cell Membrane" was exported and subtracted from the mean radius of the nuclei in the field to get the estimated distance of the spot to the nuclear center. In the set-ups where the der14 chromosome was analyzed, the

chr11-chr14 colocalization was first detected as described above and the distance to the nuclear center was measured relative to the colocalized chr11 allele. The distances from the spots to the nuclear center from one field were then normalized to the mean radius of the nuclei in the same field. No less than 100 cells were analyzed for the MCL patients (range 100-500 depending on the material availability) and no less than 200 cells for the MCL and control cell lines (range 200-500). The distributions of the resulting values for each cell were plotted as density plots. Kolmogorov-Smirnov test for the equality of the distributions was used to determine whether the distributions were significantly different; pval <0.05*, <0.01**, <0.001***, 0.0001****.

The colocalization of the FISH signals with the RNAPol II was analyzed as follows. The regions occupied by RNAPol II were detected in the blue channel using the "Add new surface" function with the surface detail set to 0.1 μm . The spots and their colocalization were determined in the channels of interest as described above. The spot was considered colocalized with the RNAPol II if it presented an overlap with the RNAPol II surface. The analysis was performed for all the spots inside the "complete" cells for each field. The percentage of colocalization relative to the "complete cells" in each field was determined and considered a technical replica. Statistical analysis was performed on the technical replicates using the ordinary one-way ANOVA with Dunnett's correction for multiple comparisons; pval <0.05*, <0.01**, <0.001***, 0.0001****.

6.7. MTT cell viability assay

The cells were seeded to 96-well plates (100 μl per well) in a concentration of 0.5 million/ml (GRANTA, UPN2, RPMI8866) or 1 million/ml (UPN1, Jeko, NCEB, Mino, BLAS, BLIT, BLYaK) and treated with 500nM Abemaciclib, 25nM, 50nM or 100nM Minnelide for 1-7 days in three technical replicates. At the end of the treatment, the cells were supplied with 0.1 mg of MTT reagent A (Merck Millipore, CT01-5) per well, incubated for 2h at 37 °C and lysed in the MTT lysis buffer (25 mM HCl, 2% acetic acid, 3% DMF, 5% SDS, pH 4.7; 100 μL per well) overnight. Next day the absorbance at 570 nm was measured on a Tecan Infinite F200 PRO plate reader. The acquired numerical data was analyzed using Excel software, wherein the average value of three technical replicates was determined. To eliminate the background noise, the value obtained by measuring the cells not supplemented with the MTT reagent was subtracted. The average absorbance values at different time points were then normalized to the average absorbance value of the non-treated control. The experiment was performed in 3-6 biological replicates. Statistical significance was determined using the ordinary one-way ANOVA with the Dunnett's multiple comparisons test. The samples treated for 1-7 days were compared to the untreated sample.

6.8. Annexin V - propidium iodide apoptosis test

0.5 $\times 10^6$ cells were seeded to the 24-well plates and treated with 0, 500 or 1000nM of Abemaciclib for 3 days or 0, 10, 25 or 50 nM of Minnelide for 7 days. After treatment,

the cells were pelleted and resuspended in 300 μ L of Annexin buffer (100 mM Hepes (pH 7.4), 150 mM NaCl, and 2.5 mM CaCl₂), incubated with 3 μ L of APC-conjugated Annexin-V (Biolegend, cat. #640920) and 3 μ L of 1 mg/ml propidium iodide (PI, #P4170-10MG, Sigma-Aldrich) for 5 minutes, and analyzed on the BD Accuri C6 Plus Flow Cytometer (BD Biosciences, San Jose, CA, USA). Flow cytometry data were analyzed using FlowJo software (BD Biosciences). The same gating was applied to all the samples within one experiment. Annexin V-positive PI-negative cells were considered early apoptotic; Annexin V-positive PI-positive cells were considered late apoptotic; Annexin V-negative PI-positive cells were considered necrotic. The percentage of apoptotic cells was defined as the sum of the early apoptotic, late apoptotic and necrotic cells divided by the total number of cells within a gate * 100%. The experiment was performed in 3-6 biological replicates. Statistical significance was determined using the ordinary one-way ANOVA with the Dunnett's multiple comparisons test.

6.9. CFSE proliferation test

The cell proliferation was analyzed using 5- (and 6-) carboxyfluorescein diacetate succinimidyl ester (CFSE) staining (CFSE Cell Division Tracker Kit, 423801; BioLegend, San Diego, CA, USA) according to the manufacturer's instructions. Briefly, 1×10^6 cells were washed with PBS, resuspended in 1% FBS/PBS to a final concentration 1×10^6 cells/mL and labeled with 1 μ L of 5 mM CFSE solution for 4 min at room temperature under shading. After incubation, 9 mL of 5% FBS/PBS was added to stop the labeling reaction. Cells were then washed once with 5% FBS/PBS and resuspended in a regular growth medium to a final concentration of 5×10^5 cells/mL. Following the labeling, the cells were treated with Abemaciclib (10, 25, 50, 100, 200, 500 and 1000 nM) or Minnelide (1, 5, 10, 25 and 50 nM) for 7 and 3 days respectively. After the treatment, CFSE fluorescence was measured on the BD Accuri C6 Plus Flow Cytometer (BD Biosciences, San Jose, CA, USA). Flow cytometry data were analyzed using FlowJo software (BD Biosciences), the same gating was applied to all samples within one experiment. The percentage of cells that have not undergone division (EGFP+) was calculated and compared with that of an untreated sample. The experiment was performed in 3-5 biological replicates. Statistical significance was determined using the ordinary one-way ANOVA with the Dunnett's multiple comparisons test.

6.10. Xenograft studies in NSG mice

GRANTA-519 MCL cells (1×10^6) were suspended in 200 μ L of mixture Dulbecco-modified phosphate buffered saline (DPBS, Sigma-Aldrich, Cat#: 59331C) and BD Matrigel Matrix (BD Biosciences; Cat#: 356234) in a ratio of 1:1, and injected subcutaneously into the right flanks of NSG mice. Tumor growth was monitored every third day using digital calipers. Tumor size was calculated as: Tumor_volume = (length \times width²)/2. Treatment with Minnelide was started on day 20 or 24 following the injection of the cells. Mice in the treatment groups (N = 5 for each group) received daily intraperitoneal injections of a volume of 0.1 mg/mL Minnelide that

achieved a final dose of 0.5 mg/kg of mouse weight. Minnelide was dissolved in PBS. Control animals (N=6) were injected with the equivalent volume of PBS that mirrored the volume of Minnelide per dose. All mice were euthanized on day 29 following the cells injection, tumors were dissected and fixed in 10% formalin for subsequent immunohistochemical analysis.

6.11. RNA-seq library preparation and sequencing

The RNA-seq samples were prepared for the two experimental set-ups. In the first set-up, total RNA was extracted from the purified B cells from MCL patients 1-4 (N=1 for each patient) and the MCL cell line GRANTA-519 (N=3) without prior manipulations. This data was used for the comparisons between the MCL cells and the control B cell from healthy donors (EGAD00001002315).

In the second set-up, the cells from an MCL patient (patient 6), MCL cell line (GRANTA-519) and control cell line (BLAS) were first treated with Minnelide (25nM, 50nM) for three days or Abemaciclib (500nM) for seven days in three technical replicates and then subjected to the RNA extraction. This data was used to compare the MCL cells with or without treatment .

In both set-ups, total RNA was extracted using a NucleoSpin RNA isolation kit (Macherey-Nagel, Germany) following manufacturer's instructions. The quantity and quality of total RNA were measured using NanoDrop2000C Spectrophotometer (Thermo Fisher Scientific). The cDNA libraries were constructed in Novogene, UK, using the Novogene NGS RNA Library Prep Set (PT042) with the polyA mRNA enrichment on the Illumina Novaseq6000 platform in the paired-end mode.

6.12. ATAC-seq library preparation and sequencing

Control (BLAS) and MCL (GRANTA-519) cells were treated or not with Minnelide (50nM, 3 days) or Abemaciclib (500nM, 7 days). The ATAC libraries were prepared using the ATAC-Seq Kit (Active Motif, 53150) according to the manufacturer's instructions. The libraries were sequenced on the Novaseq6000 platform at the sequencing facility of the Gustave Roussy Institut or in Novogene.

6.13. ChIP-seq library preparation and sequencing

Chromatin immunoprecipitation was performed on the control (BLAS) and MCL (GRANTA-519) cells using the ChIP-IT Express kit (Active Motif, 53008) according to the manufacturer's instructions. Briefly, 50 million cells per condition were fixed with formaldehyde. The nuclei were extracted and the chromatin was sheared via sonication in the 12x24mm glass tubes (Covaris 520056) on the Covaris S220 instrument with the following programme: duty factor 2%, CPB 200, PIP 105, 10 min. The sheared chromatin was immunoprecipitated with 5µg of antibodies against H3K27Ac (Active Motif 39133). The antibodies against normal rabbit IgG (Cell Signaling, 2729) was used as a negative control. The target enrichment was verified using real-time qPCR according to the instructions from the ChIP-IT Express kit (Active Motif, 53008). The Human Negative Control Primer Set 1 (Active Motif, 71001),

the Human Positive Control Primer Set GAPDH-2 (Active Motif, 71006) and the PowerUp SYBR Green Master Mix (Thermo Fisher, A25741) were used in the qPCR reaction.

The ChIP-seq libraries were prepared from the 5-10 ng of the immunoprecipitated and input chromatin using the NEBnext Ultra II DNA Library Prep Kit for Illumina (NEB, E7645) with Multiplex Oligos for Illumina (NEB, E6440s) according to the manufacturer's instructions. 11 amplification cycles were used. The libraries were sequenced in Novogene, Germany on the NovaSeq PE150 platform.

6.14. HiC library preparation and sequencing

Hi-C libraries were prepared as described elsewhere (Zakharova et al. 2022). In brief, 10^7 of control (BLAS) or MCL (GRANTA-519) cells were crosslinked for 10 min at room temperature by addition of formaldehyde (Sigma-Aldrich) to a final concentration of 1% followed by addition of glycine to a final concentration of 125 mM. Cells were washed in PBS, snap-frozen in liquid nitrogen and then stored at -80° . Thawed cells were washed and treated with the DpnII restriction endonuclease (NEB) overnight. After washing, DNA ends were biotinylated by addition of the Klenow enzyme (NEB) and the nucleotide mixture containing biotin-14-dATP (Invitrogen). After washing, DNA ends of chromatin fragments were ligated by addition of T4 DNA ligase (Thermo Fisher). Then cross-links were reversed by incubation at 65°C in the presence of Proteinase K (Sigma-Aldrich) and DNA was purified by phenol-chloroform extraction. After ethanol precipitation, the samples were treated with RNase and purified on Agencourt AMPure XP beads (Beckman Coulter) and AMICON Ultra Centrifugal Filter Units (Millipore). The samples were A-tailed using the Klenow enzyme (NEB), then the ligation junctions were purified by biotin pulldown and the Illumina TruSeq adapters were added using T4 DNA ligase. The obtained libraries were amplified by PCR and sequenced on an Illumina Novaseq 6000 in a paired-end mode.

6.15. RNA-seq analysis

RNA-seq samples from MCL patients and the control and MCL cell lines (BLAS, GRANTA-519), treated or not with Minnelide and Abemaciclib, were prepared and sequenced as described above. Additionally, raw transcriptomic data for five more MCL patients and six control naive B cell samples from healthy donors were downloaded from EGA (EGAD00001002336, EGAD00001002315) and processed together with the other samples. Raw sequencing data was processed using the nf-core/rnaseq pipeline (v3.10.1) (Patel et al. 2024) with default parameters unless stated otherwise. Briefly, the fastq files were trimmed from the sequencing adapters using TrimGalore (v 0.6.7) and aligned to the reference human genome (GRCh38) using STAR (v 2.6.1d). The reads mapping to different genomic features were then quantified by Salmon (v 1.9.0). The resulting count tables were used for the downstream analysis in RStudio.

Differential expression analysis was performed with DESeq2 (Love, Huber, and Anders 2014). The threshold of adjusted p-value (padj) of less than 0.05 was used to determine statistical significance. The genes with $\text{padj} < 0.05$ and $|\log_2\text{fold}| > 1$ were considered deregulated. The plotting of the differentially expressed genes against their chromosomal locations was performed using the karyoploteR package (v 1.26.0) (Gel and Serra 2017).

The enrichment analyses were performed on the significantly deregulated genes using the over-representation test (ORA) against the Gene Ontology Database from the clusterProfiler R package (v 4.8.2) (T. Wu et al. 2021). All the genes detected to be expressed in the corresponding RNA-seq experiment were used as the universe. The Benjamini-Hochberg correction was used to adjust the p-values. Top 10 enriched categories by adjusted p-value are shown in the figures.

6.16. ATAC-seq analysis

ATAC-seq samples from the control and MCL cell lines (BLAS, GRANTA-519) were prepared and sequenced as described above. The sequencing data from MCL patients and healthy donors was downloaded from EGA (EGAD00001002902, EGAD00001002918). Raw sequencing data was processed using the nf-core/atacseq pipeline (v 2.0) (Patel et al. 2023) with default parameters. Briefly, the files were trimmed to get rid of the sequencing adapters using TrimGalore (v 0.6.7) and aligned to the reference human genome (GRCh38) using BWA (v 0.7.17-r1188). The PCR duplicates were marked using Picard MarkDuplicates function (v 2.27.4). The alignments were filtered for duplicates, unmapped reads, reads not marked as primary alignments, multi mapping reads, reads mapping to the GRCh38 blacklist regions and mitochondrial DNA using SAMtools (v 1.16.1); for soft-clipped reads, reads with more than 4 mismatches and reads with the insert size of >2kb using BAMtools (v 2.5.2). The bigWig files with the ATAC-seq signal scaled to 1 million mapped reads were generated using BEDtools (v 2.30.0) and UCSC BedGraphToBigWig (v 377) and visualized in the IGV Genome Browser.

Peak calling was performed using MACS2 (v 2.2.7.1) with the default pipeline parameters. The procedures post-filtering were performed separately for each file and for the merged replicates. The bigWig tracks for the merged replicates are shown in the figures. The matrices for profile plotting were generated from the merged replicate files using the deepTools computeMatrix function in the reference point mode.

The aligned reads and the peaks called by MACS2 separately on each sample were subjected to the differential accessibility analysis in RStudio using DiffBind (v3.10.1) (Stark and Brown, n.d.). The peaks with the false discovery rate (FDR) of less than 0.05 were considered differentially accessible. The differentially accessible peaks were annotated to genomic features and the nearest genes using the ChIPseeker R package (v1.36.0) (Yu, Wang, and He 2015). The genes associated with the differentially accessible peaks were subjected to the enrichment analysis with the

over-representation test (ORA) against the Gene Ontology Database from the clusterProfiler R package (v4.8.2) (T. Wu et al. 2021). All the genes detected to be expressed in the MCL and control naive B cells in the RNA-seq experiment were used as the universe for the ORA test. The Benjamini-Hochberg correction was used to adjust the p-values. Top 15 enriched categories by adjusted p-value are shown in the figures.

6.17. ChIP-seq analysis

ChIP-seq samples from the control and MCL cell lines (BLAS, GRANTA-519) were prepared and sequenced as described above. The sequencing data from MCL patients and healthy donors was downloaded from EGA (EGAD00001001502, EGAD00001001519, EGAD00001002397). Raw sequencing data was processed using the nf-core/chipseq pipeline (v2.0.0) (Ewels et al. 2022) with default parameters unless mentioned otherwise. Briefly, the files were trimmed to get rid of the sequencing adapters using TrimGalore (v 0.6.7) and aligned to the reference human genome (GRCh38) using BWA (v 0.7.17-r1188). The PCR duplicates were marked using Picard MarkDuplicates function (v 2.27.4). The alignments were filtered for duplicates, unmapped reads, multi mapping reads, reads mapping to the GRCh38 blacklist regions and reads mapping for different chromosomes using SAMtools (v 1.15.1); for reads with more than 4 mismatches and the insert size of >2kb using BAMtools (v 2.5.2). The bigWig files with the ChIP-seq signal scaled to 1 million mapped reads were generated using BEDtools (v 2.30.0) and UCSC BedGraphToBigWig (v 377) and visualized in the IGV Genome Browser.

Peak calling was performed using MACS2 (v 2.2.7.1) with the mappable genome size set to 'hs', and q-value cutoff set to 0.05. NarrowPeak mode was used for the H3K27Ac mark and broadPeak mode was used for the H3K4me1 mark. The peaks consistent between the replicates/patient samples were identified using ChipR (Newell et al. 2021) with the minimum peaks between replicates required to form an intersection set to 2.

Differential H3K27Ac enrichment analysis was performed in RStudio using DiffBind (v3.10.1) (Stark and Brown, n.d.) on the aligned reads and the peaks called by MACS2. The peaks with the false discovery rate (FDR) of less than 0.05 were considered differentially enriched. The differentially enriched peaks were annotated to genomic features and the nearest genes using the ChIPseeker R package (v1.36.0) (Yu, Wang, and He 2015). The genes associated with the differentially enriched peaks were subjected to the enrichment analysis with the over-representation test (ORA) against the Gene Ontology Database from the clusterProfiler R package (v4.8.2) (Wu et al. 2021). All the genes detected to be expressed in the MCL and control naive B cells in a parallel RNA-seq experiment were used as the universe for the ORA test. The Benjamini-Hochberg correction was used to adjust the p-values. Top 15 enriched categories by adjusted p-value are shown in the figures.

6.18. Identification of enhancers and their targets

Enhancers and their target genes were identified using the activity-by-contact model of enhancer-promoter regulation (ABC) (Fulco et al. 2019), which integrates the ATAC-seq, ChIP-seq, RNA-seq and HiC data. First, the model identifies potential enhancer elements by calling peaks on the aligned ATAC-seq data using MACS2. Then, potential enhancer-gene pairs are formed: for a given element, all expressed genes within the 5Mb of the enhancer are considered potential partners. For each candidate enhancer (E) - gene (G) pair, the model calculates the ABC score which equals the Activity of E \times Contact frequency between E and G / Sum of (Activity \times Contact Frequency) over all candidate elements within 5 Mb. The activity A of an element E is calculated as the geometric mean between the ATAC-seq and H3K27Ac ChIP-seq signals in this element. The contact frequency between E and the promoter of G is inferred from the Knight-Ruiz normalized Hi-C contact map. The element-gene pairs where the element is itself a promoter are excluded, and all the remaining pairs passing the set ABC score threshold are considered valid enhancer-gene interactions.

The ABC model was run on the aligned ATAC-seq and ChIP-seq files obtained as described in the ChIP-seq analysis and ATAC-seq analysis sections of Materials and Methods, the expression data given as DESeq2-normalized counts and obtained as described in the RNA-seq analysis section, and the average HiC data for the lymphoblastoid cell line GM12878 downloaded from ftp://ftp.broadinstitute.org/outgoing/lincRNA/average_hic/average_hic.v2.191020.tar.gz. The default threshold of 0.02 was used for the ABC score.

The enhancers that are more active in the MCL cells were defined as the ones that overlap with the regions with the significantly (FDR < 0.05) increased H3K27Ac signal (see Differential enrichment analysis) by at least 50%.

6.19. Super-enhancer identification

All consistent H3K27Ac peaks passing the MACS2 q-value threshold of 0.05 were considered enhancers. As promoters can also act as enhancers, the regions within the TSS were not excluded from the regular enhancer definition. Super-enhancers were identified from the consistent H3K27Ac peaksets using rank ordering of super-enhancers (ROSE) as described in (Whyte et al. 2013). Enhancers occurring within 12.5kb of each other were stitched into a single larger enhancer domain to accurately capture dense enhancer clusters. The regions within ± 2.5 kb of TSS were excluded from the analysis this time to avoid the stitching in the dense regions with the H3K27Ac signal within the TSS only. All enhancers (stitched and non stitched except those within ± 2.5 kb of TSS) were then ranked by increasing total input-subtracted H3K27Ac occupancy and for each enhancer the total input-subtracted H3K27Ac in rpm/bp (reads per million per bp) was plotted to obtain the enhancer-distribution curve. A geometric point where a line with a slope of 1 was tangent to this curve marked the transition from low to increasingly high H3K27Ac signal density and was used as a threshold for super-enhancer definition. For each

sample, all enhancers above this point on the x axis were considered super-enhancers, and all the enhancers below this point were considered regular enhancers.

Overlapping super-enhancer regions were identified using the ChIPeakAnno package (Zhu et al. 2010). SEs with at least 80% region overlap in the samples within one condition were considered consensus SEs. Consensus SEs were further compared between the conditions with the same 80% overlap threshold to identify the SEs unique for each condition.

The genomic features nearest to the center of an SE were assigned to the respective SE and the enrichment analyses were performed on the assigned features using the ChIPeakAnno package (v 3.34.1) (Zhu et al. 2010) with the default parameters.

6.20. HiC analysis

Raw sequencing reads were obtained as described above or downloaded from EGA (EGAD00001006485). The raw fastq files were processed using the nf-core/hic pipeline (v2.1.0) (Servant et al. 2023) with the default parameters and the -digestion set to dpnii. The resulting contact maps in the mcool format were visualized using HiGlass (Kerpedjiev et al. 2018).

6.21. Statistical analysis

Statistical analyses were performed using Graphpad Prism software (v9.0.0) and R. Specific tests used to determine statistical significance are indicated in the corresponding figure legends.

6.22. Code availability

All code used to analyze the data in this study is available on GitHub (https://github.com/annaschwager/mcl_interchrom/).

MAJOR PUBLICATIONS RELATED TO THE TOPIC OF PhD THESIS

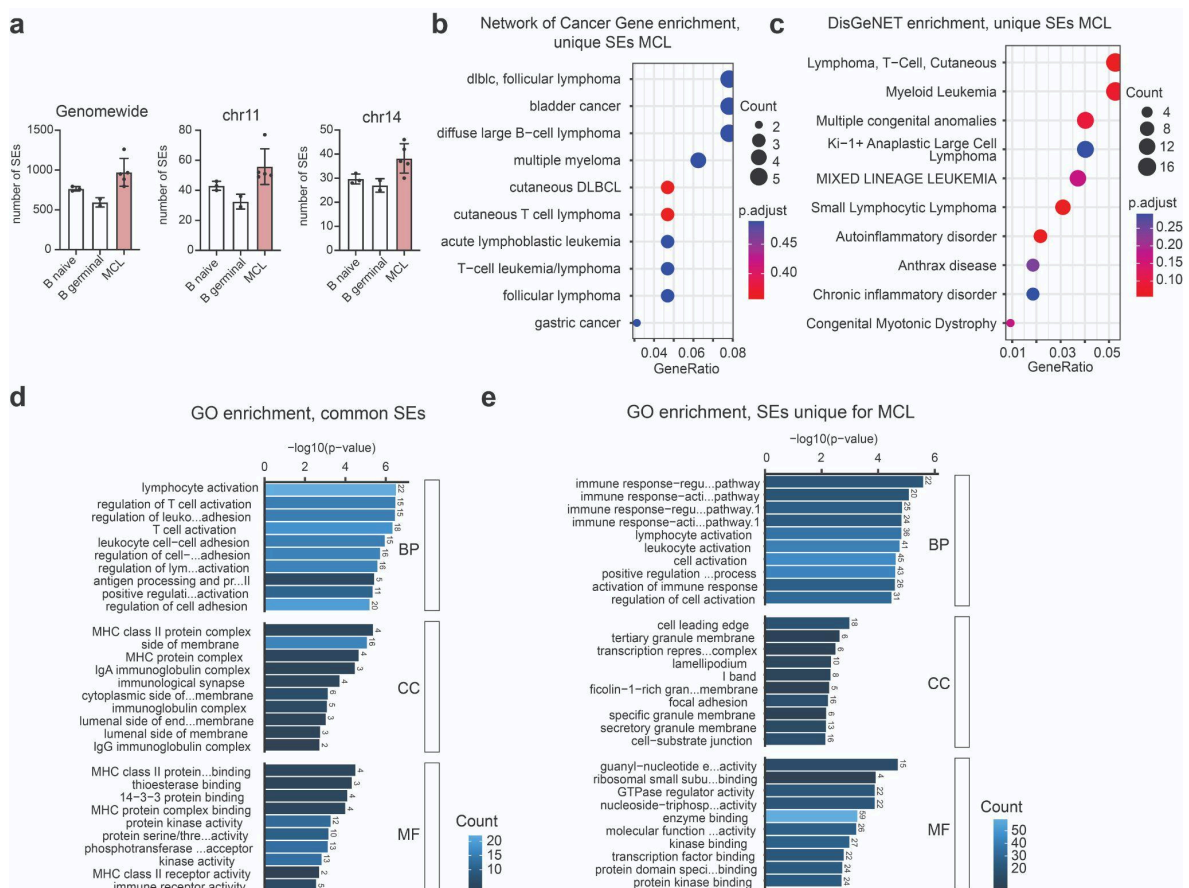
1. Canoy R.J.[†], Shmakova A.[†], **Karpukhina A.**, Lomov N., Tiukacheva E., André F., Germini D., Vassetzky Y. Breakage first drives generation of chromosomal translocations upon targeted induction of double-stranded breaks in different cell types. *NAR Cancer*. 2023. V. 5, № 3, P. zcad049. doi: 10.1093/narcan/zcad049. (Research article)
2. Tiukacheva, E., Ulianov, S., **Karpukhina, A.**, Razin, S. and Vassetzky Y.S (2023) 3D genome alterations and editing in pathology. *Molecular Therapy*, DOI: 10.1016/j.ymthe.2023.02.005 (Review)
3. Canoy R.J., Shmakova A., **Karpukhina A.**, Shepelev M., Germini D., Vassetzky Y. Factors That Affect the Formation of Chromosomal Translocations in Cells. *Cancers*. 2022. V. 14, № 20, P. 5110. doi: 10.3390/cancers14205110. (Review)

PARTICIPATIONS IN CONFERENCES

1. 08.2024 - Transcription and chromatin, EMBL Conference (poster); **Schwager (Karpukhina) A.** Tsimailo I., Sall F. B., Germini D., Vassetzky Y. A novel super-enhancer on derivative chromosome 14 contributes to Mantle Cell Lymphoma pathogenesis through interchromosomal contacts.
2. 11.2023 - Les Journées de la Recherche Gustave Roussy (poster); **Schwager (Karpukhina) A.**, Tsimailo I., Sall F. B., Germini D., Vassetzky Y. A novel super-enhancer on derivative chromosome 14 contributes to Mantle Cell Lymphoma pathogenesis through interchromosomal contacts.
3. 11.2023 - Gliwice Cancer Scientific Meeting, Gliwice, Poland (talk); **Karpukhina A.**, Tsimailo I., Sall F. B., Germini D., Vassetzky Y. Epigenetic and 3D-genome changes contribute to the pathogenesis of Mantle cell lymphoma
4. 06.2023 - 27th Wilhelm Bernhard Workshop on the Cell Nucleus, Prague, Czech Republic (talk); **Karpukhina A.**, Tsimailo I., Sall F. B., Germini D., Vassetzky Y. Targeting the 3D genomic and epigenetic changes in Mantle Cell Lymphoma
5. 05.2023 - Troisième réunion annuelle du GDR Architecture et Dynamique du Noyau et des Génomes (ADN&G) (poster) ; **Karpukhina A.**, Tsimailo I., Sall F. B., Germini D., Vassetzky Y. Targeting the 3D genomic and epigenetic changes in MCL.
6. 08.2022 - Computational biology and artificial intelligence for personalized medicine 2022, Moscow, Russia, online (invited speaker and session chairman); **Karpukhina A.** Large-scale transcriptional, epigenomic and 3D genomic changes following t(11:14) chromosomal translocation in Mantle Cell Lymphoma
7. 06.2022 – 29th annual FSHD society International Research Congress (talk); **Karpukhina A.**, Tuikacheva E, Pan Z, Ulyanov S, Vassetzky Y. dCAS-CTCF Modifies 3D Genome Organization and DUX4 Expression in FSHD
8. 03.2022 - Applied Bioinformatics in Life Sciences, VIB Conference, Belgium, Leuven (poster); **Karpukhina A.** Large-scale transcriptional, epigenomic and 3D genomic changes following t(11:14) chromosomal translocation in Mantle Cell Lymphoma
9. 09.2021 - Computational biology and artificial intelligence for personalized medicine, Moscow, Russia (poster); **Karpukhina A.**, Galkin I., Ma Y., Vassetzky Y. Analysis of genes regulated by DUX4 via oxidative stress reveals potential therapeutic targets for treatment of facioscapulohumeral dystrophy

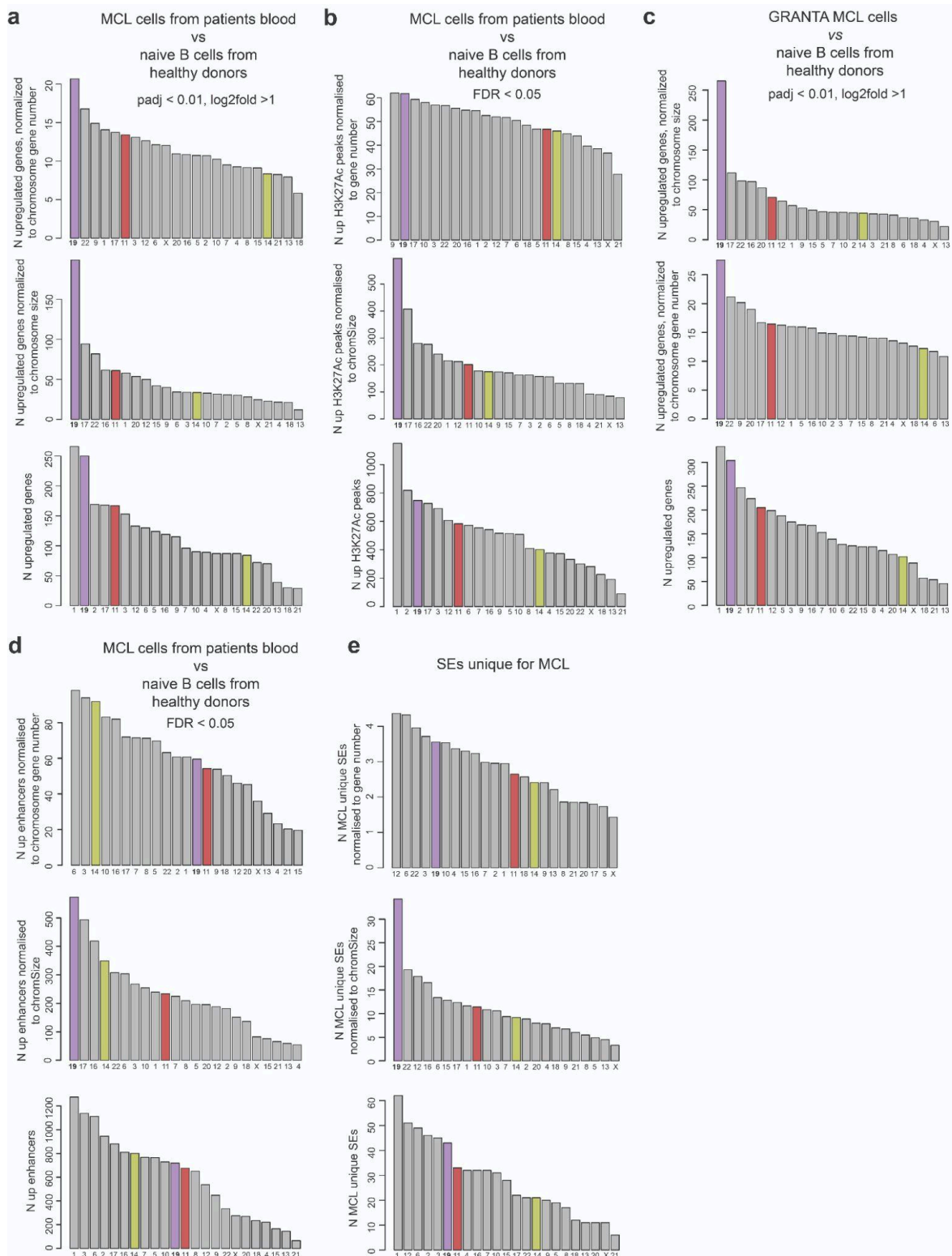
ANNEXES

Supplementary figures



Supplementary figure 1. Functional enrichment analysis of superenhancer-associated genes.

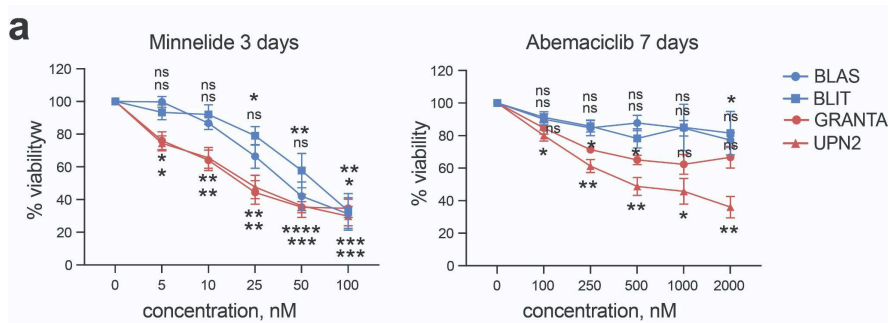
a, The numbers of SEs detected by ROSE in each individual sample of MCL patients, control naive and germinal B cells. The data is presented as mean \pm SD. **b**, The Network of Cancer Gene enrichment for the genes associated with the super-enhancers unique for MCL distance-wise. Top 10 enriched categories. **c**, DisGeNET enrichment for the genes associated with the superenhancers unique for MCL distance-wise. Top 10 enriched categories. **d**, Gene Ontology enrichment analysis for the genes associated distant-wise with the super-enhancers common for all the three groups of B cells. **e**, Gene Ontology enrichment analysis for the genes associated distant-wise with the super-enhancers unique for MCL.



Supplementary figure 2. Per-chromosome distributions of the upregulated genes, up H3K27Ac peaks, overactive enhancers and unique super-enhancers in MCL cells.

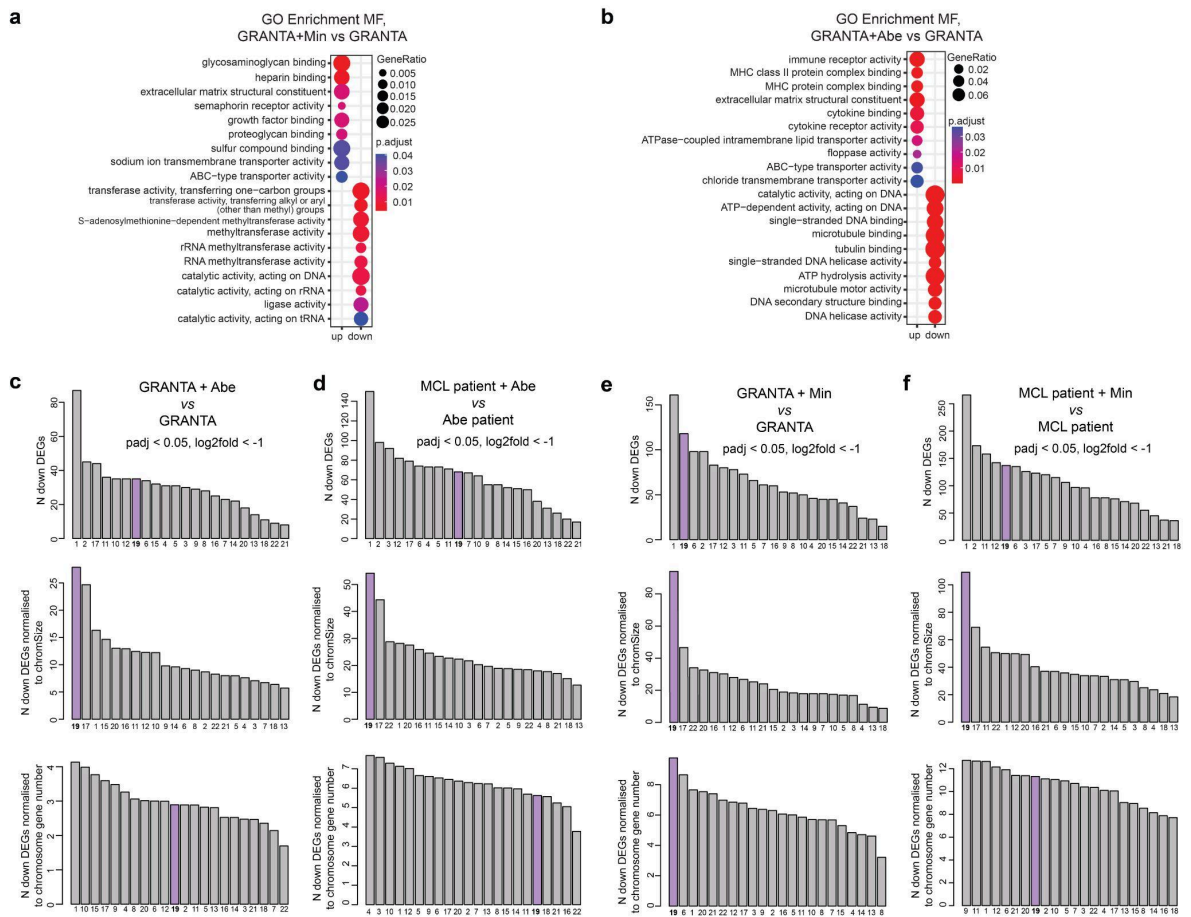
a, The numbers of upregulated genes per chromosome in MCL patients B cells vs control naive B cells from healthy donors (padj < 0.01, log2FC > 1), raw, normalized to chromosome size or to the number of genes on each chromosome. **b**, The numbers of up H3K27Ac per chromosome in MCL patients B cells vs control naive B cells from healthy donors (FDR < 0.05), raw, normalized to chromosome size or to the number

of genes on each chromosome. **c**, The numbers of upregulated genes per chromosome in MCL cell line GRANTA-519 vs control naive B cells from healthy donors ($p_{adj} < 0.01$, $\log_2FC > 1$), raw, normalized to chromosome size or to the number of genes on each chromosome. **d**, The numbers of enhancers overlapping with the up H3K27Ac peaks ($FDR < 0.05$) by at least 50% in MCL patients B cells vs control naive B cells from healthy donors; raw, normalized to chromosome size or to the number of genes on each chromosome. **e**, The numbers of super-enhancers (SEs) unique for MCL per chromosome; raw, normalized to chromosome size or to the number of genes on each chromosome.



Supplementary figure 3. Minnelide and Abemaciclib titration.

a, MTT assay of the viability of MCL (red) and control (blue) cells treated with 0-100nM of Minnelide for 3 days or 0-2000nM of Abemaciclib for 7 days. The data are shown as means \pm SEM, $N=3-6$. Statistical significance is determined relative to the untreated sample using the two-way ANOVA with Dunnett's correction for multiple comparisons. $p_{val} < 0.05^*$, $< 0.01^{**}$, $< 0.001^{***}$, 0.0001^{****} .



Supplementary figure 4. Molecular function enrichment and per-chromosome distributions of the genes downregulated by Minnelide and Abemaciclib.

a,b, Gene Ontology enrichment analysis for the molecular function of the genes upregulated ($\log_2FC > 1$, $padj < 0.05$) or downregulated ($\log_2FC < -1$, $padj < 0.05$) following Minnelide (a) or Abemaciclib (b) treatment in the MCL cell line GRANTA-519. **c,d**, The numbers of genes downregulated by Abemaciclib ($\log_2FC < -1$, $padj < 0.05$) per chromosome in the MCL cell line GRANTA-519 (c), and the PBMCs of an MCL patient (d); raw, normalized to chromosome size or to the number of genes on each chromosome. **e,f**, The numbers of genes downregulated by Minnelide ($\log_2FC < -1$, $padj < 0.05$) per chromosome in the MCL cell line GRANTA-519 (e), and the PBMCs of an MCL patient (f); raw, normalized to chromosome size or to the number of genes on each chromosome.

Articles

Article 2. Breakage first drives generation of chromosomal translocations upon targeted induction of double-stranded breaks in different cell types

Canoy R.J.[†], Shmakova A.[†], **Karpukhina A.**, Lomov N., Tiukacheva E., André F., Germini D., Vassetzky Y. Breakage first drives generation of chromosomal translocations upon targeted induction of double-stranded breaks in different cell types. *NAR Cancer*. 2023. V. 5, № 3, P. zcad049. doi: 10.1093/narcan/zcad049.

Most cancer-related chromosomal translocations are specific to certain cell types. It's not clear why different translocations happen in different cells. This could be because specific translocations occur only in certain cell types or because these translocations give a survival advantage only to specific cells.

We explored this question by inducing double-strand breaks (DSBs) at MYC, IGH, AML, and ETO gene locations in the same cell, aiming to create chromosomal translocations in different cell lineages. Our findings show that any translocation can potentially occur in any cell type. We examined various factors that could influence the frequency of these translocations and found that only the spatial proximity of gene loci after DSB induction was correlated with the frequency of resulting translocations, supporting the 'breakage-first' model.

Additionally, after culturing cells with these induced chromosomal translocations for 60 days, only the oncogenic MYC-IGH and AML-ETO translocations persisted. Overall, our results suggest that while chromosomal translocations can be generated in any type of cell after DSB induction, the persistence of these translocations in a cell population depends on whether the translocation confers a selective survival advantage to the specific cell type.

In this research paper, I carried out some experiments, statistical, bioinformatic and image analysis and also participated in writing and revision of the manuscript.

Specificity of cancer-related chromosomal translocations is linked to proximity after the DNA double-strand break and subsequent selection

Reynand Jay Canoy^{1,2,†}, Anna Shmakova^{1,3,4,†}, Anna Karpukhina^{1,4}, Nikolai Lomov⁵, Eugenia Tiukacheva^{1,4}, Yana Kozhevnikova¹, Franck André¹, Diego Germini^{1,*} and Yegor Vassetzky^{1,4,*}

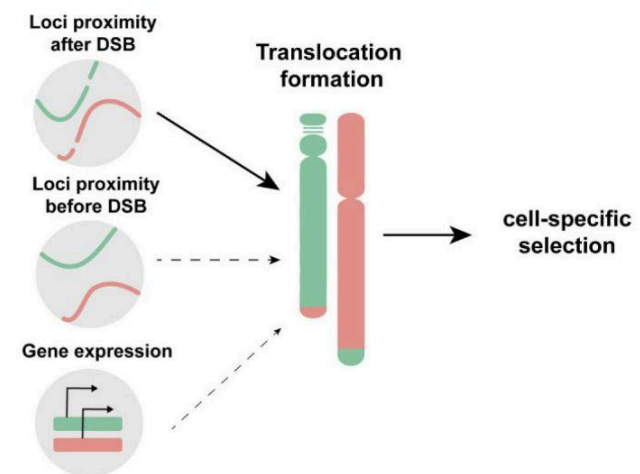
¹UMR 9018, CNRS, Univ. Paris-Sud, Université Paris Saclay, Institut Gustave Roussy, F-94805 Villejuif, France, ²Institute of Human Genetics, National Institutes of Health, University of the Philippines Manila, 1000 Manila, The Philippines, ³Laboratory of Molecular Endocrinology, Institute of Experimental Cardiology, Federal State Budgetary Organization 'National Cardiology Research Center' of the Ministry of Health of the Russian Federation, 127994 Moscow, Russia, ⁴Koltzov Institute of Developmental Biology, 117334 Moscow, Russia and ⁵Department of Molecular Biology, Faculty of Biology, Lomonosov Moscow State University, 119991 Moscow, Russia

Received March 17, 2023; Revised August 01, 2023; Editorial Decision August 30, 2023; Accepted September 14, 2023

ABSTRACT

Most cancer-related chromosomal translocations appear to be cell type specific. It is currently unknown why different chromosomal translocations occur in different cells. This can be due to either the occurrence of particular translocations in specific cell types or adaptive survival advantage conferred by translocations only in specific cells. We experimentally addressed this question by double-strand break (DSB) induction at *MYC*, *IGH*, *AML* and *ETO* loci in the same cell to generate chromosomal translocations in different cell lineages. Our results show that any translocation can potentially arise in any cell type. We have analyzed different factors that could affect the frequency of the translocations, and only the spatial proximity between gene loci after the DSB induction correlated with the resulting translocation frequency, supporting the 'breakage-first' model. Furthermore, upon long-term culture of cells with the generated chromosomal translocations, only oncogenic *MYC-IGH* and *AML-ETO* translocations persisted over a 60-day period. Overall, the results suggest that chromosomal translocation can be generated after DSB induction in any type of cell, but whether the cell with the translocation would persist in a cell population depends on the cell type-specific selective survival advantage that the chromosomal translocation confers to the cell.

GRAPHICAL ABSTRACT



INTRODUCTION

Chromosomal translocations are hallmarks of many cancers (1). More than 50% of leukemias and almost all lymphomas exhibit or are directly caused by chromosomal translocations (2–5). Functional consequences of chromosomal translocations include aberrant expression of otherwise normal genes, expression of fusion genes and/or large-scale changes in the nuclear organization (6–9).

Many of the known chromosomal translocations appear to be cell type specific (3). For example, the *MYC-IGH* translocation has only been observed in B cells and not in

*To whom correspondence should be addressed. Tel: +33 1 42 11 45 26; Email: germinidiego@gmail.com

Correspondence may also be addressed to Yegor Vassetzky. Tel: +33 1 42 11 62 83; Fax: +33 1 42 11 54 94; Email: yegor.vassetzky@cnrs.fr

†The authors wish it to be known that, in their opinion, the first two authors should be regarded as Joint First Authors.

other cell types. Why do different chromosomal translocations occur in different cells? Is this due to the fact that some translocations are more likely to occur in specific cell types due to cell-specific characteristics or do translocations occur in a similar manner in all cells, but they confer a selective advantage in a specific cell type? The generation of chromosomal translocation involves two major steps: the formation of specific double-strand breaks (DSBs) and their erroneous repair via nonhomologous end joining (NHEJ) (10). Cell-specific traits that may potentially affect translocation formation include preferential occurrence of DSBs at specific loci in specific cell types [e.g. due to chromatin state or the activity of intrinsic DNA-cutting enzymes (9,11)] and/or predetermined factors that affect DNA repair [e.g. transcriptional activity, loci spatial proximity, the activity of specific repair factors or even cell-specific expression of chromosomal aberrations stimulating long noncoding RNAs (lncRNAs) (12)]. While previous studies have extensively explored the occurrence of cell-specific DSBs, less is known about the risk factors that interfere with translocation-prone DSB repair once they are already formed in a particular cell type. Chromatin state, DSB movement and DNA damage sensing and repair mechanisms influence the generation of chromosomal translocations at this step (9). The presence of specific transcripts [e.g. lncRNAs that share homology regions for two different loci (12,13)] or certain drugs (14) can also affect the formation of chromosomal rearrangements. Understanding these risk factors is crucial for developing targeted interventions to prevent the occurrence of translocations and the development of related diseases such as cancer.

Studying randomly induced and/or naturally occurring chromosomal translocations poses challenges and serious limitations. First, translocations are rare events, for certain types of translocations literally a single event occurs in the whole organism, and cells with translocations can survive and proliferate only if translocation provides a proliferative advantage in a cell population. Second, the localization of breakpoints in naturally occurring translocations varies from kilobases to hundreds of kilobases, which requires sophisticated techniques to detect them [e.g. long-range polymerase chain reaction (PCR), fluorescence *in situ* hybridization (FISH), deep sequencing, etc.] (15,16). With the advancement of gene-editing tools that can produce DSBs at specific loci, the generation of cell lines with specific chromosomal translocations became possible (14,17–22). The CRISPR/Cas9 tool generates DSBs in both euchromatin and heterochromatin regions (23–27), which facilitates the study of factors that affect the formation of translocations across different cell types. Here, we devised a CRISPR/Cas9-based experimental strategy to induce DSBs in one cell within several specific loci that are commonly involved in oncogenic chromosomal rearrangements (*MYC*, *IGH*, *AML*, *ETO*) with the aim to stimulate the formation of chromosomal translocations between these loci. Using this strategy, we investigated different factors associated with the frequency of generated chromosomal translocations in human cells of different developmental origins. We analyzed the translocation frequencies with respect to the transcription activity, nuclear radial position and spatial proximity of the gene loci targeted by CRISPR/Cas9

and demonstrated that in all of the considered cell types the most prominent factor affecting the chromosomal translocations was the spatial proximity between the potential partner loci after the DSB induction. The colocalization of potential partner loci after the DSB induction was dependent on DNA-dependent protein kinase (DNA-Pk) activity. Our results demonstrated that virtually any type of chromosomal translocation can arise in any cell type after the induction of DSBs, but the persistence of cells with these translocations is dependent on the specific survival advantage conferred by the translocation in that cell type. This highlights the complexity of chromosomal translocations in cancer cells and underscores the importance of considering the selective survival advantage of chromosomal translocations in different cell types, adding a new dimension to our understanding of the process.

MATERIALS AND METHODS

Cell culture

All cells were handled in aseptic techniques and were kept in a humidified incubator at 37°C with 5% CO₂ until use. They were maintained in their respective cell culture growth medium and were passed at least once a week. For the recipes of the growth medium, see Supplementary Data. Cell treatments are listed in Supplementary Table S1.

gRNA design, cloning and testing

All guide RNA (gRNA) binding sites were generated from CRISPOR gRNA design online tool (<http://crispor.tefor.net/>) (28) and were inserted into the pHU6 gRNA plasmids (Addgene #53188). gRNA and Cas9 plasmids (Addgene #57818) were transformed into DH5 α competent cells via heat shock and were then subsequently clonally expanded for plasmid extraction (Machery-Nagel NucleoBond Xtra Midi or Maxi kit). gRNA efficiency was tested following the procedures provided in TIDE (29) and ENIT (30) protocols. For the sequences of the gRNA binding sites, see Supplementary Table S2.

Electrotransfection

Cells were electrotransfected following the protocol for hard-to-transfect cells in (31). Briefly, 4–8 \times 10⁶ cells were electrotransfected with 50 μ g total plasmid, 60% of which is Cas9 and the remaining 40% consists of gRNA plasmids. After 2 days, electrotransfection efficiency was checked using Accuri™ C6 Flow Cytometer (BD Biosciences). Depending on the intended number of electrotransfected cells, the electrotransfection reactions were scaled up.

Western blot

Western blot analysis was performed following the protocol in (32) using the following antibodies: Cas9 antibody (7A9-3A3) (anti-mouse, Santa Cruz Biotechnology, sc-517386), GAPDH (anti-mouse, Cell Signaling Technology, 2118) and anti-mouse peroxidase-conjugated secondary antibodies (Jackson ImmunoResearch, 315035003).

PCR and qPCR

Total DNA was extracted using NucleoSpin Tissue DNA purification kit (Macherey-Nagel) following the manufacturer's protocol. Total RNA was extracted using NucleoSpin RNA II purification kit (Macherey-Nagel) and was then converted to complementary DNA (cDNA) using Maxima H Minus cDNA Synthesis Master Mix (Thermo Fisher Scientific) following the manufacturer's protocol. PCR amplification was performed using PowerUp SYBR Green Master Mix (Thermo Scientific) following the manufacturer's protocol. For the PCR primers used, see Supplementary Tables S3 and S4.

Translocation frequency was calculated using the Pfaffl method (33) to correct for the observed varying amplification efficiencies of each primer pair (Supplementary Figure S2F). The calculated frequencies were then adjusted to the respective transfection efficiencies measured 2 days after electrotransfection, right before cell collection, using the Accuri™ C6 Flow Cytometer (BD Biosciences).

3D-FISH

3D-FISH was performed following the protocols in (18) using the following probes: AML (Empire Genomics, RP11-1056O16 blue), ETO (Empire Genomics, RP11-643O11 orange), MYC (Empire Genomics, RP11-440N18 red) and IGH (Empire Genomics, RP11-346I20 green). For image acquisition and analysis, see Supplementary Data.

Statistical analysis

All experiments were performed with at least two biological replicates and two technical replicates. Statistical analyses were performed using GraphPad Prism 9.1.0.221 and R Studio. For comparisons between the two groups, an unpaired *t*-test was done. For comparisons involving more than two groups, one-way analysis of variance (ANOVA) and Tukey's honest significant difference as the post-hoc test were performed. For the correlation analysis, the Spearman correlation between the translocation frequency and the predictors (gene expression/loci proximity before DSB/loci proximity after DSB) was performed.

RESULTS

Experimental strategy for analysis of CRISPR/Cas9-induced chromosomal translocations

With the aim to identify factors affecting the generation of chromosomal translocations across cell types, we developed a CRISPR/Cas9-based strategy to induce DSBs in one cell within several chromosomes. This would potentially generate several different chromosomal translocations upon erroneous repair of these DSBs via NHEJ (Figure 1A and Supplementary Figure S1A). The frequencies of induced chromosomal translocations were measured by quantitative PCR (qPCR) and compared in one cell type and between different cell types. We selected four loci for DSB induction: the *RUNX1* (formerly known as *ETO*) gene on chromosome 8q21, the upstream region of the *MYC* gene on chromosome 8q24, the immunoglobulin

heavy chain (*IGH*) gene locus on chromosome 14q32 and the *RUNX1* (formerly known as *AML*) gene on chromosome 21q22. These gene loci are involved in clinically relevant oncogenic translocations: t(8;21) between *AML* and *ETO* in acute myeloid leukemia and t(8;14) between *MYC* and *IGH* in Burkitt's lymphoma.

The gRNAs were designed (Supplementary Table S2) to target the above loci and cloned into pHU6 plasmids. gRNA efficiency was tested by TIDE (29) as described in the 'Materials and Methods' section and gRNAs with similar efficiencies were chosen to avoid a bias of different CRISPR/Cas9 cutting efficiencies (Supplementary Figure S2A). The cells were then electrotransfected with the Cas9-expressing plasmid to determine the Cas9 expression kinetics. The Cas9 expression started to peak 48 h after the electrotransfection (Supplementary Figure S2B). We then tested the cell survival and apoptosis after electrotransfection (Supplementary Figure S2C and D).

We designed PCR primers (Supplementary Tables S3 and S4) to detect resulting translocations. Supplementary Figure S2E shows a representative image of an agarose gel electrophoresis of PCR-amplified *MYC-IGH* translocations after electrotransfection with Cas9 and gRNAs targeting the *MYC* and *IGH*, *AML-ETO* translocations after electrotransfection with Cas9 and gRNAs targeting the *AML* and *ETO*, *IGH-ETO* translocations after electrotransfection with Cas9 and gRNAs targeting the *IGH* and *ETO*, and *AML-IGH* translocations after electrotransfection with Cas9 and gRNAs targeting the *AML* and *IGH*. The amplification efficiencies of each primer pair (Supplementary Figure S2F) were taken into account when calculating the translocation frequency (see the 'Materials and Methods' section). The translocation frequency started peaking 48 h post-transfection (Supplementary Figure S3); therefore, we selected the 48 h post-electrotransfection as the collection time point for the next experiments to avoid the effect of positive or negative selection of translocations upon subsequent cell divisions.

We used inhibitors of specific repair pathways to determine the pathway of the translocation formation in our model. We added the inhibitors of either MRE11 involved in both classical and alternative NHEJ (mirin) or DNA-Pk involved in the canonical NHEJ pathway (NU7026). We observed that treatment with NU7026 led to a 2.4-fold increase ($P = 0.0056$) in the translocation rate (Figure 1B), suggesting that translocations are mainly due to the alternative NHEJ repair as already proposed by others (34).

Simultaneous induction of DSBs results in cell type-specific translocation frequencies

To analyze the appearance of chromosomal translocations in different cell types, we induced DSBs in cell lines of different developmental origin and ploidy: RPMI8866 (lymphoid, B cell, diploid with three to four copies of chromosome 8), Jurkat (lymphoid, T cell, diploid), K562 [myeloid, nearly triploid (35)], MRC5 (lung fibroblast, diploid) and Hek-293 (embryonic kidney, epithelial, hypotriploid). These cell lines were electrotransfected with plasmids encoding for Cas9 and gRNA combinations targeting two sets of gene loci: *MYC*, *IGH* and *AML* (MIA) or

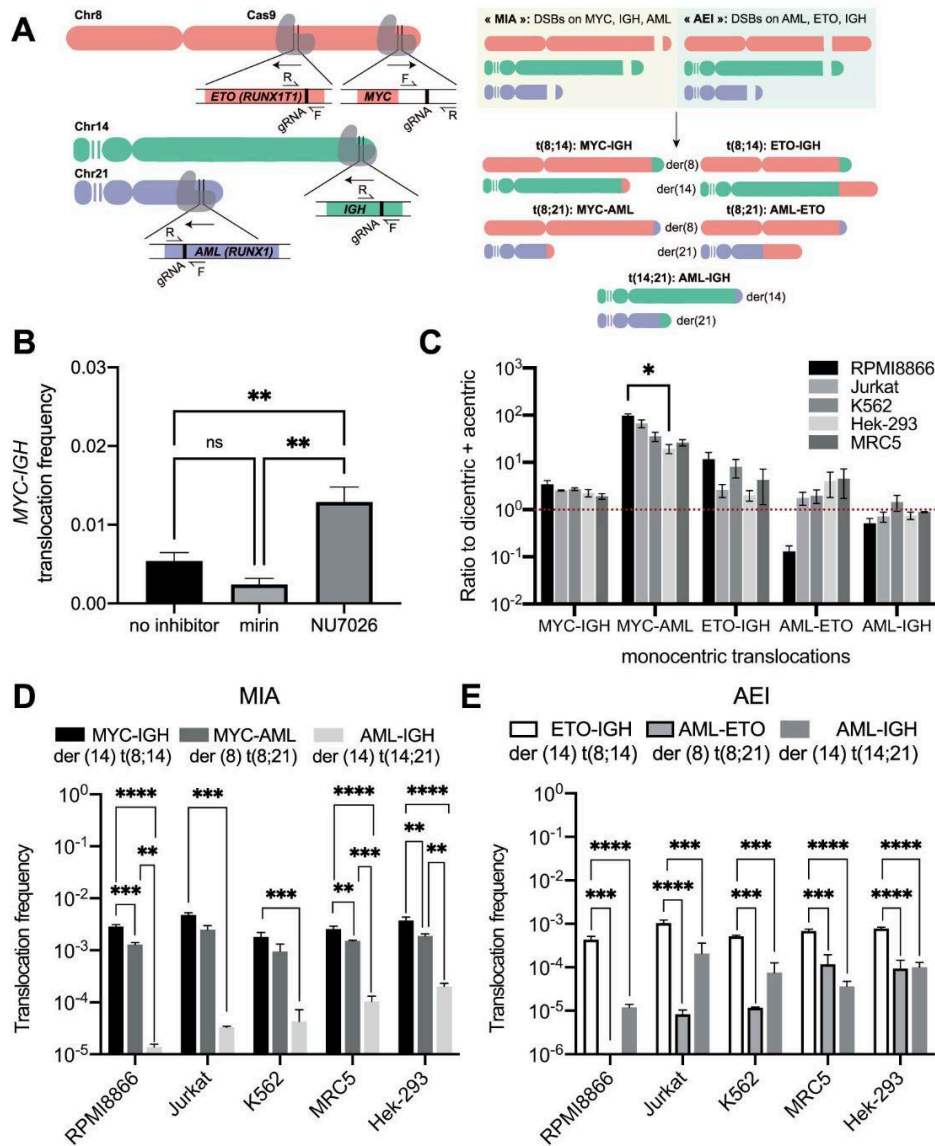


Figure 1. Translocations generated in different cells after the simultaneous induction of three DSBs on chromosomes 8, 14 and 21. (A) Positions of sites targeted by gRNA in the *ETO* (8q21.3), *MYC* (8q24.12), *IGH* (14q32.33) and *AML* (21q22.12) gene loci (left panel) and the resulting potential univalent chromosomal translocations after targeting *MYC*, *IGH* and *AML* loci (MIA) or *AML*, *ETO* and *IGH* loci (AEI) (right panel). (B) *MYC-IGH* translocation frequency after inhibition of NHEJ repair components. Six hours after electrotransfection with gRNA and Cas9 plasmids, cells were treated with either mirin (an inhibitor of MRE11) or NU7026 (an inhibitor of DNA-Pk). The number of biological replicates $n = 4-5$. (C) Ratio of the combined translocation frequencies of the two monocentric derivative chromosomes with respect to the combined translocation frequencies of the dicentric and acentric derivative chromosomes. The data are shown on a log₁₀ scale. Translocations were induced in RPMI8866, Jurkat, K562, MRC5 and Hek-293 cells via electrotransfection with gRNA and Cas9 plasmids, targeting *MYC*, *IGH* and *AML* loci or *AML*, *ETO* and *IGH* loci and the resulting translocation frequencies were measured 2 days later by qPCR with a subset of primers that target monocentric (two pairs for each translocation), dicentric and acentric derivative chromosomes. Then, the frequencies of monocentric chromosomes were added and divided by the sum of frequencies of the dicentric and acentric derivative chromosomes, providing the resulting ratio. In almost all cases, the ratio was >1, indicating that the generation of monocentric derivative chromosomes was favored over dicentric and acentric ones. The number of biological replicates $n = 2-7$. (D, E) Frequencies of translocations induced by DSBs. RPMI8866, Jurkat, K562, MRC5 and Hek-293 cells were electrotransfected with gRNA and Cas9 plasmids, targeting MIA (D) or AEI (E). After 2 days, electrotransfected cells were collected for DNA extraction and translocations were detected using qPCR with translocation-specific PCR primers. The translocation frequencies were calculated as described in the ‘Materials and Methods’ section. Only the univalent derivative chromosomes with the highest frequency compared to their reciprocal counterparts are shown in the graphs. Means \pm standard errors of the mean (SEMs) of at least two biological and two technical replicates are shown. One-way ANOVA with Tukey’s honest significant difference post-hoc test was performed to compare the translocation frequencies within each cell type: ** $P \leq 0.01$, *** $P \leq 0.001$ and **** $P \leq 0.0001$.

AML, *ETO* and *IGH* (AEI). DNA was collected 48 h later and all possible resulting translocations were quantified using qPCR as described in the ‘Materials and Methods’ section. In theory, each chromosome pair can form three types of translocations: unacentric (with one centromere; most cancer-related translocations are unacentric), dicentric (with two centromeres) and acentric (without centromeres). The latter two types of translocations are usually lost in the course of cell divisions; therefore, we concentrated on unacentric translocations.

In almost all translocations in all cell types, the combined translocation frequencies of the monocentric derivative chromosomes were higher compared to the combined dicentric and acentric derivative chromosomes after induction of three DSBs (Figure 1C), suggesting that the formation of monocentric derivative chromosomes is already favored early on. The *MYC-IGH* translocation had the highest frequency after MIA DSB induction ($2-5 \times 10^{-3}$ translocations/cell) compared to the *MYC-AML* and *AML-IGH* translocations ($1-2 \times 10^{-3}$ and $0.01-0.2 \times 10^{-3}$ translocations/cell, respectively) (Figure 1D and Supplementary Figure S4A–E). After AEI DSB induction, the *ETO-IGH* translocation had the highest frequency ($0.4-1 \times 10^{-3}$ translocations/cell) compared to the *AML-IGH* and *AML-ETO* translocations ($0.01-0.2 \times 10^{-3}$ and $0.008-0.1 \times 10^{-3}$ translocations/cell, respectively) (Figure 1E and Supplementary Figure S4F–J). Of the five cell types, Jurkat exhibited the highest translocation frequencies after induction of either MIA or AEI DSBs. The oncogenic *MYC-IGH* translocation had the highest frequency after MIA DSB induction (Figure 1D), while another oncogenic *AML-ETO* translocation had the lowest frequency after AEI DSB induction (Figure 1E), although it was relatively high in the myeloid K562 and epithelial Hek-293 cells (0.01×10^{-3} and 0.1×10^{-3} , respectively). Interestingly, the translocation frequencies involving the *MYC* locus were two to four times higher than those of the other translocations in all cell types. Another important conclusion is that while the studied cell lines had different ploidies, relative frequencies of translocations were similar across the cell lines with few exceptions.

Transcriptional activity and nuclear radial distribution of gene loci do not correlate with the translocation formation after DSB induction

We next tried to identify factors that could account for the observed translocation frequencies. Actively transcribed loci, loci with an open chromatin configuration or loci located close to each other may have higher propensities to form translocations (36–39). *MYC-IGH* and *AML-ETO* translocations will now serve as examples of our results, but all the described analyses were performed for all possible translocations.

We first correlated the frequencies of the *MYC-IGH* and *AML-ETO* translocations in different cell types (Figure 2A and B) with the transcriptional activity of the involved genes determined by quantitative reverse transcription PCR (Figure 2C) and no positive correlation was observed ($R_s = 0.24$, Figure 2D). Higher transcriptional activity did not always mean higher translocation rate. For example, both *MYC*

and *IGH* were actively transcribed in the RPMI8866 cells, and *IGH* was minimally or not transcribed in other cell types, but this did not affect the frequency of the *MYC-IGH* translocation that remained high. On the contrary, the *AML-ETO* translocation was generated at a very low frequency in K562 cells (Figure 2B) even though the *AML* and *ETO* genes were actively transcribed (Figure 2C). The *ETO-IGH* translocation in Jurkat was still generated (Figure 1E) though neither *ETO* nor *IGH* was actively transcribed (Figure 2C).

Radial positions reflect the localization of gene loci within the nucleus. Peripheral regions of the nucleus are often heterochromatin-rich and transcriptionally repressed, while central regions are transcriptionally active. We determined the nuclear radial positions of the four gene loci before the DSB induction using 3D-FISH. The *MYC*, *IGH*, *AML* and *ETO* loci were positioned near the center of the nucleus and had a roughly similar radial distribution before (Figure 2E) and after DSB induction (Figure 2F). Thus, this factor could not solely account for the variability of translocation frequencies between different gene loci across the studied cell lines in our system.

The breakage-first model accounts for translocation formation after DSB induction

As translocations are produced by NHEJ, a proximity-based mechanism (40), we next studied whether the loci involved in the translocations were proximal in the cell nuclei. We have measured the distance between fluorescent signals corresponding to the studied loci. As each 3D-FISH signal was $\sim 1 \mu\text{m}$ in diameter, two signals were considered to be proximal (colocalized) when the distance between their centers was no more than $1 \mu\text{m}$, since at this distance, spots partially or completely overlapped. The spatial proximity between the gene loci was expressed as the percentage of cells where the two loci were colocalized. Surprisingly, before the occurrence of DSB, we did not observe a positive correlation between gene proximity and translocation rate ($R_s = 0.32$; $P = 0.0331$) (Figure 3C). As DSBs are known to induce mobility of the damaged gene loci [reviewed in (41)], we also measured gene proximity after the DSB induction. We observed a significant increase of gene loci proximity after DSB induction in the case of *MYC-IGH* and *ETO-IGH* pairs in all considered cell types (Figure 3A and D, and Supplementary Figure S5A–F) and the translocations between these very gene loci were also the most frequent (Figure 3B and E). A representative image shows the positions of *MYC* and *IGH* loci before and after the DSB induction (Figure 3G). It is noteworthy that colocalization of gene loci was a predisposing factor for their translocation but did not necessarily mean that they were translocated (e.g. *AML-ETO* were colocalized in $4.4 \pm 0.3\%$ of RPMI8866 cells after DSBs, but no translocations between these loci were observed; Figure 3D and E). Overall, we observe colocalization between loci at a much higher rate than translocations; this shows that colocalization alone is not sufficient to induce translocations. The inverse is also true, as in the case of *MYC-AML* translocation, where the loci were not found to colocalize at a detectable rate and yet the translocation was still formed (Figure 3A and B). When we took into

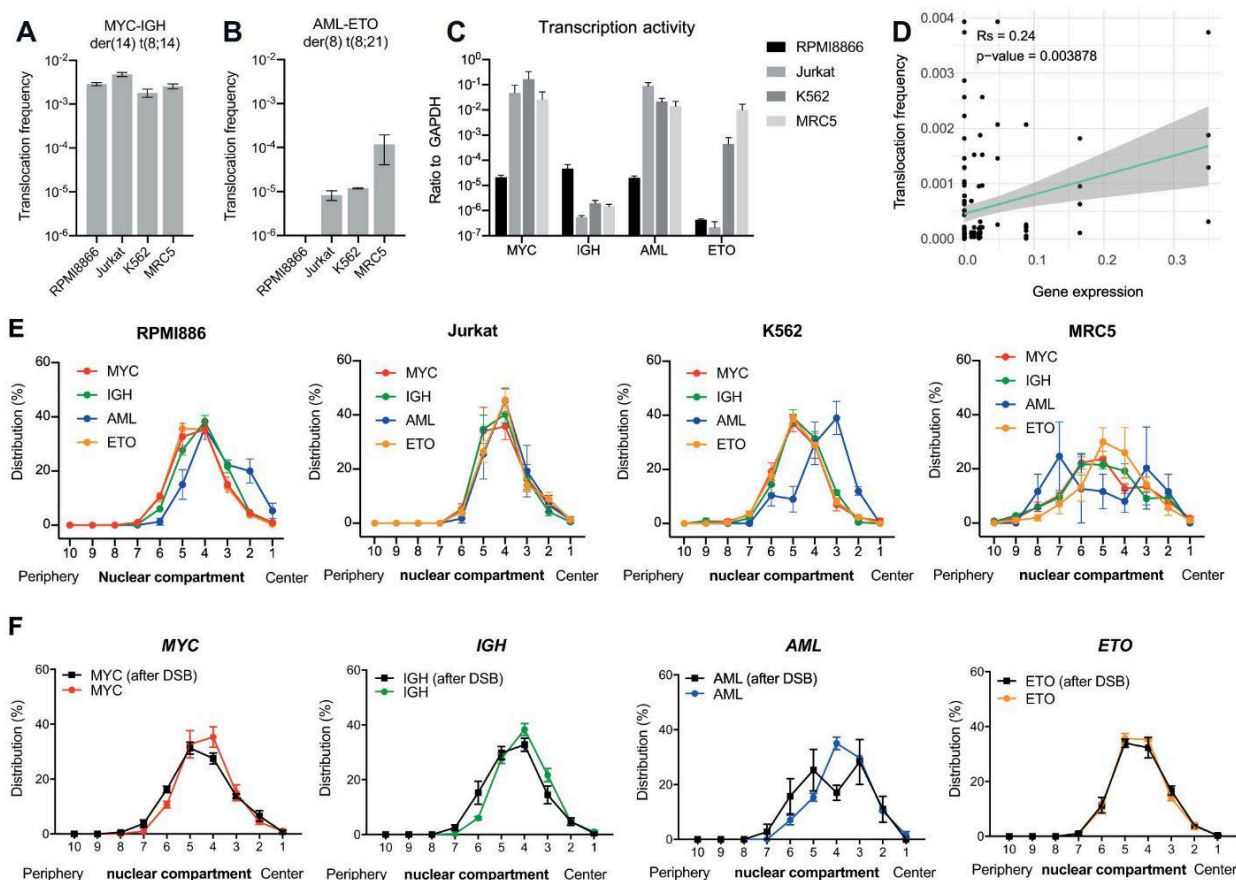


Figure 2. Transcriptional activity and nuclear radial position of gene loci do not correlate with their translocation frequency. Frequencies of the *MYC-IGH* (A) and *AML-ETO* (B) translocations across the cell lines. RPMI8866, Jurkat, K562 and MRC5 cells were electrotransfected with gRNAs and Cas9 plasmids targeting MIA (A) or AEI (B). Forty-eight hours after electrotransfection, cells were collected for DNA extraction and translocations were detected using qPCR with translocation-specific PCR primers. The translocation frequencies were calculated. Means \pm SEMs are shown representing the results of two to four biological and two technical replicates. (C) Transcriptional activity of the *MYC*, *IGH*, *AML* and *ETO* genes in the studied cell lines. RNA was extracted from cells and relative fold gene expression with respect to the housekeeping gene *GAPDH* was calculated from Ct values obtained from the qPCR results as described in the ‘Materials and Methods’ section. Means \pm SEMs of two to three biological and two technical replicates are shown. (D) Correlation plot for the gene expression and observed translocation frequencies. The Spearman correlation coefficient ($R_s = 0.24$) and its corresponding *P*-value (0.003878) are shown. The green line represents the linear regression fit and the gray area represents the 95% confidence intervals. (E) Radial position of the gene loci in the nuclear space of RPMI8866, Jurkat, K562 and MRC5 cells analyzed by 3D-FISH. (F) Radial position in the nuclear space of *MYC*, *IGH*, *AML* and *ETO* before and after DSB induction in RPMI8866. For the nuclear radial position before DSB induction, non-electrotransfected cells were collected and processed for 3D-FISH. For the nuclear radial position after DSB induction, RPMI8866 (16×10^6 cells) were electrotransfected with Cas9 and gRNA-expressing plasmids targeting either MIA or AEI. Two days after electrotransfection, cells were sorted for GFP, as the electrotransfected Cas9 plasmid also codes for GFP. The sorted cells were then processed for 3D-FISH. The images were acquired using a confocal microscope and analyzed using the Bitplane Imaris software. Each gene locus was mapped within the nucleus with respect to the 10 concentric compartments with the equal volume numbered from the center to the periphery of the nucleus. Data are presented as means \pm SEMs of three to four biological replicates. For each technical replicate, at least 100 cells were analyzed.

consideration all detected translocations in all studied cell types, we could reveal a positive correlation ($R_s = 0.55$; $P = 0.0001$) between the proximity after the DSB and the translocation frequency (Figure 3F), indicating that translocation formation was affected by the spatial proximity between gene loci after the DSB induction. In multiple linear regression of different factors that could affect translocation frequency, which also took into account the cell type, only the proximity after the DSB showed a significant association with the translocation frequency ($P = 0.012$, Table 1).

To identify factors that affected loci movement after DSB induction, we used several inhibitors: NU7026 (an

inhibitor of DNA-Pk), L67 (a DNA ligase I and III inhibitor) and KU-55933 (ATM inhibitor). We found that loci proximity after the DSB induction increased significantly in the presence of NU7026 (Figure 3H), which indicates that DNA-Pk-dependent signaling prevents loci relocation upon DSB.

Different survival outcomes of cells with chromosomal translocations

Our results show that any translocation can potentially arise in all types of cells; at the same time, the majority of described cancer-related chromosomal translocations

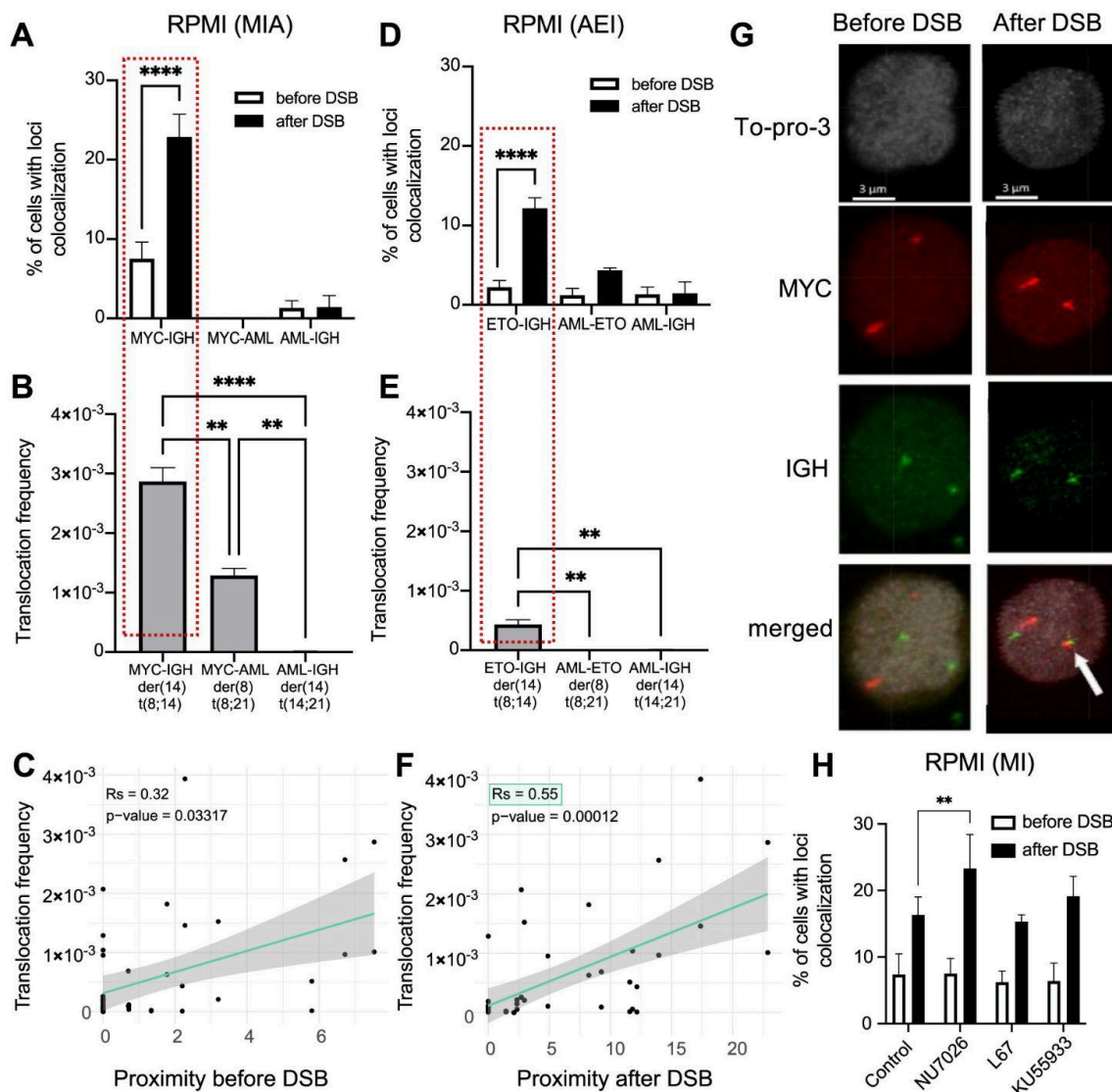


Figure 3. Spatial proximity between gene loci before and after DSB induction in RPMI8866. Spatial proximity between gene loci before and after DSB induction in MIA (A) and AEI (D) in RPMI8866. Non-electrotransfected cells ($1-2 \times 10^5$) (before DSB) and sorted cells (after DSB) ($1-2 \times 10^5$) that were electrotransfected with gRNAs and Cas9 plasmids 2 days prior were collected and processed for 3D-FISH. The slides were scanned using a confocal microscope and 3D-FISH images were analyzed in Bitplane Imaris software. The percentage of cells with the target gene loci pair located at $1 \mu\text{m}$ or less (colocalized) was calculated. The number of replicates $n = 2-8$. Translocation frequencies after DSB induction in MIA (B) and AEI (E) in RPMI8866. Only the unicentric derivative chromosomes with the highest frequency are shown. The number of replicates $n = 3$. Scatter plots of translocation frequency versus before DSB proximity (C) and after DSB proximity (F). The Spearman correlation coefficient (R_s) and its corresponding P -value are shown. (G) Representative 3D-FISH image of RPMI8866 cells before (left column) and after DSB induction (right column). The nuclei were stained with To-Pro-3 and are represented in the images as gray. Meanwhile, the *MYC* and *IGH* loci were stained with specific fluorescent probes and are represented in red and green, respectively. Colocalization between *MYC* and *IGH* is pointed out in the merged image by a white arrow. Scale bar = $3 \mu\text{m}$. (H) Spatial proximity between gene loci before and after DSB induction in *MYC* and *IGH* (MI) in RPMI8866; cells were treated with NU7026 (an inhibitor of DNA-Pk), L67 (a DNA ligase I and III inhibitor), KU-55933 (ATM inhibitor) or left untreated (control). The number of replicates $n = 3-7$. For each replicate, at least 100 cells were analyzed. For all plotted values of each graph, one-way ANOVA was performed. For each comparison, the statistical significance is shown: ** $P \leq 0.01$ and **** $P \leq 0.0001$.

Table 1. Multiple linear regression of different factors involved in translocation formation. *P*-value < 0.05 is denoted in bold

Predictors	Translocation frequency		
	Estimates	95% CI	<i>P</i> -value
Cell type			
Jurkat	−0.00	−0.07 to 0.06	0.968
K562	−0.03	−0.10 to 0.04	0.385
MRC5	0.00	−0.05 to 0.06	0.869
RPMI8866	−0.01	−0.06 to 0.04	0.620
Loci proximity before DSB	0.00	−0.01 to 0.02	0.586
Loci proximity after DSB	0.01	0.00–0.01	0.012
Gene 1 expression	0.33	−0.24 to 0.89	0.251
Gene 2 expression	0.89	−0.36 to 2.14	0.156

Number of observations = 44; $R^2/R^2_{\text{adjusted}} = 0.621/0.537$; genes 1 and 2, number involved in chromosomal translocation; 95% CI, 95% confidence intervals.

are cell type specific (3,42). This may be due to the selective advantage the translocation provides to only specific types of cells. To test this, we analyzed how the generated chromosomal translocations would be retained in different cell lines upon long-term culture. Cells transfected with CRISPR/Cas9 and gRNAs were cultured for 60 days with regular weekly passages. Translocation persistence was different in different cell types (Figure 4A–E and Supplementary Figure S6A–J). The proportion of cells bearing *MYC-IGH* translocation increased >50 times on Day 60 and attained over 10% of the total cell population as compared to Day 2 in RPMI8866 cells suggesting that *MYC-IGH* translocation could be a subject of positive selection in RPMI8866 cells. In other cell lines, *MYC-IGH* translocation either did not increase significantly or eventually decreased by Day 60. It should be noted that *IGH* is actively transcribed only in B cells and its translocation with *MYC* can lead to *MYC* overexpression in B cells (43). In addition, *MYC* expression was much lower in RPMI8866 cells prior to translocations as compared to other cell types (Figure 2C). On the other hand, the *AML-ETO* translocation was found to persist after long-term culture in MRC5 cells only (Supplementary Figure S6F–J) although still at a low frequency. These results point out that the generated chromosomal translocations either confer cell type-dependent survival advantages or are progressively eliminated from the cell population.

DISCUSSION

Why are certain chromosomal translocations observed in specific cell types? Several studies addressed this question before. They found that genes that are proximally positioned in the nuclear space, have a higher transcriptional activity or have an accessible chromatin configuration tend to have a higher propensity to form translocations in a specific cell type (22,44–52). Initial studies on chromosomal translocation formation utilized naturally occurring chromosomal translocations, as in the case of B-cell lymphomas, and then correlated their formation with the nuclear spatial position and transcription activity of the involved genes in normal cells (44,45). Naturally occurring chromosomal translocations are, however, significantly dependent on

DSBs that occur in specific gene loci in these cells. More recently, stimulated chromosomal translocations were investigated after experimental induction of DSBs, either by programmed nucleases or by ionizing radiation. The resulting chromosomal translocations were tracked using live cell microscopy to characterize the spatial and dynamic properties of translocation formation (46). Variants of massively parallel sequencing (47,48) in combination with chromosome capture techniques (4C or Hi-C) (49–52) were also used to detect the generated translocations genome-wide to demonstrate the role of spatial proximity between gene loci and DSBs, gene transcription activity, chromatin configuration and nuclear organization in translocation formation. From these studies, the factors that appear to contribute significantly to translocation formation are the spatial proximity between the gene loci and their transcription activity (46–49,51). Translocation breakpoints were also found to be close to the transcription start sites (47–49).

Chromosomal translocations are products of erroneous repair of DSBs (9,53). The error-prone NHEJ repair pathway illegitimately joins two broken chromosomal ends from nonhomologous chromosomes (54). As NHEJ is a proximity-based repair, the physical proximity of the partner loci is a prerequisite to translocation formation (37). In this context, two models are proposed to explain the formation of chromosomal translocations (55). The ‘contact-first’ model proposes that the broken chromosomal ends are immobile or have limited movement in the nuclear space and that translocation occurs to those that are initially close to each other (colocalize prior to and at the time of DSB) (55). This is supported by the occurrence of chromosomal translocations involving gene loci that were already proximal, such as *RET* and *H4* (56), *ABL* and *BCR* (57), and *PML* and *RARA* (58) loci, or gene loci that have moved closer to each other before the chromosomal breakage occurred, e.g. *MYC* and *IGH* loci upon B-lymphocyte activation (18,22,44,45,59). The ‘breakage-first’ model postulates that broken chromosomal ends can freely move around the nuclear space and that the meeting of the two ends may lead to translocation formation. In this scenario, there is a higher likelihood for translocation to occur if DSB movement and colocalization increase. This DSB movement can be directed, stochastic or both [reviewed in (41)]. DSB mobility was observed in the case of multiple DSBs induced by alpha particles or ionizing radiation (60,61).

To experimentally test these conclusions, we induced several DSBs in specific loci of one cell and compared the frequency of resulting chromosomal translocations between these loci in different cell types using the CRISPR/Cas9 system (Figure 1). The advantage of this system is that CRISPR/Cas9 induces DSBs in both euchromatin and heterochromatin regions (although Cas9 can be less efficient in heterochromatin regions) (23,24,26,27). Additionally, the repair of DSBs after Cas9 cleavage is error-prone, which prevents recutting of the same locus (62). The observed translocations were likely produced by the alternative NHEJ pathway as inhibition of DNA-Pk, an important component of the canonical NHEJ, resulted in a significant increase of translocation frequency (Figure 1B). This result is in agreement with previous studies that reported that in rodent and human cells chromosome

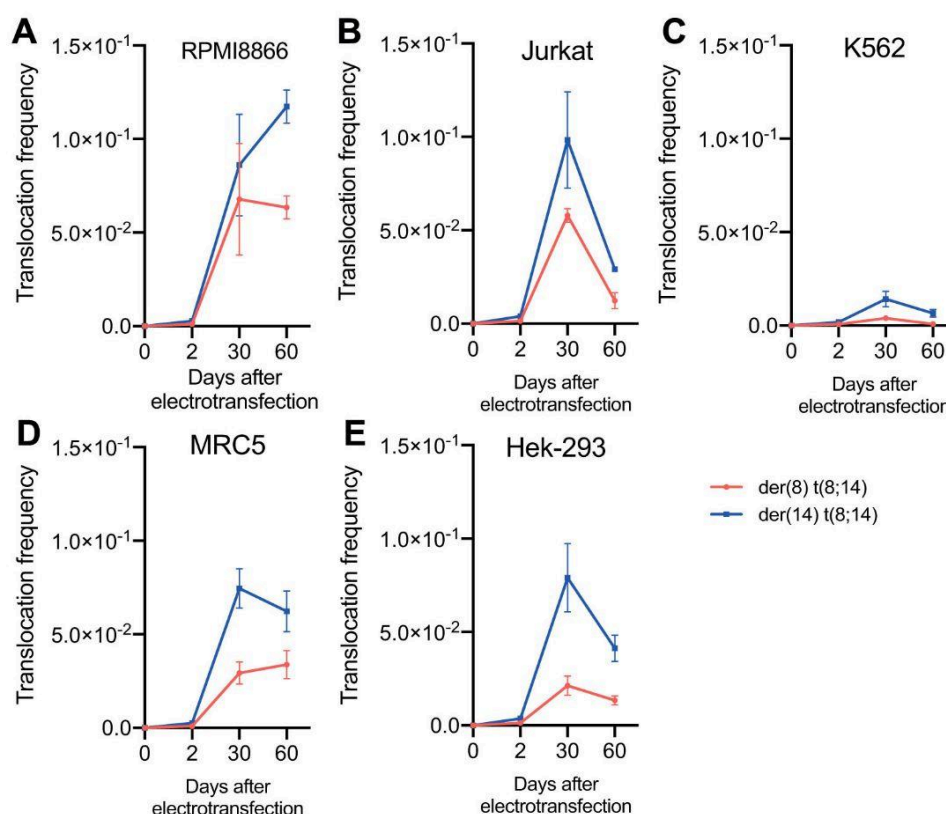


Figure 4. *MYC-IGH* translocation frequency after long-term culture. RPMI8866 (A), Jurkat (B), K562 (C), MRC5 (D) and Hek-293 (E) cells ($24\text{--}32 \times 10^6$) were electrotransfected with gRNA, targeting *MYC*, *IGH* and *AML*, and Cas9 plasmids. Two days later, the electrotransfected cells were split into two parts. The first part was collected to determine the *MYC-IGH* translocation frequency. The second part was sorted and then cultured for 60 days with regular weekly passage. Cells were collected 30 and 60 days after electrotransfection to determine the *MYC-IGH* translocation frequency. Both of the reciprocal (der8, red line; der14, blue line) *MYC-IGH* translocations are shown. Data represent means \pm SEMs of two independent biological experiments and two technical replicates.

translocations are mainly formed by the alternative NHEJ pathway (46,63–67). Nonetheless, a subset of chromosomal translocations may be generated through the canonical NHEJ pathway (68,69). The increased frequency of translocations when canonical NHEJ is abrogated can be explained by the slow kinetics of DNA repair via alternative NHEJ, which is ~ 10 -fold slower than canonical NHEJ; this permits the free movement of unrepaired DNA ends, increasing the chance to meet their translocation partner in the nuclear space (70). Likewise, we observed that inhibiting DNA-Pk increased *MYC-IGH* colocalization after the DSB (Figure 3H). The accumulation of DSB clustering upon DNA-Pk inhibition was also recently described by Zagebaum *et al.* (68).

Interestingly, all possible combinations of translocations can be generated in almost any cell type, albeit with different frequencies (Supplementary Figure S4A–J), although the generation of monocentric derivative chromosomes was favored over dicentric and acentric ones (Figure 1C). The mechanism of this preferential formation of unacentric derivative chromosomes early after DNA repair deserves a separate study. It can be noted that *MYC-IGH* translocation frequency was higher compared to the *MYC-*

AML translocation frequency in all cell lines (Figure 1D), while the ratio of monocentric versus dicentric and acentric chromosomes was much lower for *MYC-IGH* compared to *MYC-AML* in these cells (Figure 1C). From these data, it seems that pro-oncogenic *MYC* and *IGH* breaks tend to be ‘incorrectly’ repaired to a greater extent than others, i.e. more often form translocated and dicentric/acentric derivatives. We hypothesize that the DSB in *IGH* loci, located in the subtelomeric region of chromosome 14, produces a relatively small and motile chromosomal fragment of 1 Mb that can migrate larger distances more readily to meet its translocation partner compared to a larger *AML* fragment (12 Mb): both *MYC-IGH* (t8;14) and *ETO-IGH* (t8;14) translocation frequencies are higher than *MYC-AML* (t8;21) and *ETO-AML* (t8;21) translocation frequencies (Figure 1D and Supplementary Figure S1E).

The cell lines that we used were diploid, except for K562 (nearly triploid) and Hek-293 (hypotriploid). Although the cell lines had different numbers of induced DSBs, the resulting translocation frequency profiles were similar among them (Table 1), indicating that the ploidy did not play a significant role in the pattern of chromosomal translocations after simultaneous induction of DSBs.

Once DSBs are formed, shared transcription factories (71), as well as spatial positioning (72), are the potential factors influencing DSB repair and thus they could affect translocation frequency. In our system, however, the frequency of translocations was not affected by the nuclear radial position or transcription activity of the participating gene loci (Figure 2 and Table 1), but rather by their spatial proximity after the DSB induction (Figure 3 and Table 1). This favors the ‘breakage-first’ hypothesis of translocation formation. An increase in *MYC-IGH* and *ETO-IGH* colocalization frequencies, but not in *MYC-AML* or *ETO-AML* colocalization frequencies, after the respective DSBs (Figure 3A and D) corroborates the higher motility of a shorter chromosomal fragment (*IGH*) proposed above. Different loci, however, may behave differently regarding translocation frequency and colocalization after DSB induction; e.g. colocalizing *AML* and *ETO* loci did not translocate in RPMI8866 cells (Figure 3D and E), while *MYC* and *AML* were not found to colocalize at a detectable rate and yet the translocation was still formed (Figure 3A and B). The mobility of DSBs was previously described (41,61,73), and it may serve either to facilitate the search of a recombination partner (39,74) or to join common DNA repair centers (60,75). DSBs were found to cluster in DNA damage repair foci in yeasts and mammalian cells (60,75,76). However, in mammalian cells DSB clustering was mostly observed for multiple DSBs (67,68,75). An increase in chromatin movement following DSBs can result in chromosomal translocations (46).

Regarding the role of transcription, it is important to acknowledge that while we observe no significant positive correlation between basal transcriptional activity and translocation frequency in between cell line comparisons, this may not concern the changes in gene expression within one cell line and their potential influence on translocation frequency. Whether changes in gene transcriptional activity or distance from DSB to transcription start sites might affect translocation frequencies requires further exploration. Similarly, while our data did not show a significant effect of nuclear radial position on translocation frequency, we acknowledge that this may be influenced by other factors and may vary depending on the specific loci and cell types.

We next tested the persistence of the observed chromosomal translocations upon long-term culture and found that it was different in different cell types (Figure 4A–E and Supplementary Figure S6A–J). Two months after DSB induction, the proportion of cells bearing *MYC-IGH* translocation continued to increase only in RPMI8866 cells (Figure 4A), while the *AML-ETO* translocation was found to persist after long-term culture in MRC5 cells only (Supplementary Figure S6I). These results point out that the generated oncogenic chromosomal translocations confer cell type-dependent survival advantages. The persistence of chromosomal translocations may also depend on whether both derivative chromosomes are present and no genetic material is lost. That is what we supposedly observed in the case of the *MYC-IGH* translocation in RPMI8866 cells, where both derivative chromosomes were present (Figure 4A). A more precise evaluation of potential genetic material loss during such selection requires further investigation. This finding adds to the ongoing discussion on the role of

selection in the formation of cancer cells (77) and provides new evidence for the importance of considering the selective survival advantage of chromosomal translocations in different cell types.

We should also mention the limitations of our system, which provides a valid approximation but does not fully recapitulate all aspects of natural carcinogenesis in primary cells. With CRISPR/Cas9, we deliberately create several simultaneous DSBs; however, ‘naturally occurring’ DSBs can arise spontaneously and not necessarily at the same time, and their origins are diverse, encompassing external factors, e.g. irradiation, and various cellular activities, such as gene transcription, DNA replication and oxidative metabolism (31). Certain chromosomal translocations are caused by DNA-damaging enzymes (RAGs, AID, topoisomerases I and II). These enzymes are sensitive to chromatin organization, transcription and/or DNA sequence. Other chromosomal translocations are induced by random factors that are less strongly dependent on the chromatin context. These include ionizing radiation, oxidative stress, etc. As CRISPR/Cas9 is less sensitive to chromatin structure, it better reproduces the latter situation, although this does not invalidate our conclusions on translocation formation. A potential contributor to the choice of repair pathway, and thus translocation formation, is the cell cycle (78,79), which was not directly addressed in the current study. Further use of our experimental model will allow us to unravel other patterns in the generation of chromosomal translocations. The results on the persistence of the observed chromosomal translocations upon long-term culture might be limited by the fact that we used already proliferating cells; thus, the potential survival or growth rate advantages of chromosomal translocations on different cell types might not be fully estimated.

To conclude, we devised an experimental system to study the factors that drive the formation of chromosomal translocations between four distinct gene loci and five cell types; all the possible combinations of translocations can be generated in almost any cell type, albeit with different frequencies. The frequency of translocations correlates only with the spatial proximity of the partner loci after the DSB induction supporting the ‘breakage-first’ model for translocation formation. Upon long-term culture, only oncogenic *MYC-IGH* and *AML-ETO* chromosomal translocations conferred cell type-dependent survival advantages.

DATA AVAILABILITY

The data underlying this article are available in the article and in its online supplementary material.

SUPPLEMENTARY DATA

Supplementary Data are available at NAR Cancer Online.

ACKNOWLEDGEMENTS

The authors express their gratitude to Tudor Manoliu and Yann Lecluse, Gustave Roussy Cancer Campus, Plateforme Imagerie et Cytométrie—UMS 23/3655—Université Paris Saclay, Villejuif, France, for their technical help.

Authors' contributions: R.J.C. performed the experiments, analyzed and interpreted data, and wrote the original draft; A.S. and A.K. performed the experiments, analyzed and interpreted data, and wrote the paper (review and editing); N.L., E.T., Y.K. and F.A. performed the experiments; D.G. and Y.V. designed research, analyzed data and wrote the paper (review and editing). All authors read and approved the final manuscript.

FUNDING

Ministry of Science and Higher Education of the Russian Federation [075-15-2020-773]; CHED-PhilFrance Scholarship Programme (to R.J.C.).

Conflict of interest statement. The authors declare that they have no conflict of interest.

REFERENCES

- Wilch,E.S. and Morton,C.C. (2018) Historical and clinical perspectives on chromosomal translocations. In: Zhang,Y. (ed). *Advances in Experimental Medicine and Biology*. Springer, Singapore, pp. 1–14.
- Lobato,M.N., Metzler,M., Drynan,L., Forster,A., Pannell,R. and Rabbitts,T.H. (2008) Modeling chromosomal translocations using conditional alleles to recapitulate initiating events in human leukemias. *JNCI Monogr.*, **2008**, 58–63.
- Mitelman,F., Johansson,B. and Mertens,F. (2021) In: *Mitelman Database of Chromosome Aberrations and Gene Fusions in Cancer*. <https://mitelmandatabase.isb-cgc.org>.
- Nakano,K. and Takahashi,S. (2018) Translocation-related sarcomas. *Int. J. Mol. Sci.*, **19**, 3784.
- Nambiar,M. and Raghavan,S.C. (2011) How does DNA break during chromosomal translocations? *Nucleic Acids Res.*, **39**, 5813–5825.
- Bohlander,S.K., Kakadiya,P.M. and Coysh,A. (2019) Chromosome rearrangements and translocations. In: Boffetta, P. and Hainaut,P. (eds.) *Encyclopedia of Cancer*, 3rd edn. Academic Press, Oxford, pp. 389–404.
- Pannunzio,N.R. and Lieber,M.R. (2018) Concept of DNA lesion longevity and chromosomal translocations. *Trends Biochem. Sci.*, **43**, 490–498.
- Zheng,H. and Xie,W. (2019) The role of 3D genome organization in development and cell differentiation. *Nat. Rev. Mol. Cell Biol.*, **20**, 535–550.
- Canoy,R.J., Shmakova,A., Karpukhina,A., Shepelev,M., Germini,D. and Vassetzky,Y. (2022) Factors that affect the formation of chromosomal translocations in cells. *Cancers*, **14**, 5110.
- Lieber,M.R. (2010) The mechanism of double-strand DNA break repair by the nonhomologous DNA end-joining pathway. *Annu. Rev. Biochem.*, **79**, 181–211.
- Liu,M., Duke,J.L., Richter,D.J., Vinuesa,C.G., Goodnow,C.C., Kleinstein,S.H. and Schatz,D.G. (2008) Two levels of protection for the B cell genome during somatic hypermutation. *Nature*, **451**, 841–845.
- Shmakova,A. and Vassetzky,Y. (2023) lncRNA: a new danger for genome integrity. *Int. J. Cancer*, **152**, 1288–1289.
- Demin,D.E., Murashko,M.M., Uvarova,A.N., Stasevich,E.M., Shyrokova,E.Y., Gorlachev,G.E., Zaretsky,A., Korneev,K.V., Ustiugova,A.S., Tkachenko,E.A. *et al.* (2023) Adversary of DNA integrity: a long non-coding RNA stimulates driver oncogenic chromosomal rearrangement in human thyroid cells. *Int. J. Cancer*, **152**, 1452–1462.
- Shmakova,A.A., Lomov,N., Viushkov,V., Tsfasman,T., Kozhevnikova,Y., Sokolova,D., Pokrovsky,V., Syrkinina,M., Germini,D., Rubtsov,M. *et al.* (2023) Cell models with inducible oncogenic translocations allow to evaluate the potential of drugs to favor secondary translocations. *Cancer Commun.*, **43**, 154–158.
- Kovalchuk,A.L., Ansarah-Sobrinho,C., Hakim,O., Resch,W., Tolarová,H., Dubois,W., Yamane,A., Takizawa,M., Klein,I., Hager,G.L. *et al.* (2012) Mouse model of endemic Burkitt translocations reveals the long-range boundaries of Ig-mediated oncogene deregulation. *Proc. Natl Acad. Sci. U.S.A.*, **109**, 10972–10977.
- Busch,K., Keller,T., Fuchs,U., Yeh,R.-F., Harbott,J., Klose,I., Wiemels,J., Novosel,A., Reiter,A. and Borkhardt,A. (2007) Identification of two distinct MYC breakpoint clusters and their association with various IGH breakpoint regions in the t(8;14) translocations in sporadic Burkitt-lymphoma. *Leukemia*, **21**, 1739–1751.
- Brunet,E., Simsek,D., Tomishima,M., DeKelder,R., Choi,V.M., Gregory,P., Urnov,F., Weinstock,D.M. and Jasin,M. (2009) Chromosomal translocations induced at specified loci in human stem cells. *Proc. Natl Acad. Sci. U.S.A.*, **106**, 10620–10625.
- Germini,D., Tsfasman,T., Klibi,M., El-Amine,R., Pichugin,A., Iarovaia,O.V., Bilhou-Nabera,C., Subra,F., Bou Saada,Y., Sukhanova,A. *et al.* (2017) HIV Tat induces a prolonged MYC relocalization next to IGH in circulating B-cells. *Leukemia*, **31**, 2515–2522.
- Piganeau,M., Ghezraoui,H., De Cian,A., Guittat,L., Tomishima,M., Perrouault,L., René,O., Katibah,G.E., Zhang,L., Holmes,M.C. *et al.* (2013) Cancer translocations in human cells induced by zinc finger and TALE nucleases. *Genome Res.*, **23**, 1182–1193.
- Vanoli,F. and Jasin,M. (2017) Generation of chromosomal translocations that lead to conditional fusion protein expression using CRISPR–Cas9 and homology-directed repair. *Methods*, **121–122**, 138–145.
- Vanoli,F., Tomishima,M., Feng,W., Lamribet,K., Babin,L., Brunet,E. and Jasin,M. (2017) CRISPR–Cas9-guided oncogenic chromosomal translocations with conditional fusion protein expression in human mesenchymal cells. *Proc. Natl Acad. Sci. U.S.A.*, **114**, 3696–3701.
- Sall,F.B., Shmakova,A., Karpukhina,A., Tsfasman,T., Lomov,N., Canoy,R.J., Boutboul,D., Oksenhendler,E., Toure,A.O., Lipinski,M. *et al.* (2023) Epstein–Barr virus reactivation induces MYC–IGH spatial proximity and t(8;14) in B cells. *J. Med. Virol.*, **95**, e28633.
- Jain,S., Shukla,S., Yang,C., Zhang,M., Fatma,Z., Lingamaneni,M., Abesteh,S., Lane,S.T., Xiong,X., Wang,Y. *et al.* (2021) TALEN outperforms Cas9 in editing heterochromatin target sites. *Nat. Commun.*, **12**, 606.
- Mitrentsi,I. and Soutoglou,E. (2021) CRISPR/Cas9-induced breaks in heterochromatin, visualized by immunofluorescence. *Methods Mol. Biol.*, **2153**, 439–445.
- Schep,R., Brinkman,E.K., Leemans,C., Vergara,X., van der Weide,R.H., Morris,B., van Schaik,T., Manzo,S.G., Peric-Hupkes,D., van den Berg,J. *et al.* (2021) Impact of chromatin context on Cas9-induced DNA double-strand break repair pathway balance. *Mol. Cell*, **81**, 2216–2230.
- Kallimasioti-Pazi,E.M., Thelakkad Chathoth,K., Taylor,G.C., Meynert,A., Ballinger,T., Kelder,M.J.E., Lalevé,S., Sanli,I., Feil,R. and Wood,A.J. (2018) Heterochromatin delays CRISPR–Cas9 mutagenesis but does not influence the outcome of mutagenic DNA repair. *PLoS Biol.*, **16**, e2005595.
- Friskes,A., Koob,L., Krenning,L., Severson,T.M., Koeleman,E.S., Vergara,X., Schubert,M., van den Berg,J., Evers,B., Manjón,A.G. *et al.* (2022) Double-strand break toxicity is chromatin context independent. *Nucleic Acids Res.*, **50**, 9930–9947.
- Concordet,J.-P. and Haeussler,M. (2018) CRISPOR: intuitive guide selection for CRISPR/Cas9 genome editing experiments and screens. *Nucleic Acids Res.*, **46**, W242–W245.
- Brinkman,E.K., Chen,T., Amendola,M. and Van Steensel,B. (2014) Easy quantitative assessment of genome editing by sequence trace decomposition. *Nucleic Acids Res.*, **42**, e168.
- Germini,D., Saada,Y.B., Tsfasman,T., Osina,K., Robin,C., Lomov,N., Rubtsov,M., Sjakste,N., Lipinski,M. and Vassetzky,Y. (2017) A one-step PCR-based assay to evaluate the efficiency and precision of genomic DNA-editing tools. *Mol. Ther. Methods Clin. Dev.*, **5**, 43–50.
- Canoy,R.J., André,F., Shmakova,A., Wiels,J., Lipinski,M., Vassetzky,Y. and Germini,D. (2023) Easy and robust electrotransfection protocol for efficient ectopic gene expression and genome editing in human B cells. *Gene Ther.*, **30**, 167–171.
- Akbay,B., Germini,D., Bissenbaev,A.K., Musinova,Y.R., Sheval,E.V., Vassetzky,Y. and Dokudovskaya,S. (2021) HIV-1 Tat activates Akt/mTORC1 pathway and AICDA expression by

- downregulating its transcriptional inhibitors in B cells. *Int. J. Mol. Sci.*, **22**, 1588.
33. Pfaffl, M.W. (2001) A new mathematical model for relative quantification in real-time RT-PCR. *Nucleic Acids Res.*, **29**, e45.
 34. Brunet, E. and Jasin, M. (2018) Induction of chromosomal translocations with CRISPR-Cas9 and other nucleases: understanding the repair mechanisms that give rise to translocations. In: Zhang, Y. (ed.) *Chromosome Translocation, Advances in Experimental Medicine and Biology*. Springer, Singapore, pp. 15–25.
 35. Naumann, S., Reutzel, D., Speicher, M. and Decker, H.J. (2001) Complete karyotype characterization of the K562 cell line by combined application of G-banding, multiplex-fluorescence *in situ* hybridization, fluorescence *in situ* hybridization, and comparative genomic hybridization. *Leuk. Res.*, **25**, 313–322.
 36. Lin, C.-Y., Shukla, A., Grady, J.P., Fink, J.L., Dray, E. and Duijf, P.H.G. (2018) Translocation breakpoints preferentially occur in euchromatin and acrocentric chromosomes. *Cancers*, **10**, 13.
 37. Misteli, T. (2010) Higher-order genome organization in human disease. *Cold Spring Harb. Perspect. Biol.*, **2**, a000794.
 38. Osborne, C.S. (2014) Molecular pathways: transcription factories and chromosomal translocations. *Clin. Cancer Res.*, **20**, 296–300.
 39. Miné-Hattab, J. and Chiolo, I. (2020) Complex chromatin motions for DNA repair. *Front. Genet.*, **11**, 800.
 40. Pannunzio, N.R., Watanabe, G. and Lieber, M.R. (2018) Nonhomologous DNA end-joining for repair of DNA double-strand breaks. *J. Biol. Chem.*, **293**, 10512–10523.
 41. Iarovaia, O.V., Rubtsov, M., Ioudinkova, E., Tsfasman, T., Razin, S.V. and Vassetzky, Y.S. (2014) Dynamics of double strand breaks and chromosomal translocations. *Mol. Cancer*, **13**, 249.
 42. Mitelman, F., Johansson, B. and Mertens, F. (2007) The impact of translocations and gene fusions on cancer causation. *Nat. Rev. Cancer*, **7**, 233–245.
 43. Saleh, K., Michot, J.-M., Camara-Clayette, V., Vassetzky, Y. and Ribrag, V. (2020) Burkitt and Burkitt-like lymphomas: a systematic review. *Curr. Oncol. Rep.*, **22**, 33.
 44. Osborne, C.S., Chakalova, L., Mitchell, J.A., Horton, A., Wood, A.L., Bolland, D.J., Corcoran, A.E. and Fraser, P. (2007) Myc dynamically and preferentially relocates to a transcription factory occupied by Igh. *PLoS Biol.*, **5**, e192.
 45. Roix, J.J., McQueen, P.G., Munson, P.J., Parada, L.A. and Misteli, T. (2003) Spatial proximity of translocation-prone gene loci in human lymphomas. *Nat. Genet.*, **34**, 287–291.
 46. Roukos, V., Voss, T.C., Schmidt, C.K., Lee, S., Wangsa, D. and Misteli, T. (2013) Spatial dynamics of chromosome translocations in living cells. *Science*, **341**, 660–664.
 47. Chiarle, R., Zhang, Y., Frock, R.L., Lewis, S.M., Molin, B., Ho, Y.-J., Myers, D.R., Choi, V.W., Compagno, M., Malkin, D.J. *et al.* (2011) Genome-wide translocation sequencing reveals mechanisms of chromosome breaks and rearrangements in B cells. *Cell*, **147**, 107–119.
 48. Klein, I.A., Resch, W., Jankovic, M., Oliveira, T., Yamane, A., Nakahashi, H., Di Virgilio, M., Bothmer, A., Nussenzweig, A., Robbiani, D.F. *et al.* (2011) Translocation-capture sequencing reveals the extent and nature of chromosomal rearrangements in B lymphocytes. *Cell*, **147**, 95–106.
 49. Hakim, O., Resch, W., Yamane, A., Klein, I., Kieffer-Kwon, K.-R., Jankovic, M., Oliveira, T., Bothmer, A., Voss, T.C., Ansarah-Sobrinho, C. *et al.* (2012) DNA damage defines sites of recurrent chromosomal translocations in B lymphocytes. *Nature*, **484**, 69–74.
 50. Rocha, P.P., Micsinai, M., Kim, J.R., Hewitt, S.L., Souza, P.P., Trimarchi, T., Strino, F., Parisi, F., Kluger, Y. and Skok, J.A. (2012) Close proximity to Igh is a contributing factor to AID-mediated translocations. *Mol. Cell*, **47**, 873–885.
 51. Zhang, Y., McCord, R.P., Ho, Y.-J., Lajoie, B.R., Hildebrand, D.G., Simon, A.C., Becker, M.S., Alt, F.W. and Dekker, J. (2012) Spatial organization of the mouse genome and its role in recurrent chromosomal translocations. *Cell*, **148**, 908–921.
 52. Aymard, F., Aguirrebengoa, M., Guillou, E., Javierre, B.M., Bugler, B., Arnould, C., Rocher, V., Iacovoni, J.S., Biernacka, A., Skrzypczak, M. *et al.* (2017) Genome-wide mapping of long-range contacts unveils clustering of DNA double-strand breaks at damaged active genes. *Nat. Struct. Mol. Biol.*, **24**, 353–361.
 53. Roukos, V. and Misteli, T. (2014) The biogenesis of chromosome translocations. *Nat. Cell Biol.*, **16**, 293–300.
 54. Lieber, M.R., Gu, J., Lu, H., Shimazaki, N. and Tsai, A.G. (2010) Nonhomologous DNA end joining (NHEJ) and chromosomal translocations in humans. In: Nasheuer, H.-P. (ed.) *Genome Stability and Human Diseases, Subcellular Biochemistry*. Springer Netherlands, Dordrecht, pp. 279–296.
 55. Meaburn, K.J., Misteli, T. and Soutoglou, E. (2007) Spatial genome organization in the formation of chromosomal translocations. *Semin. Cancer Biol.*, **17**, 80–90.
 56. Nikiforova, M.N., Stringer, J.R., Blough, R., Medvedovic, M., Fagin, J.A. and Nikiforov, Y.E. (2000) Proximity of chromosomal loci that participate in radiation-induced rearrangements in human cells. *Science*, **290**, 138–141.
 57. Lukášová, E., Kozubek, S., Kozubek, M., Kjeronská, J., Rýznar, L., Horáková, J., Krahulcová, E. and Horneck, G. (1997) Localisation and distance between ABL and BCR genes in interphase nuclei of bone marrow cells of control donors and patients with chronic myeloid leukaemia. *Hum. Genet.*, **100**, 525–535.
 58. Neves, H., Ramos, C., da Silva, M.G., Parreira, A. and Parreira, L. (1999) The nuclear topography of ABL, BCR, PML, and RAR α genes: evidence for gene proximity in specific phases of the cell cycle and stages of hematopoietic differentiation. *Blood*, **93**, 1197–1207.
 59. Boxer, L.M. and Dang, C.V. (2001) Translocations involving c-myc and c-myc function. *Oncogene*, **20**, 5595–5610.
 60. Aten, J.A., Stap, J., Krawczyk, P.M., Oven, C.H., Hoebe, R.A., Essers, J. and Kanaar, R. (2004) Dynamics of DNA double-strand breaks revealed by clustering of damaged chromosome domains. *Science*, **303**, 92–95.
 61. Krawczyk, P.M., Borovski, T., Stap, J., Cijssouw, T., Cate, R., Medema, J.P., Kanaar, R., Franken, N.A.P. and Aten, J.A. (2012) Chromatin mobility is increased at sites of DNA double-strand breaks. *J. Cell Sci.*, **125**, 2127–2133.
 62. Brinkman, E.K., Chen, T., de Haas, M., Holland, H.A., Akhtar, W. and van Steensel, B. (2018) Kinetics and fidelity of the repair of Cas9-induced double-strand DNA breaks. *Mol. Cell*, **70**, 801–813.e6.
 63. Soni, A., Siemann, M., Pantelias, G.E. and Iliakis, G. (2015) Marked contribution of alternative end-joining to chromosome-translocation-formation by stochastically induced DNA double-strand-breaks in G2-phase human cells. *Mutat. Res. Genet. Toxicol. Environ. Mutagen.*, **793**, 2–8.
 64. Zhang, Y. and Jasin, M. (2011) An essential role for CtIP in chromosomal translocation formation through an alternative end-joining pathway. *Nat. Struct. Mol. Biol.*, **18**, 80–84.
 65. Boboila, C., Jankovic, M., Yan, C.T., Wang, J.H., Wesemann, D.R., Zhang, T., Fazeli, A., Feldman, L., Nussenzweig, A., Nussenzweig, M. *et al.* (2010) Alternative end-joining catalyzes robust IgH locus deletions and translocations in the combined absence of ligase 4 and Ku70. *Proc. Natl Acad. Sci. U.S.A.*, **107**, 3034–3039.
 66. Simsek, D. and Jasin, M. (2010) Alternative end-joining is suppressed by the canonical NHEJ component Xrcc4–ligase IV during chromosomal translocation formation. *Nat. Struct. Mol. Biol.*, **17**, 410–416.
 67. Caron, P., Choudhary, J., Clouaire, T., Bugler, B., Daburon, V., Aguirrebengoa, M., Mangeat, T., Iacovoni, J.S., Álvarez-Quilón, A., Cortés-Ledesma, F. *et al.* (2015) Non-redundant functions of ATM and DNA-PKcs in response to DNA double-strand breaks. *Cell Rep.*, **13**, 1598–1609.
 68. Zigelbaum, J., Schooley, A., Zhao, J., Schrank, B.R., Callen, E., Zha, S., Gottesman, M.E., Nussenzweig, A., Rabadan, R., Dekker, J. *et al.* (2023) Multiscale reorganization of the genome following DNA damage facilitates chromosome translocations via nuclear actin polymerization. *Nat. Struct. Mol. Biol.*, **30**, 99–106.
 69. Ghezraoui, H., Piganeau, M., Renouf, B., Renaud, J.-B., Sallmyr, A., Ruis, B., Oh, S., Tomkinson, A.E., Hendrickson, E.A., Giovannangeli, C. *et al.* (2014) Chromosomal translocations in human cells are generated by canonical nonhomologous end-joining. *Mol. Cell*, **55**, 829–842.
 70. Lieber, M.R. (2010) NHEJ and its backup pathways: relation to chromosomal translocations. *Nat. Struct. Mol. Biol.*, **17**, 393–395.
 71. Osborne, C.S., Chakalova, L., Brown, K.E., Carter, D., Horton, A., Debrand, E., Goyenechea, B., Mitchell, J.A., Lopes, S., Reik, W. *et al.* (2004) Active genes dynamically colocalize to shared sites of ongoing transcription. *Nat. Genet.*, **36**, 1065–1071.

72. Tsouroula, K., Furst, A., Rogier, M., Heyer, V., Maglott-Roth, A., Ferrand, A., Reina-San-Martin, B. and Soutoglou, E. (2016) Temporal and spatial uncoupling of DNA double strand break repair pathways within mammalian heterochromatin. *Mol. Cell*, **63**, 293–305.
73. Kruhlak, M.J., Celeste, A., Delleire, G., Fernandez-Capetillo, O., Müller, W.G., McNally, J.G., Bazett-Jones, D.P. and Nussenzweig, A. (2006) Changes in chromatin structure and mobility in living cells at sites of DNA double-strand breaks. *J. Cell Biol.*, **172**, 823–834.
74. Miné-Hattab, J. and Rothstein, R. (2012) Increased chromosome mobility facilitates homology search during recombination. *Nat. Cell Biol.*, **14**, 510–517.
75. Neumaier, T., Swenson, J., Pham, C., Polyzos, A., Lo, A.T., Yang, P., Dyball, J., Asaithamby, A., Chen, D.J., Bissell, M.J. *et al.* (2012) Evidence for formation of DNA repair centers and dose-response nonlinearity in human cells. *Proc. Natl Acad. Sci. U.S.A.*, **109**, 443–448.
76. Lisby, M., Rothstein, R. and Mortensen, U.H. (2001) Rad52 forms DNA repair and recombination centers during S phase. *Proc. Natl Acad. Sci. U.S.A.*, **98**, 8276–8282.
77. Vendramin, R., Litchfield, K. and Swanton, C. (2021) Cancer evolution: Darwin and beyond. *EMBO J.*, **40**, e108389.
78. Jasin, M. and Rothstein, R. (2013) Repair of strand breaks by homologous recombination. *Cold Spring Harb. Perspect. Biol.*, **5**, a012740.
79. Kakarougkas, A. and Jeggo, P.A. (2014) DNA DSB repair pathway choice: an orchestrated handover mechanism. *Br. J. Radiol.*, **87**, 20130685.

Article 3. Factors That Affect the Formation of Chromosomal Translocations in Cells






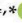
Canoy R.J., Shmakova A., **Karpukhina A.**, Shepelev M., Germini D., Vassetzky Y. Factors That Affect the Formation of Chromosomal Translocations in Cells. *Cancers*. 2022. V. 14, № 20, P. 5110. doi: 10.3390/cancers14205110. (Review)

In this review, we discuss how chromosomal translocations are formed, their mechanisms and consequences.

My role was writing a chapter on the natural sources of double strand breaks and the experimental systems for modeling translocations.

Review

Factors That Affect the Formation of Chromosomal Translocations in Cells

Reynand Jay Canoy^{1,2,3} , Anna Shmakova^{1,4} , Anna Karpukhina^{1,4} , Mikhail Shepelev⁵ ,
Diego Germini^{1,*}  and Yegor Vassetzky^{1,4,*} 

- ¹ UMR 9018, CNRS, Université Paris Saclay, Institut Gustave Roussy, F-94805 Villejuif, France
² Institute of Human Genetics, National Institutes of Health, University of the Philippines Manila, Manila 1000, Philippines
³ Scilore Asia-Pacific Corporation, Ayala-Alabang, Muntinlupa City 1780, Philippines
⁴ Koltzov Institute of Developmental Biology, 117334 Moscow, Russia
⁵ Institute of Gene Biology, 117334 Moscow, Russia
* Correspondence: germinidiego@gmail.com (D.G.); yegor.vassetzky@cnrs.fr (Y.V.)

Simple Summary: Chromosomal translocations are products of the erroneous repair of DNA double-strand breaks that result in the illegitimate joining of the two broken chromosomal ends from non-homologous chromosomes. Chromosomal translocations have been linked to aneuploidy, infertility, mental retardation, cancer and other diseases. Here we discuss how chromosomal translocations are formed and explore how different cellular factors contribute to their formation.

Abstract: Chromosomal translocations are products of the illegitimate repair of DNA double-strand breaks (DSBs). Their formation can bring about significant structural and molecular changes in the cell that can be physiologically and pathologically relevant. The induced changes may lead to serious and life-threatening diseases such as cancer. As a growing body of evidence suggests, the formation of chromosomal translocation is not only affected by the mere close spatial proximity of gene loci as potential translocation partners. Several factors may affect formation of chromosomal translocations, including chromatin motion to the potential sources of DSBs in the cell. While these can be apparently random events, certain chromosomal translocations appear to be cell-type-specific. In this review, we discuss how chromosomal translocations are formed and explore how different cellular factors contribute to their formation.

Keywords: chromosomal translocation; cancer; translocation formation; spatial proximity



Citation: Canoy, R.J.; Shmakova, A.; Karpukhina, A.; Shepelev, M.; Germini, D.; Vassetzky, Y. Factors That Affect the Formation of Chromosomal Translocations in Cells. *Cancers* **2022**, *14*, 5110. <https://doi.org/10.3390/cancers14205110>

Academic Editor: Frederic Chibon

Received: 28 September 2022

Accepted: 17 October 2022

Published: 18 October 2022

Publisher's Note: MDPI stays neutral with regard to jurisdictional claims in published maps and institutional affiliations.



Copyright: © 2022 by the authors. Licensee MDPI, Basel, Switzerland. This article is an open access article distributed under the terms and conditions of the Creative Commons Attribution (CC BY) license (<https://creativecommons.org/licenses/by/4.0/>).

1. Introduction

Chromosomal translocations are the products of an illegitimate proximity-based repair of DNA double-strand breaks (DSBs), where the proximity of DNA ends from different non-homologous chromosomes can result in their erroneous joining. The appearance of a chromosomal translocation results in substantial structural and molecular alterations in the cell and may have perilous pathological consequences. The mechanisms of chromosomal translocation generation, as well as their contribution to human diseases, were extensively reviewed before (e.g., [1–4]). Still, it is currently unknown why certain chromosomal translocations are observed in specific cell types. In the current review we aim to summarize cellular factors that contribute to the formation of chromosomal translocations and that, among other things, could explain the specificity of the occurrence of certain chromosomal translocations.

1.1. History of Chromosomal Translocations in Cancer

The link between an aberrant number of chromosomes and cancer was first described by Theodor Boveri, who postulated that “growth stimulatory chromosomes” triggered

the unlimited growth of tumor cells [5,6]. Then, in 1960, the Philadelphia chromosome, which appeared to be smaller than chromosomes 21 and 22, was described in patients with chronic myeloid leukemia (CML) [7]. However, it was not until 1973 that Janet Rowley showed that this chromosome is the truncated derivative of chromosome 22 fused to the fragment of chromosome 9 [8–10]. This report was the first to demonstrate that the novel chromosomes, which were usually reported to be present in tumor cells, were actually the products of chromosomal translocations.

1.2. Types of Chromosomal Translocations

Chromosomal translocations are generated when non-homologous chromosomes exchange their parts with each other. A few types of chromosomal translocations have been described [11,12]. Chromosomal translocations are considered reciprocal (Figure 1A) if the exchange between chromosomes is bidirectional. Non-reciprocal chromosomal translocations result from the unidirectional transfer of one chromosomal part to another chromosome (Figure 1B). Chromosomal translocations can also be classified as balanced (no net loss or gain of genomic material) or unbalanced if genetic material is lost or amplified. In reciprocal translocations, one of the three sets of possible derivative chromosomes can be produced [13]:

- (1) Two chromosomes produce monocentric derivative chromosomes with one centromere (Figure 1A);
- (2) Two chromosomes produce a derivative chromosome with two centromeres (dicentric) and a derivative chromosome without a centromere (acentric) (Figure 1A);
- (3) Two acrocentric chromosomes fuse at the centromere (Figure 1C) (Robertsonian translocation; [14,15]). The remnants of the short p arms of the two chromosomes also fuse and the small reciprocal product are usually lost, which may not be deleterious for the cell [16].

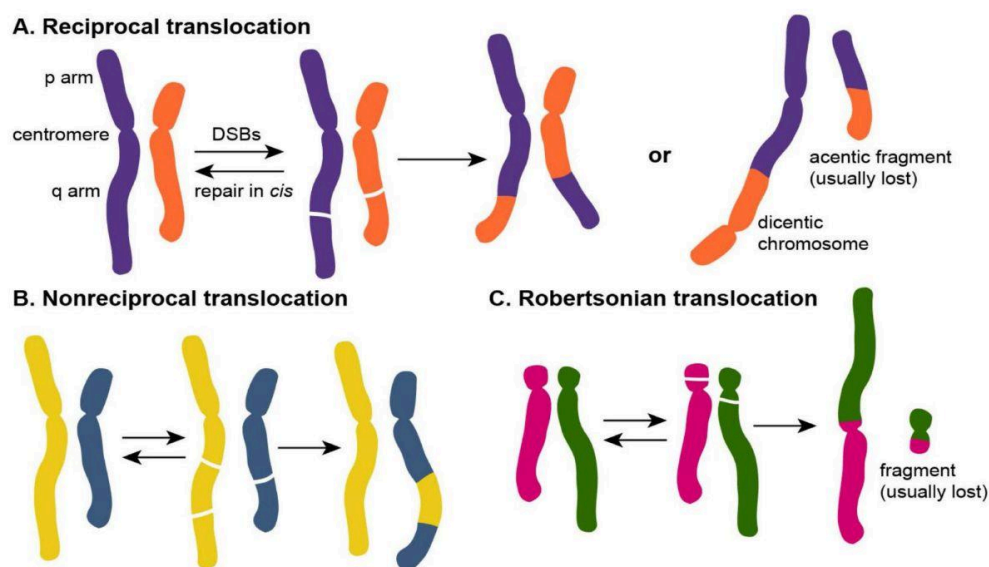


Figure 1. Types of chromosomal translocations. The illegitimate repair of the two DSBs in two non-homologous chromosomes can produce (A) reciprocal translocations if the exchange between two translocating chromosomes is bidirectional or (B) non-reciprocal translocations if the exchange is unidirectional. (C) Robertsonian translocations occur between two acrocentric chromosomes that are fused at the centromere.

The dicentric and acentric chromosomes are often lost after several rounds of cell divisions as they are either lethal or unstable [11], while Robertsonian translocations may persist in meiosis and even produce gametes [12].

1.3. Chromosomal Translocations Affect the Normal Cell Functions

The mere rearrangement of chromosome parts can cause significant consequences in the cell. Chromosomal translocations have been linked to aneuploidy, infertility, mental retardation, cancer, and other diseases [17–22]. Chromosomal translocations may result in the formation of fusion proteins (Figure 2A) with unique or atypical functions or activity, as in the case of the BCR-ABL fusion protein in CML [23–25]. In addition, they can result in the aberrant expression (upregulation or downregulation) of an otherwise normal gene if it is positioned next to the new cis-regulatory elements (Figure 2B). Usually these aberrantly expressed genes are proto-oncogenes that are controlled by a potent gene promoter or enhancer after the translocation. Either of these two can significantly affect the cell and can lead to its transformation and malignancy. This is exemplified by Burkitt's lymphoma, where the *MYC* gene on chromosome 8 is translocated next to the *IGH* locus on chromosome 14; this triggers its overexpression [26–30]. Recently, large-scale changes in the nuclear organization have also been attributed to chromosomal translocations, further expanding our understanding of the consequences of chromosomal translocations for the cell [11,31–36].

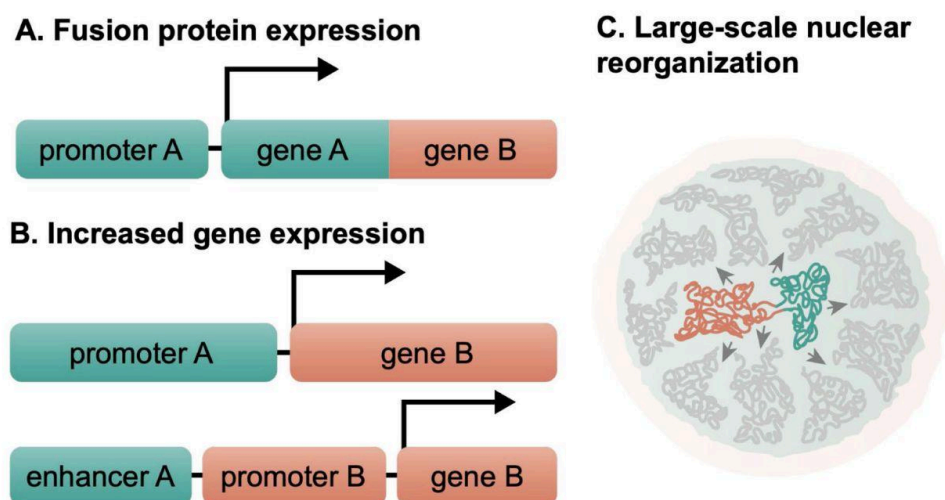


Figure 2. Molecular and functional consequences of chromosomal translocations. Chromosomal translocations can bring about the formation of fusion protein (A) or the (B) aberrant expression of an otherwise normal gene as well as (C) large-scale changes in the nuclear organization have also been attributed to chromosomal translocations.

Chromosomal translocations are characteristic for many types of cancer [37,38], including carcinomas [39,40], lymphomas, leukemias [19,37], and soft tissue sarcomas [20,41,42]. The Mitelman Database of Chromosome Aberrations and Gene Fusions in Cancer (<https://mitelmandatabase.isb-cgc.org/> (accessed on 27 September 2022)) contains exhaustive data related to chromosomal aberrations, including translocations and cancer [43].

2. Sources of DSBs In Vivo and Their Experimental Modeling for Studying Translocations

2.1. Sources of DSBs

The sources of DSBs can be grouped into extrinsic and intrinsic ones. The former include environmental factors such as the ionizing radiation of X-rays and alpha particles [44–49], UV light, or exposure to genotoxic chemical agents (e.g., chemotherapy). Cellular activities that involve DNA-cutting enzymes or produce nonspecific DNA damage, are the potential intrinsic sources of DSBs. In meiotic recombination, DSBs are induced mainly by SPO11 [50,51] during the segregation of chromosomes to convert the cell from diploid to haploid [52,53]. DSBs are consequently produced in lymphocytes during the V(D)J recombination in maturing B and T cells [54–56]. Furthermore, DSBs are also formed during the somatic hypermutation (SHM) and the immunoglobulin class switching or class switch recombination (CSR) in mature B cells [57,58]. The breaks in V(D)J recombination are initiated by the recombination-activating gene (RAG) 1/2 complex [59], while the breaks in SHM and CSR are initiated by the activation-induced deaminase (AID) [60]. Although AID has a special affinity for immunoglobulin genes, it is able to target a large number of other genes (~25% of all expressed genes in B cells) [61]. This programmed DNA damage is considered as a major contributing factor to the susceptibility of B-cells to chromosomal translocations [1]. On the other hand, there are cellular activities that unintentionally produce DSBs such as gene transcription [62–67], DNA replication [68,69] and oxidative metabolism [70,71].

Apparently, different sources of DSB and the chromosome regions targeted by these DSBs differently affect the formation of chromosomal translocations; different sources of DSBs might also determine which factors influence the formation of translocations and thus, translocation specificity, which is discussed below. For instance, CRISPR/Cas9 mostly induce DSBs independently of the chromatin context, which makes the generation of CRISPR/Cas9-induced translocations dependent on the spatial proximity of DNA ends and the choice of DSB repair pathway [72–74]. This should also be taken into account when modeling chromosomal translocations by various methods of DSB induction.

2.2. Experimental Models of Chromosomal Translocations

Translocations can be induced either randomly (e.g., by treatment with γ -rays or H_2O_2) or specifically (e.g., by engineered programmed nucleases) [75]. The advent of engineered nucleases provided a new opportunity to precisely study translocations by introducing DSBs in the regions of interest. Specific chromosomal translocations can now be generated from precisely induced DSBs using programmed nucleases such as zinc finger nucleases (ZFN), transcription activator-like effector nucleases (TALEN), and clustered regularly interspaced short palindromic repeats (CRISPR) [76–84]. A more sophisticated way to induce chromosomal translocations in cells would be to use proteins that naturally induce DNA damage and are known to be implicated in chromosomal translocations, reviewed in [85,86]. In B cells, the chromosome breaks are usually caused by either AID, involved in class switch recombination and somatic hypermutation, or RAG endonuclease, essential for V(D)J recombination together with its RAG2 cofactor. Consequently, physiological or aberrant activation of these genes may induce DSBs and chromosomal translocations. These translocations can then be identified by next-generation sequencing [87,88]. A subset of chromosomal translocations in hematological and solid tumors are driven by DNA topoisomerase II (TOP2) [89]. TOP2 poisons, such as the anticancer agent etoposide, which trap DNA-TOP2 complexes, can be used to induce and identify chromosomal translocations [90]. The factors favoring chromosomal translocations (Figure 3) identified in these and other studies are considered below.

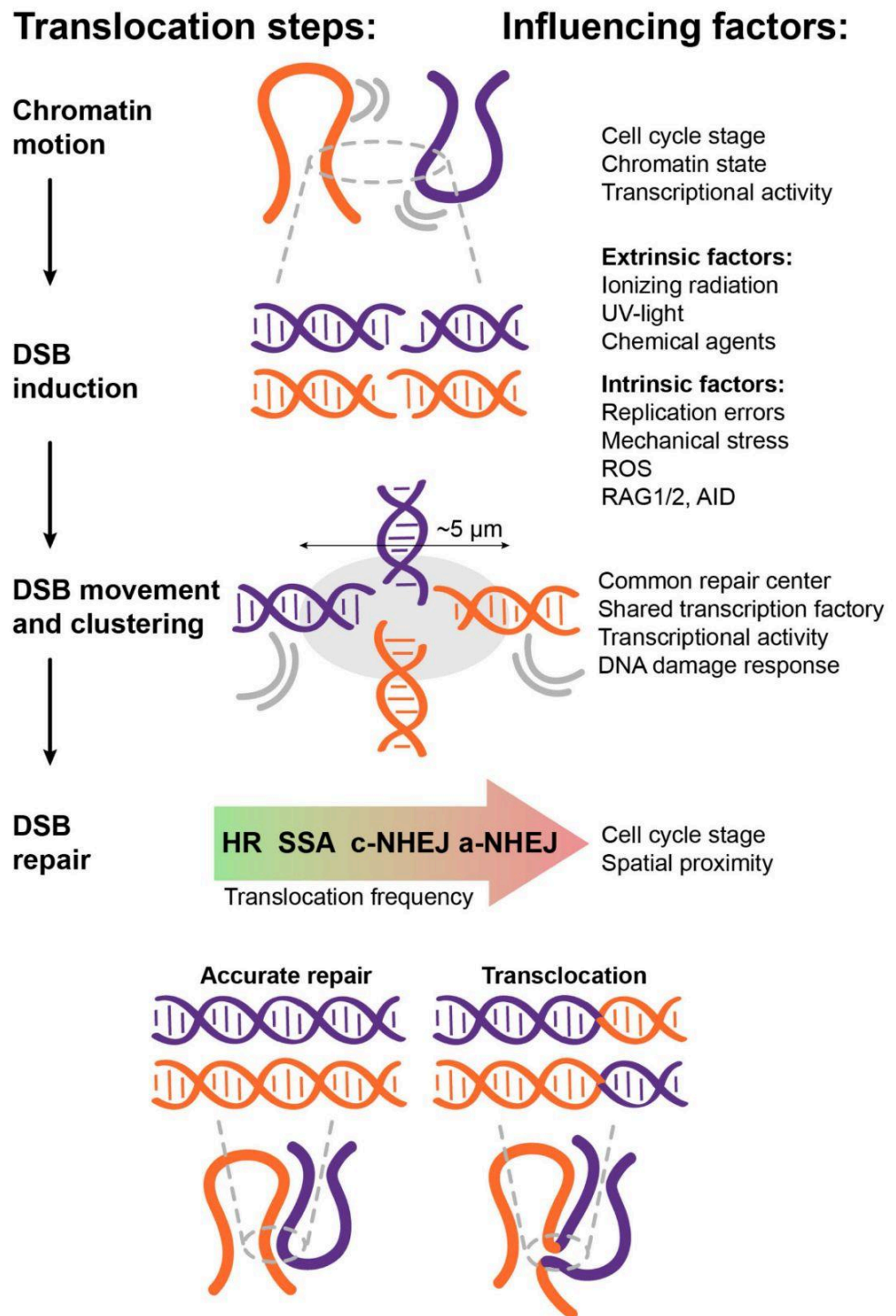


Figure 3. Different factors affect the formation of chromosomal translocations. These cellular factors are not mutually exclusive and can influence each other to affect the multiple stages of chromosomal translocation formation.

3. How Do the Different Factors Affect the Formation of Chromosomal Translocations?

3.1. Spatial Proximity

The erroneous repair of DSBs on different non-homologous chromosomes can result in their joining; this mechanism of chromosomal translocation generation largely relies on

the spatial proximity of DNA ends. However, whether the potential translocation partners should be initially proximally close when the breaks occur or they can move in the nuclear space after the break to get closer is still an open question. In this regard, the “contact first” and “break first” models of translocation formation have been proposed, which assume that the movement of intact chromatin or the movement of DSBs, respectively, contribute to the eventual proximity of DNA ends and translocation [3,75,91,92].

In the nuclear landscape of mammalian cells, chromosomes are organized into spatially distinct territories where they interact with each other more than with those belonging to the other different territories [93]. The term chromosome territory (CT) was actually first introduced by Boveri in the early 1900s in his studies on the blastomere stages of horse roundworms [94,95]. These CTs are composed of chromatin fibers [96]. Different types of cells and tissues have been observed to have different patterns of CTs in their nuclei [97,98]. The proximity of translocation-prone loci (e.g., *MYC/IGH* or *IGH/BCL6*) is largely determined by the higher order chromosome territory positioning [99]. In contrast to higher eukaryotes, yeasts do not exhibit this manner of organization of their chromosomes [100].

The nuclear genome architecture can be visualized using fluorescence in situ hybridization (FISH) using conventional or high-resolution microscopy, or it can be inferred using chromosome conformation structure (3C) and its spin-offs [101,102]. Using FISH, it was found that the gene loci that are commonly involved in oncogenic chromosomal translocation are already proximal to each other in pre-cancerous cells, supporting the “contact first” model of translocation formation. This was the case of the *ABL-BCR* translocation involving chromosomes 9 and 22 in CML [103], the *PML-RARA* translocation involving chromosomes 15 and 17 in acute promyelocytic leukemia [104], and the translocations of *MYC* in chromosome 8 with either of the three of the immunoglobulin genes: *IGH* in chromosome 14, *IGL* in chromosome 22, and *IGK* in chromosome 2 in Burkitt’s lymphoma [99]. The *MYC* gene has been often found to be close to the *IGH* gene locus compared with the *IGL* and *IGK* gene loci, which may explain why the *MYC-IGH* translocation is observed in around 80% of Burkitt’s lymphoma cases while the remaining *MYC-IGK* and *MYC-IGL* translocations occupy the rest [105]. Interestingly, the specific chromosomal position of the *MYC* gene, but not its sequence, was proven to affect its involvement in translocations, since the replacement with *MYCN* sequence does not affect its role as a translocation partner [106].

With the advent of advanced staining and imaging technologies, the preservation of the overall 3D structure of the nucleus and the 3D imaging of the whole chromosome have become possible. Using the technology of 3D structured illumination microscopy (3D-SIM) with pan-chromosome-specific paints, Sathitruangsak et al. investigated the positioning of chromosomes 4, 9, 11, 14, 16, 18, 19, and 22 in normal lymphocytes and myeloma cells from treatment-naïve patients with monoclonal gammopathy of undetermined significance or multiple myeloma [107]. They calculated the overlap between five chromosomal pairs and found out that the pair of chromosomes 18 and 19, which does not usually engage in chromosomal translocation in multiple myeloma, has up to 50% less overlap compared to the remaining pairs, which are usually involved in translocations, both in normal and malignant nuclei. The chromosomal pair which has less overlap has fewer chances of physical interaction or proximity, which can then negatively affect translocation formation.

FISH methods examine the distance between and the relative position of specific gene loci in the nucleus while Hi-C methods determine the interactions of the gene loci with each other on the genome-wide scale. In this line, Zhang et al. demonstrated the positive correlation between inter-chromosomal contacts and translocation frequency [108]. They built a high resolution Hi-C spatial organization map of G1-arrested mouse pro-B cells and used high-throughput translocation sequencing to detect the translocations after DSB induction by ionizing radiation. They found that in the condition when DNA damage is random (i.e., DSBs happen with the same frequency in different sites), the spatial proximity between loci is the main factor contributing to translocation formation (Figure 3).

To further demonstrate the role of spatial proximity in oncogenic translocations, the publicly available Hi-C datasets on genome-wide interaction maps of a lymphoblastoid cell line (GM06990) and an erythroleukemic cell line (K562) were analyzed along with the collections of 1533 chromosomal translocations from cancer and germline genomes [91]. They observed that the gene loci that are usually involved in oncogenic translocations, such as *MYC-IGH* and *BCR-ABL*, have high Hi-C contact frequencies in normal cells. With these findings, the authors were able to show that the high contact interaction between any two gene loci can influence translocation formation if DSBs are formed in them.

To conclude, the overall nuclear genome architecture has been shown to have a significant influence on the formation of chromosomal translocation by virtue of spatial proximity, which can be analyzed by measuring the physical distance or calculating the contact frequency between potential translocation partners.

3.2. Transcriptional Activity

Transcriptional activity can influence the genome's vulnerability to DNA damage and its access to the cellular repair machinery. Endogenous DSBs or DSBs caused by DNA replication inhibitors favorably occur in transcriptionally active genomic regions [87,109,110], which could be explained by transcription-induced DNA damage or the collision of transcriptional and replication forks in S phase. Transcriptionally active chromatin is also more vulnerable to DSB formation induced by ionizing radiation [111]. Consistently, it was observed that genetic rearrangements such as chromosomal translocations preferentially occur in coding regions and in actively transcribed genes compared to the intergenic regions and transcriptionally silent genes [88]. Active gene transcription can cause DNA damage in several ways. Transcription produces short DNA–RNA hybrids called R loops that leave the non-template DNA single strand susceptible to mutagenic activities, including DSBs [63,64,112–115]. In B cells, AID was observed to bind R loops formed at the *MYC* and *IGH* gene loci and to produce DSBs [116–118]. Moreover, AID, through its interaction with Spt5, can be recruited to gene promoters occupied by stalled RNA polymerase II, which explains the prevalence of AID-mediated damages within transcription start sites [119,120].

DNA topoisomerase III beta (TOPB3) has been found to relax the negative supercoiled DNA, reducing the transcription-generated R loops and *MYC-IGH* translocation in mammalian cells [121]. Recent studies have shown that other repair factors suppress chromosomal translocations by modulating the R loop formation [115]. In particular, ATM is a known suppressor of the *MYC-IGH* translocation in vivo [122], and it can also prevent the formation of R loops in proliferating cells [123]. BRCA2, which plays a key role in the HR pathway by recruiting Rad51 to the DSBs, has also been found to prevent R loop formation [124]. The R loop suppression activity of BRCA2 could be part of the coordinated roles between BRCA1 and BRCA2 in the HR pathway, or it could be part of the Fanconi anemia pathway to protect the replication fork [115,125].

However, in the study of mutations in different cancers, euchromatin had a lower mutation rate due to transcription-coupled repair, while heterochromatin and nucleosomal DNA were less accessible to repair machinery and had a higher cancer mutation rate [126]. Meanwhile, a relationship between transcriptional activity and chromatin movement was observed in HeLa cells, where inhibition of transcription with actinomycin D abolished increased transcriptional chromatin mobility and configurational changes during early S phase [127]. Moreover, actively transcribed genes are recruited into shared transcription factories, which increases their spatial proximity and promotes translocation in case DSBs occur among them [128]. This was shown for the genes that are usually involved in chromosomal translocations that cause Burkitt's lymphoma: *MYC*, *IGH*, *IGL*, and *IGK*, where they share a common translocation factory [129]. The correlation between high gene transcription, their spatial proximity within the nuclear space, and chromosomal translocation appearance have also been observed in diffuse large B-cell lymphoma [130], anaplastic cell lymphoma [131], and prostate cancer [132].

3.3. DNA Damage Response

Eukaryotic cells have evolved complex and tightly regulated mechanisms that coordinate the detection, signaling, and repair of DNA damage [133]. These mechanisms are not always efficient, and the formation of chromosomal translocations is one example when the DNA repair machinery incorrectly repairs DSBs. Chromosome translocations are normally found in peripheral blood cells and the non-neoplastic tissues of healthy individuals [134–139], which indicates that their formation should not be seen as a pathological cellular event but rather as an inevitable outcome of DNA repair activities. Only when the chromosomal translocation results in molecular and functional consequences that can disrupt the normal physiological processes and then confer selective survival advantage to the cell does it become pathologically relevant.

DNA breaks are repaired either by homologous recombination (HR) or the non-homologous end joining (NHEJ). The HR pathway is mostly used during S phase of the cell cycle. HR uses the homologous template from the unbroken strand to repair the breakage with high fidelity [140,141]. The NHEJ pathway is cell cycle-independent; it ligates the broken ends together and does not require an extended homology template [142,143]. The DNA ends can be either resected during S/G2 stages or suppressed in the G1 stage; this affects the choice of the repair pathway [144]. The resected DNA produces 3' overhangs coated with Rad51, forming the nucleoprotein filament that is essential in the strand invasion of a homologous template to start the repair [145]. If the homologous template is provided by the sister chromatid, then faithful repair is performed by the HR pathway as opposed to the protected ends in NHEJ [144]. In the absence of a homologous template from a sister chromatid, the resected DNA end can then be repaired by the alternative NHEJ pathway (a-NHEJ) that uses a microhomology of around less than 100 bp, thus requiring limited resection [146]. Additionally, resected DNA ends can be repaired by single-strand annealing (SSA), but this needs annealing of repeats that are more than 100 bp, thus requiring extensive resection [147,148]. Because of the absence of a repair template, the NHEJ pathway results in erroneous repair, ranging from the small indels or mutations at the broken ends up to the relocation of the broken segments leading to chromosomal rearrangements [149]. Whichever pathway the cell utilizes, the repair usually takes from minutes to hours [150]. Both the HR and NHEJ pathways can compete for or even collaborate in DSB repair [151]. DNA repair initiated by the HR pathway can be completed by the NHEJ pathway in some cases [152–154], but when it comes to translocation formation, NHEJ is the most proficient, followed by the SSA pathway [149].

Translocations result from erroneous DNA repair mediated by one of the three different DNA damage response and repair (DDR) pathways: the classical NHEJ (cNHEJ; mediated by DNA-PKcs and Lig4); alternative NHEJ (aNHEJ; mediated by CtIP, Parp1 and Lig1/Lig3); and the single-strand annealing (SSA; mediated by Rad-52) pathway. Chromosome translocations in rodent and human cells are mainly formed by the alternative NHEJ pathway [155–158]. SSA-mediated translocations occur predominantly within repetitive DNA elements [159]. The choice of these pathways depends on several factors.

Kinetic aspect. The cNHEJ pathway proceeds very fast (within 2–4 h) [160,161], which makes it the cellular “first-line therapy” of DSBs. Fast kinetics explains the low frequency of translocation formation with cNHEJ [156]: right after the lesion, DSBs are situated close to each other and their direct joining is favored. Consistently, when cNHEJ is slowed down in G1 (a related process known as Artemis- or resection-dependent cNHEJ), the probability of translocation formation is increased [160,162]. An impairment or slow progression of cNHEJ allows aNHEJ to manifest as a backup process [156,161]. The HR pathway proceeds slower than the NHEJ pathway [163] and has a priority over NHEJ in G2 in repairing DSBs situated in heterochromatin regions, complex, or slow-to-repair lesions [163–165]. Abrogated or stalled HR can be rescued by the aNHEJ pathway [161].

Spatial aspect. Different types of DNA repair have a spatial selectivity as well, which is influenced by the chromatin context. In the study of CRISPR/Cas9-induced DSBs, cNHEJ was found to largely comprise the main DNA repair mechanism both for euchromatin and

heterochromatin, while aNHEJ participates in a small proportion of DSBs repair, although its contribution to DSB repair increases in heterochromatin regions [74]. Another study has shown that the DSBs induced by CRISPR/Cas9 in pericentric heterochromatin are immobile and repaired by NHEJ in G1, while in S/G2 they move to the periphery of heterochromatin and are repaired by HR [166]. In addition, the centromeric DSBs that are majorly peripheral recruit both NHEJ and HR factors throughout the cell cycle [166].

Cell type aspect. The demand for sister chromatids as repair templates restricts HR to S/G2 phase; thus, NHEJ is considered as the dominant repair pathway in most of the human cells. There are, however, some notable exceptions. DSB repair in human embryonic stem cells is largely dependent on HR due to the prolonged S phase, which facilitates the accurate repair of DNA breaks [167]. The differentiation of human embryonic stem cells decreases DNA repair through HR [168]. In some cases, cell differentiation accompanied by chromatin condensation may even completely suppress DSB repair response [169]. Cancer cells often grow in hypoxic conditions, which may also preferentially inhibit HR and contribute to increased rates of mutation [170].

3.4. Chromatin State and Mobility

The DNA in eukaryotic cells is packaged into nucleosomes and then further compacted into denser chromatin [171]. Each nucleosome is composed of around 150 bp DNA that is wrapped around a set of histone octamer [172] containing two copies of H2A, H2B, H3, and H4 [173,174]. The realization of the highly dynamic nature of chromatin has uncovered various regulatory mechanisms that affect different cellular activities such as cell division, DNA replication, DNA repair, and gene expression [175,176]. Chromatin contains epigenetic marks which consist of histone modifications, histone variants, and regions of open chromatin whose distribution and activity are shown to be different in different cell types and diseases [177,178]. The combination of these marks in their spatial context constitutes the chromatin state that encompasses genomic elements such as promoters, enhancers and different regions which are either transcribed, repressed or repetitive [179,180]. Using live cell tracking of chromosome loci tagged with either GFP or fluorescent topoisomerase II, scientists were able to show in yeasts and in *Drosophila* that the chromatin moves in a suggestive Brownian motion, right into a confined subregion of the nucleus [181]. This constrained motion of chromatin was also observed in bacteria and mammalian cells whose chromatin movement ranges from 10^{-4} to 10^{-3} $\mu\text{m}^2/\text{s}$ [182]. However, chromatin movement does not fully follow the Brownian motion. Chromatin movement has been shown to be dependent on ATP levels and is affected by temperature [183–185]. It was also shown that movement of the intact chromatin can be affected by the cell cycle [127,186–190], transcription activity [184,191–193], and chromatin condensation [184,194,195]. Physiological chromatin movements occurring within the cell nucleus many times a day can predispose to the chromosomal translocation formation; however, other events should take place to produce translocations.

The chromatin state was shown to affect the chromatin mobility as chromatin decondensation without changes in transcription activity resulted in the repositioning of genes [195] in a manner similar to that of the transcription-induced chromosomal repositioning [191]. In yeasts, actin-dependent increase of chromatin mobility [194] was observed after targeting the nucleosome remodeling complex INO80 and INO80-dependent nucleosome remodeling [184]. On the other hand, a 30–40% reduction in chromatin density in mammalian cells was observed after DSB induction [196]. In *Drosophila*, the DSBs located in the heterochromatic region move out from their original domain to be repaired [197]. Specifically, the DSBs in yeasts and mammalian cells were found to move out into the periphery of the heterochromatin [198,199], and this was independent of chromatin state, at least in mammalian cells [166]. However, DSBs associated with the nuclear lamina were observed to be repaired differently compared to relocated DSBs [200]. On the other hand, an increase in condensin II activity was found to promote chromatin condensation, spatial

separation of CTs, decreased CT contacts and intermixing, and, as a result, decreased translocation frequency after DSBs induction in *Drosophila* cells [201].

3.5. DSB Movement and Clustering

Upon DNA damage, repair factors flock the sites of breakage and form the microscopically-detectable DNA repair foci [202]. The movement of DSBs is usually investigated using time-lapse microscopy on fluorescently tagged DNA repair foci. Upon DSB induction, the resulting chromosomal breaks in yeast and mammals were observed to remain physically close to each other and were positionally stable over time [203–205].

In yeasts, DSBs were observed to group together in common repair centers [206]. In contrast in mammalian cells, live cell tracking of several DSBs revealed that DSBs did not group together or form clusters, although there were instances when they did, but they were only transient and were observed to be reversible [196,207]. The DNA repair foci after induction of up to four DSBs were also tracked and were found to remain separated [92,205]; they only came together or clustered to a common repair focus if they were to be translocated [92]. The DSBs in mammalian cells were only observed to cluster in common repair foci in case of induction of multiple DSBs (around 100 per cell) [208]. The clustering of multiple DSBs in common repair foci in mammalian cells could be due to the random motion of the breaks, increasing the probability that they meet and group together, or it could be due to the overall control mechanism, as placing the DSBs together in common repair foci can increase the chances that they be illegitimately joined and produce oncogenic translocations [182]. Another possibility is that there are just a limited number of repair foci which the cell can form, thus DSBs are driven to these repair foci similarly to genes recruited into shared transcription factories [128]. The nucleolus is a hub for many nuclear functions [209] formed by rDNA genes located on acrocentric chromosomes. Acrocentric chromosomes are actively involved in chromosomal translocations [210] and several derivative chromosomes remain associated with the nucleolus; this affects expression of proto-oncogenes [31]. Recently, genes whose transcription was inhibited by DSBs were shown to cluster in the vicinity of the nucleolus [211,212]; this potentially increases the probability of translocation, including those with the acrocentric chromosomes.

In mammalian cells, DSBs exhibit similar mobility with that of intact chromatin with a mean displacement of around $1 \mu\text{m}^2/\text{h}$ [182,196,207]. This includes DSBs formed after exposure to ultrasoft X-rays [213] and DSBs induced by endonucleases [205]. On the other hand, large-scale DNA damage from exposure to α -particles resulted in an extensive movement and clustering of DSB-containing chromosome domains [214]. This was also the case after exposure to γ irradiation, where DSB mobility was observed to be at least twice as high as that of the intact loci [186]. γ Irradiation was shown to induce repositioning of *ABL* and *BCR* genes in the nuclear center of lymphocytes [103]. When breaks were induced by I-SceI endonuclease, the translocating DSBs were observed to exhibit higher mobility compared to the non-translocating DSBs; 5% of the translocating DSBs were capable of traveling long distance (up to $5 \mu\text{m}$) [92]. This observation supported the notion that DSBs do search and move to find their respective translocation partner, supporting the “breakage first” model of translocation formation.

In yeasts, breakage induced by I-SceI resulted in the increased mobility of both the induced DSBs and the intact chromatin [215–218]. The increased DSB mobility in yeasts was shown to be dependent on the homologous recombination factors such as Rad51 [215,217,219–222] as yeasts do not have other repair pathways than the HR pathway and DSBs need to search the entire nucleus for homology [140].

3.6. Cell Cycle

Cell cycle stage determines the state of cellular chromatin and how it is repaired when DSBs occur. As such, it can potentially affect translocation formation. Chromatin mobility has been observed to be different across cell stages, with the highest mobility observed during the early G1 phase and thereafter, the chromosome territories remain quite stable

from mid G1 to late G2 [187,189]. During the S phase, the highest mobility can be observed in the early S phase [127]. However in a study where the entire cell cycle phases were considered, no significant differences in chromatin movement were observed between cells in G1, S, and G2 [190]. Nonetheless, the chromatin movement can lead to distancing or approaching of specific gene loci during the cell cycle. Namely, it was shown that the spatial proximity between *ABL-BCR* and *PML-RARA* pairs increases in the period from late S to G2 in hematopoietic precursors and lymphoid cells [104]. The “natural” mobility of intact chromatin does not always reflect the mobility of DSBs that occurs throughout the cell cycle. It was shown that DSBs, induced by ionizing radiation, had decreased mobility during S phase compared with G1/G2 [186]. In contrast, DSBs induced by CRISPR/Cas9 in pericentric heterochromatic regions were shown to be positionally stable in G1 and then move towards the periphery in G2 [166].

How the cell decides which DNA repair pathway to utilize to repair DSBs can be affected by its cell cycle stage: the accurate HR pathway takes place in late S and G2, while the NHEJ pathway is active throughout the cell cycle [140,164]. However in centromeric heterochromatin regions, it was shown that the HR pathway is active both in G1 and S/G2 [166]. Surprisingly, the HR pathway does not have a priority over NHEJ in repairing DSBs during G2 and only accounts for the repair of ~15% of ionizing radiation-induced DSBs [163]. The NHEJ pathway has the highest activity observed in the G1 phase, while the HR pathway has its highest activity in S phase [223]. Although the S/G2 phase requires accurate DNA repair to maintain genomic stability, chromosomal translocations can still be generated at any time as the NHEJ pathway is active all throughout the cell cycle. However, experimentally, no changes in DSB pairing and translocation formation were detected at different cell cycle stages after IScE1-induced DSBs in NIH3T3duo cells [92]. Perhaps this observation could be due to site- and cell-specific conditions, and extrapolating this to the general conclusion about the role of cell cycle stage on translocation formation is still premature.

4. Conclusions

Spatial proximity of the potential translation partners primarily affects translocation formation, perhaps largely because chromosomal translocation is a product of a proximity-based DSB misrepair. However, several other factors come into play and influence each other to affect multiple stages in chromosomal translocation formation (Figure 3), highlighting the sheer complexity of this potentially serious and life-threatening occurrence.

Author Contributions: Writing—original draft preparation, R.J.C., A.S., A.K. and M.S.; writing—review and editing, D.G. and Y.V. All authors have read and agreed to the published version of the manuscript.

Funding: This study was supported by Ministry of Science and Higher Education of the Russian Federation (075-15-2020-773). RJC was a recipient of the CHED-PhilFrance Scholarship Programme.

Conflicts of Interest: The authors declare no conflict of interest. The funders had no role in the design of the study; in the collection, analyses, or interpretation of data; in the writing of the manuscript; or in the decision to publish the results.

References

1. Nussenzweig, A.; Nussenzweig, M.C. Origin of Chromosomal Translocations in Lymphoid Cancer. *Cell* **2010**, *141*, 27–38. [[CrossRef](#)] [[PubMed](#)]
2. Ramsden, D.A.; Nussenzweig, A. Mechanisms Driving Chromosomal Translocations: Lost in Time and Space. *Oncogene* **2021**, *40*, 4263–4270. [[CrossRef](#)] [[PubMed](#)]
3. Roukos, V.; Misteli, T. The Biogenesis of Chromosome Translocations. *Nat. Cell Biol.* **2014**, *16*, 293–300. [[CrossRef](#)] [[PubMed](#)]
4. Zheng, J. Oncogenic Chromosomal Translocations and Human Cancer (Review). *Oncol. Rep.* **2013**, *30*, 2011–2019. [[CrossRef](#)] [[PubMed](#)]
5. Balmain, A. Cancer Genetics: From Boveri and Mendel to Microarrays. *Nat. Rev. Cancer* **2001**, *1*, 77–82. [[CrossRef](#)] [[PubMed](#)]
6. Boveri, T. Concerning the Origin of Malignant Tumours by Theodor Boveri. Translated and Annotated by Henry Harris. *J. Cell Sci.* **2008**, *121*, 1–84. [[CrossRef](#)] [[PubMed](#)]

7. Nowell, P.C.; Hungerford, D.A. Chromosome Studies on Normal and Leukemic Human Leukocytes. *J. Natl. Cancer Inst.* **1960**, *25*, 85–109. [CrossRef]
8. Levan, A. Some Current Problems of Cancer Cytogenetics. *Hereditas* **1967**, *57*, 343–355. [CrossRef]
9. Rowley, J.D. A New Consistent Chromosomal Abnormality in Chronic Myelogenous Leukaemia Identified by Quinacrine Fluorescence and Giemsa Staining. *Nature* **1973**, *243*, 290–293. [CrossRef]
10. Rowley, J.D. Identification of a Translocation with Quinacrine Fluorescence in a Patient with Acute Leukemia. *Ann. De Genet.* **1973**, *16*, 109–112.
11. Bohlander, S.K.; Kakadiya, P.M.; Coysh, A. Chromosome Rearrangements and Translocations. In *Encyclopedia of Cancer*, 3rd ed.; Boffetta, P., Hainaut, P., Eds.; Academic Press: Oxford, UK, 2019; pp. 389–404. ISBN 978-0-12-812485-7.
12. Morin, S.J.; Eccles, J.; Iturriaga, A.; Zimmerman, R.S. Translocations, Inversions and Other Chromosome Rearrangements. *Fertil. Steril.* **2017**, *107*, 19–26. [CrossRef]
13. Barra, V.; Fachinetti, D. The Dark Side of Centromeres: Types, Causes and Consequences of Structural Abnormalities Implicating Centromeric DNA. *Nat. Commun.* **2018**, *9*, 4340. [CrossRef]
14. Robertson, W.R.B. Chromosome Studies. I. Taxonomic Relationships Shown in the Chromosomes of Tettigidae and Acrididae: V-Shaped Chromosomes and Their Significance in Acrididae, Locustidae, and Gryllidae: Chromosomes and Variation. *J. Morphol.* **1916**, *27*, 179–331. [CrossRef]
15. Matveevsky, S.; Tretiakov, A.; Kashintsova, A.; Bakloushinskaya, I.; Kolomiets, O. Meiotic Nuclear Architecture in Distinct Mole Vole Hybrids with Robertsonian Translocations: Chromosome Chains, Stretched Centromeres, and Distorted Recombination. *Int. J. Mol. Sci.* **2020**, *21*, 7630. [CrossRef]
16. Spinner, N.B.; Conlin, L.K.; Mulchandani, S.; Emanuel, B.S. Chapter 45—Deletions and Other Structural Abnormalities of the Autosomes. In *Emery and Rimoin's Principles and Practice of Medical Genetics*, 6th ed.; Rimoin, D., Pyeritz, R., Korf, B., Eds.; Academic Press: Oxford, UK, 2013; pp. 1–37. ISBN 978-0-12-383834-6.
17. Eykelenboom, J.E.; Briggs, G.J.; Bradshaw, N.J.; Soares, D.C.; Ogawa, F.; Christie, S.; Malavasi, E.L.V.; Makedonopoulou, P.; Mackie, S.; Malloy, M.P.; et al. A t(1;11) Translocation Linked to Schizophrenia and Affective Disorders Gives Rise to Aberrant Chimeric DISC1 Transcripts That Encode Structurally Altered, Deleterious Mitochondrial Proteins. *Hum. Mol. Genet.* **2012**, *21*, 3374–3386. [CrossRef]
18. Fraccaro, M.; Maraschio, P.; Pasquali, F.; Tiepolo, L.; Zuffardi, O.; Giarola, A. Male Infertility and 13–14 Translocation. *Lancet* **1973**, *1*, 488. [CrossRef]
19. Mitelman, F.; Johansson, B.; Mertens, F. Mitelman Database of Chromosome Aberrations and Gene Fusions in Cancer. Available online: <https://mitelmandatabase.isb-cgc.org> (accessed on 5 July 2021).
20. Nakano, K.; Takahashi, S. Translocation-Related Sarcomas. *Int. J. Mol. Sci.* **2018**, *19*, 3784. [CrossRef]
21. Prasher, V.P. Presenile Dementia Associated with Unbalanced Robertsonian Translocation Form of Down's Syndrome. *Lancet* **1993**, *342*, 686–687. [CrossRef]
22. Zhang, H.-G.; Wang, R.-X.; Pan, Y.; Zhang, H.; Li, L.-L.; Zhu, H.-B.; Liu, R.-Z. A Report of Nine Cases and Review of the Literature of Infertile Men Carrying Balanced Translocations Involving Chromosome 5. *Mol. Cytogenet* **2018**, *11*, 10. [CrossRef]
23. Daley, G.Q.; Baltimore, D. Transformation of an Interleukin 3-Dependent Hematopoietic Cell Line by the Chronic Myelogenous Leukemia-Specific P210(Bcr/Abl) Protein. *Proc. Natl. Acad. Sci. USA* **1988**, *85*, 9312–9316. [CrossRef]
24. Daley, G.Q.; Van Etten, R.A.; Baltimore, D. Induction of Chronic Myelogenous Leukemia in Mice by the P210 Bcr/Abl Gene of the Philadelphia Chromosome. *Science* **1990**, *247*, 824–830. [CrossRef]
25. Gishizky, M.L.; Johnson-White, J.; Witte, O.N. Efficient Transplantation of BCR-ABL-Induced Chronic Myelogenous Leukemia-like Syndrome in Mice. *Proc. Natl. Acad. Sci. USA* **1993**, *90*, 3755–3759. [CrossRef]
26. Adams, J.M.; Harris, A.W.; Pinkert, C.A.; Corcoran, L.M.; Alexander, W.S.; Cory, S.; Palmiter, R.D.; Brinster, R.L. The C-Myc Oncogene Driven by Immunoglobulin Enhancers Induces Lymphoid Malignancy in Transgenic Mice. *Nature* **1985**, *318*, 533–538. [CrossRef]
27. Ar-Rushdi, A.; Nishikura, K.; Erikson, J.; Watt, R.; Rovera, G.; Croce, C.M. Differential Expression of the Translocated and the Untranslocated C-Myc Oncogene in Burkitt Lymphoma. *Science* **1983**, *222*, 390–393. [CrossRef]
28. Dalla-Favera, R.; Bregni, M.; Erikson, J.; Patterson, D.; Gallo, R.C.; Croce, C.M. Human C-Myc Onc Gene Is Located on the Region of Chromosome 8 That Is Translocated in Burkitt Lymphoma Cells. *Proc. Natl. Acad. Sci. USA* **1982**, *79*, 7824–7827. [CrossRef]
29. Taub, R.; Kirsch, I.; Morton, C.; Lenoir, G.; Swan, D.; Tronick, S.; Aaronson, S.; Leder, P. Translocation of the C-Myc Gene into the Immunoglobulin Heavy Chain Locus in Human Burkitt Lymphoma and Murine Plasmacytoma Cells. *Proc. Natl. Acad. Sci. USA* **1982**, *79*, 7837–7841. [CrossRef]
30. Zech, L.; Haglund, U.; Nilsson, K.; Klein, G. Characteristic Chromosomal Abnormalities in Biopsies and Lymphoid-cell Lines from Patients with Burkitt and Non-burkitt Lymphomas. *Int. J. Cancer* **1976**, *17*, 47–56. [CrossRef]
31. Allinne, J.; Pichugin, A.; Iarovaia, O.; Klibi, M.; Barat, A.; Zlotek-Zlotkiewicz, E.; Markozashvili, D.; Petrova, N.; Camara-Clayette, V.; Ioudinkova, E.; et al. Perinucleolar Relocalization and Nucleolin as Crucial Events in the Transcriptional Activation of Key Genes in Mantle Cell Lymphoma. *Blood* **2014**, *123*, 2044–2053. [CrossRef]
32. Bickmore, W.A.; van Steensel, B. Genome Architecture: Domain Organization of Interphase Chromosomes. *Cell* **2013**, *152*, 1270–1284. [CrossRef]

33. Harewood, L.; Schutz, F.; Boyle, S.; Perry, P.; Delorenzi, M.; Bickmore, W.A.; Reymond, A. The Effect of Translocation-Induced Nuclear Reorganization on Gene Expression. *Genome Res.* **2010**, *20*, 554–564. [CrossRef]
34. Meaburn, K.J. Spatial Genome Organization and Its Emerging Role as a Potential Diagnosis Tool. *Front. Genet.* **2016**, *7*, 134. [CrossRef] [PubMed]
35. Pannunzio, N.R.; Lieber, M.R. Concept of DNA Lesion Longevity and Chromosomal Translocations. *Trends Biochem. Sci.* **2018**, *43*, 490–498. [CrossRef] [PubMed]
36. Zheng, H.; Xie, W. The Role of 3D Genome Organization in Development and Cell Differentiation. *Nat. Rev. Mol. Cell Biol.* **2019**, *20*, 535–550. [CrossRef] [PubMed]
37. Mitelman, F.; Johansson, B.; Mertens, F. The Impact of Translocations and Gene Fusions on Cancer Causation. *Nat. Rev. Cancer* **2007**, *7*, 233–245. [CrossRef]
38. Robbiani, D.F.; Nussenzweig, M.C. Chromosome Translocation, B Cell Lymphoma, and Activation-Induced Cytidine Deaminase. *Annu. Rev. Pathol. Mech. Dis.* **2013**, *8*, 79–103. [CrossRef]
39. Bray, F.; Ferlay, J.; Soerjomataram, I.; Siegel, R.L.; Torre, L.A.; Jemal, A. Global Cancer Statistics 2018: GLOBOCAN Estimates of Incidence and Mortality Worldwide for 36 Cancers in 185 Countries. *CA A Cancer J. Clin.* **2018**, *68*, 394–424. [CrossRef]
40. Ferlay, J.; Colombet, M.; Soerjomataram, I.; Mathers, C.; Parkin, D.M.; Piñeros, M.; Znaor, A.; Bray, F. Estimating the Global Cancer Incidence and Mortality in 2018: GLOBOCAN Sources and Methods. *Int. J. Cancer* **2019**, *144*, 1941–1953. [CrossRef]
41. Lobato, M.N.; Metzler, M.; Drynan, L.; Forster, A.; Pannell, R.; Rabbitts, T.H. Modeling Chromosomal Translocations Using Conditional Alleles to Recapitulate Initiating Events in Human Leukemias. *JNCI Monogr.* **2008**, *2008*, 58–63. [CrossRef]
42. Nambiar, M.; Raghavan, S.C. How Does DNA Break during Chromosomal Translocations? *Nucleic Acids Res.* **2011**, *39*, 5813–5825. [CrossRef]
43. Mitelman, F.; Johansson, B.; Mertens, F. Mitelman Database Chromosome Aberrations and Gene Fusions in Cancer. Available online: <https://mitelmandatabase.isb-cgc.org/about> (accessed on 28 January 2020).
44. Cannan, W.J.; Pederson, D.S. Mechanisms and Consequences of Double-Strand DNA Break Formation in Chromatin. *J. Cell. Physiol.* **2016**, *231*, 3–14. [CrossRef]
45. Georgakilas, A.G. Processing of DNA Damage Clusters in Human Cells: Current Status of Knowledge. *Mol. BioSystems* **2008**, *4*, 30–35. [CrossRef]
46. Sax, K. Chromosome Aberrations Induced by X-Rays. *Genetics* **1938**, *23*, 494–516. [CrossRef]
47. Shikazono, N.; Noguchi, M.; Fujii, K.; Urushibara, A.; Yokoya, A. The Yield, Processing, and Biological Consequences of Clustered DNA Damage Induced by Ionizing Radiation. *J. Radiat Res.* **2009**, *50*, 27–36. [CrossRef]
48. Sutherland, B.M.; Bennett, P.V.; Sutherland, J.C.; Laval, J. Clustered DNA Damages Induced by X Rays in Human Cells. *Rare* **2002**, *157*, 611–616. [CrossRef]
49. Ward, J.F. DNA Damage Produced by Ionizing Radiation in Mammalian Cells: Identities, Mechanisms of Formation, and Reparability. In *Progress in Nucleic Acid Research and Molecular Biology*; Cohn, W.E., Moldave, K., Eds.; Academic Press: Cambridge, MA, USA, 1988; Volume 35, pp. 95–125.
50. Cao, L.; Alani, E.; Kleckner, N. A Pathway for Generation and Processing of Double-Strand Breaks during Meiotic Recombination in *S. Cerevisiae*. *Cell* **1990**, *61*, 1089–1101. [CrossRef]
51. Keeney, S.; Giroux, C.N.; Kleckner, N. Meiosis-Specific DNA Double-Strand Breaks Are Catalyzed by Spo11, a Member of a Widely Conserved Protein Family. *Cell* **1997**, *88*, 375–384. [CrossRef]
52. De Massy, B. Initiation of Meiotic Recombination: How and Where? Conservation and Specificities Among Eukaryotes. *Annu. Rev. Genet.* **2013**, *47*, 563–599. [CrossRef]
53. Paigen, K.; Petkov, P. Mammalian Recombination Hot Spots: Properties, Control and Evolution. *Nat. Rev. Genet.* **2010**, *11*, 221–233. [CrossRef]
54. Cobb, R.M.; Oestreich, K.J.; Osipovich, O.A.; Oltz, E.M. Accessibility Control of V(D)J Recombination. In *Advances in Immunology*; Academic Press: Cambridge, MA, USA, 2006; Volume 91, pp. 45–109.
55. Davis, M.M.; Bjorkman, P.J. T-Cell Antigen Receptor Genes and T-Cell Recognition. *Nature* **1988**, *334*, 395–402. [CrossRef]
56. Krangel, M.S. Mechanics of T Cell Receptor Gene Rearrangement. *Curr. Opin. Immunol.* **2009**, *21*, 133–139. [CrossRef]
57. Chaudhuri, J.; Basu, U.; Zarrin, A.; Yan, C.; Franco, S.; Perlot, T.; Vuong, B.; Wang, J.; Phan, R.T.; Datta, A.; et al. Evolution of the Immunoglobulin Heavy Chain Class Switch Recombination Mechanism. In *Advances in Immunology*; AID for Immunoglobulin Diversity; Academic Press: Cambridge, MA, USA, 2007; Volume 94, pp. 157–214.
58. Di Noia, J.M.; Neuberger, M.S. Molecular Mechanisms of Antibody Somatic Hypermutation. *Annu. Rev. Biochem.* **2007**, *76*, 1–22. [CrossRef]
59. Schatz, D.G.; Baltimore, D. Uncovering the V(D)J Recombinase. *Cell* **2004**, *116*, S103–S108. [CrossRef]
60. Honjo, T.; Kinoshita, K.; Muramatsu, M. Molecular Mechanism of Class Switch Recombination: Linkage with Somatic Hypermutation. *Annu. Rev. Immunol.* **2002**, *20*, 165–196. [CrossRef]
61. Liu, M.; Duke, J.L.; Richter, D.J.; Vinuesa, C.G.; Goodnow, C.C.; Kleinstein, S.H.; Schatz, D.G. Two Levels of Protection for the B Cell Genome during Somatic Hypermutation. *Nature* **2008**, *451*, 841–845. [CrossRef] [PubMed]
62. Helmrich, A.; Stout-Weider, K.; Hermann, K.; Schrock, E.; Heiden, T. Common Fragile Sites Are Conserved Features of Human and Mouse Chromosomes and Relate to Large Active Genes. *Genome Res.* **2006**, *16*, 1222–1230. [CrossRef] [PubMed]

63. Helmrich, A.; Ballarino, M.; Tora, L. Collisions between Replication and Transcription Complexes Cause Common Fragile Site Instability at the Longest Human Genes. *Mol. Cell* **2011**, *44*, 966–977. [[CrossRef](#)] [[PubMed](#)]
64. Huertas, P.; Aguilera, A. Cotranscriptionally Formed DNA:RNA Hybrids Mediate Transcription Elongation Impairment and Transcription-Associated Recombination. *Mol. Cell* **2003**, *12*, 711–721. [[CrossRef](#)]
65. Iannelli, F.; Galbiati, A.; Capozzo, I.; Nguyen, Q.; Magnuson, B.; Michelini, F.; D'Alessandro, G.; Cabrini, M.; Roncador, M.; Francia, S.; et al. A Damaged Genome's Transcriptional Landscape through Multilayered Expression Profiling around in Situ-Mapped DNA Double-Strand Breaks. *Nat. Commun.* **2017**, *8*, 15656. [[CrossRef](#)]
66. Le Tallec, B.; Dutrillaux, B.; Lachages, A.-M.; Millot, G.A.; Brison, O.; Debatisse, M. Molecular Profiling of Common Fragile Sites in Human Fibroblasts. *Nat. Struct. Mol. Biol.* **2011**, *18*, 1421–1423. [[CrossRef](#)]
67. Sutherland, G.R. Heritable Fragile Sites on Human Chromosomes II. Distribution, Phenotypic Effects, and Cytogenetics. *Am. J. Hum. Genet.* **1979**, *31*, 136–148.
68. Pfeiffer, P.; Goedecke, W.; Obe, G. Mechanisms of DNA Double-Strand Break Repair and Their Potential to Induce Chromosomal Aberrations. *Mutagenesis* **2000**, *15*, 289–302. [[CrossRef](#)]
69. Syeda, A.H.; Hawkins, M.; McGlynn, P. Recombination and Replication. *Cold Spring Harb Perspect Biol.* **2014**, *6*, a016550. [[CrossRef](#)]
70. Fraga, C.G.; Shigenaga, M.K.; Park, J.W.; Degan, P.; Ames, B.N. Oxidative Damage to DNA during Aging: 8-Hydroxy-2'-Deoxyguanosine in Rat Organ DNA and Urine. *Proc. Natl. Acad. Sci. USA* **1990**, *87*, 4533–4537. [[CrossRef](#)]
71. Lindahl, T.; Nyberg, B. Rate of Depurination of Native Deoxyribonucleic Acid. *Biochemistry* **1972**, *11*, 3610–3618. [[CrossRef](#)]
72. Jain, S.; Shukla, S.; Yang, C.; Zhang, M.; Fatma, Z.; Lingamaneni, M.; Abesteh, S.; Lane, S.T.; Xiong, X.; Wang, Y.; et al. TALEN Outperforms Cas9 in Editing Heterochromatin Target Sites. *Nat. Commun.* **2021**, *12*, 606. [[CrossRef](#)]
73. Mitrentsi, I.; Soutoglou, E. CRISPR/Cas9-Induced Breaks in Heterochromatin, Visualized by Immunofluorescence. *Methods Mol. Biol.* **2021**, *2153*, 439–445. [[CrossRef](#)]
74. Schep, R.; Brinkman, E.K.; Leemans, C.; Vergara, X.; van der Weide, R.H.; Morris, B.; van Schaik, T.; Manzo, S.G.; Peric-Hupkes, D.; van den Berg, J.; et al. Impact of Chromatin Context on Cas9-Induced DNA Double-Strand Break Repair Pathway Balance. *Mol. Cell* **2021**, *81*, 2216–2230.e10. [[CrossRef](#)]
75. Iarovaia, O.V.; Rubtsov, M.; Ioudinkova, E.; Tsfasman, T.; Razin, S.V.; Vassetzky, Y.S. Dynamics of Double Strand Breaks and Chromosomal Translocations. *Mol. Cancer* **2014**, *13*, 249. [[CrossRef](#)]
76. Brunet, E.; Simsek, D.; Tomishima, M.; DeKolver, R.; Choi, V.M.; Gregory, P.; Urnov, F.; Weinstock, D.M.; Jasin, M. Chromosomal Translocations Induced at Specified Loci in Human Stem Cells. *Proc. Natl. Acad. Sci. USA* **2009**, *106*, 10620–10625. [[CrossRef](#)]
77. Germini, D.; Saada, Y.B.; Tsfasman, T.; Osina, K.; Robin, C.; Lomov, N.; Rubtsov, M.; Sjakste, N.; Lipinski, M.; Vassetzky, Y. A One-Step PCR-Based Assay to Evaluate the Efficiency and Precision of Genomic DNA-Editing Tools. *Mol. Ther. Methods Clin. Dev.* **2017**, *5*, 43–50. [[CrossRef](#)]
78. Piganeau, M.; Ghezraoui, H.; De Cian, A.; Guittat, L.; Tomishima, M.; Perrouault, L.; René, O.; Katibah, G.E.; Zhang, L.; Holmes, M.C.; et al. Cancer Translocations in Human Cells Induced by Zinc Finger and TALE Nucleases. *Genome Res.* **2013**, *23*, 1182–1193. [[CrossRef](#)]
79. Torres, R.; Martin, M.C.; Garcia, A.; Cigudosa, J.C.; Ramirez, J.C.; Rodriguez-Perales, S. Engineering Human Tumour-Associated Chromosomal Translocations with the RNA-Guided CRISPR–Cas9 System. *Nat. Commun.* **2014**, *5*, 3964. [[CrossRef](#)]
80. Vanoli, F.; Jasin, M. Generation of Chromosomal Translocations That Lead to Conditional Fusion Protein Expression Using CRISPR-Cas9 and Homology-Directed Repair. *Methods* **2017**, *121–122*, 138–145. [[CrossRef](#)]
81. Shmakova, A.A.; Germini, D.; Vassetzky, Y.S. Exploring the Features of Burkitt's Lymphoma-Associated t(8;14) Translocations Generated via a CRISPR/Cas9-Based System. *Biopolym. Cell* **2019**, *35*, 232–233. [[CrossRef](#)]
82. Canoy, R.J.; André, F.; Shmakova, A.; Wiels, J.; Lipinski, M.; Vassetzky, Y.; Germini, D. Easy and Robust Electrotransfection Protocol for Efficient Ectopic Gene Expression and Genome Editing in Human B Cells. *Gene Ther.* **2020**, *1–5*. [[CrossRef](#)]
83. Shmakova, A.A.; Lomov, N.; Viushkov, V.; Tsfasman, T.; Kozhevnikova, Y.; Sokolova, D.; Pokrovsky, V.; Syrkina, M.; Germini, D.; Rubtsov, M.; et al. Cell Models with Inducible Oncogenic Translocations Allow to Evaluate the Potential of Drugs to Favor Secondary Translocations. *Cancer Commun.* **2022**, in press. [[CrossRef](#)]
84. Shmakova, A.A.; Shmakova, O.P.; Karpukhina, A.A.; Vassetzky, Y.S. CRISPR/Cas: History and Perspectives. *Russ. J. Dev. Biol.* **2022**, *53*, 272–282. [[CrossRef](#)]
85. Byrne, M.; Wray, J.; Reinert, B.; Wu, Y.; Nickoloff, J.; Lee, S.-H.; Hromas, R.; Williamson, E. Mechanisms of Oncogenic Chromosomal Translocations. *Ann. New York Acad. Sci.* **2014**, *1310*, 89–97. [[CrossRef](#)]
86. Lieber, M.R. Mechanisms of Human Lymphoid Chromosomal Translocations. *Nat. Rev. Cancer* **2016**, *16*, 387–398. [[CrossRef](#)]
87. Chiarle, R.; Zhang, Y.; Frock, R.L.; Lewis, S.M.; Molinie, B.; Ho, Y.J.; Myers, D.R.; Choi, V.W.; Compagno, M.; Malkin, D.J.; et al. Genome-Wide Translocation Sequencing Reveals Mechanisms of Chromosome Breaks and Rearrangements in B Cells. *Cell* **2011**, *147*, 107–119. [[CrossRef](#)]
88. Klein, I.A.; Resch, W.; Jankovic, M.; Oliveira, T.; Yamane, A.; Nakahashi, H.; Di Virgilio, M.; Bothmer, A.; Nussenzweig, A.; Robbiani, D.F.; et al. Translocation-Capture Sequencing Reveals the Extent and Nature of Chromosomal Rearrangements in B Lymphocytes. *Cell* **2011**, *147*, 95–106. [[CrossRef](#)]
89. Haffner, M.C.; Aryee, M.J.; Toubaji, A.; Esopi, D.M.; Albadine, R.; Gurel, B.; Isaacs, W.B.; Bova, G.S.; Liu, W.; Xu, J.; et al. Androgen-Induced TOP2B-Mediated Double-Strand Breaks and Prostate Cancer Gene Rearrangements. *Nat. Genet.* **2010**, *42*, 668–675. [[CrossRef](#)]

90. Canela, A.; Maman, Y.; Huang, S.N.; Wutz, G.; Tang, W.; Zagnoli-Vieira, G.; Callen, E.; Wong, N.; Day, A.; Peters, J.-M.; et al. Topoisomerase II-Induced Chromosome Breakage and Translocation Is Determined by Chromosome Architecture and Transcriptional Activity. *Mol. Cell* **2019**, *75*, 252–266.e8. [\[CrossRef\]](#)
91. Engreitz, J.M.; Agarwala, V.; Mirny, L.A. Three-Dimensional Genome Architecture Influences Partner Selection for Chromosomal Translocations in Human Disease. *PLoS ONE* **2012**, *7*, e44196. [\[CrossRef\]](#)
92. Roukos, V.; Voss, T.C.; Schmidt, C.K.; Lee, S.; Wangsa, D.; Misteli, T. Spatial Dynamics of Chromosome Translocations in Living Cells. *Science* **2013**, *341*, 660–664. [\[CrossRef\]](#)
93. Cremer, T.; Cremer, M.; Dietzel, S.; Müller, S.; Solovei, I.; Fakan, S. Chromosome Territories—A Functional Nuclear Landscape. *Curr. Opin. Cell Biol.* **2006**, *18*, 307–316. [\[CrossRef\]](#)
94. Boveri, T. Die Blastomerenkerne von *Ascaris Megalocephala* Und Die Theorie Der Chromosomenindividualität. *Arch. Zellforsch* **1909**, *3*, 181–268.
95. Cremer, T.; Cremer, M. Chromosome Territories. *Cold Spring Harb Perspect Biol.* **2010**, *2*, a003889. [\[CrossRef\]](#)
96. Belmont, A.S.; Bruce, K. Visualization of G1 Chromosomes: A Folded, Twisted, Supercoiled Chromonema Model of Interphase Chromatid Structure. *J. Cell Biol.* **1994**, *127*, 287–302. [\[CrossRef\]](#)
97. Marella, N.V.; Bhattacharya, S.; Mukherjee, L.; Xu, J.; Berezney, R. Cell Type Specific Chromosome Territory Organization in the Interphase Nucleus of Normal and Cancer Cells. *J. Cell. Physiol.* **2009**, *221*, 130–138. [\[CrossRef\]](#)
98. Parada, L.A.; McQueen, P.G.; Misteli, T. Tissue-Specific Spatial Organization of Genomes. *Genome Biol.* **2004**, *5*, R44. [\[CrossRef\]](#)
99. Roix, J.J.; McQueen, P.G.; Munson, P.J.; Parada, L.A.; Misteli, T. Spatial Proximity of Translocation-Prone Gene Loci in Human Lymphomas. *Nat. Genet.* **2003**, *34*, 287–291. [\[CrossRef\]](#)
100. Haber, J.E.; Leung, W.-Y. Lack of Chromosome Territoriality in Yeast: Promiscuous Rejoining of Broken Chromosome Ends. *Proc. Natl. Acad. Sci. USA* **1996**, *93*, 13949–13954. [\[CrossRef\]](#)
101. Fraser, J.; Williamson, I.; Bickmore, W.A.; Dostie, J. An Overview of Genome Organization and How We Got There: From FISH to Hi-C. *Microbiol. Mol. Biol. Rev.* **2015**, *79*, 347–372. [\[CrossRef\]](#)
102. Fritz, A.J.; Barutcu, A.R.; Martin-Buley, L.; van Wijnen, A.J.; Zaidi, S.K.; Imbalzano, A.N.; Lian, J.B.; Stein, J.L.; Stein, G.S. Chromosomes at Work: Organization of Chromosome Territories in the Interphase Nucleus. *J. Cell. Biochem.* **2016**, *117*, 9–19. [\[CrossRef\]](#)
103. Lukášová, E.; Kozubek, S.; Kozubek, M.; Kjeronská, J.; Rýznar, L.; Horáková, J.; Krahulcová, E.; Horneck, G. Localisation and Distance between ABL and BCR Genes in Interphase Nuclei of Bone Marrow Cells of Control Donors and Patients with Chronic Myeloid Leukaemia. *Hum. Genet.* **1997**, *100*, 525–535. [\[CrossRef\]](#)
104. Neves, H.; Ramos, C.; da Silva, M.G.; Parreira, A.; Parreira, L. The Nuclear Topography of ABL, BCR, PML, and RARalpha Genes: Evidence for Gene Proximity in Specific Phases of the Cell Cycle and Stages of Hematopoietic Differentiation. *Blood* **1999**, *93*, 1197–1207. [\[CrossRef\]](#)
105. Boxer, L.M.; Dang, C.V. Translocations Involving C- Myc and c- Myc Function. *Oncogene* **2001**, *20*, 5595–5610. [\[CrossRef\]](#)
106. Gostissa, M.; Ranganath, S.; Bianco, J.M.; Alt, F.W. Chromosomal Location Targets Different MYC Family Gene Members for Oncogenic Translocations. *Proc. Natl. Acad. Sci. USA* **2009**, *106*, 2265–2270. [\[CrossRef\]](#)
107. Sathitruangsak, C.; Righolt, C.H.; Klewes, L.; Chang, D.T.; Kotb, R.; Mai, S. Distinct and Shared Three-Dimensional Chromosome Organization Patterns in Lymphocytes, Monoclonal Gammopathy of Undetermined Significance and Multiple Myeloma. *Int. J. Cancer* **2017**, *140*, 400–410. [\[CrossRef\]](#)
108. Zhang, Y.; McCord, R.P.; Ho, Y.-J.; Lajoie, B.R.; Hildebrand, D.G.; Simon, A.C.; Becker, M.S.; Alt, F.W.; Dekker, J. Spatial Organization of the Mouse Genome and Its Role in Recurrent Chromosomal Translocations. *Cell* **2012**, *148*, 908–921. [\[CrossRef\]](#)
109. Crosetto, N.; Mitra, A.; Silva, M.J.; Bienko, M.; Dojer, N.; Wang, Q.; Karaca, E.; Chiarle, R.; Skrzypczak, M.; Ginalski, K.; et al. Nucleotide-Resolution DNA Double-Strand Breaks Mapping by next-Generation Sequencing. *Nat. Methods* **2013**, *10*, 361–365. [\[CrossRef\]](#)
110. Lensing, S.V.; Marsico, G.; Hänsel-Hertsch, R.; Lam, E.Y.; Tannahill, D.; Balasubramanian, S. DSB-Capture: In Situ Capture and Sequencing of DNA Breaks. *Nat. Methods* **2016**, *13*, 855–857. [\[CrossRef\]](#)
111. Falk, M.; Lukášová, E.; Kozubek, S. Chromatin Structure Influences the Sensitivity of DNA to Gamma-Radiation. *Biochim. Biophys. Acta* **2008**, *1783*, 2398–2414. [\[CrossRef\]](#)
112. Aguilera, A. The Connection between Transcription and Genomic Instability. *EMBO J.* **2002**, *21*, 195–201. [\[CrossRef\]](#)
113. Ginno, P.A.; Lott, P.L.; Christensen, H.C.; Korf, I.; Chédin, F. R-Loop Formation Is a Distinctive Characteristic of Unmethylated Human CpG Island Promoters. *Mol. Cell* **2012**, *45*, 814–825. [\[CrossRef\]](#)
114. Santos-Pereira, J.M.; Aguilera, A. R Loops: New Modulators of Genome Dynamics and Function. *Nat. Rev. Genet.* **2015**, *16*, 583–597. [\[CrossRef\]](#)
115. Stirling, P.C.; Hieter, P. Canonical DNA Repair Pathways Influence R-Loop-Driven Genome Instability. *J. Mol. Biol.* **2017**, *429*, 3132–3138. [\[CrossRef\]](#) [\[PubMed\]](#)
116. Boerma, E.G.; Siebert, R.; Kluin, P.M.; Baudis, M. Translocations Involving 8q24 in Burkitt Lymphoma and Other Malignant Lymphomas: A Historical Review of Cytogenetics in the Light of Today's Knowledge. *Leukemia* **2009**, *23*, 225–234. [\[CrossRef\]](#) [\[PubMed\]](#)
117. Duquette, M.L.; Pham, P.; Goodman, M.F.; Maizels, N. AID Binds to Transcription-Induced Structures in c- MYC That Map to Regions Associated with Translocation and Hypermethylation. *Oncogene* **2005**, *24*, 5791–5798. [\[CrossRef\]](#)

118. Yu, K.; Chedin, F.; Hsieh, C.-L.; Wilson, T.E.; Lieber, M.R. R-Loops at Immunoglobulin Class Switch Regions in the Chromosomes of Stimulated B Cells. *Nat. Immunol.* **2003**, *4*, 442–451. [[CrossRef](#)]
119. Pavri, R.; Gazumyan, A.; Jankovic, M.; Di Virgilio, M.; Klein, I.; Ansarah-Sobrinho, C.; Resch, W.; Yamane, A.; Reina San-Martin, B.; Barreto, V.; et al. Activation-Induced Cytidine Deaminase Targets DNA at Sites of RNA Polymerase II Stalling by Interaction with Spt5. *Cell* **2010**, *143*, 122–133. [[CrossRef](#)]
120. Yamane, A.; Resch, W.; Kuo, N.; Kuchen, S.; Li, Z.; Sun, H.; Robbiani, D.F.; McBride, K.; Nussenzweig, M.C.; Casellas, R. Deep-Sequencing Identification of the Genomic Targets of the Cytidine Deaminase AID and Its Cofactor RPA in B Lymphocytes. *Nat. Immunol.* **2011**, *12*, 62–69. [[CrossRef](#)]
121. Yang, Y.; McBride, K.M.; Hensley, S.; Lu, Y.; Chedin, F.; Bedford, M.T. Arginine Methylation Facilitates the Recruitment of TOP3B to Chromatin to Prevent R Loop Accumulation. *Mol. Cell* **2014**, *53*, 484–497. [[CrossRef](#)]
122. Ramiro, A.R.; Jankovic, M.; Callen, E.; Difilippantonio, S.; Chen, H.-T.; McBride, K.M.; Eisenreich, T.R.; Chen, J.; Dickins, R.A.; Lowe, S.W.; et al. Role of Genomic Instability and P53 in AID-Induced c-Myc—Igh Translocations. *Nature* **2006**, *440*, 105–109. [[CrossRef](#)]
123. Yeo, A.J.; Becherel, O.J.; Luff, J.E.; Cullen, J.K.; Wongsurawat, T.; Jenjaroenpoon, P.; Kuznetsov, V.A.; McKinnon, P.J.; Lavin, M.F. R-Loops in Proliferating Cells but Not in the Brain: Implications for AOA2 and Other Autosomal Recessive Ataxias. *PLoS ONE* **2014**, *9*, e90219. [[CrossRef](#)]
124. Bhatia, V.; Barroso, S.I.; García-Rubio, M.L.; Tumini, E.; Herrera-Moyano, E.; Aguilera, A. BRCA2 Prevents R-Loop Accumulation and Associates with TREX-2 mRNA Export Factor PCID2. *Nature* **2014**, *511*, 362–365. [[CrossRef](#)]
125. Schlacher, K.; Wu, H.; Jasin, M. A Distinct Replication Fork Protection Pathway Connects Fanconi Anemia Tumor Suppressors to RAD51-BRCA1/2. *Cancer Cell* **2012**, *22*, 106–116. [[CrossRef](#)]
126. Roberts, S.A.; Gordenin, D.A. Hypermutation in Human Cancer Genomes: Footprints and Mechanisms. *Nat. Rev. Cancer* **2014**, *14*, 786–800. [[CrossRef](#)]
127. Pliss, A.; Malyavantham, K.; Bhattacharya, S.; Zeitz, M.; Berezney, R. Chromatin Dynamics Is Correlated with Replication Timing. *Chromosoma* **2009**, *118*, 459–470. [[CrossRef](#)]
128. Osborne, C.S.; Chakalova, L.; Brown, K.E.; Carter, D.; Horton, A.; Debrand, E.; Goyenechea, B.; Mitchell, J.A.; Lopes, S.; Reik, W.; et al. Active Genes Dynamically Colocalize to Shared Sites of Ongoing Transcription. *Nat. Genet.* **2004**, *36*, 1065–1071. [[CrossRef](#)]
129. Osborne, C.S.; Chakalova, L.; Mitchell, J.A.; Horton, A.; Wood, A.L.; Bolland, D.J.; Corcoran, A.E.; Fraser, P. Myc Dynamically and Preferentially Relocates to a Transcription Factory Occupied by Igh. *PLoS Biol.* **2007**, *5*, e192. [[CrossRef](#)]
130. Barlow, J.; Faryabi, R.B.; Callen, E.; Wong, N.; Malhowski, A.; Chen, H.T.; Gutierrez-Cruz, G.; Sun, H.-W.; McKinnon, P.; Wright, G.; et al. A Novel Class of Early Replicating Fragile Sites That Contribute to Genome Instability in B Cell Lymphomas. *Cell* **2013**, *152*, 620–632. [[CrossRef](#)]
131. Mathas, S.; Kreher, S.; Meaburn, K.J.; Jöhrens, K.; Lamprecht, B.; Assaf, C.; Sterry, W.; Kadin, M.E.; Daibata, M.; Joos, S.; et al. Gene Deregulation and Spatial Genome Reorganization near Breakpoints Prior to Formation of Translocations in Anaplastic Large Cell Lymphoma. *Proc. Natl. Acad. Sci. USA* **2009**, *106*, 5831–5836. [[CrossRef](#)]
132. Lin, C.; Yang, L.; Tanasa, B.; Hutt, K.; Ju, B.; Ohgi, K.; Zhang, J.; Rose, D.; Fu, X.-D.; Glass, C.K.; et al. Nuclear Receptor-Induced Chromosomal Proximity and DNA Breaks Underlie Specific Translocations in Cancer. *Cell* **2009**, *139*, 1069–1083. [[CrossRef](#)]
133. Ciccia, A.; Elledge, S.J. The DNA Damage Response: Making It Safe to Play with Knives. *Mol. Cell* **2010**, *40*, 179–204. [[CrossRef](#)]
134. Janz, S.; Potter, M.; Rabkin, C.S. Lymphoma- and Leukemia-Associated Chromosomal Translocations in Healthy Individuals. *Genes Chromosomes Cancer* **2003**, *36*, 211–223. [[CrossRef](#)]
135. Rabkin, C.S.; Hirt, C.; Janz, S.; Dölken, G. T(14;18) Translocations and Risk of Follicular Lymphoma. *J. Natl. Cancer Inst. Monogr.* **2008**, *39*, 48–51. [[CrossRef](#)]
136. Schüler, F.; Hirt, C.; Dölken, G. Chromosomal Translocation t(14;18) in Healthy Individuals. *Semin. Cancer Biol.* **2003**, *13*, 203–209. [[CrossRef](#)]
137. Bäsecke, J.; Griesinger, F.; Trümper, L.; Brittinger, G. Leukemia- and Lymphoma-Associated Genetic Aberrations in Healthy Individuals. *Ann. Hematol.* **2002**, *81*, 64–75. [[CrossRef](#)]
138. Brassesco, M.S.; Montaldi, A.P.; Gras, D.E.; de Paula Queiroz, R.G.; Martinez-Rossi, N.M.; Tone, L.G.; Sakamoto-Hojo, E.T. MLL Leukemia-Associated Rearrangements in Peripheral Blood Lymphocytes from Healthy Individuals. *Genet. Mol. Biol.* **2009**, *32*, 234–241. [[CrossRef](#)] [[PubMed](#)]
139. Nambiar, M.; Raghavan, S.C. Chromosomal Translocations among the Healthy Human Population: Implications in Oncogenesis. *Cell Mol. Life Sci.* **2013**, *70*, 1381–1392. [[CrossRef](#)] [[PubMed](#)]
140. Jasin, M.; Rothstein, R. Repair of Strand Breaks by Homologous Recombination. *Cold Spring Harb Perspect Biol.* **2013**, *5*, a012740. [[CrossRef](#)] [[PubMed](#)]
141. Prakash, R.; Zhang, Y.; Feng, W.; Jasin, M. Homologous Recombination and Human Health: The Roles of BRCA1, BRCA2, and Associated Proteins. *Cold Spring Harb Perspect Biol.* **2015**, *7*, a016600. [[CrossRef](#)]
142. Boboila, C.; Alt, F.W.; Schwer, B. Chapter One—Classical and Alternative End-Joining Pathways for Repair of Lymphocyte-Specific and General DNA Double-Strand Breaks. In *Advances in Immunology*; Alt, F.W., Ed.; Academic Press: Cambridge, MA, USA, 2012; Volume 116, pp. 1–49.
143. Lieber, M.R. The Mechanism of Double-Strand DNA Break Repair by the Nonhomologous DNA End-Joining Pathway. *Annu. Rev. Biochem.* **2010**, *79*, 181–211. [[CrossRef](#)]

144. Symington, L.S.; Gautier, J. Double-Strand Break End Resection and Repair Pathway Choice. *Annu. Rev. Genet.* **2011**, *45*, 247–271. [[CrossRef](#)]
145. Moynahan, M.E.; Jasin, M. Mitotic Homologous Recombination Maintains Genomic Stability and Suppresses Tumorigenesis. *Nat. Rev. Mol. Cell Biol.* **2010**, *11*, 196–207. [[CrossRef](#)]
146. Sfeir, A.; Symington, L.S. Microhomology-Mediated End Joining: A Back-up Survival Mechanism or Dedicated Pathway? *Trends Biochem. Sci.* **2015**, *40*, 701–714. [[CrossRef](#)]
147. Brunet, E.; Jasin, M. Induction of Chromosomal Translocations with CRISPR-Cas9 and Other Nucleases: Understanding the Repair Mechanisms That Give Rise to Translocations. In *Chromosome Translocation*; Zhang, Y., Ed.; Advances in Experimental Medicine and Biology; Springer: Singapore, 2018; pp. 15–25. ISBN 9789811305931.
148. Stark, J.M.; Pierce, A.J.; Oh, J.; Pastink, A.; Jasin, M. Genetic Steps of Mammalian Homologous Repair with Distinct Mutagenic Consequences. *Mol. Cell Biol.* **2004**, *24*, 9305–9316. [[CrossRef](#)]
149. Weinstock, D.M.; Richardson, C.A.; Elliott, B.; Jasin, M. Modeling Oncogenic Translocations: Distinct Roles for Double-Strand Break Repair Pathways in Translocation Formation in Mammalian Cells. *DNA Repair* **2006**, *5*, 1065–1074. [[CrossRef](#)]
150. Ghosh, R.; Das, D.; Franco, S. The Role for the DSB Response Pathway in Regulating Chromosome Translocations. In *Chromosome Translocation*; Zhang, Y., Ed.; Advances in Experimental Medicine and Biology; Springer: Singapore, 2018; pp. 65–87. ISBN 9789811305931.
151. Kass, E.M.; Jasin, M. Collaboration and Competition between DNA Double-Strand Break Repair Pathways. *FEBS Lett.* **2010**, *584*, 3703–3708. [[CrossRef](#)]
152. Costantino, L.; Sotiriou, S.K.; Rantala, J.K.; Magin, S.; Mladenov, E.; Helleday, T.; Haber, J.E.; Iliakis, G.; Kallioniemi, O.P.; Halazonetis, T.D. Break-Induced Replication Repair of Damaged Forks Induces Genomic Duplications in Human Cells. *Science* **2014**, *343*, 88–91. [[CrossRef](#)]
153. Johnson, R.D.; Jasin, M. Sister Chromatid Gene Conversion Is a Prominent Double-Strand Break Repair Pathway in Mammalian Cells. *EMBO J.* **2000**, *19*, 3398–3407. [[CrossRef](#)]
154. Richardson, C.; Jasin, M. Coupled Homologous and Nonhomologous Repair of a Double-Strand Break Preserves Genomic Integrity in Mammalian Cells. *Mol. Cell Biol.* **2000**, *20*, 9068–9075. [[CrossRef](#)]
155. Soni, A.; Siemann, M.; Pantelias, G.E.; Iliakis, G. Marked Contribution of Alternative End-Joining to Chromosome-Translocation-Formation by Stochastically Induced DNA Double-Strand-Breaks in G2-Phase Human Cells. *Mutat. Res./Genet. Toxicol. Environ. Mutagen.* **2015**, *793*, 2–8. [[CrossRef](#)]
156. Simsek, D.; Jasin, M. Alternative End-Joining Is Suppressed by the Canonical NHEJ Component Xrcc4-Ligase IV during Chromosomal Translocation Formation. Available online: <https://pubmed.ncbi.nlm.nih.gov/20208544/> (accessed on 29 November 2020).
157. Zhang, Y.; Jasin, M. An Essential Role for CtIP in Chromosomal Translocation Formation through an Alternative End-Joining Pathway. *Nat. Struct. Mol. Biol.* **2011**, *18*, 80–84. [[CrossRef](#)]
158. Boboila, C.; Jankovic, M.; Yan, C.T.; Wang, J.H.; Wesemann, D.R.; Zhang, T.; Fazeli, A.; Feldman, L.; Nussenzweig, A.; Nussenzweig, M.; et al. Alternative End-Joining Catalyzes Robust IgH Locus Deletions and Translocations in the Combined Absence of Ligase 4 and Ku70. *Proc. Natl. Acad. Sci. USA* **2010**, *107*, 3034–3039. [[CrossRef](#)]
159. Elliott, B.; Richardson, C.; Jasin, M. Chromosomal Translocation Mechanisms at Intronic Alu Elements in Mammalian Cells. *Mol. Cell* **2005**, *17*, 885–894. [[CrossRef](#)]
160. Löbrich, M.; Jeggo, P. A Process of Resection-Dependent Nonhomologous End Joining Involving the Goddess Artemis. *Trends Biochem. Sci.* **2017**, *42*, 690–701. [[CrossRef](#)]
161. Iliakis, G.; Murmann, T.; Soni, A. Alternative End-Joining Repair Pathways Are the Ultimate Backup for Abrogated Classical Non-Homologous End-Joining and Homologous Recombination Repair: Implications for the Formation of Chromosome Translocations. *Mutat. Res./Genet. Toxicol. Environ. Mutagen.* **2015**, *793*, 166–175. [[CrossRef](#)]
162. Biehs, R.; Steinlage, M.; Barton, O.; Juhász, S.; Künzel, J.; Spies, J.; Shibata, A.; Jeggo, P.A.; Löbrich, M. DNA Double-Strand Break Resection Occurs during Non-Homologous End Joining in G1 but Is Distinct from Resection during Homologous Recombination. *Mol. Cell* **2017**, *65*, 671–684.e5. [[CrossRef](#)]
163. Beucher, A.; Birraux, J.; Tchouandong, L.; Barton, O.; Shibata, A.; Conrad, S.; Goodarzi, A.A.; Krempler, A.; Jeggo, P.A.; Löbrich, M. ATM and Artemis Promote Homologous Recombination of Radiation-Induced DNA Double-Strand Breaks in G2. *EMBO J.* **2009**, *28*, 3413–3427. [[CrossRef](#)]
164. Kakarougkas, A.; Jeggo, P.A. DNA DSB Repair Pathway Choice: An Orchestrated Handover Mechanism. *Br. J. Radiol.* **2014**, *87*, 20130685. [[CrossRef](#)]
165. Shibata, A.; Conrad, S.; Birraux, J.; Geuting, V.; Barton, O.; Ismail, A.; Kakarougkas, A.; Meek, K.; Taucher-Scholz, G.; Löbrich, M.; et al. Factors Determining DNA Double-Strand Break Repair Pathway Choice in G2 Phase. *EMBO J.* **2011**, *30*, 1079–1092. [[CrossRef](#)]
166. Tsuroula, K.; Furst, A.; Rogier, M.; Heyer, V.; Maglott-Roth, A.; Ferrand, A.; Reina-San-Martin, B.; Soutoglou, E. Temporal and Spatial Uncoupling of DNA Double Strand Break Repair Pathways within Mammalian Heterochromatin. *Mol. Cell* **2016**, *63*, 293–305. [[CrossRef](#)]
167. Choi, E.-H.; Yoon, S.; Koh, Y.E.; Seo, Y.-J.; Kim, K.P. Maintenance of Genome Integrity and Active Homologous Recombination in Embryonic Stem Cells. *Exp. Mol. Med.* **2020**, *52*, 1220–1229. [[CrossRef](#)] [[PubMed](#)]

168. Mujoo, K.; Pandita, R.K.; Tiwari, A.; Charaka, V.; Chakraborty, S.; Singh, D.K.; Hambarde, S.; Hittelman, W.N.; Horikoshi, N.; Hunt, C.R.; et al. Differentiation of Human Induced Pluripotent or Embryonic Stem Cells Decreases the DNA Damage Repair by Homologous Recombination. *Stem Cell Rep.* **2017**, *9*, 1660–1674. [[CrossRef](#)] [[PubMed](#)]
169. Lukášová, E.; Kořistek, Z.; Klabusay, M.; Ondřej, V.; Grigoryev, S.; Bačíková, A.; Řezáčová, M.; Falk, M.; Vávrová, J.; Kohútová, V.; et al. Granulocyte Maturation Determines Ability to Release Chromatin NETs and Loss of DNA Damage Response; These Properties Are Absent in Immature AML Granulocytes. *Biochim. Biophys. Acta* **2013**, *1833*, 767–779. [[CrossRef](#)] [[PubMed](#)]
170. Bristow, R.G.; Hill, R.P. Hypoxia and Metabolism. Hypoxia, DNA Repair and Genetic Instability. *Nat. Rev. Cancer* **2008**, *8*, 180–192. [[CrossRef](#)]
171. Lee, J.Y.; Orr-Weaver, T.L. Chromatin. In *Encyclopedia of Genetics*; Brenner, S., Miller, J.H., Eds.; Academic Press: New York, NY, USA, 2001; pp. 340–343. ISBN 978-0-12-227080-2.
172. Thomas, J.O.; Kornberg, R.D. An Octamer of Histones in Chromatin and Free in Solution. *Proc. Natl. Acad. Sci. USA* **1975**, *72*, 2626–2630. [[CrossRef](#)]
173. Arents, G.; Burlingame, R.W.; Wang, B.C.; Love, W.E.; Moudrianakis, E.N. The Nucleosomal Core Histone Octamer at 3.1 Å Resolution: A Tripartite Protein Assembly and a Left-Handed Superhelix. *Proc. Natl. Acad. Sci. USA* **1991**, *88*, 10148–10152. [[CrossRef](#)]
174. Luger, K.; Mäder, A.W.; Richmond, R.K.; Sargent, D.F.; Richmond, T.J. Crystal Structure of the Nucleosome Core Particle at 2.8 Å Resolution. *Nature* **1997**, *389*, 251–260. [[CrossRef](#)]
175. Campos, E.I.; Reinberg, D. Histones: Annotating Chromatin. *Annu. Rev. Genet.* **2009**, *43*, 559–599. [[CrossRef](#)]
176. Misteli, T. The Cell Biology of Genomes: Bringing the Double Helix to Life. *Cell* **2013**, *152*, 1209–1212. [[CrossRef](#)]
177. Ernst, J.; Kheradpour, P.; Mikkelsen, T.S.; Shores, N.; Ward, L.D.; Epstein, C.B.; Zhang, X.; Wang, L.; Issner, R.; Coyne, M.; et al. Mapping and Analysis of Chromatin State Dynamics in Nine Human Cell Types. *Nature* **2011**, *473*, 43–49. [[CrossRef](#)]
178. Maurano, M.T.; Humbert, R.; Rynes, E.; Thurman, R.E.; Haugen, E.; Wang, H.; Reynolds, A.P.; Sandstrom, R.; Qu, H.; Brody, J.; et al. Systematic Localization of Common Disease-Associated Variation in Regulatory DNA. *Science* **2012**, *337*, 1190–1195. [[CrossRef](#)]
179. Ernst, J.; Kellis, M. Discovery and Characterization of Chromatin States for Systematic Annotation of the Human Genome. *Nature Biotechnology* **2010**, *28*, 817–825. [[CrossRef](#)]
180. Ernst, J.; Kellis, M. Chromatin-State Discovery and Genome Annotation with ChromHMM. *Nat. Protoc.* **2017**, *12*, 2478–2492. [[CrossRef](#)]
181. Marshall, W.F.; Straight, A.; Marko, J.F.; Swedlow, J.; Dernburg, A.; Belmont, A.; Murray, A.W.; Agard, D.A.; Sedat, J.W. Interphase Chromosomes Undergo Constrained Diffusional Motion in Living Cells. *Curr. Biol.* **1997**, *7*, 930–939. [[CrossRef](#)]
182. Gothe, H.J.; Minneker, V.; Roukos, V. Dynamics of Double-Strand Breaks: Implications for the Formation of Chromosome Translocations. In *Chromosome Translocation*; Zhang, Y., Ed.; Advances in Experimental Medicine and Biology; Springer: Singapore, 2018; pp. 27–38. ISBN 9789811305931.
183. Heun, P.; Laroche, T.; Shimada, K.; Furrer, P.; Gasser, S.M. Chromosome Dynamics in the Yeast Interphase Nucleus. *Science* **2001**, *294*, 2181–2186. [[CrossRef](#)]
184. Neumann, F.R.; Dion, V.; Gehlen, L.R.; Tsai-Pflugfelder, M.; Schmid, R.; Taddei, A.; Gasser, S.M. Targeted INO80 Enhances Subnuclear Chromatin Movement and Ectopic Homologous Recombination. *Genes Dev.* **2012**, *26*, 369–383. [[CrossRef](#)] [[PubMed](#)]
185. Weber, S.C.; Spakowitz, A.J.; Theriot, J.A. Nonthermal ATP-Dependent Fluctuations Contribute to the in Vivo Motion of Chromosomal Loci. *Proc. Natl. Acad. Sci. USA* **2012**, *109*, 7338. [[CrossRef](#)] [[PubMed](#)]
186. Krawczyk, P.M.; Borovski, T.; Stap, J.; Cijssouw, T.; ten Cate, R.; Medema, J.P.; Kanaar, R.; Franken, N.a.P.; Aten, J.A. Chromatin Mobility Is Increased at Sites of DNA Double-Strand Breaks. *J. Cell Sci.* **2012**, *125*, 2127–2133. [[CrossRef](#)] [[PubMed](#)]
187. Thomson, I.; Gilchrist, S.; Bickmore, W.A.; Chubb, J.R. The Radial Positioning of Chromatin Is Not Inherited through Mitosis but Is Established De Novo in Early G1. *Curr. Biol.* **2004**, *14*, 166–172. [[CrossRef](#)] [[PubMed](#)]
188. Vazquez, J.; Belmont, A.S.; Sedat, J.W. Multiple Regimes of Constrained Chromosome Motion Are Regulated in the Interphase Drosophila Nucleus. *Curr. Biol.* **2001**, *11*, 1227–1239. [[CrossRef](#)]
189. Walter, J.; Schermelleh, L.; Cremer, M.; Tashiro, S.; Cremer, T. Chromosome Order in HeLa Cells Changes during Mitosis and Early G1, but Is Stably Maintained during Subsequent Interphase Stages. *J. Cell Biol.* **2003**, *160*, 685–697. [[CrossRef](#)]
190. Wiesmeijer, K.; Krouwels, I.M.; Tanke, H.J.; Dirks, R.W. Chromatin Movement Visualized with Photoactivable GFP-Labeled Histone H4. *Differentiation* **2008**, *76*, 83–90. [[CrossRef](#)]
191. Chuang, C.-H.; Carpenter, A.E.; Fuchsova, B.; Johnson, T.; de Lanerolle, P.; Belmont, A.S. Long-Range Directional Movement of an Interphase Chromosome Site. *Curr. Biol.* **2006**, *16*, 825–831. [[CrossRef](#)]
192. Dundr, M.; Ospina, J.K.; Sung, M.-H.; John, S.; Upender, M.; Ried, T.; Hager, G.L.; Matera, A.G. Actin-Dependent Intranuclear Repositioning of an Active Gene Locus in Vivo. *J. Cell Biol.* **2007**, *179*, 1095–1103. [[CrossRef](#)]
193. Tumber, T.; Belmont, A.S. Interphase Movements of a DNA Chromosome Region Modulated by VP16 Transcriptional Activator. *Nat. Cell Biol.* **2001**, *3*, 134–139. [[CrossRef](#)]
194. Spichal, M.; Brion, A.; Herbert, S.; Cournac, A.; Marbouty, M.; Zimmer, C.; Koszul, R.; Fabre, E. Evidence for a Dual Role of Actin in Regulating Chromosome Organization and Dynamics in Yeast. *J. Cell Sci.* **2016**, *129*, 681–692. [[CrossRef](#)]
195. Therizols, P.; Illingworth, R.S.; Courilleau, C.; Boyle, S.; Wood, A.J.; Bickmore, W.A. Chromatin Decondensation Is Sufficient to Alter Nuclear Organization in Embryonic Stem Cells. *Science* **2014**, *346*, 1238–1242. [[CrossRef](#)]

196. Kruhlak, M.J.; Celeste, A.; Dellaire, G.; Fernandez-Capetillo, O.; Müller, W.G.; McNally, J.G.; Bazett-Jones, D.P.; Nussenzweig, A. Changes in Chromatin Structure and Mobility in Living Cells at Sites of DNA Double-Strand Breaks. *J. Cell Biol.* **2006**, *172*, 823–834. [[CrossRef](#)]
197. Chiolo, I.; Minoda, A.; Colmenares, S.U.; Polyzos, A.; Costes, S.V.; Karpen, G.H. Double-Strand Breaks in Heterochromatin Move Outside of a Dynamic HP1a Domain to Complete Recombinational Repair. *Cell* **2011**, *144*, 732–744. [[CrossRef](#)]
198. Jakob, B.; Splinter, J.; Conrad, S.; Voss, K.-O.; Zink, D.; Durante, M.; Löbrich, M.; Taucher-Scholz, G. DNA Double-Strand Breaks in Heterochromatin Elicit Fast Repair Protein Recruitment, Histone H2AX Phosphorylation and Relocation to Euchromatin. *Nucleic Acids Res.* **2011**, *39*, 6489–6499. [[CrossRef](#)]
199. Kim, J.-A.; Kruhlak, M.; Dotiwala, F.; Nussenzweig, A.; Haber, J.E. Heterochromatin Is Refractory to γ -H2AX Modification in Yeast and Mammals. *J. Cell Biol.* **2007**, *178*, 209–218. [[CrossRef](#)]
200. Lemaitre, C.; Grabarz, A.; Tsouroula, K.; Andronov, L.; Furst, A.; Pankotai, T.; Heyer, V.; Rogier, M.; Attwood, K.M.; Kessler, P.; et al. Nuclear Position Dictates DNA Repair Pathway Choice. *Genes Dev.* **2014**, *28*, 2450–2463. [[CrossRef](#)]
201. Rosin, L.F.; Crocker, O.; Isenhardt, R.L.; Nguyen, S.C.; Xu, Z.; Joyce, E.F. Chromosome Territory Formation Attenuates the Translocation Potential of Cells. *eLife* **2019**, *8*, e49553. [[CrossRef](#)]
202. Lukas, J.; Lukas, C.; Bartek, J. More than Just a Focus: The Chromatin Response to DNA Damage and Its Role in Genome Integrity Maintenance. *Nat. Cell Biol.* **2011**, *13*, 1161–1169. [[CrossRef](#)]
203. Kaye, J.A.; Melo, J.A.; Cheung, S.K.; Vaze, M.B.; Haber, J.E.; Toczyski, D.P. DNA Breaks Promote Genomic Instability by Impeding Proper Chromosome Segregation. *Curr. Biol.* **2004**, *14*, 2096–2106. [[CrossRef](#)]
204. Lobachev, K.; Vitriol, E.; Stemple, J.; Resnick, M.A.; Bloom, K. Chromosome Fragmentation after Induction of a Double-Strand Break Is an Active Process Prevented by the RMX Repair Complex. *Curr. Biol.* **2004**, *14*, 2107–2112. [[CrossRef](#)]
205. Soutoglou, E.; Dorn, J.F.; Sengupta, K.; Jasin, M.; Nussenzweig, A.; Ried, T.; Danuser, G.; Misteli, T. Positional Stability of Single Double-Strand Breaks in Mammalian Cells. *Nat. Cell Biol.* **2007**, *9*, 675–682. [[CrossRef](#)]
206. Lisby, M.; Mortensen, U.H.; Rothstein, R. Colocalization of Multiple DNA Double-Strand Breaks at a Single Rad52 Repair Centre. *Nat. Cell Biol.* **2003**, *5*, 572–577. [[CrossRef](#)]
207. Jakob, B.; Splinter, J.; Durante, M.; Taucher-Scholz, G. Live Cell Microscopy Analysis of Radiation-Induced DNA Double-Strand Break Motion. *Proc. Natl. Acad. Sci. USA* **2009**, *106*, 3172–3177. [[CrossRef](#)]
208. Caron, P.; Choudhary, J.; Clouaire, T.; Bugler, B.; Daburon, V.; Aguirrebengoa, M.; Mangeat, T.; Iacovoni, J.S.; Álvarez-Quilón, A.; Cortés-Ledesma, F.; et al. Non-Redundant Functions of ATM and DNA-PKcs in Response to DNA Double-Strand Breaks. *Cell Rep.* **2015**, *13*, 1598–1609. [[CrossRef](#)]
209. Iarovaia, O.V.; Minina, E.P.; Sheval, E.V.; Onichtchouk, D.; Dokudovskaya, S.; Razin, S.V.; Vassetzky, Y.S. Nucleolus: A Central Hub for Nuclear Functions. *Trends Cell Biol.* **2019**, *29*, 647–659. [[CrossRef](#)]
210. Lin, C.-Y.; Shukla, A.; Grady, J.P.; Fink, J.L.; Dray, E.; Duijf, P.H.G. Translocation Breakpoints Preferentially Occur in Euchromatin and Acrocentric Chromosomes. *Cancers (Basel)* **2018**, *10*, 13. [[CrossRef](#)] [[PubMed](#)]
211. Yasuhara, T.; Xing, Y.-H.; Bauer, N.C.; Lee, L.; Dong, R.; Yadav, T.; Soberman, R.J.; Rivera, M.N.; Zou, L. Condensates Induced by Transcription Inhibition Localize Active Chromatin to Nucleoli. *Mol. Cell* **2022**, *82*, 2738–2753.e6. [[CrossRef](#)]
212. Ramanand, S.G.; Mani, R.S. Stress and the CIT1. *Mol. Cell* **2022**, *82*, 2730–2731. [[CrossRef](#)]
213. Nelms, B.E.; Maser, R.S.; MacKay, J.F.; Lagally, M.G.; Petrini, J.H.J. In Situ Visualization of DNA Double-Strand Break Repair in Human Fibroblasts. *Science* **1998**, *280*, 590–592. [[CrossRef](#)]
214. Aten, J.A.; Stap, J.; Krawczyk, P.M.; van Oven, C.H.; Hoebe, R.A.; Essers, J.; Kanaar, R. Dynamics of DNA Double-Strand Breaks Revealed by Clustering of Damaged Chromosome Domains. *Science* **2004**, *303*, 92–95. [[CrossRef](#)] [[PubMed](#)]
215. Dion, V.; Kalck, V.; Horigome, C.; Towbin, B.D.; Gasser, S.M. Increased Mobility of Double-Strand Breaks Requires Mec1, Rad9 and the Homologous Recombination Machinery. *Nat. Cell Biol.* **2012**, *14*, 502–509. [[CrossRef](#)]
216. Dion, V.; Kalck, V.; Seeber, A.; Schleker, T.; Gasser, S.M. Cohesin and the Nucleolus Constrain the Mobility of Spontaneous Repair Foci. *EMBO Rep.* **2013**, *14*, 984–991. [[CrossRef](#)] [[PubMed](#)]
217. Miné-Hattab, J.; Rothstein, R. Increased Chromosome Mobility Facilitates Homology Search during Recombination. *Nat. Cell Biol.* **2012**, *14*, 510–517. [[CrossRef](#)] [[PubMed](#)]
218. Saad, H.; Gallardo, F.; Dalvai, M.; Tanguy-le-Gac, N.; Lane, D.; Bystricky, K. DNA Dynamics during Early Double-Strand Break Processing Revealed by Non-Intrusive Imaging of Living Cells. *PLoS Genet.* **2014**, *10*, e1004187. [[CrossRef](#)] [[PubMed](#)]
219. Forget, A.L.; Kowalczykowski, S.C. Single-Molecule Imaging of DNA Pairing by RecA Reveals a Three-Dimensional Homology Search. *Nature* **2012**, *482*, 423–427. [[CrossRef](#)]
220. Ragunathan, K.; Liu, C.; Ha, T. RecA Filament Sliding on DNA Facilitates Homology Search. *eLife* **2012**, *1*, e00067. [[CrossRef](#)]
221. Renkawitz, J.; Lademann, C.A.; Kalocsay, M.; Jentsch, S. Monitoring Homology Search during DNA Double-Strand Break Repair In Vivo. *Mol. Cell* **2013**, *50*, 261–272. [[CrossRef](#)]
222. Seeber, A.; Dion, V.; Gasser, S.M. Checkpoint Kinases and the INO80 Nucleosome Remodeling Complex Enhance Global Chromatin Mobility in Response to DNA Damage. *Genes Dev.* **2013**, *27*, 1999–2008. [[CrossRef](#)]
223. Mao, Z.; Bozzella, M.; Seluanov, A.; Gorbunova, V. DNA Repair by Nonhomologous End Joining and Homologous Recombination during Cell Cycle in Human Cells. *Cell Cycle* **2008**, *7*, 2902–2906. [[CrossRef](#)]

REFERENCES

- Abrahamsson, Anna, Alexandra Albertsson-Lindblad, Peter N. Brown, Stefanie Baumgartner-Wennerholm, Lars M. Pedersen, Francesco D'Amore, Herman Nilsson-Ehle, et al. 2014. 'Real World Data on Primary Treatment for Mantle Cell Lymphoma: A Nordic Lymphoma Group Observational Study'. *Blood* 124 (8): 1288–95. <https://doi.org/10.1182/blood-2014-03-559930>.
- Abranches, R., A. P. Santos, E. Wegel, S. Williams, A. Castilho, P. Christou, P. Shaw, and E. Stoger. 2000. 'Widely Separated Multiple Transgene Integration Sites in Wheat Chromosomes Are Brought Together at Interphase'. *The Plant Journal: For Cell and Molecular Biology* 24 (6): 713–23. <https://doi.org/10.1046/j.1365-313x.2000.00908.x>.
- Advani, Ranjana H., Joseph J. Buggy, Jeff P. Sharman, Sonali M. Smith, Thomas E. Boyd, Barbara Grant, Kathryn S. Kolibaba, et al. 2013. 'Bcr Tyrosine Kinase Inhibitor Ibrutinib (PCI-32765) Has Significant Activity in Patients with Relapsed/Refractory B-Cell Malignancies'. *Journal of Clinical Oncology: Official Journal of the American Society of Clinical Oncology* 31 (1): 88–94. <https://doi.org/10.1200/JCO.2012.42.7906>.
- Agarwal, Rishu, Yih-Chih Chan, Constantine S. Tam, Tane Hunter, Dane Vassiliadis, Charis E. Teh, Rachel Thijssen, et al. 2019. 'Dynamic Molecular Monitoring Reveals That SWI–SNF Mutations Mediate Resistance to Ibrutinib plus Venetoclax in Mantle Cell Lymphoma'. *Nature Medicine* 25 (1): 119–29. <https://doi.org/10.1038/s41591-018-0243-z>.
- Alaggio, Rita, Catalina Amador, Ioannis Anagnostopoulos, Ayoma D. Attygalle, Iguaracyra Barreto de Oliveira Araujo, Emilio Berti, Govind Bhagat, et al. 2022. 'The 5th Edition of the World Health Organization Classification of Haematolymphoid Tumours: Lymphoid Neoplasms'. *Leukemia* 36 (7): 1720–48. <https://doi.org/10.1038/s41375-022-01620-2>.
- Allen, Christopher D. C., K. Mark Ansel, Caroline Low, Robin Lesley, Hirokazu Tamamura, Nobutaka Fujii, and Jason G. Cyster. 2004. 'Germinal Center Dark and Light Zone Organization Is Mediated by CXCR4 and CXCR5'. *Nature Immunology* 5 (9): 943–52. <https://doi.org/10.1038/ni1100>.
- Allinne, Jeanne, Andrei Pichugin, Olga Iarovaia, Manel Klibi, Ana Barat, Ewa Zlotek-Zlotkiewicz, Diana Markozashvili, et al. 2014a. 'Perinucleolar Relocalization and Nucleolin as Crucial Events in the Transcriptional Activation of Key Genes in Mantle Cell Lymphoma'. *Blood* 123 (13): 2044–53. <https://doi.org/10.1182/blood-2013-06-510511>.
- Andersen, N. S., J. K. Larsen, J. Christiansen, L. B. Pedersen, N. S. Christophersen, C. H. Geisler, and J. Jurlander. 2000. 'Soluble CD40 Ligand Induces Selective Proliferation of Lymphoma Cells in Primary Mantle Cell Lymphoma Cell Cultures'. *Blood* 96 (6): 2219–25.

- Annese, Tiziana, Giuseppe Ingravallo, Roberto Tamma, Michelina De Giorgis, Eugenio Maiorano, Tommasina Perrone, Francesco Albano, Giorgina Specchia, and Domenico Ribatti. 2020. 'Inflammatory Infiltrate and Angiogenesis in Mantle Cell Lymphoma'. *Translational Oncology* 13 (3): 100744. <https://doi.org/10.1016/j.tranon.2020.100744>.
- Ansell, Stephen M., David J. Inwards, Kendrith M. Rowland, Patrick J. Flynn, Roscoe F. Morton, Dennis F. Moore, Scott H. Kaufmann, et al. 2008. 'Low-Dose, Single-Agent Temsirolimus for Relapsed Mantle Cell Lymphoma: A Phase 2 Trial in the North Central Cancer Treatment Group'. *Cancer* 113 (3): 508–14. <https://doi.org/10.1002/cncr.23580>.
- Apostolou, Effie, and Dimitris Thanos. 2008. 'Virus Infection Induces NF- κ B-Dependent Interchromosomal Associations Mediating Monoallelic IFN- β Gene Expression'. *Cell* 134 (1): 85–96. <https://doi.org/10.1016/j.cell.2008.05.052>.
- Aran, Dvir, Gidon Toperoff, Michael Rosenberg, and Asaf Hellman. 2011. 'Replication Timing-Related and Gene Body-Specific Methylation of Active Human Genes'. *Human Molecular Genetics* 20 (4): 670–80. <https://doi.org/10.1093/hmg/ddq513>.
- Archambeau, Jérôme, Alice Blondel, and Rémy Pedoux. 2019. 'Focus-ING on DNA Integrity: Implication of ING Proteins in Cell Cycle Regulation and DNA Repair Modulation'. *Cancers* 12 (1): 58. <https://doi.org/10.3390/cancers12010058>.
- Argatoff, L. H., J. M. Connors, R. J. Klasa, D. E. Horsman, and R. D. Gascoyne. 1997. 'Mantle Cell Lymphoma: A Clinicopathologic Study of 80 Cases'. *Blood* 89 (6): 2067–78.
- Au, Wing Y., Randy D. Gascoyne, David S. Viswanatha, Joseph M. Connors, Richard J. Klasa, and Douglas E. Horsman. 2002. 'Cytogenetic Analysis in Mantle Cell Lymphoma: A Review of 214 Cases'. *Leukemia & Lymphoma* 43 (4): 783–91. <https://doi.org/10.1080/10428190290016890>.
- Aukema, Sietse M., Eva Hoster, Andreas Rosenwald, Danielle Canoni, Marie-Hélène Delfau-Larue, Grzegorz Rymkiewicz, Christoph Thorns, et al. 2018. 'Expression of TP53 Is Associated with the Outcome of MCL Independent of MIPI and Ki-67 in Trials of the European MCL Network'. *Blood* 131 (4): 417–20. <https://doi.org/10.1182/blood-2017-07-797019>.
- Baba, Yoshihiro, Shoji Hashimoto, Masato Matsushita, Dai Watanabe, Tadamitsu Kishimoto, Tomohiro Kurosaki, and Satoshi Tsukada. 2001. 'BLNK Mediates Syk-Dependent Btk Activation'. *Proceedings of the National Academy of Sciences of the United States of America* 98 (5): 2582–86. <https://doi.org/10.1073/pnas.051626198>.
- Bajénoff, Marc, Jackson G. Egen, Lily Y. Koo, Jean Pierre Laugier, Frédéric Brau, Nicolas Glaichenhaus, and Ronald N. Germain. 2006. 'Stromal Cell Networks Regulate Lymphocyte Entry, Migration, and Territoriality in Lymph Nodes'. *Immunity* 25 (6): 989–1001. <https://doi.org/10.1016/j.immuni.2006.10.011>.

- Balsas, Patricia, Jara Palomero, Álvaro Eguileor, Marta Leonor Rodríguez, Maria Carmela Vegliante, Ester Planas-Rigol, Marta Sureda-Gómez, Maria C. Cid, Elias Campo, and Virginia Amador. 2017. 'SOX11 Promotes Tumor Protective Microenvironment Interactions through CXCR4 and FAK Regulation in Mantle Cell Lymphoma'. *Blood* 130 (4): 501–13. <https://doi.org/10.1182/blood-2017-04-776740>.
- Balsas, Patricia, Luis Veloza, Guillem Clot, Marta Sureda-Gómez, Marta-Leonor Rodríguez, Christos Masaoutis, Gerard Frigola, et al. 2021. 'SOX11, CD70, and Treg Cells Configure the Tumor-Immune Microenvironment of Aggressive Mantle Cell Lymphoma'. *Blood* 138 (22): 2202–15. <https://doi.org/10.1182/blood.2020010527>.
- Banerji, J., S. Rusconi, and W. Schaffner. 1981. 'Expression of a Beta-Globin Gene Is Enhanced by Remote SV40 DNA Sequences'. *Cell* 27 (2 Pt 1): 299–308. [https://doi.org/10.1016/0092-8674\(81\)90413-x](https://doi.org/10.1016/0092-8674(81)90413-x).
- Bannerji, Rajat, Jon E. Arnason, Ranjana H. Advani, Jennifer R. Brown, John N. Allan, Stephen M. Ansell, Jeffrey A. Barnes, et al. 2022. 'Odronextamab, a Human CD20×CD3 Bispecific Antibody in Patients with CD20-Positive B-Cell Malignancies (ELM-1): Results from the Relapsed or Refractory Non-Hodgkin Lymphoma Cohort in a Single-Arm, Multicentre, Phase 1 Trial'. *The Lancet. Haematology* 9 (5): e327–39. [https://doi.org/10.1016/S2352-3026\(22\)00072-2](https://doi.org/10.1016/S2352-3026(22)00072-2).
- Bao, Shiwei, Mei Yi, Bo Xiang, and Pan Chen. 2024. 'Antitumor Mechanisms and Future Clinical Applications of the Natural Product Triptolide'. *Cancer Cell International* 24 (1): 150. <https://doi.org/10.1186/s12935-024-03336-y>.
- Bao, Shunshun, Mohammad Darvishi, Ali H Amin, Maysoon T. Al-Haideri, Indrajit Patra, Khadisha Kashikova, Irfan Ahmad, et al. 2023. 'CXC Chemokine Receptor 4 (CXCR4) Blockade in Cancer Treatment'. *Journal of Cancer Research and Clinical Oncology* 149 (10): 7945–68. <https://doi.org/10.1007/s00432-022-04444-w>.
- Bassam, Mohamad, Matthew J Maurer, Mary Stenson, Linda E Wellik, Christine Allmer, Brian K Link, James R Cerhan, Thomas E Witzig, and Mamta Gupta. 2013. 'Elevated Soluble IL-2Ra Levels Are Associated With Inferior Outcome and Is Independent Of MIPI Score in Patients With Mantle Cell Lymphoma'. *Blood* 122 (21): 4256. <https://doi.org/10.1182/blood.V122.21.4256.4256>.
- Basso, Katia, and Riccardo Dalla-Favera. 2012. 'Roles of BCL6 in Normal and Transformed Germinal Center B Cells'. *Immunological Reviews* 247 (1): 172–83. <https://doi.org/10.1111/j.1600-065X.2012.01112.x>.
- Beà, Sílvia, Rafael Valdés-Mas, Alba Navarro, Itziar Salaverria, David Martín-García, Pedro Jares, Eva Giné, et al. 2013. 'Landscape of Somatic Mutations and Clonal Evolution in Mantle Cell Lymphoma'. *Proceedings of the National Academy of Sciences* 110 (45): 18250–55. <https://doi.org/10.1073/pnas.1314608110>.

- Beà, Sílvia, Maria Ribas, Jesús M. Hernández, Francesc Bosch, Magda Pinyol, Luis Hernández, Juan Luis García, et al. 1999. 'Increased Number of Chromosomal Imbalances and High-Level DNA Amplifications in Mantle Cell Lymphoma Are Associated With Blastoid Variants'. *Blood* 93 (12): 4365–74. <https://doi.org/10.1182/blood.V93.12.4365>.
- Beerman, Isabel, Christoph Bock, Brian S. Garrison, Zachary D. Smith, Hongcang Gu, Alexander Meissner, and Derrick J. Rossi. 2013. 'Proliferation-Dependent Alterations of the DNA Methylation Landscape Underlie Hematopoietic Stem Cell Aging'. *Cell Stem Cell* 12 (4): 413–25. <https://doi.org/10.1016/j.stem.2013.01.017>.
- Bellis, S. L., J. T. Miller, and C. E. Turner. 1995. 'Characterization of Tyrosine Phosphorylation of Paxillin in Vitro by Focal Adhesion Kinase'. *The Journal of Biological Chemistry* 270 (29): 17437–41. <https://doi.org/10.1074/jbc.270.29.17437>.
- Beltran, Elena, Vicente Fresquet, Javier Martinez-Useros, Jose A. Richter-Larrea, Ainara Sagardoy, Izaskun Sesma, Luciana L. Almada, et al. 2011. 'A Cyclin-D1 Interaction with BAX Underlies Its Oncogenic Role and Potential as a Therapeutic Target in Mantle Cell Lymphoma'. *Proceedings of the National Academy of Sciences* 108 (30): 12461–66. <https://doi.org/10.1073/pnas.1018941108>.
- Benoist, C., and P. Chambon. 1981. 'In Vivo Sequence Requirements of the SV40 Early Promotor Region'. *Nature* 290 (5804): 304–10. <https://doi.org/10.1038/290304a0>.
- Berlin, C., D. J. Kowalewski, H. Schuster, N. Mirza, S. Walz, M. Handel, B. Schmid-Horch, et al. 2015. 'Mapping the HLA Ligandome Landscape of Acute Myeloid Leukemia: A Targeted Approach toward Peptide-Based Immunotherapy'. *Leukemia* 29 (3): 647–59. <https://doi.org/10.1038/leu.2014.233>.
- Betancur, Paola A., Brian J. Abraham, Ying Y. Yiu, Stephen B. Willingham, Farnaz Khameneh, Mark Zarnegar, Angera H. Kuo, et al. 2017. 'A CD47-Associated Super-Enhancer Links pro-Inflammatory Signalling to CD47 Upregulation in Breast Cancer'. *Nature Communications* 8 (1): 14802. <https://doi.org/10.1038/ncomms14802>.
- Bhatt, Vijaya R., Fausto R. Loberiza, Lynette M. Smith, James O. Armitage, Timothy C. Greiner, Martin Bast, Matthew A. Lunning, Philip J. Bierman, Julie M. Vose, and R. Gregory Bociek. 2016. 'Clinicopathologic Features, Management and Outcomes of Blastoid Variant of Mantle Cell Lymphoma: A Nebraska Lymphoma Study Group Experience'. *Leukemia & Lymphoma* 57 (6): 1327–34. <https://doi.org/10.3109/10428194.2015.1094801>.
- Bodrug, S. E., B. J. Warner, M. L. Bath, G. J. Lindeman, A. W. Harris, and J. M. Adams. 1994. 'Cyclin D1 Transgene Impedes Lymphocyte Maturation and Collaborates in Lymphomagenesis with the Myc Gene'. *The EMBO Journal* 13 (9): 2124–30.

- <https://doi.org/10.1002/j.1460-2075.1994.tb06488.x>.
- Bolzer, Andreas, Gregor Kreth, Irina Solovei, Daniela Koehler, Kaan Saracoglu, Christine Fauth, Stefan Müller, et al. 2005. 'Three-Dimensional Maps of All Chromosomes in Human Male Fibroblast Nuclei and Prometaphase Rosettes'. *PLoS Biology* 3 (5): e157.
<https://doi.org/10.1371/journal.pbio.0030157>.
- Borazanci, Erkut, Ashok Saluja, Jon Gockerman, Mohana Velagapudi, Ronald Korn, Daniel Von Hoff, and Ed Greeno. 2024. 'First-in-Human Phase I Study of Minnelide in Patients With Advanced Gastrointestinal Cancers: Safety, Pharmacokinetics, Pharmacodynamics, and Antitumor Activity'. *The Oncologist* 29 (2): 132–41. <https://doi.org/10.1093/oncolo/oyad278>.
- Bortnick, Alexandra, Zhaoren He, Megan Aubrey, Vivek Chandra, Matthew Denholtz, Kenian Chen, Yin C. Lin, and Cornelis Murre. 2018. 'An Inter-Chromosomal Transcription Hub Activates the Unfolded Protein Response in Plasma Cells'. bioRxiv. <https://doi.org/10.1101/295915>.
- Bosch, F., A. López-Guillermo, E. Campo, J. M. Ribera, E. Conde, M. A. Piris, T. Vallespi, S. Woessner, and E. Montserrat. 1998. 'Mantle Cell Lymphoma: Presenting Features, Response to Therapy, and Prognostic Factors'. *Cancer* 82 (3): 567–75.
[https://doi.org/10.1002/\(sici\)1097-0142\(19980201\)82:3<567::aid-cnrcr20>3.0.co;2-z](https://doi.org/10.1002/(sici)1097-0142(19980201)82:3<567::aid-cnrcr20>3.0.co;2-z).
- Boyd, Robert S., Rebekah Jukes-Jones, Renata Walewska, David Brown, Martin J. S. Dyer, and Kelvin Cain. 2009. 'Protein Profiling of Plasma Membranes Defines Aberrant Signaling Pathways in Mantle Cell Lymphoma'. *Molecular & Cellular Proteomics: MCP* 8 (7): 1501–15.
<https://doi.org/10.1074/mcp.M800515-MCP200>.
- Branco, Miguel R., and Ana Pombo. 2006. 'Intermingling of Chromosome Territories in Interphase Suggests Role in Translocations and Transcription-Dependent Associations'. *PLoS Biology* 4 (5): e138.
<https://doi.org/10.1371/journal.pbio.0040138>.
- Camacho, Emma, Luis Hernández, Silvia Hernández, Frederic Tort, Beatriz Bellosillo, Silvia Beà, Francesc Bosch, et al. 2002. 'ATM Gene Inactivation in Mantle Cell Lymphoma Mainly Occurs by Truncating Mutations and Missense Mutations Involving the Phosphatidylinositol-3 Kinase Domain and Is Associated with Increasing Numbers of Chromosomal Imbalances'. *Blood* 99 (1): 238–44.
<https://doi.org/10.1182/blood.V99.1.238>.
- Campo, Elias, Elaine S. Jaffe, James R. Cook, Leticia Quintanilla-Martinez, Steven H. Swerdlow, Kenneth C. Anderson, Pierre Brousset, et al. 2022. 'The International Consensus Classification of Mature Lymphoid Neoplasms: A Report from the Clinical Advisory Committee'. *Blood* 140 (11): 1229–53. <https://doi.org/10.1182/blood.2022015851>.
- Canoy, Reynand Jay, Anna Shmakova, Anna Karpukhina, Nikolai Lomov, Eugenia Tiukacheva, Yana Kozhevnikova, Franck André, Diego Germini,

- and Yegor Vassetzky. 2023. 'Specificity of Cancer-Related Chromosomal Translocations Is Linked to Proximity after the DNA Double-Strand Break and Subsequent Selection'. *NAR Cancer* 5 (3): zcad049. <https://doi.org/10.1093/narcan/zcad049>.
- Carvajal-Cuenca, Alejandra, Luz F. Sua, Nhora M. Silva, Stefania Pittaluga, Cristina Royo, Joo Y. Song, Rachel L. Sargent, et al. 2012. 'In Situ Mantle Cell Lymphoma: Clinical Implications of an Incidental Finding with Indolent Clinical Behavior'. *Haematologica* 97 (2): 270–78. <https://doi.org/10.3324/haematol.2011.052621>.
- Casella, Alex M., Carlo Colantuoni, and Seth A. Ament. 2022. 'Identifying Enhancer Properties Associated with Genetic Risk for Complex Traits Using Regulome-Wide Association Studies'. *PLoS Computational Biology* 18 (9): e1010430. <https://doi.org/10.1371/journal.pcbi.1010430>.
- Castillo, R., J. Mascarenhas, W. Telford, A. Chadburn, S. M. Friedman, and E. J. Schattner. 2000. 'Proliferative Response of Mantle Cell Lymphoma Cells Stimulated by CD40 Ligation and IL-4'. *Leukemia* 14 (2): 292–98. <https://doi.org/10.1038/sj.leu.2401664>.
- Catera, Rosa, Gregg J. Silverman, Katerina Hatzi, Till Seiler, Sebastien Didier, Lu Zhang, Maxime Hervé, et al. 2008. 'Chronic Lymphocytic Leukemia Cells Recognize Conserved Epitopes Associated with Apoptosis and Oxidation'. *Molecular Medicine (Cambridge, Mass.)* 14 (11–12): 665–74. <https://doi.org/10.2119/2008-00102.Catera>.
- Chang, Betty Y., Michelle Francesco, Martin F. M. De Rooij, Padmaja Magadala, Susanne M. Steggerda, Min Mei Huang, Annemieke Kuil, et al. 2013. 'Egress of CD19(+)CD5(+) Cells into Peripheral Blood Following Treatment with the Bruton Tyrosine Kinase Inhibitor Ibrutinib in Mantle Cell Lymphoma Patients'. *Blood* 122 (14): 2412–24. <https://doi.org/10.1182/blood-2013-02-482125>.
- Chapuy, Bjoern, Michael R. McKeown, Charles Y. Lin, Stefano Monti, Margaretha G. M. Roemer, Jun Qi, Peter B. Rahl, et al. 2013. 'Discovery and Characterization of Super-Enhancer-Associated Dependencies in Diffuse Large B Cell Lymphoma'. *Cancer Cell* 24 (6): 777–90. <https://doi.org/10.1016/j.ccr.2013.11.003>.
- Che, Yuxuan, Yang Liu, Yixin Yao, Holly A. Hill, Yijing Li, Qingsong Cai, Fangfang Yan, et al. 2023. 'Exploiting PRMT5 as a Target for Combination Therapy in Mantle Cell Lymphoma Characterized by Frequent ATM and TP53 Mutations'. *Blood Cancer Journal* 13 (1): 27. <https://doi.org/10.1038/s41408-023-00799-6>.
- Chen, Yang, Ya-ran Wu, Hong-ying Yang, Xin-zhe Li, Meng-meng Jie, Chang-jiang Hu, Yu-yun Wu, Shi-ming Yang, and Ying-bin Yang. 2018. 'Prolyl Isomerase Pin1: A Promoter of Cancer and a Target for Therapy'. *Cell Death & Disease* 9 (9): 1–17. <https://doi.org/10.1038/s41419-018-0844-y>.
- Chen, Yu, Haiping Zhang, Zhu Xu, Huanyin Tang, Anke Geng, Bailian Cai, Tao

- Su, et al. 2019. 'A PARP1-BRG1-SIRT1 Axis Promotes HR Repair by Reducing Nucleosome Density at DNA Damage Sites'. *Nucleic Acids Research* 47 (16): 8563–80. <https://doi.org/10.1093/nar/gkz592>.
- Chen, Yu, Yang Zhang, Yuchuan Wang, Liguozhang, Eva K. Brinkman, Stephen A. Adam, Robert Goldman, Bas van Steensel, Jian Ma, and Andrew S. Belmont. 2018. 'Mapping 3D Genome Organization Relative to Nuclear Compartments Using TSA-Seq as a Cytological Ruler'. *The Journal of Cell Biology* 217 (11): 4025–48. <https://doi.org/10.1083/jcb.201807108>.
- Chiarle, Roberto, Leo M. Budel, Jeffrey Skolnik, Glauco Frizzera, Marco Chilosi, Alessandra Corato, Gianni Pizzolo, et al. 2000. 'Increased Proteasome Degradation of Cyclin-Dependent Kinase Inhibitor P27 Is Associated with a Decreased Overall Survival in Mantle Cell Lymphoma'. *Blood* 95 (2): 619–26. <https://doi.org/10.1182/blood.V95.2.619>.
- Chilà, Rosaria, Alessandra Basana, Monica Lupi, Federica Guffanti, Eugenio Gaudio, Andrea Rinaldi, Luciano Cascione, et al. 2014. 'Combined Inhibition of Chk1 and Wee1 as a New Therapeutic Strategy for Mantle Cell Lymphoma'. *Oncotarget* 6 (5): 3394–3408.
- Chim, C. S., K. Y. Wong, F. Loong, W. W. Lam, and G. Srivastava. 2007. 'Frequent Epigenetic Inactivation of *Rb1* in Addition to *P15* and *P16* in Mantle Cell and Follicular Lymphoma'. *Human Pathology* 38 (12): 1849–57. <https://doi.org/10.1016/j.humpath.2007.05.009>.
- Chipumuro, Edmond, Eugenio Marco, Camilla L. Christensen, Nicholas Kwiatkowski, Tinghu Zhang, Clark M. Hatheway, Brian J. Abraham, et al. 2014. 'CDK7 Inhibition Suppresses Super-Enhancer-Linked Oncogenic Transcription in MYCN-Driven Cancer'. *Cell* 159 (5): 1126–39. <https://doi.org/10.1016/j.cell.2014.10.024>.
- Cho, Won-Ki, Jan-Hendrik Spille, Micca Hecht, Choongman Lee, Charles Li, Valentin Grube, and Ibrahim I. Cisse. 2018. 'Mediator and RNA Polymerase II Clusters Associate in Transcription-Dependent Condensates'. *Science (New York, N.Y.)* 361 (6400): 412–15. <https://doi.org/10.1126/science.aar4199>.
- Choe, Ji-Young, Ji Yun Yun, Hee Young Na, Jooryung Huh, Su-Jin Shin, Hyun-Jung Kim, Jin Ho Paik, et al. 2016. 'MYC Overexpression Correlates with MYC Amplification or Translocation, and Is Associated with Poor Prognosis in Mantle Cell Lymphoma'. *Histopathology* 68 (3): 442–49. <https://doi.org/10.1111/his.12760>.
- Choi, Michael Y., George F. Widhopf, Christina C. N. Wu, Bing Cui, Fitzgerald Lao, Anil Sadarangani, Joy Cavagnaro, et al. 2015. 'Pre-Clinical Specificity and Safety of UC-961, a First-In-Class Monoclonal Antibody Targeting ROR1'. *Clinical Lymphoma, Myeloma & Leukemia* 15 Suppl (0): S167-169. <https://doi.org/10.1016/j.clml.2015.02.010>.
- Chong, Shasha, Claire Dugast-Darzacq, Zhe Liu, Peng Dong, Gina M. Dailey, Claudia Cattoglio, Alec Heckert, et al. 2018. 'Imaging Dynamic and Selective Low-Complexity Domain Interactions That Control Gene

- Transcription'. *Science (New York, N.Y.)* 361 (6400): eaar2555.
<https://doi.org/10.1126/science.aar2555>.
- Chowdhary, Surabhi, Amoldeep S. Kainth, David Pincus, and David S. Gross. 2019. 'Heat Shock Factor 1 Drives Intergenic Association of Its Target Gene Loci upon Heat Shock'. *Cell Reports* 26 (1): 18.
<https://doi.org/10.1016/j.celrep.2018.12.034>.
- Chu, Charles C., Rosa Catera, Lu Zhang, Sebastien Didier, Briana M. Agagnina, Rajendra N. Damle, Matthew S. Kaufman, et al. 2010. 'Many Chronic Lymphocytic Leukemia Antibodies Recognize Apoptotic Cells with Exposed Nonmuscle Myosin Heavy Chain IIA: Implications for Patient Outcome and Cell of Origin'. *Blood* 115 (19): 3907–15.
<https://doi.org/10.1182/blood-2009-09-244251>.
- Chüeh, Anderly C., Janson W. T. Tse, Michael Dickinson, Paul Ioannidis, Laura Jenkins, Lars Tögel, BeeShin Tan, et al. 2017. 'ATF3 Repression of BCL-XL Determines Apoptotic Sensitivity to HDAC Inhibitors across Tumor Types'. *Clinical Cancer Research: An Official Journal of the American Association for Cancer Research* 23 (18): 5573–84.
<https://doi.org/10.1158/1078-0432.CCR-17-0466>.
- Cinar, Munewver, Farid Saei Hamedani, Zhicheng Mo, Bekir Cinar, Hesham M. Amin, and Serhan Alkan. 2013. 'Bcr Tyrosine Kinase Is Commonly Overexpressed in Mantle Cell Lymphoma and Its Attenuation by Ibrutinib Induces Apoptosis'. *Leukemia Research* 37 (10): 1271–77.
<https://doi.org/10.1016/j.leukres.2013.07.028>.
- Cobaleda, César, Wolfram Jochum, and Meinrad Busslinger. 2007. 'Conversion of Mature B Cells into T Cells by Dedifferentiation to Uncommitted Progenitors'. *Nature* 449 (7161): 473–77.
<https://doi.org/10.1038/nature06159>.
- Cohen, Andrea J., Alina Saiakhova, Olivia Corradin, Jennifer M. Luppino, Katreya Lovrenert, Cynthia F. Bartels, James J. Morrow, et al. 2017. 'Hotspots of Aberrant Enhancer Activity Punctuate the Colorectal Cancer Epigenome'. *Nature Communications* 8 (1): 14400.
<https://doi.org/10.1038/ncomms14400>.
- Conrotto, Paolo, Ulrika Andréasson, Venera Kuci, Carl A. K. Borrebaeck, and Sara Ek. 2011. 'Knock-down of SOX11 Induces Autotaxin-Dependent Increase in Proliferation in Vitro and More Aggressive Tumors in Vivo'. *Molecular Oncology* 5 (6): 527–37.
<https://doi.org/10.1016/j.molonc.2011.08.001>.
- Cremer, M., J. von Hase, T. Volm, A. Brero, G. Kreth, J. Walter, C. Fischer, I. Solovei, C. Cremer, and T. Cremer. 2001. 'Non-Random Radial Higher-Order Chromatin Arrangements in Nuclei of Diploid Human Cells'. *Chromosome Research: An International Journal on the Molecular, Supramolecular and Evolutionary Aspects of Chromosome Biology* 9 (7): 541–67. <https://doi.org/10.1023/a:1012495201697>.
- Cremer, T., C. Cremer, H. Baumann, E. K. Luedtke, K. Sperling, V. Teuber, and

- C. Zorn. 1982. 'Rabl's Model of the Interphase Chromosome Arrangement Tested in Chinese Hamster Cells by Premature Chromosome Condensation and Laser-UV-Microbeam Experiments'. *Human Genetics* 60 (1): 46–56. <https://doi.org/10.1007/BF00281263>.
- Cremer, Thomas, and Marion Cremer. 2010. 'Chromosome Territories'. *Cold Spring Harbor Perspectives in Biology* 2 (3): a003889. <https://doi.org/10.1101/cshperspect.a003889>.
- Dal Bo, Michele, Riccardo Bomben, Luis Hernández, and Valter Gattei. 2015. 'The MYC/miR-17-92 Axis in Lymphoproliferative Disorders: A Common Pathway with Therapeutic Potential'. *Oncotarget* 6 (23): 19381–92.
- Dal Col, Jessica, Paola Zancai, Liliana Terrin, Massimo Guidoboni, Maurilio Ponzoni, Alessandro Pavan, Michele Spina, et al. 2008. 'Distinct Functional Significance of Akt and mTOR Constitutive Activation in Mantle Cell Lymphoma'. *Blood* 111 (10): 5142–51. <https://doi.org/10.1182/blood-2007-07-103481>.
- Das, Nando D., Jen-Chien Chang, Chung-Chau Hon, S. Thomas Kelly, Shinsuke Ito, Marina Lizio, Bogumil Kaczkowski, et al. 2023. 'Defining Super-Enhancers by Highly Ranked Histone H4 Multi-Acetylation Levels Identifies Transcription Factors Associated with Glioblastoma Stem-like Properties'. *BMC Genomics* 24 (1): 574. <https://doi.org/10.1186/s12864-023-09659-w>.
- Davids, Matthew S., Andrew W. Roberts, Vaishalee P. Kenkre, William G. Wierda, Abhijeet Kumar, Thomas J. Kipps, Michelle Boyer, et al. 2021. 'Long-Term Follow-up of Patients with Relapsed or Refractory Non-Hodgkin Lymphoma Treated with Venetoclax in a Phase I, First-in-Human Study'. *Clinical Cancer Research: An Official Journal of the American Association for Cancer Research* 27 (17): 4690–95. <https://doi.org/10.1158/1078-0432.CCR-20-4842>.
- Del Giudice, Ilaria, Monica Messina, Sabina Chiaretti, Simona Santangelo, Simona Tavolaro, Maria Stefania De Propriis, Mauro Nanni, et al. 2012. 'Behind the Scenes of Non-Nodal MCL: Downmodulation of Genes Involved in Actin Cytoskeleton Organization, Cell Projection, Cell Adhesion, Tumour Invasion, TP53 Pathway and Mutated Status of Immunoglobulin Heavy Chain Genes'. *British Journal of Haematology* 156 (5): 601–11. <https://doi.org/10.1111/j.1365-2141.2011.08962.x>.
- Delfau-Larue, Marie-Hélène, Wolfram Klapper, Françoise Berger, Fabrice Jardin, Josette Briere, Gilles Salles, Olivier Casasnovas, et al. 2015. 'High-Dose Cytarabine Does Not Overcome the Adverse Prognostic Value of CDKN2A and TP53 Deletions in Mantle Cell Lymphoma'. *Blood* 126 (5): 604–11. <https://doi.org/10.1182/blood-2015-02-628792>.
- Demosthenous, Christos, Shiv K. Gupta, Jing Sun, Yongsun Wang, Tammy P. Troska, and Mamta Gupta. 2020. 'Deregulation of Polycomb Repressive Complex-2 in Mantle Cell Lymphoma Confers Growth Advantage by Epigenetic Suppression of Cdkn2b'. *Frontiers in Oncology* 10 (July):1226.

<https://doi.org/10.3389/fonc.2020.01226>.

- Derby, Lyudmyla, Gopichand Pendurti, George Deeb, Sheila Sait, Annmarie Block, and Francisco J. Hernandez-Ilizaliturri. 2010. 'Blastoid Variant of Mantle Cell Lymphoma (MCL) Is Associated with P53 Abnormalities and Have a Shorter Progression-Free Survival (PFS) and Overall Survival (OS) Despite Upfront Chemo-Immunotherapy Followed by High Dose Chemotherapy and Autologous Stem Cell Support (HDC-ASCS)'. *Blood* 116 (21): 1773. <https://doi.org/10.1182/blood.V116.21.1773.1773>.
- Dictor, Michael, Sara Ek, Maria Sundberg, Janina Warenholt, Czabafy György, Sandra Sernbo, Elin Gustavsson, Waleed Abu-Alsoud, Torkel Wadström, and Carl Borrebaeck. 2009. 'Strong Lymphoid Nuclear Expression of SOX11 Transcription Factor Defines Lymphoblastic Neoplasms, Mantle Cell Lymphoma and Burkitt's Lymphoma'. *Haematologica* 94 (11): 1563–68. <https://doi.org/10.3324/haematol.2009.008474>.
- Dixon, Jesse R., Siddarth Selvaraj, Feng Yue, Audrey Kim, Yan Li, Yin Shen, Ming Hu, Jun S. Liu, and Bing Ren. 2012. 'Topological Domains in Mammalian Genomes Identified by Analysis of Chromatin Interactions'. *Nature* 485 (7398): 376–80. <https://doi.org/10.1038/nature11082>.
- Donehower, L. A., M. Harvey, B. L. Slagle, M. J. McArthur, C. A. Montgomery, J. S. Butel, and A. Bradley. 1992. 'Mice Deficient for P53 Are Developmentally Normal but Susceptible to Spontaneous Tumours'. *Nature* 356 (6366): 215–21. <https://doi.org/10.1038/356215a0>.
- Dong, Jiaqiang, Jiong Li, Yang Li, Zhikun Ma, Yongxin Yu, and Cun-Yu Wang. 2021. 'Transcriptional Super-Enhancers Control Cancer Stemness and Metastasis Genes in Squamous Cell Carcinoma'. *Nature Communications* 12 (1): 3974. <https://doi.org/10.1038/s41467-021-24137-1>.
- Dreyling, Martin, Jeanette Doorduijn, Eva Giné, Mats Jerkeman, Jan Walewski, Martin Hutchings, Ulrich Mey, et al. 2024. 'Ibrutinib Combined with Immunochemotherapy with or without Autologous Stem-Cell Transplantation versus Immunochemotherapy and Autologous Stem-Cell Transplantation in Previously Untreated Patients with Mantle Cell Lymphoma (TRIANGLE): A Three-Arm, Randomised, Open-Label, Phase 3 Superiority Trial of the European Mantle Cell Lymphoma Network'. *The Lancet* 403 (10441): 2293–2306. [https://doi.org/10.1016/S0140-6736\(24\)00184-3](https://doi.org/10.1016/S0140-6736(24)00184-3).
- Dreyling, Martin, Wolfram Klapper, and Simon Rule. 2018. 'Blastoid and Pleomorphic Mantle Cell Lymphoma: Still a Diagnostic and Therapeutic Challenge!' *Blood* 132 (26): 2722–29. <https://doi.org/10.1182/blood-2017-08-737502>.
- Dubovsky, Jason A., Kyle A. Beckwith, Gayathri Natarajan, Jennifer A. Woyach, Samantha Jaglowski, Yiming Zhong, Joshua D. Hessler, et al. 2013. 'Ibrutinib Is an Irreversible Molecular Inhibitor of ITK Driving a Th1-Selective Pressure in T Lymphocytes'. *Blood* 122 (15): 2539–49. <https://doi.org/10.1182/blood-2013-06-507947>.

- Dudgeon, Crissy, Chang Chan, Wenfeng Kang, Yvonne Sun, Ryan Emerson, Harlan Robins, and Arnold J. Levine. 2014. 'The Evolution of Thymic Lymphomas in P53 Knockout Mice'. *Genes & Development* 28 (23): 2613–20. <https://doi.org/10.1101/gad.252148.114>.
- Dy, Peter, Alfredo Penzo-Méndez, Hongzhe Wang, Carlos E. Pedraza, Wendy B. Macklin, and Véronique Lefebvre. 2008. 'The Three SoxC Proteins--Sox4, Sox11 and Sox12--Exhibit Overlapping Expression Patterns and Molecular Properties'. *Nucleic Acids Research* 36 (9): 3101–17. <https://doi.org/10.1093/nar/gkn162>.
- E, Elhassadi, Hennessy B, Kumar S, Swan D, Lee E, Barrett N, Doyle M, Shilling C, and Catherwood M. 2019. 'TP53 Status in Mantle Cell Lymphoma (MCL) - A 10-Year Single Center Experience'. *Hematology and Medical Oncology* 4 (3). <https://doi.org/10.15761/HMO.1000185>.
- Ek, Sara, Michael Dictor, Mats Jerkeman, Karin Jirström, and Carl A. K. Borrebaeck. 2008. 'Nuclear Expression of the Non B-Cell Lineage Sox11 Transcription Factor Identifies Mantle Cell Lymphoma'. *Blood* 111 (2): 800–805. <https://doi.org/10.1182/blood-2007-06-093401>.
- Elhassadi, Ezzat, Brian Hennessy, Senthil Kumar, Louise Sutton, Michelle Griffin, Osasere Osarhieme, Rehman Faryal, et al. 2021. 'Impact of P53 Disruption on Mantle Cell Lymphoma (MCL) Treatment out-Come, Multi-Centre Retrospective Study'. *Blood* 138 (November):4514. <https://doi.org/10.1182/blood-2021-149653>.
- Elsnerova, Katerina, Alena Bartakova, Josef Tihlarik, Jiri Bouda, Lukas Rob, Petr Skapa, Martin Hrudá, et al. 2017. 'Gene Expression Profiling Reveals Novel Candidate Markers of Ovarian Carcinoma Intraperitoneal Metastasis'. *Journal of Cancer* 8 (17): 3598–3606. <https://doi.org/10.7150/jca.20766>.
- Engreitz, Jesse M., Vineeta Agarwala, and Leonid A. Mirny. 2012. 'Three-Dimensional Genome Architecture Influences Partner Selection for Chromosomal Translocations in Human Disease'. *PLOS ONE* 7 (9): e44196. <https://doi.org/10.1371/journal.pone.0044196>.
- Enjuanes, Anna, Verònica Fernández, Luis Hernández, Alba Navarro, Sílvia Beà, Magda Pinyol, Armando López-Guillermo, et al. 2011. 'Identification of Methylated Genes Associated with Aggressive Clinicopathological Features in Mantle Cell Lymphoma'. *PLoS ONE* 6 (5): e19736. <https://doi.org/10.1371/journal.pone.0019736>.
- Epperla, Narendranath, Mehdi Hamadani, Timothy S. Fenske, and Luciano J. Costa. 2018. 'Incidence and Survival Trends in Mantle Cell Lymphoma'. *British Journal of Haematology* 181 (5): 703–6. <https://doi.org/10.1111/bjh.14699>.
- Epron, G., P. Ame-Thomas, J. Le Priol, C. Pangault, J. Dulong, T. Lamy, T. Fest, and K. Tarte. 2012. 'Monocytes and T Cells Cooperate to Favor Normal and Follicular Lymphoma B-Cell Growth: Role of IL-15 and CD40L Signaling'. *Leukemia* 26 (1): 139–48.

- <https://doi.org/10.1038/leu.2011.179>.
- Erokhin, Maksim, Yegor Vassetzky, Pavel Georgiev, and Darya Chetverina. 2015. 'Eukaryotic Enhancers: Common Features, Regulation, and Participation in Diseases'. *Cellular and Molecular Life Sciences: CMLS* 72 (12): 2361–75. <https://doi.org/10.1007/s00018-015-1871-9>.
- Eskelund, Christian W., Christina Dahl, Jakob W. Hansen, Maj Westman, Arne Kolstad, Lone B. Pedersen, Carmen P. Montano-Almendras, et al. 2017. 'TP53 Mutations Identify Younger Mantle Cell Lymphoma Patients Who Do Not Benefit from Intensive Chemoimmunotherapy'. *Blood* 130 (17): 1903–10. <https://doi.org/10.1182/blood-2017-04-779736>.
- Evens, Andrew M., Sriram Balasubramanian, Julie M. Vose, Wael Harb, Leo I. Gordon, Robert Langdon, Julian Sprague, et al. 2016. 'A Phase I/II Multicenter, Open-Label Study of the Oral Histone Deacetylase Inhibitor Abexinostat in Relapsed/Refractory Lymphoma'. *Clinical Cancer Research: An Official Journal of the American Association for Cancer Research* 22 (5): 1059–66. <https://doi.org/10.1158/1078-0432.CCR-15-0624>.
- Fang, Nicole Y., Timothy C. Greiner, Dennis D. Weisenburger, Wing C. Chan, Julie M. Vose, Lynette M. Smith, James O. Armitage, et al. 2003. 'Oligonucleotide Microarrays Demonstrate the Highest Frequency of ATM Mutations in the Mantle Cell Subtype of Lymphoma'. *Proceedings of the National Academy of Sciences of the United States of America* 100 (9): 5372–77. <https://doi.org/10.1073/pnas.0831102100>.
- Fernández, Verónica, Olga Salamero, Blanca Espinet, Francesc Solé, Cristina Royo, Alba Navarro, Francisca Camacho, et al. 2010. 'Genomic and Gene Expression Profiling Defines Indolent Forms of Mantle Cell Lymphoma'. *Cancer Research* 70 (4): 1408–18. <https://doi.org/10.1158/0008-5472.CAN-09-3419>.
- Ferrer, Ana, Itziar Salaverria, Francesc Bosch, Neus Villamor, María Rozman, Silvia Beà, Eva Giné, Armando López-Guillermo, Elías Campo, and Emili Montserrat. 2007. 'Leukemic Involvement Is a Common Feature in Mantle Cell Lymphoma'. *Cancer* 109 (12): 2473–80. <https://doi.org/10.1002/cncr.22715>.
- Ferrero, Simone, Davide Rossi, Andrea Rinaldi, Alessio Brusca, Valeria Spina, Christian W. Eskelund, Andrea Evangelista, et al. 2020. 'KMT2D Mutations and TP53 Disruptions Are Poor Prognostic Biomarkers in Mantle Cell Lymphoma Receiving High-Dose Therapy: A FIL Study'. *Haematologica* 105 (6): 1604–12. <https://doi.org/10.3324/haematol.2018.214056>.
- Fiancette, Rémi, Rada Amin, Véronique Truffinet, Christelle Vincent-Fabert, Nadine Cogné, Michel Cogné, and Yves Denizot. 2010. 'A Myeloma Translocation-like Model Associating CCND1 with the Immunoglobulin Heavy-Chain Locus 3' Enhancers Does Not Promote by Itself B-Cell Malignancies'. *Leukemia Research* 34 (8): 1043–51. <https://doi.org/10.1016/j.leukres.2009.11.017>.

- Finlan, Lee E., Duncan Sproul, Inga Thomson, Shelagh Boyle, Elizabeth Kerr, Paul Perry, Bauke Ylstra, Jonathan R. Chubb, and Wendy A. Bickmore. 2008. 'Recruitment to the Nuclear Periphery Can Alter Expression of Genes in Human Cells'. *PLOS Genetics* 4 (3): e1000039. <https://doi.org/10.1371/journal.pgen.1000039>.
- Fisher, Richard I., Steven H. Bernstein, Brad S. Kahl, Benjamin Djulbegovic, Michael J. Robertson, Sven de Vos, Elliot Epner, et al. 2006. 'Multicenter Phase II Study of Bortezomib in Patients with Relapsed or Refractory Mantle Cell Lymphoma'. *Journal of Clinical Oncology: Official Journal of the American Society of Clinical Oncology* 24 (30): 4867–74. <https://doi.org/10.1200/JCO.2006.07.9665>.
- Fiskus, Warren, Christopher P. Mill, Dimuthu Perera, Christine Birdwell, Qing Deng, Haopeng Yang, Bernardo H. Lara, et al. 2021. 'BET Proteolysis Targeted Chimera-Based Therapy of Novel Models of Richter Transformation-Diffuse Large B-Cell Lymphoma'. *Leukemia* 35 (9): 2621–34. <https://doi.org/10.1038/s41375-021-01181-w>.
- Fitz-James, Maximilian H., Gonzalo Sabarís, Peter Sarkies, Frédéric Bantignies, and Giacomo Cavalli. 2023. 'Interchromosomal Contacts between Regulatory Regions Trigger Stable Transgenerational Epigenetic Inheritance in *Drosophila*'. bioRxiv. <https://doi.org/10.1101/2023.07.13.548806>.
- Flinsenberg, Thijs W.H., Charnelle C. Tromedjo, Nan Hu, Ye Liu, Yin Guo, Kevin Y.T. Thia, Tahereh Noori, et al. 2020. 'Differential Effects of BTK Inhibitors Ibrutinib and Zanubrutinib on NK-Cell Effector Function in Patients with Mantle Cell Lymphoma'. *Haematologica* 105 (2): e76–79. <https://doi.org/10.3324/haematol.2019.220590>.
- Fortin, Jean-Philippe, and Kasper D. Hansen. 2015. 'Reconstructing A/B Compartments as Revealed by Hi-C Using Long-Range Correlations in Epigenetic Data'. *Genome Biology* 16 (1): 180. <https://doi.org/10.1186/s13059-015-0741-y>.
- Freeman, Ciara L., Prasath Pararajalingam, Ling Jin, Sriram Balasubramanian, Aixiang Jiang, Wendan Xu, Michael Grau, et al. 2022. 'Molecular Determinants of Outcomes in Relapsed or Refractory Mantle Cell Lymphoma Treated with Ibrutinib or Temsirolimus in the MCL3001 (RAY) Trial'. *Leukemia* 36 (10): 2479–87. <https://doi.org/10.1038/s41375-022-01658-2>.
- Friedberg, Jonathan W., Jeff Sharman, John Sweetenham, Patrick B. Johnston, Julie M. Vose, Ann Lacasce, Julia Schaefer-Cuttillo, et al. 2010. 'Inhibition of Syk with Fostamatinib Disodium Has Significant Clinical Activity in Non-Hodgkin Lymphoma and Chronic Lymphocytic Leukemia'. *Blood* 115 (13): 2578–85. <https://doi.org/10.1182/blood-2009-08-236471>.
- Fu, Shuangshuang, Michael Wang, David R. Lairson, Ruosha Li, Bo Zhao, and Xianglin L. Du. 2017. 'Trends and Variations in Mantle Cell Lymphoma Incidence from 1995 to 2013: A Comparative Study between Texas and

- National SEER Areas'. *Oncotarget* 8 (68): 112516–29.
<https://doi.org/10.18632/oncotarget.22367>.
- Fuente, Hortensia de la, Aranzazu Cruz-Adalia, Gloria Martinez Del Hoyo, Danay Cibrián-Vera, Pedro Bonay, Daniel Pérez-Hernández, Jesús Vázquez, et al. 2014. 'The Leukocyte Activation Receptor CD69 Controls T Cell Differentiation through Its Interaction with Galectin-1'. *Molecular and Cellular Biology* 34 (13): 2479–87.
<https://doi.org/10.1128/MCB.00348-14>.
- Fulco, Charles P., Joseph Nasser, Thouis R. Jones, Glen Munson, Drew T. Bergman, Vidya Subramanian, Sharon R. Grossman, et al. 2019. 'Activity-by-Contact Model of Enhancer–Promoter Regulation from Thousands of CRISPR Perturbations'. *Nature Genetics* 51 (12): 1664–69.
<https://doi.org/10.1038/s41588-019-0538-0>.
- Gambino, Simona, Francesca Maria Quaglia, Marilisa Galasso, Chiara Cavallini, Roberto Chignola, Ornella Lovato, Luca Giacobazzi, et al. 2024. 'B-Cell Receptor Signaling Activity Identifies Patients with Mantle Cell Lymphoma at Higher Risk of Progression'. *Scientific Reports* 14 (1): 6595.
<https://doi.org/10.1038/s41598-024-55728-9>.
- Gaudio, Francesco, Michele Dicataldo, Fabrizia Di Giovanni, Gerardo Cazzato, Antonio d'Amati, Tommasina Perrone, Pierluigi Masciopinto, et al. 2023. 'Prognostic Role of CDKN2A Deletion and P53 Expression and Association With MIPIb in Mantle Cell Lymphoma'. *Clinical Lymphoma, Myeloma & Leukemia* 23 (8): 599–605.
<https://doi.org/10.1016/j.clml.2023.04.004>.
- Geisler, Christian H., Arne Kolstad, Anna Laurell, Niels S. Andersen, Lone B. Pedersen, Mats Jerkeman, Mikael Eriksson, et al. 2008. 'Long-Term Progression-Free Survival of Mantle Cell Lymphoma after Intensive Front-Line Immunochemotherapy with in Vivo-Purged Stem Cell Rescue: A Nonrandomized Phase 2 Multicenter Study by the Nordic Lymphoma Group'. *Blood* 112 (7): 2687–93.
<https://doi.org/10.1182/blood-2008-03-147025>.
- Gel, Bernat, and Eduard Serra. 2017. 'karyoploteR: An R/Bioconductor Package to Plot Customizable Genomes Displaying Arbitrary Data'. *Bioinformatics* 33 (19): 3088–90. <https://doi.org/10.1093/bioinformatics/btx346>.
- Gelbert, Lawrence M., Shufen Cai, Xi Lin, Concepcion Sanchez-Martinez, Miriam Del Prado, Maria Jose Lallena, Raquel Torres, et al. 2014. 'Preclinical Characterization of the CDK4/6 Inhibitor LY2835219: In-Vivo Cell Cycle-Dependent/Independent Anti-Tumor Activities Alone/in Combination with Gemcitabine'. *Investigational New Drugs* 32 (5): 825–37.
<https://doi.org/10.1007/s10637-014-0120-7>.
- Gerdtsen, Anna Sandström, Joana de Matos Rodrigues, Christian Winther Eskelund, Simon Husby, Kirsten Grønbaek, Riikka Rätty, Arne Kolstad, et al. 2023. 'Overexpression of the Key Metabolic Protein CPT1A Defines Mantle Cell Lymphoma Patients with Poor Response to Standard

- High-Dose Chemotherapy Independent of MIPI and Complement Established Highrisk Factors'. *Haematologica* 108 (4): 1092–1104. <https://doi.org/10.3324/haematol.2022.281420>.
- Gerstel, D., F. Wegwitz, K. Jannasch, P. Ludewig, K. Scheike, F. Alves, N. Beauchemin, W. Deppert, C. Wagener, and A. K. Horst. 2011. 'CEACAM1 Creates a Pro-Angiogenic Tumor Microenvironment That Supports Tumor Vessel Maturation'. *Oncogene* 30 (41): 4275–88. <https://doi.org/10.1038/onc.2011.146>.
- Gibson, Bryan A., Lynda K. Doolittle, Maximillian W. G. Schneider, Liv E. Jensen, Nathan Gamarra, Lisa Henry, Daniel W. Gerlich, Sy Redding, and Michael K. Rosen. 2019. 'Organization of Chromatin by Intrinsic and Regulated Phase Separation'. *Cell* 179 (2): 470-484.e21. <https://doi.org/10.1016/j.cell.2019.08.037>.
- Goy, Andre, Rajni Sinha, Michael E. Williams, Sevgi Kalayoglu Besisik, Johannes Drach, Radhakrishnan Ramchandren, Lei Zhang, Sherri Cicero, Tommy Fu, and Thomas E. Witzig. 2013. 'Single-Agent Lenalidomide in Patients with Mantle-Cell Lymphoma Who Relapsed or Progressed after or Were Refractory to Bortezomib: Phase II MCL-001 (EMERGE) Study'. *Journal of Clinical Oncology: Official Journal of the American Society of Clinical Oncology* 31 (29): 3688–95. <https://doi.org/10.1200/JCO.2013.49.2835>.
- Goy, Andre, Anas Younes, Peter McLaughlin, Barbara Pro, Jorge E. Romaguera, Frederick Hagemeister, Luis Fayad, et al. 2005. 'Phase II Study of Proteasome Inhibitor Bortezomib in Relapsed or Refractory B-Cell Non-Hodgkin's Lymphoma'. *Journal of Clinical Oncology: Official Journal of the American Society of Clinical Oncology* 23 (4): 667–75. <https://doi.org/10.1200/JCO.2005.03.108>.
- Greiner, TC, MJ Moynihan, WC Chan, DM Lytle, A Pedersen, JR Anderson, and DD Weisenburger. 1996. 'P53 Mutations in Mantle Cell Lymphoma Are Associated with Variant Cytology and Predict a Poor Prognosis'. *Blood* 87 (10): 4302–10. <https://doi.org/10.1182/blood.V87.10.4302.bloodjournal87104302>.
- Greiner, Timothy C., Chiranjib Dasgupta, Vincent V. Ho, Dennis D. Weisenburger, Lynette M. Smith, James C. Lynch, Julie M. Vose, et al. 2006. 'Mutation and Genomic Deletion Status of Ataxia Telangiectasia Mutated (ATM) and P53 Confer Specific Gene Expression Profiles in Mantle Cell Lymphoma'. *Proceedings of the National Academy of Sciences of the United States of America* 103 (7): 2352–57. <https://doi.org/10.1073/pnas.0510441103>.
- Grubert, Fabian, Rohith Srivas, Damek V. Spacek, Maya Kasowski, Mariana Ruiz-Velasco, Nasa Sinnott-Armstrong, Peyton Greenside, et al. 2020. 'Landscape of Cohesin-Mediated Chromatin Loops in the Human Genome'. *Nature* 583 (7818): 737–43. <https://doi.org/10.1038/s41586-020-2151-x>.
- Guangzhou Lupeng Pharmaceutical Company LTD. 2023. 'An Open Label,

- Single Arm, Multicenter Phase II Study of the Efficacy and Safety of LP-168 Monotherapy for Recurrent or Refractory Mantle Cell Lymphoma'. Clinical trial registration NCT05716087. [clinicaltrials.gov. https://clinicaltrials.gov/study/NCT05716087.](https://clinicaltrials.gov/study/NCT05716087)
- Guo, Hui, Dongfeng Zeng, Hui Zhang, Taylor Bell, Jun Yao, Yang Liu, Shengjian Huang, et al. 2019. 'Dual Inhibition of PI3K Signaling and Histone Deacetylation Halts Proliferation and Induces Lethality in Mantle Cell Lymphoma'. *Oncogene* 38 (11): 1802–14. [https://doi.org/10.1038/s41388-018-0550-3.](https://doi.org/10.1038/s41388-018-0550-3)
- Guo, Lingyu, Tian An, Haibin Zhou, Ziyang Wan, Zhixin Huang, and Tie Chong. 2023. 'MMP9 and TYROBP Affect the Survival of Circulating Tumor Cells in Clear Cell Renal Cell Carcinoma by Adapting to Tumor Immune Microenvironment'. *Scientific Reports* 13 (1): 6982. [https://doi.org/10.1038/s41598-023-34317-2.](https://doi.org/10.1038/s41598-023-34317-2)
- Guo, Wenjun, and Filippo G. Giancotti. 2004. 'Integrin Signalling during Tumour Progression'. *Nature Reviews Molecular Cell Biology* 5 (10): 816–26. [https://doi.org/10.1038/nrm1490.](https://doi.org/10.1038/nrm1490)
- Gupta, Mamta, Stephen M. Ansell, Anne J. Novak, Shaji Kumar, Scott H. Kaufmann, and Thomas E. Witzig. 2009. 'Inhibition of Histone Deacetylase Overcomes Rapamycin-Mediated Resistance in Diffuse Large B-Cell Lymphoma by Inhibiting Akt Signaling through mTORC2'. *Blood* 114 (14): 2926–35. [https://doi.org/10.1182/blood-2009-05-220889.](https://doi.org/10.1182/blood-2009-05-220889)
- Gurumurthy, Aishwarya, David T. Yu, Jared R. Stees, Pamela Chamales, Ekaterina Gavrilova, Paul Wassel, Lu Li, et al. 2021. 'Super-Enhancer Mediated Regulation of Adult β -Globin Gene Expression: The Role of eRNA and Integrator'. *Nucleic Acids Research* 49 (3): 1383–96. [https://doi.org/10.1093/nar/gkab002.](https://doi.org/10.1093/nar/gkab002)
- Gustavsson, Elin, Sandra Sernbo, Elin Andersson, Donal J. Brennan, Michael Dictor, Mats Jerkeman, Carl A. K. Borrebaeck, and Sara Ek. 2010. 'SOX11 Expression Correlates to Promoter Methylation and Regulates Tumor Growth in Hematopoietic Malignancies'. *Molecular Cancer* 9 (1): 187. [https://doi.org/10.1186/1476-4598-9-187.](https://doi.org/10.1186/1476-4598-9-187)
- Hagner, Patrick R., Hsiling Chiu, Maria Ortiz, Benedetta Apollonio, Maria Wang, Suzana Couto, Michelle F. Waldman, et al. 2017. 'Activity of Lenalidomide in Mantle Cell Lymphoma Can Be Explained by NK Cell-Mediated Cytotoxicity'. *British Journal of Haematology* 179 (3): 399–409. [https://doi.org/10.1111/bjh.14866.](https://doi.org/10.1111/bjh.14866)
- Hangaishi, Akira, Seishi Ogawa, Ying Qiao, Lili Wang, Noriko Hosoya, Koichiro Yuji, Yoichi Imai, Kengo Takeuchi, Shuichi Miyawaki, and Hisamaru Hirai. 2002. 'Mutations of Chk2 in Primary Hematopoietic Neoplasms'. *Blood* 99 (8): 3075–77. [https://doi.org/10.1182/blood.V99.8.3075.](https://doi.org/10.1182/blood.V99.8.3075)
- Harada, Akihito, Chandrashekhara Mallappa, Seiji Okada, John T. Butler, Stephen P. Baker, Jeanne B. Lawrence, Yasuyuki Ohkawa, and Anthony N. Imbalzano. 2015. 'Spatial Re-Organization of Myogenic Regulatory

- Sequences Temporally Controls Gene Expression'. *Nucleic Acids Research* 43 (4): 2008–21. <https://doi.org/10.1093/nar/gkv046>.
- Hardell, Lennart, Michael Carlberg, Marie Nordström, and Mikael Eriksson. 2023. 'Exposure to Phenoxyacetic Acids and Glyphosate as Risk Factors for Non-Hodgkin Lymphoma- Pooled Analysis of Three Swedish Case-Control Studies Including the Sub-Type Hairy Cell Leukemia'. *Leukemia & Lymphoma* 64 (5): 997–1004. <https://doi.org/10.1080/10428194.2023.2190434>.
- Haritunians, T., A. Mori, J. O'Kelly, Q. T. Luong, F. J. Giles, and H. P. Koeffler. 2007. 'Antiproliferative Activity of RAD001 (Everolimus) as a Single Agent and Combined with Other Agents in Mantle Cell Lymphoma'. *Leukemia* 21 (2): 333–39. <https://doi.org/10.1038/sj.leu.2404471>.
- Hartmann, Elena M., Elias Campo, George Wright, Georg Lenz, Itziar Salaverria, Pedro Jares, Wenming Xiao, et al. 2010. 'Pathway Discovery in Mantle Cell Lymphoma by Integrated Analysis of High-Resolution Gene Expression and Copy Number Profiling'. *Blood* 116 (6): 953–61. <https://doi.org/10.1182/blood-2010-01-263806>.
- Hathcock, Karen S., Hesed M. Padilla-Nash, Jordi Camps, Dong-Mi Shin, Daniel Triner, Arthur L. Shaffer, Robert W. Maul, et al. 2015. 'ATM Deficiency Promotes Development of Murine B-Cell Lymphomas That Resemble Diffuse Large B-Cell Lymphoma in Humans'. *Blood* 126 (20): 2291–2301. <https://doi.org/10.1182/blood-2015-06-654749>.
- Hay, Deborah, Jim R. Hughes, Christian Babbs, James O. J. Davies, Bryony J. Graham, Lars Hanssen, Mira T. Kassouf, et al. 2016. 'Genetic Dissection of the α -Globin Super-Enhancer in Vivo'. *Nature Genetics* 48 (8): 895–903. <https://doi.org/10.1038/ng.3605>.
- Hayakawa, Kyoko, Anthony M. Formica, Yuka Nakao, Daiju Ichikawa, Susan A. Shinton, Joni Brill-Dashoff, Mitchell R. Smith, Herbert C. Morse, and Richard R. Hardy. 2018. 'Early Generated B-1-Derived B Cells Have the Capacity To Progress To Become Mantle Cell Lymphoma-like Neoplasia in Aged Mice'. *The Journal of Immunology Author Choice* 201 (2): 804–13. <https://doi.org/10.4049/jimmunol.1800400>.
- Hayakawa, Kyoko, Yue-Sheng Li, Susan A. Shinton, Srinivasa R. Bandi, Anthony M. Formica, Joni Brill-Dashoff, and Richard R. Hardy. 2019. 'Crucial Role of Increased Arid3a at the Pre-B and Immature B Cell Stages for B1a Cell Generation'. *Frontiers in Immunology* 10:457. <https://doi.org/10.3389/fimmu.2019.00457>.
- He, Qing-Li, Denis V. Titov, Jing Li, Minjia Tan, Zhaohui Ye, Yingming Zhao, Daniel Romo, and Jun O. Liu. 2015. 'Covalent Modification of a Cysteine Residue in the XPB Subunit of the General Transcription Factor TFIIH through Single Epoxide Cleavage of the Transcription Inhibitor Triptolide'. *Angewandte Chemie (International Ed. in English)* 54 (6): 1859–63. <https://doi.org/10.1002/anie.201408817>.
- Hedditch, Ellen L., Bo Gao, Amanda J. Russell, Yi Lu, Catherine Emmanuel,

- Jonathan Beesley, Sharon E. Johnatty, et al. 2014. 'ABCA Transporter Gene Expression and Poor Outcome in Epithelial Ovarian Cancer'. *Journal of the National Cancer Institute* 106 (7): dju149. <https://doi.org/10.1093/jnci/dju149>.
- Heesters, Balthasar A., Riley C. Myers, and Michael C. Carroll. 2014. 'Follicular Dendritic Cells: Dynamic Antigen Libraries'. *Nature Reviews Immunology* 14 (7): 495–504. <https://doi.org/10.1038/nri3689>.
- Hermine, Olivier, Eva Hoster, Jan Walewski, André Bosly, Stephan Stilgenbauer, Catherine Thieblemont, Michal Szymczyk, et al. 2016. 'Addition of High-Dose Cytarabine to Immunochemotherapy before Autologous Stem-Cell Transplantation in Patients Aged 65 Years or Younger with Mantle Cell Lymphoma (MCL Younger): A Randomised, Open-Label, Phase 3 Trial of the European Mantle Cell Lymphoma Network'. *Lancet (London, England)* 388 (10044): 565–75. [https://doi.org/10.1016/S0140-6736\(16\)00739-X](https://doi.org/10.1016/S0140-6736(16)00739-X).
- Hernández, Luis, Silvia Beà, Magda Pinyol, German Ott, Tiemo Katzenberger, Andreas Rosenwald, Francesc Bosch, et al. 2005. 'CDK4 and MDM2 Gene Alterations Mainly Occur in Highly Proliferative and Aggressive Mantle Cell Lymphomas with Wild-Type INK4a/ARF Locus'. *Cancer Research* 65 (6): 2199–2206. <https://doi.org/10.1158/0008-5472.CAN-04-1526>.
- Hess, Georg, Raoul Herbrecht, Jorge Romaguera, Gregor Verhoef, Michael Crump, Christian Gisselbrecht, Anna Laurell, et al. 2009. 'Phase III Study to Evaluate Temsirolimus Compared with Investigator's Choice Therapy for the Treatment of Relapsed or Refractory Mantle Cell Lymphoma'. *Journal of Clinical Oncology: Official Journal of the American Society of Clinical Oncology* 27 (23): 3822–29. <https://doi.org/10.1200/JCO.2008.20.7977>.
- Hide, Takuichiro, Tatsuya Takezaki, Yuka Nakatani, Hideo Nakamura, Jun-ichi Kuratsu, and Toru Kondo. 2009. 'Sox11 Prevents Tumorigenesis of Glioma-Initiating Cells by Inducing Neuronal Differentiation'. *Cancer Research* 69 (20): 7953–59. <https://doi.org/10.1158/0008-5472.CAN-09-2006>.
- Hill, Louisa, Anja Ebert, Markus Jaritz, Gordana Wutz, Kota Nagasaka, Hiromi Tagoh, Daniela Kostanova-Poliakova, et al. 2020. 'Wapl Repression by Pax5 Promotes V Gene Recombination by Igh Loop Extrusion'. *Nature* 584 (7819): 142–47. <https://doi.org/10.1038/s41586-020-2454-y>.
- Hipp, Susanne, Ingo Ringshausen, Madlene Oelsner, Christian Bogner, Christian Peschel, and Thomas Decker. 2005. 'Inhibition of the Mammalian Target of Rapamycin and the Induction of Cell Cycle Arrest in Mantle Cell Lymphoma Cells'. *Haematologica* 90 (10): 1433–34.
- Horta, A., K. Monahan, E. Bashkirova, and S. Lomvardas. 2018. 'Cell Type-Specific Interchromosomal Interactions as a Mechanism for Transcriptional Diversity'. bioRxiv. <https://doi.org/10.1101/287532>.
- Hoster, Eva, Martin Dreyling, Wolfram Klapper, Christian Gisselbrecht, Achiel

- van Hoof, Hanneke C. Kluin-Nelemans, Michael Pfreundschuh, et al. 2008. 'A New Prognostic Index (MIPI) for Patients with Advanced-Stage Mantle Cell Lymphoma'. *Blood* 111 (2): 558–65. <https://doi.org/10.1182/blood-2007-06-095331>.
- Hou, Weihua, Ping Wei, Jianlan Xie, Yuanyuan Zheng, Yanlin Zhang, and Xiaoge Zhou. 2018. 'The Degree of Overlap between the Follicular Dendritic Cell Meshwork and Tumor Cells in Mantle Cell Lymphoma Is Associated with Prognosis'. *Pathology, Research and Practice* 214 (4): 513–20. <https://doi.org/10.1016/j.prp.2018.02.015>.
- Hu, Ying-Li, Shaoying Lu, Kai W. Szeto, Jie Sun, Yingxiao Wang, Juan C. Lasheras, and Shu Chien. 2014. 'FAK and Paxillin Dynamics at Focal Adhesions in the Protrusions of Migrating Cells'. *Scientific Reports* 4 (1): 6024. <https://doi.org/10.1038/srep06024>.
- Hu, Zhihong, L. Jeffrey Medeiros, Zi Chen, Weina Chen, Shaoying Li, Sergej N. Konoplev, Xinyan Lu, et al. 2017. 'Mantle Cell Lymphoma With MYC Rearrangement: A Report of 17 Patients'. *The American Journal of Surgical Pathology* 41 (2): 216–24. <https://doi.org/10.1097/PAS.0000000000000758>.
- Hummel, M., J. Tamaru, B. Kalvelage, and H. Stein. 1994. 'Mantle Cell (Previously Centrocytic) Lymphomas Express VH Genes with No or Very Little Somatic Mutations like the Physiologic Cells of the Follicle Mantle'. *Blood* 84 (2): 403–7.
- Ishov, Alexander M., Aishwarya Gurumurthy, and Jörg Bungert. 2020. 'Coordination of Transcription, Processing, and Export of Highly Expressed RNAs by Distinct Biomolecular Condensates'. *Emerging Topics in Life Sciences* 4 (3): 281–91. <https://doi.org/10.1042/ETLS20190160>.
- Jackson, D.a., A.b. Hassan, R.j. Errington, and P.r. Cook. 1993. 'Visualization of Focal Sites of Transcription within Human Nuclei.' *The EMBO Journal* 12 (3): 1059–65. <https://doi.org/10.1002/j.1460-2075.1993.tb05747.x>.
- Jain, Preetesh, Krystle Nomie, Nikita Kotlov, Vitaly Segodin, Holly Hill, Chi Young Ok, Ahmed Fetooh, et al. 2023. 'Immune-Depleted Tumor Microenvironment Is Associated with Poor Outcomes and BTK Inhibitor Resistance in Mantle Cell Lymphoma'. *Blood Cancer Journal* 13 (1): 156. <https://doi.org/10.1038/s41408-023-00927-2>.
- Jain, Preetesh, and Michael Wang. 2019. 'Mantle Cell Lymphoma: 2019 Update on the Diagnosis, Pathogenesis, Prognostication, and Management'. *American Journal of Hematology* 94 (6): 710–25. <https://doi.org/10.1002/ajh.25487>.
- Jeong, Seri, Yu Jin Park, Woobin Yun, Seung-Tae Lee, Jong Rak Choi, Cheolwon Suh, Jae-Cheol Jo, et al. 2020. 'Genetic Heterogeneity and Prognostic Impact of Recurrent ANK2 and TP53 Mutations in Mantle Cell Lymphoma: A Multi-Centre Cohort Study'. *Scientific Reports* 10 (1): 13359. <https://doi.org/10.1038/s41598-020-70310-9>.
- Jian, Xing, and Gary Felsenfeld. 2018. 'Insulin Promoter in Human Pancreatic β

- Cells Contacts Diabetes Susceptibility Loci and Regulates Genes Affecting Insulin Metabolism'. *Proceedings of the National Academy of Sciences of the United States of America* 115 (20): E4633–41. <https://doi.org/10.1073/pnas.1803146115>.
- Jiang, Yan-Yi, De-Chen Lin, Anand Mayakonda, Masaharu Hazawa, Ling-Wen Ding, Wen-Wen Chien, Liang Xu, et al. 2017. 'Targeting Super-Enhancer-Associated Oncogenes in Oesophageal Squamous Cell Carcinoma'. *Gut* 66 (8): 1358–68. <https://doi.org/10.1136/gutjnl-2016-311818>.
- Jiang, Ying, Qian Ding, Xiaoling Xie, Richard T. Libby, Veronique Lefebvre, and Lin Gan. 2013. 'Transcription Factors SOX4 and SOX11 Function Redundantly to Regulate the Development of Mouse Retinal Ganglion Cells'. *The Journal of Biological Chemistry* 288 (25): 18429–38. <https://doi.org/10.1074/jbc.M113.478503>.
- Johnston, Robert J., and Claude Desplan. 2014. 'Interchromosomal Communication Coordinates Intrinsically Stochastic Expression Between Alleles'. *Science* 343 (6171): 661–65. <https://doi.org/10.1126/science.1243039>.
- Jones, S. M., and A. Kazlauskas. 2001. 'Growth-Factor-Dependent Mitogenesis Requires Two Distinct Phases of Signalling'. *Nature Cell Biology* 3 (2): 165–72. <https://doi.org/10.1038/35055073>.
- Joo, Jaegeon, Sunghyun Cho, Sukbum Hong, Sunwoo Min, Kyukwang Kim, Rajeev Kumar, Jeong-Mo Choi, Yongdae Shin, and Inkyung Jung. 2023. 'Probabilistic Establishment of Speckle-Associated Inter-Chromosomal Interactions'. *Nucleic Acids Research* 51 (11): 5377–95. <https://doi.org/10.1093/nar/gkad211>.
- Kagiyama, Yuki, Shuhei Fujita, Yutaka Shima, Kazutsune Yamagata, Takuo Katsumoto, Makoto Nakagawa, Daisuke Honma, et al. 2021. 'CDKN1C-Mediated Growth Inhibition by an EZH1/2 Dual Inhibitor Overcomes Resistance of Mantle Cell Lymphoma to Ibrutinib'. *Cancer Science* 112 (6): 2314–24. <https://doi.org/10.1111/cas.14905>.
- Kahl, Brad S., Stephen E. Spurgeon, Richard R. Furman, Ian W. Flinn, Steven E. Coutre, Jennifer R. Brown, Don M. Benson, et al. 2014. 'A Phase 1 Study of the PI3K δ Inhibitor Idelalisib in Patients with Relapsed/Refractory Mantle Cell Lymphoma (MCL)'. *Blood* 123 (22): 3398–3405. <https://doi.org/10.1182/blood-2013-11-537555>.
- Kalhor, Reza, Harianto Tjong, Nimanthi Jayathilaka, Frank Alber, and Lin Chen. 2012. 'Genome Architectures Revealed by Tethered Chromosome Conformation Capture and Population-Based Modeling'. *Nature Biotechnology* 30 (1): 90–98. <https://doi.org/10.1038/nbt.2057>.
- Kanduri, Meena, Birgitta Sander, Stavroula Ntoufa, Nikos Papakonstantinou, Lesley-Ann Sutton, Kostas Stamatopoulos, Chandrasekhar Kanduri, and Richard Rosenquist. 2013. 'A Key Role for EZH2 in Epigenetic Silencing of HOX Genes in Mantle Cell Lymphoma'. *Epigenetics* 8 (12): 1280–88.

<https://doi.org/10.4161/epi.26546>.

- Karimi, Yasmin, Herve Ghesquieres, Wojciech Jurczak, Chan Cheah, Michael Clausen, Pieternella Lugtenburg, David Cunningham, et al. 2023. 'Effect of Follow-up Time on the Ability of Subcutaneous Epcoritamab to Induce Deep and Durable Complete Remissions in Patients with Relapsed/Refractory Large B-Cell Lymphoma: Updated Results from the Pivotal EPCORE NHL-1 Trial.' *Journal of Clinical Oncology* 41 (16_suppl): 7525–7525. https://doi.org/10.1200/JCO.2023.41.16_suppl.7525.
- Karolová, J., D. Kazantsev, M. Svatoň, L. Tušková, K. Forsterová, D. Maláriková, K. Benešová, et al. 2023. 'Sequencing-Based Analysis of Clonal Evolution of 25 Mantle Cell Lymphoma Patients at Diagnosis and after Failure of Standard Immunochemotherapy'. *American Journal of Hematology* 98 (10): 1627–36. <https://doi.org/10.1002/ajh.27044>.
- Kawaji-Kanayama, Yuka, Taku Tsukamoto, Masakazu Nakano, Yuichi Tokuda, Hiroaki Nagata, Kentaro Mizuhara, Yoko Katsuragawa-Taminishi, et al. 2023. 'miR-17-92 Cluster-BTG2 Axis Regulates B-Cell Receptor Signaling in Mantle Cell Lymphoma'. *Cancer Science*, December. <https://doi.org/10.1111/cas.16027>.
- Ke, Liangru, Hufeng Zhou, Chong Wang, Geng Xiong, Yanqun Xiang, Yihong Ling, Abdelmajid Khabir, et al. 2017. 'Nasopharyngeal Carcinoma Super-Enhancer-Driven ETV6 Correlates with Prognosis'. *Proceedings of the National Academy of Sciences* 114 (36): 9683–88. <https://doi.org/10.1073/pnas.1705236114>.
- Keats, Jeffrey A., Arleide Lee, Jeremy C. Cunniff, Weiqing Chen, Revonda Mehovic, Vania Estanek, Crag Markwood, et al. 2021. 'Abstract 1161: EZH2 Inhibitor Tazemetostat Demonstrates Activity in Preclinical Models of Bruton's Tyrosine Kinase Inhibitor-Resistant Relapsed/Refractory Mantle Cell Lymphoma'. *Cancer Research* 81 (13_Supplement): 1161. <https://doi.org/10.1158/1538-7445.AM2021-1161>.
- Kerpedjiev, Peter, Nezar Abdennur, Fritz Lekschas, Chuck McCallum, Kasper Dinkla, Hendrik Strobel, Jacob M. Lubert, et al. 2018. 'HiGlass: Web-Based Visual Exploration and Analysis of Genome Interaction Maps'. *Genome Biology* 19 (1): 125. <https://doi.org/10.1186/s13059-018-1486-1>.
- Khodadoust, Michael S., Niclas Olsson, Lisa E. Wagar, Ole A. W. Haabeth, Binbin Chen, Kavya Swaminathan, Keith Rawson, et al. 2017. 'Antigen Presentation Profiling Reveals Recognition of Lymphoma Immunoglobulin Neoantigens'. *Nature* 543 (7647): 723–27. <https://doi.org/10.1038/nature21433>.
- Khurana, Dianne, Laura N. Arneson, Renee A. Schoon, Christopher J. Dick, and Paul J. Leibson. 2007. 'Differential Regulation of Human NK Cell-Mediated Cytotoxicity by the Tyrosine Kinase Itk'. *Journal of Immunology (Baltimore, Md.: 1950)* 178 (6): 3575–82. <https://doi.org/10.4049/jimmunol.178.6.3575>.

- Kienle, Dirk, Alexander Kröber, Tiemo Katzenberger, German Ott, Elke Leupolt, Thomas F. E. Barth, Peter Möller, et al. 2003. 'VH Mutation Status and VDJ Rearrangement Structure in Mantle Cell Lymphoma: Correlation with Genomic Aberrations, Clinical Characteristics, and Outcome'. *Blood* 102 (8): 3003–9. <https://doi.org/10.1182/blood-2003-05-1383>.
- Kim, Do Hwan, Saima Siddiqui, Preetesh Jain, Michael Wang, Beenu Thakral, Shaoying Li, Roberto Miranda, Francisco Vega, L. Jeffrey Medeiros, and Chi Young Ok. 2024. 'TP53 Mutation Is Frequent in Mantle Cell Lymphoma with EZH2 Expression and Have Dismal Outcome When Both Are Present'. *Human Pathology* 146 (April):1–7. <https://doi.org/10.1016/j.humpath.2024.03.002>.
- Kim, Yeun Ju, Fujio Sekiya, Benoit Poulin, Yun Soo Bae, and Sue Goo Rhee. 2004. 'Mechanism of B-Cell Receptor-Induced Phosphorylation and Activation of Phospholipase C-Gamma2'. *Molecular and Cellular Biology* 24 (22): 9986–99. <https://doi.org/10.1128/MCB.24.22.9986-9999.2004>.
- Kim, Yu-Ri, and Ki-Seong Eom. 2014. 'Simultaneous Inhibition of CXCR4 and VLA-4 Exhibits Combinatorial Effect in Overcoming Stroma-Mediated Chemotherapy Resistance in Mantle Cell Lymphoma Cells'. *Immune Network* 14 (6): 296–306. <https://doi.org/10.4110/in.2014.14.6.296>.
- Kind, Jop, Ludo Pagie, Sandra S. de Vries, Leila Nahidiazar, Siddharth S. Dey, Magda Bienko, Ye Zhan, et al. 2015. 'Genome-Wide Maps of Nuclear Lamina Interactions in Single Human Cells'. *Cell* 163 (1): 134–47. <https://doi.org/10.1016/j.cell.2015.08.040>.
- Kirschbaum, Mark, Paul Frankel, Leslie Popplewell, Jasmine Zain, Maria Delioukina, Vinod Pullarkat, Deron Matsuoka, et al. 2011. 'Phase II Study of Vorinostat for Treatment of Relapsed or Refractory Indolent Non-Hodgkin's Lymphoma and Mantle Cell Lymphoma'. *Journal of Clinical Oncology: Official Journal of the American Society of Clinical Oncology* 29 (9): 1198–1203. <https://doi.org/10.1200/JCO.2010.32.1398>.
- Kluin-Nelemans, H. C., E. Hoster, O. Hermine, J. Walewski, M. Trneny, C. H. Geisler, S. Stilgenbauer, et al. 2012. 'Treatment of Older Patients with Mantle-Cell Lymphoma'. *The New England Journal of Medicine* 367 (6): 520–31. <https://doi.org/10.1056/NEJMoa1200920>.
- Kluin-Nelemans, Hanneke C., Eva Hoster, Olivier Hermine, Jan Walewski, Christian H. Geisler, Marek Trneny, Stephan Stilgenbauer, et al. 2020. 'Treatment of Older Patients With Mantle Cell Lymphoma (MCL): Long-Term Follow-Up of the Randomized European MCL Elderly Trial'. *Journal of Clinical Oncology* 38 (3): 248–56. <https://doi.org/10.1200/JCO.19.01294>.
- Kodet, Roman. 2009. 'Molecular and Immunohistochemical Analyses of BCL2, KI-67, and Cyclin D1 Expression in Synovial Sarcoma'. *Cancer Genetics and Cytogenetics*, January. https://www.academia.edu/19994350/Molecular_and_immunohistochemical_analyses_of_BCL2_KI_67_and_cyclin_D1_expression_in_synovial_sa

rcoma.

- Koff, Jean L., Rachel Kositsky, David L. Jaye, Michael C. Churnetski, Katelin Baird, Colin B. O'Leary, Christopher R. Flowers, et al. 2022. 'Mutations of ATM Confer a Risk of Inferior Survival in Patients with TP53-Wild Type Mantle Cell Lymphoma'. *Blood* 140 (Supplement 1): 3500–3503. <https://doi.org/10.1182/blood-2022-168002>.
- Kolar, Grant R., Darshna Mehta, Rosana Pelayo, and J. Donald Capra. 2007. 'A Novel Human B Cell Subpopulation Representing the Initial Germinal Center Population to Express AID'. *Blood* 109 (6): 2545–52. <https://doi.org/10.1182/blood-2006-07-037150>.
- Kopparapu, Pradeep Kumar, Sujata Bhoi, Larry Mansouri, Laleh S. Arabanian, Karla Plevova, Sarka Pospisilova, Agata M. Wasik, et al. 2016. 'Epigenetic Silencing of miR-26A1 in Chronic Lymphocytic Leukemia and Mantle Cell Lymphoma: Impact on EZH2 Expression'. *Epigenetics* 11 (5): 335–43. <https://doi.org/10.1080/15592294.2016.1164375>.
- Kowalewski, Daniel J., Heiko Schuster, Linus Backert, Claudia Berlin, Stefan Kahn, Lothar Kanz, Helmut R. Salih, Hans-Georg Rammensee, Stefan Stevanovic, and Juliane Sarah Stickel. 2015. 'HLA Ligandome Analysis Identifies the Underlying Specificities of Spontaneous Antileukemia Immune Responses in Chronic Lymphocytic Leukemia (CLL)'. *Proceedings of the National Academy of Sciences* 112 (2): E166–75. <https://doi.org/10.1073/pnas.1416389112>.
- Kridel, Robert, Barbara Meissner, Sanja Rogic, Merrill Boyle, Adele Telenius, Bruce Woolcock, Jay Gunawardana, et al. 2012. 'Whole Transcriptome Sequencing Reveals Recurrent NOTCH1 Mutations in Mantle Cell Lymphoma'. *Blood* 119 (9): 1963–71. <https://doi.org/10.1182/blood-2011-11-391474>.
- Kuci, Venera, Lena Nordström, Paolo Conrotto, and Sara Ek. 2016. 'SOX11 and HIG-2 Are Cross-Regulated and Affect Growth in Mantle Cell Lymphoma'. *Leukemia & Lymphoma* 57 (8): 1883–92. <https://doi.org/10.3109/10428194.2015.1121257>.
- Kuo, Pei-Yu, Shashidhar S. Jatiani, Adeeb H. Rahman, Donna Edwards, Zewei Jiang, Katya Ahr, Deepak Perumal, et al. 2018. 'SOX11 Augments BCR Signaling to Drive MCL-like Tumor Development'. *Blood* 131 (20): 2247–55. <https://doi.org/10.1182/blood-2018-02-832535>.
- Kuo, P.-Y., V. V. Leshchenko, M. J. Fazzari, D. Perumal, T. Gellen, T. He, J. Iqbal, et al. 2015. 'High-Resolution Chromatin Immunoprecipitation (ChIP) Sequencing Reveals Novel Binding Targets and Prognostic Role for SOX11 in Mantle Cell Lymphoma'. *Oncogene* 34 (10): 1231–40. <https://doi.org/10.1038/onc.2014.44>.
- Küppers, R., U. Klein, M. L. Hansmann, and K. Rajewsky. 1999. 'Cellular Origin of Human B-Cell Lymphomas'. *The New England Journal of Medicine* 341 (20): 1520–29. <https://doi.org/10.1056/NEJM199911113412007>.
- Kurozumi, Sasagu, Yuri Yamaguchi, Hiroshi Matsumoto, Masafumi Kurosumi,

- Shin-ichi Hayashi, Takaaki Fujii, Jun Horiguchi, Ken Shirabe, and Kenichi Inoue. 2019. 'Utility of Ki67 Labeling Index, Cyclin D1 Expression, and ER-Activity Level in Postmenopausal ER-Positive and HER2-Negative Breast Cancer with Neoadjuvant Chemo-Endocrine Therapy'. *PLoS ONE* 14 (5): e0217279. <https://doi.org/10.1371/journal.pone.0217279>.
- Kurtova, Antonina V., Archito T. Tamayo, Richard J. Ford, and Jan A. Burger. 2009. 'Mantle Cell Lymphoma Cells Express High Levels of CXCR4, CXCR5, and VLA-4 (CD49d): Importance for Interactions with the Stromal Microenvironment and Specific Targeting'. *Blood* 113 (19): 4604–13. <https://doi.org/10.1182/blood-2008-10-185827>.
- Kwon, H., A. N. Imbalzano, P. A. Khavari, R. E. Kingston, and M. R. Green. 1994. 'Nucleosome Disruption and Enhancement of Activator Binding by a Human SW1/SNF Complex'. *Nature* 370 (6489): 477–81. <https://doi.org/10.1038/370477a0>.
- Lancho, Olga, and Daniel Herranz. 2018. 'The MYC Enhancer-Ome: Long-Range Transcriptional Regulation of MYC in Cancer'. *Trends in Cancer* 4 (12): 810–22. <https://doi.org/10.1016/j.trecan.2018.10.003>.
- Landan, Gilad, Netta Mendelson Cohen, Zohar Mukamel, Amir Bar, Alina Molchadsky, Ran Brosh, Shirley Horn-Saban, et al. 2012. 'Epigenetic Polymorphism and the Stochastic Formation of Differentially Methylated Regions in Normal and Cancerous Tissues'. *Nature Genetics* 44 (11): 1207–14. <https://doi.org/10.1038/ng.2442>.
- Le Gouill Steven, Thieblemont Catherine, Oberic Lucie, Moreau Anne, Bouabdallah Krime, Dartigeas Caroline, Damaj Gandhi, et al. 2017. 'Rituximab after Autologous Stem-Cell Transplantation in Mantle-Cell Lymphoma'. *New England Journal of Medicine* 377 (13): 1250–60. <https://doi.org/10.1056/NEJMoa1701769>.
- Le, Kang, Jing Sun, Javid Ghaemmaghami, Mitchell R. Smith, W. K. Eddie Ip, Tycel Phillips, and Mamta Gupta. 2023. 'Blockade of CCR1 Induces a Phenotypic Shift in Macrophages and Triggers a Favorable Antilymphoma Activity'. *Blood Advances* 7 (15): 3952–67. <https://doi.org/10.1182/bloodadvances.2022008722>.
- Le, Kang, Jing Sun, Hunain Khawaja, Maho Shibata, Sanjay B. Maggirwar, Mitchell R. Smith, and Mamta Gupta. 2021. 'Mantle Cell Lymphoma Polarizes Tumor-Associated Macrophages into M2-like Macrophages, Which in Turn Promote Tumorigenesis'. *Blood Advances* 5 (14): 2863–78. <https://doi.org/10.1182/bloodadvances.2020003871>.
- Lecluse, Y., P. Lebailly, S. Roulland, A.-C. Gac, B. Nadel, and P. Gauduchon. 2009. 'T(11;14)-Positive Clones Can Persist over a Long Period of Time in the Peripheral Blood of Healthy Individuals'. *Leukemia* 23 (6): 1190–93. <https://doi.org/10.1038/leu.2009.31>.
- Lee, Christina, Xiangao Huang, Maurizio Di Liberto, Peter Martin, and Selina Chen-Kiang. 2020. 'Targeting CDK4/6 in Mantle Cell Lymphoma'. *Annals of Lymphoma* 4 (March):1. <https://doi.org/10.21037/aol.2019.12.01>.

- Lee, Hyewon, Hyeon Jin Park, Eun-Hye Park, Hee Young Ju, Chang-Mo Oh, Hyun-Joo Kong, Kyu-Won Jung, et al. 2017. 'Nationwide Statistical Analysis of Lymphoid Malignancies in Korea'. *Cancer Research and Treatment* 50 (1): 222–38. <https://doi.org/10.4143/crt.2017.093>.
- Lee, Ji-Hoon, and Tanya T. Paull. 2021. 'Cellular Functions of the Protein Kinase ATM and Their Relevance to Human Disease'. *Nature Reviews. Molecular Cell Biology* 22 (12): 796–814. <https://doi.org/10.1038/s41580-021-00394-2>.
- Lee, Ling-Ling, Cong Zhu, Brianna Feldmeier, Yao Chen, Wenyu Li, Yu Chen, Stephen P. Anthony, et al. 2023. 'Pre-Clinical Evaluation of a New-Generation Orally Bioavailable Dual Bcl-2/Bcl-XI Inhibitor LP-118 in Mantle Cell Lymphoma'. *Blood* 142 (Supplement 1): 3640. <https://doi.org/10.1182/blood-2023-180190>.
- Lee, Michael S., Wenji Sun, and Tonya J. Webb. 2020. 'Sphingosine Kinase Blockade Leads to Increased Natural Killer T Cell Responses to Mantle Cell Lymphoma'. *Cells* 9 (4): 1030. <https://doi.org/10.3390/cells9041030>.
- Lee, Seung-Cheol, Alexander A. Shestov, Lili Guo, Qian Zhang, Jeffrey C. Roman, Xiaobin Liu, Hong Y. Wang, et al. 2019. 'Metabolic Detection of Bruton's Tyrosine Kinase Inhibition in Mantle Cell Lymphoma Cells'. *Molecular Cancer Research: MCR* 17 (6): 1365–77. <https://doi.org/10.1158/1541-7786.MCR-18-0256>.
- Leonard, John P., Ann S. LaCasce, Mitchell R. Smith, Ariela Noy, Lucian R. Chirieac, Scott J. Rodig, Jian Q. Yu, et al. 2012. 'Selective CDK4/6 Inhibition with Tumor Responses by PD0332991 in Patients with Mantle Cell Lymphoma'. *Blood* 119 (20): 4597–4607. <https://doi.org/10.1182/blood-2011-10-388298>.
- Leux, Christophe, Marc Maynadié, Xavier Troussard, Quentin Cabrera, Aurélie Herry, Sandra Le Guyader-Peyrou, Steven Le Gouill, and Alain Monnereau. 2014. 'Mantle Cell Lymphoma Epidemiology: A Population-Based Study in France'. *Annals of Hematology* 93 (8): 1327–33. <https://doi.org/10.1007/s00277-014-2049-5>.
- Levine, Arnold J. 2020. 'P53: 800 Million Years of Evolution and 40 Years of Discovery'. *Nature Reviews. Cancer* 20 (8): 471–80. <https://doi.org/10.1038/s41568-020-0262-1>.
- Lewin, Jeremy, Jean-Charles Soria, Anastasios Stathis, Jean-Pierre Delord, Solange Peters, Ahmad Awada, Philippe G. Aftimos, et al. 2018. 'Phase Ib Trial With Birabresib, a Small-Molecule Inhibitor of Bromodomain and Extraterminal Proteins, in Patients With Selected Advanced Solid Tumors'. *Journal of Clinical Oncology: Official Journal of the American Society of Clinical Oncology* 36 (30): 3007–14. <https://doi.org/10.1200/JCO.2018.78.2292>.
- Li, Jian-Yong, Fanny Gaillard, Anne Moreau, Jean-Luc Harousseau, Christian Laboisie, Noël Milpied, Régis Bataille, and Hervé Avet-Loiseau. 1999. 'Detection of Translocation t(11;14)(Q13;Q32) in Mantle Cell Lymphoma

- by Fluorescence in Situ Hybridization'. *The American Journal of Pathology* 154 (5): 1449–52.
- Li, Jin, Jiayu Zhu, Olivia Gray, Débora R. Sobreira, David Wu, Ru-Ting Huang, Bernadette Miao, et al. 2024. 'Mechanosensitive Super-Enhancers Regulate Genes Linked to Atherosclerosis in Endothelial Cells'. *The Journal of Cell Biology* 223 (3): e202211125. <https://doi.org/10.1083/jcb.202211125>.
- Li, Peipei, Lee Marshall, Gabriel Oh, Jennifer L. Jakubowski, Daniel Groot, Yu He, Ting Wang, Arturas Petronis, and Viviane Labrie. 2019. 'Epigenetic Dysregulation of Enhancers in Neurons Is Associated with Alzheimer's Disease Pathology and Cognitive Symptoms'. *Nature Communications* 10 (1): 2246. <https://doi.org/10.1038/s41467-019-10101-7>.
- Li, Philippa, Ji Yuan, Fahad Shabbir Ahmed, Austin McHenry, Kai Fu, Guohua Yu, Hongxia Cheng, Mina L. Xu, David L. Rimm, and Zenggang Pan. 2021. 'High Counts of CD68+ and CD163+ Macrophages in Mantle Cell Lymphoma Are Associated With Inferior Prognosis'. *Frontiers in Oncology* 11:701492. <https://doi.org/10.3389/fonc.2021.701492>.
- Liang, Jin-Hua, Yi-Min Ren, Kai-Xin Du, Rui Gao, Zi-Wen Duan, Jing-Ran Guo, Tong-Yao Xing, et al. 2023. 'MYC-Induced Cytidine Metabolism Regulates Survival and Drug Resistance via cGas-STING Pathway in Mantle Cell Lymphoma'. *British Journal of Haematology* 202 (3): 550–65. <https://doi.org/10.1111/bjh.18878>.
- Lieberman-Aiden, Erez, Nynke L. van Berkum, Louise Williams, Maxim Imakaev, Tobias Ragoczy, Agnes Telling, Ido Amit, et al. 2009. 'Comprehensive Mapping of Long-Range Interactions Reveals Folding Principles of the Human Genome'. *Science (New York, N.Y.)* 326 (5950): 289–93. <https://doi.org/10.1126/science.1181369>.
- Lipfert, L., B. Haimovich, M. D. Schaller, B. S. Cobb, J. T. Parsons, and J. S. Brugge. 1992. 'Integrin-Dependent Phosphorylation and Activation of the Protein Tyrosine Kinase pp125FAK in Platelets'. *The Journal of Cell Biology* 119 (4): 905–12. <https://doi.org/10.1083/jcb.119.4.905>.
- Liu, Qing, Lapo Alinari, Ching-Shih Chen, Fengting Yan, James T. Dalton, Rosa Lapalombella, Xiaoli Zhang, et al. 2010. 'FTY720 Shows Promising in Vitro and in Vivo Preclinical Activity by Downmodulating Cyclin D1 and Phospho-Akt in Mantle Cell Lymphoma'. *Clinical Cancer Research: An Official Journal of the American Association for Cancer Research* 16 (12): 3182–92. <https://doi.org/10.1158/1078-0432.CCR-09-2484>.
- Liu, Shouchun, Sheila M. Thomas, Darren G. Woodside, David M. Rose, William B. Kiosses, Martin Pfaff, and Mark H. Ginsberg. 1999. 'Binding of Paxillin to A4 Integrins Modifies Integrin-Dependent Biological Responses'. *Nature* 402 (6762): 676–81. <https://doi.org/10.1038/45264>.
- Liu, Yunxia, Shuichi Kimpara, Nguyet M. Hoang, Anusara Daenthanasanmak, Yangguang Li, Li Lu, Vu N. Ngo, et al. 2023. 'EGR1-Mediated Metabolic Reprogramming to Oxidative Phosphorylation Contributes to Ibrutinib

- Resistance in B-Cell Lymphoma'. *Blood* 142 (22): 1879–94.
<https://doi.org/10.1182/blood.2023020142>.
- Lomvardas, Stavros, Gilad Barnea, David J. Pisapia, Monica Mendelsohn, Jennifer Kirkland, and Richard Axel. 2006. 'Interchromosomal Interactions and Olfactory Receptor Choice'. *Cell* 126 (2): 403–13.
<https://doi.org/10.1016/j.cell.2006.06.035>.
- Long, Mackenzie Elizabeth, Shirsha Koirala, Shelby Sloan, Fiona Brown-Burke, Christoph Weigel, Lynda Villagomez, Kara Corps, et al. 2023. 'Resistance to PRMT5-Targeted Therapy in Mantle Cell Lymphoma'. *Blood Advances* 8 (1): 150–63. <https://doi.org/10.1182/bloodadvances.2023010554>.
- Love, Michael I., Wolfgang Huber, and Simon Anders. 2014. 'Moderated Estimation of Fold Change and Dispersion for RNA-Seq Data with DESeq2'. *Genome Biology* 15 (12): 550.
<https://doi.org/10.1186/s13059-014-0550-8>.
- Lovec, H, A Grzeschiczek, M B Kowalski, and T Möröy. 1994. 'Cyclin D1/Bcl-1 Cooperates with Myc Genes in the Generation of B-Cell Lymphoma in Transgenic Mice.' *The EMBO Journal* 13 (15): 3487–95.
- Lovén, Jakob, Heather A. Hoke, Charles Y. Lin, Ashley Lau, David A. Orlando, Christopher R. Vakoc, James E. Bradner, Tong Ihn Lee, and Richard A. Young. 2013. 'Selective Inhibition of Tumor Oncogenes by Disruption of Super-Enhancers'. *Cell* 153 (2): 320–34.
<https://doi.org/10.1016/j.cell.2013.03.036>.
- Lu, Huasong, Dan Yu, Anders S. Hansen, Sourav Ganguly, Rongdiao Liu, Alec Heckert, Xavier Darzacq, and Qiang Zhou. 2018. 'Phase-Separation Mechanism for C-Terminal Hyperphosphorylation of RNA Polymerase II'. *Nature* 558 (7709): 318–23. <https://doi.org/10.1038/s41586-018-0174-3>.
- Lu, Jiajie, Yuecheng Peng, Rihong Huang, Zejia Feng, Yongyang Fan, Haojian Wang, Zhaorong Zeng, Yunxiang Ji, Yezhong Wang, and Zhaotao Wang. 2021. 'Elevated TYROBP Expression Predicts Poor Prognosis and High Tumor Immune Infiltration in Patients with Low-Grade Glioma'. *BMC Cancer* 21 (1): 723. <https://doi.org/10.1186/s12885-021-08456-6>.
- Luanpitpong, Sudjit, Nawin Chanthra, Montira Janan, Jirarat Poohadsuan, Parinya Samart, Yaowalak U-Pratya, Yon Rojanasakul, and Surapol Issaragrisil. 2018. 'Inhibition of O-GlcNAcase Sensitizes Apoptosis and Reverses Bortezomib Resistance in Mantle Cell Lymphoma through Modification of Truncated Bid'. *Molecular Cancer Therapeutics* 17 (2): 484–96. <https://doi.org/10.1158/1535-7163.MCT-17-0390>.
- Lupiáñez, Darío G., Katerina Kraft, Verena Heinrich, Peter Krawitz, Francesco Brancati, Eva Klopocki, Denise Horn, et al. 2015. 'Disruptions of Topological Chromatin Domains Cause Pathogenic Rewiring of Gene-Enhancer Interactions'. *Cell* 161 (5): 1012–25.
<https://doi.org/10.1016/j.cell.2015.04.004>.
- Ma, Jiao, Pin Lu, Ailin Guo, Shuhua Cheng, Hongliang Zong, Peter Martin, Morton Coleman, and Y. Lynn Wang. 2014. 'Characterization of

- Ibrutinib-Sensitive and -Resistant Mantle Lymphoma Cells'. *British Journal of Haematology* 166 (6): 849–61.
<https://doi.org/10.1111/bjh.12974>.
- Mahy, Nicola L., Paul E. Perry, and Wendy A. Bickmore. 2002. 'Gene Density and Transcription Influence the Localization of Chromatin Outside of Chromosome Territories Detectable by FISH'. *Journal of Cell Biology* 159 (5): 753–63. <https://doi.org/10.1083/jcb.200207115>.
- Malarikova, Diana, Adela Berkova, Ales Obr, Petra Blahovcova, Michael Svaton, Kristina Forsterova, Eva Kriegova, et al. 2020. 'Concurrent TP53 and CDKN2A Gene Aberrations in Newly Diagnosed Mantle Cell Lymphoma Correlate with Chemoresistance and Call for Innovative Upfront Therapy'. *Cancers* 12 (8): 2120.
<https://doi.org/10.3390/cancers12082120>.
- Mandala, Suzanne, Richard Hajdu, James Bergstrom, Elizabeth Quackenbush, Jenny Xie, James Milligan, Rosemary Thornton, et al. 2002. 'Alteration of Lymphocyte Trafficking by Sphingosine-1-Phosphate Receptor Agonists'. *Science (New York, N.Y.)* 296 (5566): 346–49.
<https://doi.org/10.1126/science.1070238>.
- Manfroi, B., J. Moreaux, C. Righini, F. Ghiringhelli, N. Sturm, and B. Huard. 2018. 'Tumor-Associated Neutrophils Correlate with Poor Prognosis in Diffuse Large B-Cell Lymphoma Patients'. *Blood Cancer Journal* 8 (7): 66.
<https://doi.org/10.1038/s41408-018-0099-y>.
- Manzo, Stefano Giustino, Zhao-Li Zhou, Ying-Qing Wang, Jessica Marinello, Jin-Xue He, Yuan-Chao Li, Jian Ding, Giovanni Capranico, and Ze-Hong Miao. 2012. 'Natural Product Triptolide Mediates Cancer Cell Death by Triggering CDK7-Dependent Degradation of RNA Polymerase II'. *Cancer Research* 72 (20): 5363–73.
<https://doi.org/10.1158/0008-5472.CAN-12-1006>.
- Markozashvili, Diana, Andrei Pichugin, Ana Barat, Valerie Camara-Clayette, Natalia V. Vasilyeva, Hélène Lelièvre, Laurence Kraus-Berthier, Stéphane Depil, Vincent Ribrag, and Yegor Vassetzky. 2016. 'Histone Deacetylase Inhibitor Abexinostat Affects Chromatin Organization and Gene Transcription in Normal B Cells and in Mantle Cell Lymphoma'. *Gene* 580 (2): 134–43. <https://doi.org/10.1016/j.gene.2016.01.017>.
- Martinez-Baquero, Diana, Ali Sakhdari, Huan Mo, Do Hwan Kim, Rashmi Kanagal-Shamanna, Shaoying Li, Ken H. Young, et al. 2021. 'EZH2 Expression Is Associated with Inferior Overall Survival in Mantle Cell Lymphoma'. *Modern Pathology: An Official Journal of the United States and Canadian Academy of Pathology, Inc* 34 (12): 2183–91.
<https://doi.org/10.1038/s41379-021-00885-9>.
- Mastrangelo, I A, A J Courey, J S Wall, S P Jackson, and P V Hough. 1991. 'DNA Looping and Sp1 Multimer Links: A Mechanism for Transcriptional Synergism and Enhancement.' *Proceedings of the National Academy of Sciences* 88 (13): 5670–74. <https://doi.org/10.1073/pnas.88.13.5670>.

- Mato, Anthony R., Nirav N. Shah, Wojciech Jurczak, Chan Y. Cheah, John M. Pagel, Jennifer A. Woyach, Bitá Fakhri, et al. 2021. 'Pirtobrutinib in Relapsed or Refractory B-Cell Malignancies (BRUIN): A Phase 1/2 Study'. *Lancet (London, England)* 397 (10277): 892–901. [https://doi.org/10.1016/S0140-6736\(21\)00224-5](https://doi.org/10.1016/S0140-6736(21)00224-5).
- Medina, Daniel J., Lauri Goodell, John Glod, Céline Gélinas, Arnold B. Rabson, and Roger K. Strair. 2012. 'Mesenchymal Stromal Cells Protect Mantle Cell Lymphoma Cells from Spontaneous and Drug-Induced Apoptosis through Secretion of B-Cell Activating Factor and Activation of the Canonical and Non-Canonical Nuclear Factor κ B Pathways'. *Haematologica* 97 (8): 1255–63. <https://doi.org/10.3324/haematol.2011.040659>.
- Menezes, Daniel L., Jenny Holt, Yan Tang, Jiajia Feng, Paul Barsanti, Yue Pan, Majid Ghodusi, et al. 2015. 'A Synthetic Lethal Screen Reveals Enhanced Sensitivity to ATR Inhibitor Treatment in Mantle Cell Lymphoma with ATM Loss-of-Function'. *Molecular Cancer Research: MCR* 13 (1): 120–29. <https://doi.org/10.1158/1541-7786.MCR-14-0240>.
- Meng, Jingshu, Chan Chang, Huaxiong Pan, Fang Zhu, Yin Xiao, Tao Liu, Xiu Nie, Gang Wu, and Liling Zhang. 2018. 'Epidemiologic Characteristics of Malignant Lymphoma in Hubei, China: A Single-Center 5-Year Retrospective Study'. *Medicine* 97 (35): e12120. <https://doi.org/10.1097/MD.00000000000012120>.
- Miao, Qi, Matthew C. Hill, Fengju Chen, Qianxing Mo, Amy T. Ku, Carlos Ramos, Elisabeth Sock, Véronique Lefebvre, and Hoang Nguyen. 2019. 'SOX11 and SOX4 Drive the Reactivation of an Embryonic Gene Program during Murine Wound Repair'. *Nature Communications* 10 (September):4042. <https://doi.org/10.1038/s41467-019-11880-9>.
- Minden, Marcus Dühren-von, Rudolf Übelhart, Dunja Schneider, Thomas Wossning, Martina P. Bach, Maike Buchner, Daniel Hofmann, et al. 2012. 'Chronic Lymphocytic Leukaemia Is Driven by Antigen-Independent Cell-Autonomous Signalling'. *Nature* 489 (7415): 309–12. <https://doi.org/10.1038/nature11309>.
- Mittal, Priya, and Charles W. M. Roberts. 2020. 'The SWI/SNF Complex in Cancer — Biology, Biomarkers and Therapy'. *Nature Reviews Clinical Oncology* 17 (7): 435–48. <https://doi.org/10.1038/s41571-020-0357-3>.
- Mohanty, Atish, Natalie Sandoval, Manasi Das, Raju Pillai, Lu Chen, Robert W. Chen, Hesham M. Amin, et al. 2016. 'CCND1 Mutations Increase Protein Stability and Promote Ibrutinib Resistance in Mantle Cell Lymphoma'. *Oncotarget* 7 (45): 73558–72. <https://doi.org/10.18632/oncotarget.12434>.
- Mohanty, Suchismita, Atish Mohanty, Natalie Sandoval, Victoria Bedell, Joyce Murata-Collins, Jun Wu, Anna Scuto, Dennis D. Weisenburger, and Vu N Ngo. 2013. 'Cyclin D1 Maintains Mantle Cell Lymphoma Through CDK4-Independent Regulation Of DNA Replicative Checkpoints'. *Blood* 122 (21): 2512. <https://doi.org/10.1182/blood.V122.21.2512.2512>.

- Mohanty, Suchismita, Atish Mohanty, Natalie Sandoval, Thai Tran, Victoria Bedell, Jun Wu, Anna Scuto, Joyce Murata-Collins, Dennis D. Weisenburger, and Vu N. Ngo. 2017. 'Cyclin D1 Depletion Induces DNA Damage in Mantle Cell Lymphoma Lines'. *Leukemia & Lymphoma* 58 (3): 676–88. <https://doi.org/10.1080/10428194.2016.1198958>.
- Morschhauser, Franck, Kamal Bouabdallah, Stephan Stilgenbauer, Catherine Thieblemont, Sophie de Guibert, Florian Zettl, Lawrence M. Gelbert, et al. 2021. 'Clinical Activity of Abemaciclib in Patients with Relapsed or Refractory Mantle Cell Lymphoma - a Phase II Study'. *Haematologica* 106 (3): 859–62. <https://doi.org/10.3324/haematol.2019.224535>.
- Mota, Ana, Szymon Berezicki, Erik Wernersson, Luuk Harbers, Xiaoze Li-Wang, Katarina Gradin, Christiane Peuckert, Nicola Crosetto, and Magda Bienko. 2022a. 'FRET-FISH Probes Chromatin Compaction at Individual Genomic Loci in Single Cells'. *Nature Communications* 13 (1): 6680. <https://doi.org/10.1038/s41467-022-34183-y>.
- Mozos, Ana, Cristina Royo, Elena Hartmann, Daphne De Jong, Cristina Baró, Alexandra Valera, Kai Fu, et al. 2009. 'SOX11 Expression Is Highly Specific for Mantle Cell Lymphoma and Identifies the Cyclin D1-Negative Subtype'. *Haematologica* 94 (11): 1555–62. <https://doi.org/10.3324/haematol.2009.010264>.
- Muramatsu, M., K. Kinoshita, S. Fagarasan, S. Yamada, Y. Shinkai, and T. Honjo. 2000. 'Class Switch Recombination and Hypermutation Require Activation-Induced Cytidine Deaminase (AID), a Potential RNA Editing Enzyme'. *Cell* 102 (5): 553–63. [https://doi.org/10.1016/s0092-8674\(00\)00078-7](https://doi.org/10.1016/s0092-8674(00)00078-7).
- Mushimiyimana, Isidore, Henri Niskanen, Mustafa Beter, Johanna P. Laakkonen, Minna U. Kaikkonen, Seppo Ylä-Herttuala, and Nihay Laham-Karam. 2021. 'Characterization of a Functional Endothelial Super-Enhancer That Regulates ADAMTS18 and Angiogenesis'. *Nucleic Acids Research* 49 (14): 8078–96. <https://doi.org/10.1093/nar/gkab633>.
- Myklebust, June H., Joshua Brody, Holbrook E. Kohrt, Arne Kolstad, Debra K. Czerwinski, Sébastien Wälchli, Michael R. Green, et al. 2017. 'Distinct Patterns of B-Cell Receptor Signaling in Non-Hodgkin Lymphomas Identified by Single-Cell Profiling'. *Blood* 129 (6): 759–70. <https://doi.org/10.1182/blood-2016-05-718494>.
- Nadeu, Ferran, David Martin-Garcia, Guillem Clot, Ander Díaz-Navarro, Martí Duran-Ferrer, Alba Navarro, Roser Vilarrasa-Blasi, et al. 2020. 'Genomic and Epigenomic Insights into the Origin, Pathogenesis, and Clinical Behavior of Mantle Cell Lymphoma Subtypes'. *Blood* 136 (12): 1419–32. <https://doi.org/10.1182/blood.2020005289>.
- Nakayama, Robert T., John L. Pulice, Alfredo M. Valencia, Matthew J. McBride, Zachary M. McKenzie, Mark A. Gillespie, Wai Lim Ku, et al. 2017. 'SMARCB1 Is Required for Widespread BAF Complex-Mediated Activation of Enhancers and Bivalent Promoters'. *Nature Genetics* 49 (11):

- 1613–23. <https://doi.org/10.1038/ng.3958>.
- Navarro, Alba, Guillem Clot, Miriam Prieto, Cristina Royo, Maria Carmela Vegliante, Virginia Amador, Elena Hartmann, et al. 2013. 'microRNA Expression Profiles Identify Subtypes of Mantle Cell Lymphoma with Different Clinicobiological Characteristics'. *Clinical Cancer Research: An Official Journal of the American Association for Cancer Research* 19 (12): 3121–29. <https://doi.org/10.1158/1078-0432.CCR-12-3077>.
- Navarro, Alba, Guillem Clot, Cristina Royo, Pedro Jares, Anastasia Hadzidimitriou, Andreas Agathangelidis, Vasilis Bikos, et al. 2012. 'Molecular Subsets of Mantle Cell Lymphoma Defined by the IGHV Mutational Status and SOX11 Expression Have Distinct Biologic and Clinical Features'. *Cancer Research* 72 (20): 5307–16. <https://doi.org/10.1158/0008-5472.CAN-12-1615>.
- Nawaratne, Vindhya, Anya K. Sondhi, Omar Abdel-Wahab, and Justin Taylor. 2024. 'New Means and Challenges in the Targeting of BTK'. *Clinical Cancer Research* 30 (11): 2333–41. <https://doi.org/10.1158/1078-0432.CCR-23-0409>.
- Nera, Kalle-Pekka, Pekka Kohonen, Elli Narvi, Anne Peippo, Laura Mustonen, Perttu Terho, Kimmo Koskela, Jean-Marie Buerstedde, and Olli Lassila. 2006. 'Loss of Pax5 Promotes Plasma Cell Differentiation'. *Immunity* 24 (3): 283–93. <https://doi.org/10.1016/j.immuni.2006.02.003>.
- Newell, Rhys, Richard Pienaar, Brad Balderson, Michael Piper, Alexandra Essebier, and Mikael Bodén. 2021. 'ChIP-R: Assembling Reproducible Sets of ChIP-Seq and ATAC-Seq Peaks from Multiple Replicates'. *Genomics* 113 (4): 1855–66. <https://doi.org/10.1016/j.ygeno.2021.04.026>.
- Nierengarten, Mary Beth. 2023. 'FDA Grants Accelerated Approval of Mosunetuzumab for Relapsed, Refractory Follicular Lymphoma'. *Cancer* 129 (10): 1465–66. <https://doi.org/10.1002/cncr.34810>.
- Nodit, Laurentia, David W. Bahler, Samuel A. Jacobs, Joseph Locker, and Steven H. Swerdlow. 2003. 'Indolent Mantle Cell Lymphoma with Nodal Involvement and Mutated Immunoglobulin Heavy Chain Genes'. *Human Pathology* 34 (10): 1030–34. [https://doi.org/10.1053/s0046-8177\(03\)00410-6](https://doi.org/10.1053/s0046-8177(03)00410-6).
- Noel, Pawan, Shaimaa Hussein, Serina Ng, Corina E. Antal, Wei Lin, Emily Rodela, Priscilla Delgado, et al. 2020. 'Triptolide Targets Super-Enhancer Networks in Pancreatic Cancer Cells and Cancer-Associated Fibroblasts'. *Oncogenesis* 9 (11): 1–12. <https://doi.org/10.1038/s41389-020-00285-9>.
- Noma, Ken-ichi, Hugh P. Cam, Richard J. Maraia, and Shiv I. S. Grewal. 2006. 'A Role for TFIIIC Transcription Factor Complex in Genome Organization'. *Cell* 125 (5): 859–72. <https://doi.org/10.1016/j.cell.2006.04.028>.
- Noordermeer, Daan, Elzo de Wit, Petra Klous, Harmen van de Werken, Marieke Simonis, Melissa Lopez-Jones, Bert Eussen, Annelies de Klein, Robert H. Singer, and Wouter de Laat. 2011. 'Variegated Gene Expression Caused by Cell-Specific Long-Range DNA Interactions'.

- Nature Cell Biology* 13 (8): 944–51. <https://doi.org/10.1038/ncb2278>.
- Nordström, Lena, Sandra Sernbo, Patrik Eden, Kirsten Grønbaek, Arne Kolstad, Riikka Rätty, Marja-Liisa Karjalainen, et al. 2014. 'SOX11 and TP53 Add Prognostic Information to MIPI in a Homogenously Treated Cohort of Mantle Cell Lymphoma--a Nordic Lymphoma Group Study'. *British Journal of Haematology* 166 (1): 98–108. <https://doi.org/10.1111/bjh.12854>.
- Nott, Alexi, Inge R. Holtman, Nicole G. Coufal, Johannes C. M. Schlachetzki, Miao Yu, Rong Hu, Claudia Z. Han, et al. 2019. 'Brain Cell Type-Specific Enhancer-Promoter Interactome Maps and Disease-Risk Association'. *Science (New York, N.Y.)* 366 (6469): 1134–39. <https://doi.org/10.1126/science.aay0793>.
- Nygren, Lina, Stefanie Baumgartner Wennerholm, Monika Klimkowska, Birger Christensson, Eva Kimby, and Birgitta Sander. 2012. 'Prognostic Role of SOX11 in a Population-Based Cohort of Mantle Cell Lymphoma'. *Blood* 119 (18): 4215–23. <https://doi.org/10.1182/blood-2011-12-400580>.
- Nygren, Lina, Agata M. Wasik, Stefanie Baumgartner-Wennerholm, Åsa Jeppsson-Ahlberg, Monika Klimkowska, Patrik Andersson, Daren Buhrkuhl, et al. 2014. 'T-Cell Levels Are Prognostic in Mantle Cell Lymphoma'. *Clinical Cancer Research: An Official Journal of the American Association for Cancer Research* 20 (23): 6096–6104. <https://doi.org/10.1158/1078-0432.CCR-14-0889>.
- Obrador-Hevia, Antònia, Margalida Serra-Sitjar, José Rodríguez, Lamiae Belayachi, Leyre Bento, Marta García-Recio, Jose María Sánchez, Priam Villalonga, Antonio Gutiérrez, and Silvia Fernández de Mattos. 2016. 'Efficacy of the GemOx-R Regimen Leads to the Identification of Oxaliplatin as a Highly Effective Drug against Mantle Cell Lymphoma'. *British Journal of Haematology* 174 (6): 899–910. <https://doi.org/10.1111/bjh.14141>.
- O'Connor, Owen A., John Wright, Craig Moskowitz, Jamie Muzzy, Barbara MacGregor-Cortelli, Michael Stubblefield, David Straus, et al. 2005. 'Phase II Clinical Experience with the Novel Proteasome Inhibitor Bortezomib in Patients with Indolent Non-Hodgkin's Lymphoma and Mantle Cell Lymphoma'. *Journal of Clinical Oncology: Official Journal of the American Society of Clinical Oncology* 23 (4): 676–84. <https://doi.org/10.1200/JCO.2005.02.050>.
- Ogiwara, H., A. Ui, A. Otsuka, H. Satoh, I. Yokomi, S. Nakajima, A. Yasui, J. Yokota, and T. Kohno. 2011. 'Histone Acetylation by CBP and P300 at Double-Strand Break Sites Facilitates SWI/SNF Chromatin Remodeling and the Recruitment of Non-Homologous End Joining Factors'. *Oncogene* 30 (18): 2135–46. <https://doi.org/10.1038/onc.2010.592>.
- Ogura, Michinori, Kiyoshi Ando, Tatsuya Suzuki, Kenichi Ishizawa, Sung Yong Oh, Kuniaki Itoh, Kazuhito Yamamoto, et al. 2014. 'A Multicentre Phase II Study of Vorinostat in Patients with Relapsed or Refractory Indolent

- B-Cell Non-Hodgkin Lymphoma and Mantle Cell Lymphoma'. *British Journal of Haematology* 165 (6): 768–76.
<https://doi.org/10.1111/bjh.12819>.
- Ollion, Jean, François Loll, Julien Cochenec, Thomas Boudier, and Christophe Escudé. 2015. 'Proliferation-Dependent Positioning of Individual Centromeres in the Interphase Nucleus of Human Lymphoblastoid Cell Lines'. *Molecular Biology of the Cell* 26 (13): 2550–60.
<https://doi.org/10.1091/mbc.E14-05-1002>.
- Orchard, Jenny, Richard Garand, Zadi Davis, Gavin Babbage, Surinder Sahota, Estella Matutes, Daniel Catovsky, Peter W. Thomas, Hervé Avet-Loiseau, and David Oscier. 2003. 'A Subset of t(11;14) Lymphoma with Mantle Cell Features Displays Mutated IgVH Genes and Includes Patients with Good Prognosis, Nonnodal Disease'. *Blood* 101 (12): 4975–81.
<https://doi.org/10.1182/blood-2002-06-1864>.
- Ørom, Ulf Andersson, Thomas Derrien, Malte Beringer, Kiranmai Gumireddy, Alessandro Gardini, Giovanni Bussotti, Fan Lai, et al. 2010. 'Long Noncoding RNAs with Enhancer-like Function in Human Cells'. *Cell* 143 (1): 46–58. <https://doi.org/10.1016/j.cell.2010.09.001>.
- Ortiz, Angela B., Diego Garcia, Yolanda Vicente, Magda Palka, Carmen Bellas, and Paloma Martin. 2017. 'Prognostic Significance of Cyclin D1 Protein Expression and Gene Amplification in Invasive Breast Carcinoma'. *PLOS ONE* 12 (11): e0188068. <https://doi.org/10.1371/journal.pone.0188068>.
- Osborne, Cameron S., Lyubomira Chakalova, Karen E. Brown, David Carter, Alice Horton, Emmanuel Debrand, Beatriz Goyenechea, et al. 2004. 'Active Genes Dynamically Colocalize to Shared Sites of Ongoing Transcription'. *Nature Genetics* 36 (10): 1065–71.
<https://doi.org/10.1038/ng1423>.
- Osborne, Cameron S., Lyubomira Chakalova, Jennifer A. Mitchell, Alice Horton, Andrew L. Wood, Daniel J. Bolland, Anne E. Corcoran, and Peter Fraser. 2007. 'Myc Dynamically and Preferentially Relocates to a Transcription Factory Occupied by Igh'. *PLOS Biology* 5 (8): e192.
<https://doi.org/10.1371/journal.pbio.0050192>.
- Oyama, T., K. Kashiwabara, K. Yoshimoto, A. Arnold, and F. Koerner. 1998. 'Frequent Overexpression of the Cyclin D1 Oncogene in Invasive Lobular Carcinoma of the Breast'. *Cancer Research* 58 (13): 2876–80.
- Ozkal, Sermin, Jennifer C. Paterson, Sara Tedoldi, Martin-Leo Hansmann, Aydanur Kargi, Sanjiv Manek, David Y. Mason, and Teresa Marafioti. 2009. 'Focal Adhesion Kinase (FAK) Expression in Normal and Neoplastic Lymphoid Tissues'. *Pathology, Research and Practice* 205 (11): 781–88.
<https://doi.org/10.1016/j.prp.2009.07.002>.
- Palanichamy, Jayanth Kumar, Tiffany M. Tran, Jennifer K. King, Sol Katzman, Alexander J. Ritter, Gunjan Sharma, Christine Tso, et al. 2023. 'Distinct Oncogenic Phenotypes in Hematopoietic Specific Deletions of Trp53'. *Scientific Reports* 13 (1): 7490.

- <https://doi.org/10.1038/s41598-023-33949-8>.
- Palomero, J., M. C. Vegliante, A. Eguileor, M. L. Rodríguez, P. Balsas, D. Martínez, E. Campo, and V. Amador. 2016. 'SOX11 Defines Two Different Subtypes of Mantle Cell Lymphoma through Transcriptional Regulation of BCL6'. *Leukemia* 30 (7): 1596–99. <https://doi.org/10.1038/leu.2015.355>.
- Palomero, Jara, Maria Carmela Vegliante, Marta Leonor Rodríguez, Álvaro Eguileor, Giancarlo Castellano, Ester Planas-Rigol, Pedro Jares, et al. 2014. 'SOX11 Promotes Tumor Angiogenesis through Transcriptional Regulation of PDGFA in Mantle Cell Lymphoma'. *Blood* 124 (14): 2235–47. <https://doi.org/10.1182/blood-2014-04-569566>.
- Paoluzzi, Luca, Luigi Scotto, Enrica Marchi, Jasmine Zain, Venkatraman E. Seshan, and Owen A. O'Connor. 2010. 'Romidepsin and Belinostat Synergize the Antineoplastic Effect of Bortezomib in Mantle Cell Lymphoma'. *Clinical Cancer Research: An Official Journal of the American Association for Cancer Research* 16 (2): 554–65. <https://doi.org/10.1158/1078-0432.CCR-09-1937>.
- Parada, Luis A., Philip G. McQueen, Peter J. Munson, and Tom Misteli. 2002. 'Conservation of Relative Chromosome Positioning in Normal and Cancer Cells'. *Current Biology: CB* 12 (19): 1692–97. [https://doi.org/10.1016/s0960-9822\(02\)01166-1](https://doi.org/10.1016/s0960-9822(02)01166-1).
- Parker, Stephen C. J., Michael L. Stitzel, D. Leland Taylor, Jose Miguel Orozco, Michael R. Erdos, Jennifer A. Akiyama, Kelly Lammerts van Bueren, et al. 2013. 'Chromatin Stretch Enhancer States Drive Cell-Specific Gene Regulation and Harbor Human Disease Risk Variants'. *Proceedings of the National Academy of Sciences of the United States of America* 110 (44): 17921–26. <https://doi.org/10.1073/pnas.1317023110>.
- Patel, Harshil, Jose Espinosa-Carrasco, Björn Langer, Phil Ewels, nf-core bot, Maxime U. Garcia, Robert Syme, et al. 2023. 'Nf-Core/Atacseq: [2.1.2] - 2022-08-07'. Zenodo. <https://doi.org/10.5281/zenodo.8222875>.
- Pérez-Galán, Patricia, Gaël Roué, Neus Villamor, Emili Montserrat, Elias Campo, and Dolores Colomer. 2006. 'The Proteasome Inhibitor Bortezomib Induces Apoptosis in Mantle-Cell Lymphoma through Generation of ROS and Noxa Activation Independent of P53 Status'. *Blood* 107 (1): 257–64. <https://doi.org/10.1182/blood-2005-05-2091>.
- Petrakis, Georgios, Luis Veloza, Guillem Clot, Eva Gine, Blanca Gonzalez-Farre, Alba Navarro, Silvia Bea, et al. 2019. 'Increased Tumour Angiogenesis in SOX11-Positive Mantle Cell Lymphoma'. *Histopathology* 75 (5): 704–14. <https://doi.org/10.1111/his.13935>.
- Pham, Lan V., Archito T. Tamayo, Linda C. Yoshimura, Piao Lo, and Richard J. Ford. 2003. 'Inhibition of Constitutive NF-Kappa B Activation in Mantle Cell Lymphoma B Cells Leads to Induction of Cell Cycle Arrest and Apoptosis'. *Journal of Immunology (Baltimore, Md.: 1950)* 171 (1): 88–95. <https://doi.org/10.4049/jimmunol.171.1.88>.

- Pham, Lan V., Muychi T. Vang, Archito T. Tamayo, Gary Lu, Pramoda Challagundla, Jeffrey L. Jorgensen, Alex A. Rollo, et al. 2015. 'Involvement of Tumor-Associated Macrophage Activation in Vitro during Development of a Novel Mantle Cell Lymphoma Cell Line, PF-1, Derived from a Typical Patient with Relapsed Disease'. *Leukemia & Lymphoma* 56 (1): 186–93. <https://doi.org/10.3109/10428194.2014.901511>.
- Pighi, Chiara, Stefano Barbi, Anna Bertolaso, and Alberto Zamò. 2013. 'Mantle Cell Lymphoma Cell Lines Show No Evident Immunoglobulin Heavy Chain Stereotypy but Frequent Light Chain Stereotypy'. *Leukemia & Lymphoma* 54 (8): 1747–55. <https://doi.org/10.3109/10428194.2012.758843>.
- Pighi, Chiara, Ting-Lei Gu, Irene Dalai, Stefano Barbi, Claudia Parolini, Anna Bertolaso, Serena Pedron, et al. 2011. 'Phospho-Proteomic Analysis of Mantle Cell Lymphoma Cells Suggests a pro-Survival Role of B-Cell Receptor Signaling'. *Cellular Oncology (Dordrecht)* 34 (2): 141–53. <https://doi.org/10.1007/s13402-011-0019-7>.
- Pinyol, Magda, Silvia Bea, Laura Plà, Vincent Ribrag, Jacques Bosq, Andreas Rosenwald, Elias Campo, and Pedro Jares. 2007. 'Inactivation of RB1 in Mantle-Cell Lymphoma Detected by Nonsense-Mediated mRNA Decay Pathway Inhibition and Microarray Analysis'. *Blood* 109 (12): 5422–29. <https://doi.org/10.1182/blood-2006-11-057208>.
- Pope, Benjamin D., Tyrone Ryba, Vishnu Dileep, Feng Yue, Weisheng Wu, Olger Denas, Daniel L. Vera, et al. 2014. 'Topologically Associating Domains Are Stable Units of Replication-Timing Regulation'. *Nature* 515 (7527): 402–5. <https://doi.org/10.1038/nature13986>.
- Prager, Isabel, and Carsten Watzl. 2019. 'Mechanisms of Natural Killer Cell-Mediated Cellular Cytotoxicity'. *Journal of Leukocyte Biology* 105 (6): 1319–29. <https://doi.org/10.1002/JLB.MR0718-269R>.
- Pugongchai, Apiwat, Andrey Bychkov, and Pichet Sampatanukul. 2017. 'Promoter Hypermethylation of SOX11 Correlates with Adverse Clinicopathological Features of Human Prostate Cancer'. *International Journal of Experimental Pathology* 98 (6): 341–46. <https://doi.org/10.1111/iep.12257>.
- Qi, Wenjing, Ruoxi Wang, Hongyu Chen, Xiaolin Wang, Ting Xiao, Istvan Boldogh, Xueqing Ba, Liping Han, and Xianlu Zeng. 2015. 'BRG1 Promotes the Repair of DNA Double-Strand Breaks by Facilitating the Replacement of RPA with RAD51'. *Journal of Cell Science* 128 (2): 317–30. <https://doi.org/10.1242/jcs.159103>.
- Queirós, Ana C., Renée Beekman, Roser Vilarrasa-Blasi, Martí Duran-Ferrer, Guillem Clot, Angelika Merkel, Emanuele Raineri, et al. 2016. 'Decoding the DNA Methylome of Mantle Cell Lymphoma in the Light of the Entire B Cell Lineage'. *Cancer Cell* 30 (5): 806–21. <https://doi.org/10.1016/j.ccell.2016.09.014>.
- Quintanilla-Martinez, Leticia, Theresa Davies-Hill, Falko Fend, Julia

- Calzada-Wack, Lynn Sorbara, Elias Campo, Elaine S. Jaffe, and Mark Raffeld. 2003. 'Sequestration of p27Kip1 Protein by Cyclin D1 in Typical and Blastic Variants of Mantle Cell Lymphoma (MCL): Implications for Pathogenesis'. *Blood* 101 (8): 3181–87.
<https://doi.org/10.1182/blood-2002-01-0263>.
- Rao, Suhas S. P., Su-Chen Huang, Brian Glenn St Hilaire, Jesse M. Engreitz, Elizabeth M. Perez, Kyong-Rim Kieffer-Kwon, Adrian L. Sanborn, et al. 2017. 'Cohesin Loss Eliminates All Loop Domains'. *Cell* 171 (2): 305–320.e24. <https://doi.org/10.1016/j.cell.2017.09.026>.
- Rao, Suhas S. P., Miriam H. Huntley, Neva C. Durand, Elena K. Stamenova, Ivan D. Bochkov, James T. Robinson, Adrian L. Sanborn, et al. 2014. 'A 3D Map of the Human Genome at Kilobase Resolution Reveals Principles of Chromatin Looping'. *Cell* 159 (7): 1665–80.
<https://doi.org/10.1016/j.cell.2014.11.021>.
- Razin, S. V., A. A. Gavrillov, A. Pichugin, M. Lipinski, O. V. Iarovaia, and Yegor S. Vassetzky. 2011. 'Transcription Factories in the Context of the Nuclear and Genome Organization'. *Nucleic Acids Research* 39 (21): 9085–92.
<https://doi.org/10.1093/nar/gkr683>.
- Reaper, Philip M., Matthew R. Griffiths, Joanna M. Long, Jean-Damien Charrier, Somhairle Maccormick, Peter A. Charlton, Julian M. C. Golec, and John R. Pollard. 2011. 'Selective Killing of ATM- or P53-Deficient Cancer Cells through Inhibition of ATR'. *Nature Chemical Biology* 7 (7): 428–30.
<https://doi.org/10.1038/nchembio.573>.
- Reif, Karin, Eric H. Eklund, Lars Ohl, Hideki Nakano, Martin Lipp, Reinhold Förster, and Jason G. Cyster. 2002. 'Balanced Responsiveness to Chemoattractants from Adjacent Zones Determines B-Cell Position'. *Nature* 416 (6876): 94–99. <https://doi.org/10.1038/416094a>.
- Renner, Christoph, Pier Luigi Zinzani, Rémy Gressin, Dirk Klingbiel, Pierre-Yves Dietrich, Felicitas Hitz, Mario Bargetzi, et al. 2012. 'A Multicenter Phase II Trial (SAKK 36/06) of Single-Agent Everolimus (RAD001) in Patients with Relapsed or Refractory Mantle Cell Lymphoma'. *Haematologica* 97 (7): 1085–91. <https://doi.org/10.3324/haematol.2011.053173>.
- Ribera-Cortada, Inmaculada, Daniel Martinez, Virginia Amador, Cristina Royo, Alba Navarro, Silvia Beà, Eva Gine, et al. 2015. 'Plasma Cell and Terminal B-Cell Differentiation in Mantle Cell Lymphoma Mainly Occur in the SOX11-Negative Subtype'. *Modern Pathology* 28 (11): 1435–47.
<https://doi.org/10.1038/modpathol.2015.99>.
- Rinaldi, Andrea, Ivo Kwee, Monica Taborelli, Cristina Largo, Silvia Uccella, Vittoria Martin, Giulia Poretti, et al. 2006. 'Genomic and Expression Profiling Identifies the B-Cell Associated Tyrosine Kinase Syk as a Possible Therapeutic Target in Mantle Cell Lymphoma'. *British Journal of Haematology* 132 (3): 303–16.
<https://doi.org/10.1111/j.1365-2141.2005.05883.x>.
- Rizzatti, Edgar Gil, Helena Mora-Jensen, Marc Andrée Weniger, Federica

- Gibellini, Elinor Lee, Masanori Daibata, Raymond Lai, and Adrian Wiestner. 2008. 'Noxa Mediates Bortezomib Induced Apoptosis in Both Sensitive and Intrinsically Resistant Mantle Cell Lymphoma Cells and This Effect Is Independent of Constitutive Activity of the AKT and NF-kappaB Pathways'. *Leukemia & Lymphoma* 49 (4): 798–808. <https://doi.org/10.1080/10428190801910912>.
- Robak, Tadeusz, Jie Jin, Halyna Pylypenko, Gregor Verhoef, Noppadol Siritanaratkul, Johannes Drach, Markus Raderer, et al. 2018. 'Frontline Bortezomib, Rituximab, Cyclophosphamide, Doxorubicin, and Prednisone (VR-CAP) versus Rituximab, Cyclophosphamide, Doxorubicin, Vincristine, and Prednisone (R-CHOP) in Transplantation-Ineligible Patients with Newly Diagnosed Mantle Cell Lymphoma: Final Overall Survival Results of a Randomised, Open-Label, Phase 3 Study'. *The Lancet. Oncology* 19 (11): 1449–58. [https://doi.org/10.1016/S1470-2045\(18\)30685-5](https://doi.org/10.1016/S1470-2045(18)30685-5).
- Rodrigues, Joana M., May Hassan, Catja Freiburghaus, Christian W. Eskelund, Christian Geisler, Riikka Rätty, Arne Kolstad, et al. 2020. 'P53 Is Associated with High-risk and Pinpoints TP53 Missense Mutations in Mantle Cell Lymphoma'. *British Journal of Haematology* 191 (5): 796. <https://doi.org/10.1111/bjh.17023>.
- Rodrigues, Joana M., Peter Hollander, Lina Schmidt, Eirinaios Gkika, Masoud Razmara, Darshan Kumar, Christian Geisler, et al. 2020. 'MYC Protein Is a High-Risk Factor in Mantle Cell Lymphoma and Identifies Cases beyond Morphology, Proliferation and TP53/P53 – a Nordic Lymphoma Group Study'. *Haematologica*. <https://doi.org/10.3324/haematol.2023.283352>.
- Rodrigues, Joana M., Anna Nikkarinen, Peter Hollander, Caroline E. Weibull, Riikka Rätty, Arne Kolstad, Rose-Marie Amini, et al. 2021. 'Infiltration of CD163-, PD-L1- and FoxP3-Positive Cells Adversely Affects Outcome in Patients with Mantle Cell Lymphoma Independent of Established Risk Factors'. *British Journal of Haematology* 193 (3): 520–31. <https://doi.org/10.1111/bjh.17366>.
- Rosenthal, Allison C., Javier L. Munoz, and J. C. Villasboas. 2023. 'Clinical Advances in Epigenetic Therapies for Lymphoma'. *Clinical Epigenetics* 15 (1): 39. <https://doi.org/10.1186/s13148-023-01452-6>.
- Rosenwald, Andreas, George Wright, Adrian Wiestner, Wing C Chan, Joseph M Connors, Elias Campo, Randy D Gascoyne, et al. 2003. 'The Proliferation Gene Expression Signature Is a Quantitative Integrator of Oncogenic Events That Predicts Survival in Mantle Cell Lymphoma'. *Cancer Cell* 3 (2): 185–97. [https://doi.org/10.1016/S1535-6108\(03\)00028-X](https://doi.org/10.1016/S1535-6108(03)00028-X).
- Rossjohn, Jamie, Daniel G. Pellicci, Onisha Patel, Laurent Gapin, and Dale I. Godfrey. 2012. 'Recognition of CD1d-Restricted Antigens by Natural Killer T Cells'. *Nature Reviews. Immunology* 12 (12): 845–57. <https://doi.org/10.1038/nri3328>.

- Rowley, R. B., A. L. Burkhardt, H. G. Chao, G. R. Matsueda, and J. B. Bolen. 1995. 'Syk Protein-Tyrosine Kinase Is Regulated by Tyrosine-Phosphorylated Ig Alpha/Ig Beta Immunoreceptor Tyrosine Activation Motif Binding and Autophosphorylation'. *The Journal of Biological Chemistry* 270 (19): 11590–94. <https://doi.org/10.1074/jbc.270.19.11590>.
- Royo, C., A. Navarro, G. Clot, I. Salaverria, E. Giné, P. Jares, D. Colomer, et al. 2012. 'Non-Nodal Type of Mantle Cell Lymphoma Is a Specific Biological and Clinical Subgroup of the Disease'. *Leukemia* 26 (8): 1895–98. <https://doi.org/10.1038/leu.2012.72>.
- Ruan, Jia, Peter Martin, Paul Christos, Leandro Cerchietti, Wayne Tam, Bijal Shah, Stephen J. Schuster, et al. 2018. 'Five-Year Follow-up of Lenalidomide plus Rituximab as Initial Treatment of Mantle Cell Lymphoma'. *Blood* 132 (19): 2016–25. <https://doi.org/10.1182/blood-2018-07-859769>.
- Rudelius, Martina, Stefania Pittaluga, Satoshi Nishizuka, Trinh H.-T. Pham, Falko Fend, Elaine S. Jaffe, Leticia Quintanilla-Martinez, and Mark Raffeld. 2006. 'Constitutive Activation of Akt Contributes to the Pathogenesis and Survival of Mantle Cell Lymphoma'. *Blood* 108 (5): 1668–76. <https://doi.org/10.1182/blood-2006-04-015586>.
- Rudelius, Martina, Mathias Tillmann Rosenfeldt, Ellen Leich, Hilka Rauert-Wunderlich, Antonio Giovanni Solimando, Andreas Beilhack, German Ott, and Andreas Rosenwald. 2018. 'Inhibition of Focal Adhesion Kinase Overcomes Resistance of Mantle Cell Lymphoma to Ibrutinib in the Bone Marrow Microenvironment'. *Haematologica* 103 (1): 116–25. <https://doi.org/10.3324/haematol.2017.177162>.
- Ryu, Jayoung, Hyunwoong Kim, Dongchan Yang, Andrew J. Lee, and Inkyung Jung. 2019. 'A New Class of Constitutively Active Super-Enhancers Is Associated with Fast Recovery of 3D Chromatin Loops'. *BMC Bioinformatics* 20 (3): 127. <https://doi.org/10.1186/s12859-019-2646-3>.
- Saba, Nakhle S., Delong Liu, Sarah E. M. Herman, Chingiz Underbayev, Xin Tian, David Behrend, Marc A. Weniger, et al. 2016. 'Pathogenic Role of B-Cell Receptor Signaling and Canonical NF- κ B Activation in Mantle Cell Lymphoma'. *Blood* 128 (1): 82–92. <https://doi.org/10.1182/blood-2015-11-681460>.
- Sabari, Benjamin R., Alessandra Dall'Agnese, Ann Boija, Isaac A. Klein, Eliot L. Coffey, Krishna Shrinivas, Brian J. Abraham, et al. 2018. 'Coactivator Condensation at Super-Enhancers Links Phase Separation and Gene Control'. *Science (New York, N.Y.)* 361 (6400): eaar3958. <https://doi.org/10.1126/science.aar3958>.
- Sadeghi, Laia, Gustav Arvidsson, Magali Merrien, Agata M. Wasik, André Görgens, C.I. Edvard Smith, Birgitta Sander, and Anthony P. Wright. 2020. 'Differential B-Cell Receptor Signaling Requirement for Adhesion of Mantle Cell Lymphoma Cells to Stromal Cells'. *Cancers* 12 (5): 1143. <https://doi.org/10.3390/cancers12051143>.

- Sadeghi, Laia, and Anthony P. H. Wright. 2023. 'GSK-J4 Inhibition of KDM6B Histone Demethylase Blocks Adhesion of Mantle Cell Lymphoma Cells to Stromal Cells by Modulating NF- κ B Signaling'. *Cells* 12 (15): 2010. <https://doi.org/10.3390/cells12152010>.
- Sadoni, N., S. Langer, C. Fauth, G. Bernardi, T. Cremer, B. M. Turner, and D. Zink. 1999. 'Nuclear Organization of Mammalian Genomes. Polar Chromosome Territories Build up Functionally Distinct Higher Order Compartments'. *The Journal of Cell Biology* 146 (6): 1211–26. <https://doi.org/10.1083/jcb.146.6.1211>.
- Saijo, Kaoru, Christian Schmedt, I.-Hsin Su, Hajime Karasuyama, Clifford A. Lowell, Michael Reth, Takahiro Adachi, Alina Patke, Angela Santana, and Alexander Tarakhovsky. 2003. 'Essential Role of Src-Family Protein Tyrosine Kinases in NF-kappaB Activation during B Cell Development'. *Nature Immunology* 4 (3): 274–79. <https://doi.org/10.1038/ni893>.
- Salaverria, Itziar, Andreas Zettl, Sílvia Beà, Victor Moreno, Joan Valls, Elena Hartmann, German Ott, et al. 2007. 'Specific Secondary Genetic Alterations in Mantle Cell Lymphoma Provide Prognostic Information Independent of the Gene Expression-Based Proliferation Signature'. *Journal of Clinical Oncology: Official Journal of the American Society of Clinical Oncology* 25 (10): 1216–22. <https://doi.org/10.1200/JCO.2006.08.4251>.
- Sarkozy, Clémentine, Christine Terré, Fabrice Jardin, Isabelle Radford, Catherine Roche-Lestienne, Dominique Penther, Christian Bastard, et al. 2014. 'Complex Karyotype in Mantle Cell Lymphoma Is a Strong Prognostic Factor for the Time to Treatment and Overall Survival, Independent of the MCL International Prognostic Index'. *Genes, Chromosomes & Cancer* 53 (1): 106–16. <https://doi.org/10.1002/gcc.22123>.
- Schaffner, Claudia, Irina Idler, Stephan Stilgenbauer, Hartmut Döhner, and Peter Lichter. 2000. 'Mantle Cell Lymphoma Is Characterized by Inactivation of the ATM Gene'. *Proceedings of the National Academy of Sciences of the United States of America* 97 (6): 2773–78.
- Scharer, Christopher D., Benjamin G. Barwick, Muyao Guo, Alexander P. R. Bally, and Jeremy M. Boss. 2018. 'Plasma Cell Differentiation Is Controlled by Multiple Cell Division-Coupled Epigenetic Programs'. *Nature Communications* 9 (1): 1698. <https://doi.org/10.1038/s41467-018-04125-8>.
- Schede, Halima H., Pradeep Natarajan, Arup K. Chakraborty, and Krishna Shrinivas. 2023. 'A Model for Organization and Regulation of Nuclear Condensates by Gene Activity'. *Nature Communications* 14 (1): 4152. <https://doi.org/10.1038/s41467-023-39878-4>.
- Scheubeck, Gabriel, Linmiao Jiang, Olivier Hermine, Hanneke C. Kluin-Nelemans, Christian Schmidt, Michael Unterhalt, Andreas Rosenwald, et al. 2023. 'Clinical Outcome of Mantle Cell Lymphoma

- Patients with High-Risk Disease (High-Risk MIPI-c or High P53 Expression)'. *Leukemia* 37 (9): 1887–94.
<https://doi.org/10.1038/s41375-023-01977-y>.
- Schoenfelder, Stefan, Tom Sexton, Lyubomira Chakalova, Nathan F. Cope, Alice Horton, Simon Andrews, Sreenivasulu Kurukuti, et al. 2010. 'Preferential Associations between Co-Regulated Genes Reveal a Transcriptional Interactome in Erythroid Cells'. *Nature Genetics* 42 (1): 53–61. <https://doi.org/10.1038/ng.496>.
- Schrader, Carsten, Peter Meusers, Günter Brittinger, Dirk Janssen, Afshin Teymoortash, Jens U. Siebmann, Reza Parwaresch, and Markus Tiemann. 2006. 'Growth Pattern and Distribution of Follicular Dendritic Cells in Mantle Cell Lymphoma: A Clinicopathological Study of 96 Patients'. *Virchows Archiv: An International Journal of Pathology* 448 (2): 151–59. <https://doi.org/10.1007/s00428-005-0049-5>.
- Schraders, Margit, Rolph Pfundt, Huub M. P. Straatman, Irene M. Janssen, Ad Geurts van Kessel, Eric F. P. M. Schoenmakers, Johan H. J. M. van Krieken, and Patricia J. T. A. Groenen. 2005. 'Novel Chromosomal Imbalances in Mantle Cell Lymphoma Detected by Genome-Wide Array-Based Comparative Genomic Hybridization'. *Blood* 105 (4): 1686–93. <https://doi.org/10.1182/blood-2004-07-2730>.
- Seaton, Gillian, Hannah Smith, Andrea Brancale, Andrew D. Westwell, and Richard Clarkson. 2024. 'Multifaceted Roles for BCL3 in Cancer: A Proto-Oncogene Comes of Age'. *Molecular Cancer* 23 (1): 7. <https://doi.org/10.1186/s12943-023-01922-8>.
- Sehgal, Nitasha, Andrew J. Fritz, Jaromira Vecerova, Hu Ding, Zihe Chen, Branislav Stojkovic, Sambit Bhattacharya, Jinhui Xu, and Ronald Berezney. 2016. 'Large-Scale Probabilistic 3D Organization of Human Chromosome Territories'. *Human Molecular Genetics* 25 (3): 419–36. <https://doi.org/10.1093/hmg/ddv479>.
- Sekihara, Kazumasa, Kaori Saitoh, Lina Han, Stefan Ciurea, Shinichi Yamamoto, Mika Kikkawa, Saiko Kazuno, et al. 2017. 'Targeting Mantle Cell Lymphoma Metabolism and Survival through Simultaneous Blockade of mTOR and Nuclear Transporter Exportin-1'. *Oncotarget* 8 (21): 34552–64. <https://doi.org/10.18632/oncotarget.16602>.
- Servant, Nicolas, nf-core bot, Phil Ewels, Maxime U. Garcia, Adam Talbot, Alexander Peltzer, Edmund Miller, et al. 2023. 'Nf-Core/Hic: Nf-Core/Hic v2.1.0'. Zenodo. <https://doi.org/10.5281/zenodo.7994878>.
- Shen, Wei, Linda J. Bendall, David J. Gottlieb, and Kenneth F. Bradstock. 2001. 'The Chemokine Receptor CXCR4 Enhances Integrin-Mediated in Vitro Adhesion and Facilitates Engraftment of Leukemic Precursor-B Cells in the Bone Marrow'. *Experimental Hematology* 29 (12): 1439–47. [https://doi.org/10.1016/S0301-472X\(01\)00741-X](https://doi.org/10.1016/S0301-472X(01)00741-X).
- Shen, Y., C. S. Park, K. Suppipat, T.-A. Mistretta, M. Puppi, T. M. Horton, K. Rabin, N. S. Gray, J. P. P. Meijerink, and H. D. Lacorazza. 2017.

- 'Inactivation of KLF4 Promotes T-Cell Acute Lymphoblastic Leukemia and Activates the MAP2K7 Pathway'. *Leukemia* 31 (6): 1314–24.
<https://doi.org/10.1038/leu.2016.339>.
- Shevra, CR, A Ghosh, and M Kumar. 2015. 'Cyclin D1 and Ki-67 Expression in Normal, Hyperplastic and Neoplastic Endometrium'. *Journal of Postgraduate Medicine* 61 (1): 15–20.
<https://doi.org/10.4103/0022-3859.147025>.
- Shi, Conglin, Liuting Chen, Hui Pi, Henglu Cui, Chenyang Fan, Fangzheng Tan, Xuanhao Qu, et al. 2023. 'Identifying a Locus in Super-Enhancer and Its Resident NFE2L1/MAFG as Transcriptional Factors That Drive PD-L1 Expression and Immune Evasion'. *Oncogenesis* 12 (1): 56.
<https://doi.org/10.1038/s41389-023-00500-3>.
- Shi, Yijiang, Huajun Yan, Patrick Frost, Joseph Gera, and Alan Lichtenstein. 2005. 'Mammalian Target of Rapamycin Inhibitors Activate the AKT Kinase in Multiple Myeloma Cells by Up-Regulating the Insulin-like Growth Factor Receptor/Insulin Receptor Substrate-1/Phosphatidylinositol 3-Kinase Cascade'. *Molecular Cancer Therapeutics* 4 (10): 1533–40.
<https://doi.org/10.1158/1535-7163.MCT-05-0068>.
- Shin, Dong-Yeop, Seok Jin Kim, Dok Hyun Yoon, Yong Park, Jee Hyun Kong, Jeong-A. Kim, Byung-Su Kim, et al. 2016. 'Results of a Phase II Study of Vorinostat in Combination with Intravenous Fludarabine, Mitoxantrone, and Dexamethasone in Patients with Relapsed or Refractory Mantle Cell Lymphoma: An Interim Analysis'. *Cancer Chemotherapy and Pharmacology* 77 (4): 865–73.
<https://doi.org/10.1007/s00280-016-3005-y>.
- Shirley, Matt. 2023. 'Glofitamab: First Approval'. *Drugs* 83 (10): 935–41.
<https://doi.org/10.1007/s40265-023-01894-5>.
- Shoker, B. S., C. Jarvis, M. P. Davies, M. Iqbal, D. R. Sibson, and J. P. Sloane. 2001. 'Immunodetectable Cyclin D(1)Is Associated with Oestrogen Receptor but Not Ki67 in Normal, Cancerous and Precancerous Breast Lesions'. *British Journal of Cancer* 84 (8): 1064–69.
<https://doi.org/10.1054/bjoc.2001.1705>.
- Siegmund, Kimberly D., Paul Marjoram, Yen-Jung Woo, Simon Tavaré, and Darryl Shibata. 2009. 'Inferring Clonal Expansion and Cancer Stem Cell Dynamics from DNA Methylation Patterns in Colorectal Cancers'. *Proceedings of the National Academy of Sciences of the United States of America* 106 (12): 4828–33. <https://doi.org/10.1073/pnas.0810276106>.
- Silkenstedt, Elisabeth, and Martin Dreyling. 2023. 'Mantle Cell Lymphoma—Update on Molecular Biology, Prognostication and Treatment Approaches'. *Hematological Oncology* 41 (S1): 36–42.
<https://doi.org/10.1002/hon.3149>.
- Simonis, Marieke, Petra Klous, Erik Splinter, Yuri Moshkin, Rob Willemsen, Elzo de Wit, Bas van Steensel, and Wouter de Laat. 2006. 'Nuclear

- Organization of Active and Inactive Chromatin Domains Uncovered by Chromosome Conformation Capture-on-Chip (4C). *Nature Genetics* 38 (11): 1348–54. <https://doi.org/10.1038/ng1896>.
- Sklyar, Ilya, Olga V. Iarovaia, Alexey A. Gavrillov, Andrey Pichugin, Diego Germini, Tatiana Tsfasman, Gersende Caron, et al. 2016. 'Distinct Patterns of Colocalization of the CCND1 and CMYC Genes With Their Potential Translocation Partner IGH at Successive Stages of B-Cell Differentiation'. *Journal of Cellular Biochemistry* 117 (7): 1506–10. <https://doi.org/10.1002/jcb.25516>.
- Skorupan, Nebojsa, Mehwish I. Ahmad, Seth M. Steinberg, Jane B. Trepel, Derek Cridebring, Haiyong Han, Daniel D. Von Hoff, and Christine Alewine. 2022. 'A Phase II Trial of the Super-Enhancer Inhibitor Minnelide™ in Advanced Refractory Adenosquamous Carcinoma of the Pancreas'. *Future Oncology (London, England)* 18 (20): 2475–81. <https://doi.org/10.2217/fon-2021-1609>.
- Sloan, Shelby L., Fiona Brown, Mackenzie Long, Christoph Weigel, Shirsha Koirala, Ji-Hyun Chung, Betsy Pray, et al. 2023. 'PRMT5 Supports Multiple Oncogenic Pathways in Mantle Cell Lymphoma'. *Blood* 142 (10): 887–902. <https://doi.org/10.1182/blood.2022019419>.
- Sonbol, Mohamad B., Matthew J. Maurer, Mary J. Stenson, Cristine Allmer, Betsy R. LaPlant, George J. Weiner, William R. Macon, James R. Cerhan, Thomas E. Witzig, and Mamta Gupta. 2014. 'Elevated Soluble IL-2R α , IL-8, and MIP-1 β Levels Are Associated with Inferior Outcome and Are Independent of MIPI Score in Patients with Mantle Cell Lymphoma'. *American Journal of Hematology* 89 (12): E223-227. <https://doi.org/10.1002/ajh.23838>.
- Song, Kai, Brett H. Herzog, Minjia Sheng, Jianxin Fu, J. Michael McDaniel, Jia Ruan, and Lijun Xia. 2013. 'Lenalidomide Inhibits Lymphangiogenesis in Preclinical Models of Mantle Cell Lymphoma'. *Cancer Research* 73 (24): 7254–64. <https://doi.org/10.1158/0008-5472.CAN-13-0750>.
- Spaargaren, Marcel, Esther A. Beuling, Mette L. Rurup, Helen P. Meijer, Melanie D. Klok, Sabine Middendorp, Rudolf W. Hendriks, and Steven T. Pals. 2003. 'The B Cell Antigen Receptor Controls Integrin Activity through Btk and PLC γ 2'. *The Journal of Experimental Medicine* 198 (10): 1539–50. <https://doi.org/10.1084/jem.20011866>.
- Speiser, Daniel E., Obinna Chijioke, Karin Schaeuble, and Christian Münz. 2023. 'CD4+ T Cells in Cancer'. *Nature Cancer* 4 (3): 317–29. <https://doi.org/10.1038/s43018-023-00521-2>.
- Spilianakis, Charalampos G., Maria D. Lalioti, Terrence Town, Gap Ryol Lee, and Richard A. Flavell. 2005. 'Interchromosomal Associations between Alternatively Expressed Loci'. *Nature* 435 (7042): 637–45. <https://doi.org/10.1038/nature03574>.
- Spurgeon, Stephen E., Kamal Sharma, David F. Claxton, Christopher Ehmann, Jeffrey Pu, Sara Shimko, August Stewart, et al. 2019. 'Phase 1-2 Study of

- Vorinostat (SAHA), Cladribine and Rituximab (SCR) in Relapsed B-Cell Non-Hodgkin Lymphoma and Previously Untreated Mantle Cell Lymphoma'. *British Journal of Haematology* 186 (6): 845–54. <https://doi.org/10.1111/bjh.16008>.
- Starczynski, Jane, William Simmons, Joanne R. Flavell, Phillip J. Byrd, Grant S. Stewart, Harjit S. Kullar, Alix Groom, et al. 2003. 'Variations in ATM Protein Expression During Normal Lymphoid Differentiation and Among B-Cell-Derived Neoplasias'. *The American Journal of Pathology* 163 (2): 423–32.
- Stark, Rory, and Gord Brown. n.d. 'DiffBind: Differential Binding Analysis of ChIP-Seq Peak Data', 75.
- Streich, Lukas, Madina Sukhanova, Xinyan Lu, Yi-Hua Chen, Girish Venkataraman, Stephanie Mathews, Shanxiang Zhang, et al. 2020. 'Aggressive Morphologic Variants of Mantle Cell Lymphoma Characterized with High Genomic Instability Showing Frequent Chromothripsis, CDKN2A/B Loss, and TP53 Mutations: A Multi-Institutional Study'. *Genes, Chromosomes and Cancer* 59 (8): 484–94. <https://doi.org/10.1002/gcc.22849>.
- Su, Jun-Han, Pu Zheng, Seon S. Kinrot, Bogdan Bintu, and Xiaowei Zhuang. 2020a. 'Genome-Scale Imaging of the 3D Organization and Transcriptional Activity of Chromatin'. *Cell* 182 (6): 1641-1659.e26. <https://doi.org/10.1016/j.cell.2020.07.032>.
- Sun, Baohua, Saradhi Mallampati, Yun Gong, Donghai Wang, Véronique Lefebvre, and Xiaoping Sun. 2013. 'Sox4 Is Required for the Survival of Pro-B Cells'. *The Journal of Immunology* 190 (5): 2080–89. <https://doi.org/10.4049/jimmunol.1202736>.
- Suzuki, Osamu, Yoshihiro Nozawa, and Masafumi Abe. 2004. 'Regulatory Roles of N-Glycosylation of Immunoglobulin M in CD40-CD40L-Mediated Cell Survival of Human Diffuse Large B Cell Lymphoma'. *Oncology Reports* 11 (5): 1031–39.
- Swerdlow, Steven H., Elias Campo, Stefano A. Pileri, Nancy Lee Harris, Harald Stein, Reiner Siebert, Ranjana Advani, et al. 2016. 'The 2016 Revision of the World Health Organization Classification of Lymphoid Neoplasms'. *Blood* 127 (20): 2375–90. <https://doi.org/10.1182/blood-2016-01-643569>.
- Tchurikov, Nickolai A., Elena S. Klushevskaya, Ildar R. Alembekov, Antonina N. Kretova, Vladimir R. Chechetkin, Galina I. Kravatskaya, and Yuri V. Kravatsky. 2023. 'Induction of the Erythroid Differentiation of K562 Cells Is Coupled with Changes in the Inter-Chromosomal Contacts of rDNA Clusters'. *International Journal of Molecular Sciences* 24 (12): 9842. <https://doi.org/10.3390/ijms24129842>.
- Telaraja, Deepti, Yvette L. Kasamon, Justin S. Collazo, Ruby Leong, Kun Wang, Ping Li, Elyes Dahmane, et al. 2024. 'FDA Approval Summary: Pirtobrutinib for Relapsed or Refractory Mantle Cell Lymphoma'. *Clinical Cancer Research: An Official Journal of the American Association for Cancer*

- Research* 30 (1): 17–22. <https://doi.org/10.1158/1078-0432.CCR-23-1272>.
- Teras, Lauren R., Carol E. DeSantis, James R. Cerhan, Lindsay M. Morton, Ahmedin Jemal, and Christopher R. Flowers. 2016. '2016 US Lymphoid Malignancy Statistics by World Health Organization Subtypes'. *CA: A Cancer Journal for Clinicians* 66 (6): 443–59. <https://doi.org/10.3322/caac.21357>.
- Tessoulin, Benoit, David Chiron, Catherine Thieblemont, Lucie Oberic, Kamal Bouadballah, Emmanuel Gyan, Gandhi Damaj, et al. 2021. 'Oxaliplatin before Autologous Transplantation in Combination with High-Dose Cytarabine and Rituximab Provides Longer Disease Control than Cisplatin or Carboplatin in Patients with Mantle-Cell Lymphoma: Results from the LyMA Prospective Trial'. *Bone Marrow Transplantation* 56 (7): 1700–1709. <https://doi.org/10.1038/s41409-020-01198-2>.
- The AACR Project GENIE Consortium, The AACR Project GENIE Consortium, Fabrice André, Monica Arnedos, Alexander S. Baras, José Baselga, Philippe L. Bedard, et al. 2017. 'AACR Project GENIE: Powering Precision Medicine through an International Consortium'. *Cancer Discovery* 7 (8): 818–31. <https://doi.org/10.1158/2159-8290.CD-17-0151>.
- Thein, Daniela C., Johannes M. Thalhammer, Anna C. Hartwig, E. Bryan Crenshaw, Veronique Lefebvre, Michael Wegner, and Elisabeth Sock. 2010. 'The Closely Related Transcription Factors Sox4 and Sox11 Function as Survival Factors during Spinal Cord Development'. *Journal of Neurochemistry* 115 (1): 131–41. <https://doi.org/10.1111/j.1471-4159.2010.06910.x>.
- Thieblemont, Catherine, Remi Houlgatte, Pascal Felman, Alexandra Traverse-Glehen, Lucile Baseggio, Delphine Rolland, Evelyne Callet-Bauchu, Gilles Salles, Françoise Berger, and Bertrand Coiffier. 2008. 'Indolent Mantle Cell Lymphoma (MCL): A Retrospective Detailed Clinical and Morphological Analysis of 21 Patients, with Histological, Cytological, Cytogenetic, Interphase Genetic, Immunoglobulin Gene, and Gene Expression Profiling Analysis.' *Blood* 112 (November):1780–1780. <https://doi.org/10.1182/blood.V112.11.1780.1780>.
- Tiemann, Katrin, Jessica V. Alluin, Anja Honegger, Pritsana Chomchan, Shikha Gaur, Yen Yun, Stephen J. Forman, John J. Rossi, and Robert W. Chen. 2011. 'Small Interfering RNAs Targeting Cyclin D1 and Cyclin D2 Enhance the Cytotoxicity of Chemotherapeutic Agents in Mantle Cell Lymphoma Cell Lines'. *Leukemia & Lymphoma* 52 (11): 2148–54. <https://doi.org/10.3109/10428194.2011.593272>.
- Till, Kathleen J., Mariah Abdullah, Tahera Alnassfan, Gallardo Zapata Janet, Thomas Marks, Silvia Coma, David T. Weaver, Jonathan A. Pachter, Andrew R. Pettitt, and Joseph R. Slupsky. 2023. 'Roles of PI3Ky and PI3Kδ in Mantle Cell Lymphoma Proliferation and Migration Contributing to Efficacy of the PI3Ky/δ Inhibitor Duvelisib'. *Scientific Reports* 13 (1): 3793. <https://doi.org/10.1038/s41598-023-30148-3>.

- Titov, Denis V., Benjamin Gilman, Qing-Li He, Shridhar Bhat, Woon-Kai Low, Yongjun Dang, Michael Smeaton, et al. 2011. 'XPB, a Subunit of TFIIH, Is a Target of the Natural Product Triptolide'. *Nature Chemical Biology* 7 (3): 182–88. <https://doi.org/10.1038/nchembio.522>.
- Togashi, Yosuke, Kohei Shitara, and Hiroyoshi Nishikawa. 2019. 'Regulatory T Cells in Cancer Immunosuppression - Implications for Anticancer Therapy'. *Nature Reviews. Clinical Oncology* 16 (6): 356–71. <https://doi.org/10.1038/s41571-019-0175-7>.
- Tort, F., S. Hernández, S. Beà, E. Camacho, V. Fernández, M. Esteller, M. F. Fraga, et al. 2005. 'Checkpoint Kinase 1 (CHK1) Protein and mRNA Expression Is Downregulated in Aggressive Variants of Human Lymphoid Neoplasms'. *Leukemia* 19 (1): 112–17. <https://doi.org/10.1038/sj.leu.2403571>.
- Tort, Frederic, Silvia Hernández, Silvia Beà, Antonio Martínez, Manel Esteller, James G. Herman, Xavier Puig, et al. 2002. 'CHK2-Decreased Protein Expression and Infrequent Genetic Alterations Mainly Occur in Aggressive Types of Non-Hodgkin Lymphomas'. *Blood* 100 (13): 4602–8. <https://doi.org/10.1182/blood-2002-04-1078>.
- Toure, Mohammed A., and Angela N. Koehler. 2023. 'Addressing Transcriptional Dysregulation in Cancer through CDK9 Inhibition'. *Biochemistry* 62 (6): 1114–23. <https://doi.org/10.1021/acs.biochem.2c00609>.
- Trněný, Marek, Thierry Lamy, Jan Walewski, David Belada, Jiri Mayer, John Radford, Wojciech Jurczak, et al. 2016. 'Lenalidomide versus Investigator's Choice in Relapsed or Refractory Mantle Cell Lymphoma (MCL-002; SPRINT): A Phase 2, Randomised, Multicentre Trial'. *The Lancet. Oncology* 17 (3): 319–31. [https://doi.org/10.1016/S1470-2045\(15\)00559-8](https://doi.org/10.1016/S1470-2045(15)00559-8).
- Tsang, Siu Man, Erik Oliemuller, and Beatrice A. Howard. 2020. 'Regulatory Roles for SOX11 in Development, Stem Cells and Cancer'. *Seminars in Cancer Biology, SOX family in Developmental Progression and Cancer Biology*, 67 (December):3–11. <https://doi.org/10.1016/j.semcancer.2020.06.015>.
- Tsukamoto, Taku, Shingo Nakahata, Ryuichi Sato, Akinori Kanai, Masakazu Nakano, Yoshiaki Chinen, Saori Maegawa-Matsui, et al. 2020. 'BRD4-Regulated Molecular Targets in Mantle Cell Lymphoma: Insights into Targeted Therapeutic Approach'. *Cancer Genomics & Proteomics* 17 (1): 77–89. <https://doi.org/10.21873/cgp.20169>.
- Tut, V M, K L Braithwaite, B Angus, D E Neal, J Lunec, and J K Mellon. 2001. 'Cyclin D1 Expression in Transitional Cell Carcinoma of the Bladder: Correlation with P53, Waf1, pRb and Ki67'. *British Journal of Cancer* 84 (2): 270–75. <https://doi.org/10.1054/bjoc.2000.1557>.
- Uy, Benjamin R., Marcos Simoes-Costa, Daniel E. S. Koo, Tatjana Sauka-Spengler, and Marianne E. Bronner. 2015. 'Evolutionarily

- Conserved Role for SoxC Genes in Neural Crest Specification and Neuronal Differentiation'. *Developmental Biology* 397 (2): 282–92. <https://doi.org/10.1016/j.ydbio.2014.09.022>.
- Vahedi, Golnaz, Yuka Kanno, Yasuko Furumoto, Kan Jiang, Stephen C. J. Parker, Michael R. Erdos, Sean R. Davis, et al. 2015. 'Super-Enhancers Delineate Disease-Associated Regulatory Nodes in T Cells'. *Nature* 520 (7548): 558–62. <https://doi.org/10.1038/nature14154>.
- Valentin Hansen, Simone, Marcus Høy Hansen, Oriane Cédile, Michael Boe Møller, Jacob Haaber, Niels Abildgaard, and Charlotte Guldborg Nyvold. 2021. 'Detailed Characterization of the Transcriptome of Single B Cells in Mantle Cell Lymphoma Suggesting a Potential Use for SOX4'. *Scientific Reports* 11 (September):19092. <https://doi.org/10.1038/s41598-021-98560-1>.
- Vandenbergh, E., C. De Wolf-Peeters, J. van den Oord, I. Wlodarska, J. Delabie, M. Stul, J. Thomas, J. L. Michaux, C. Mecucci, and J. J. Cassiman. 1991. 'Translocation (11;14): A Cytogenetic Anomaly Associated with B-Cell Lymphomas of Non-Follicle Centre Cell Lineage'. *The Journal of Pathology* 163 (1): 13–18. <https://doi.org/10.1002/path.1711630104>.
- Vegliante, Maria Carmela, Jara Palomero, Patricia Pérez-Galán, Gaël Roué, Giancarlo Castellano, Alba Navarro, Guillem Clot, et al. 2013. 'SOX11 Regulates PAX5 Expression and Blocks Terminal B-Cell Differentiation in Aggressive Mantle Cell Lymphoma'. *Blood* 121 (12): 2175–85. <https://doi.org/10.1182/blood-2012-06-438937>.
- Vegliante, Maria Carmela, Cristina Royo, Jara Palomero, Itziar Salaverria, Balazs Balint, Idoia Martín-Guerrero, Xabier Agirre, et al. 2011. 'Epigenetic Activation of SOX11 in Lymphoid Neoplasms by Histone Modifications'. *PLoS ONE* 6 (6): e21382. <https://doi.org/10.1371/journal.pone.0021382>.
- Velders, G. A., J. C. Kluin-Nelemans, C. J. De Boer, J. Hermans, E. M. Noordijk, E. Schuurung, M. H. Kramer, et al. 1996. 'Mantle-Cell Lymphoma: A Population-Based Clinical Study'. *Journal of Clinical Oncology: Official Journal of the American Society of Clinical Oncology* 14 (4): 1269–74. <https://doi.org/10.1200/JCO.1996.14.4.1269>.
- Veloza, Luis, Inmaculada Ribera-Cortada, and Elias Campo. 2019. 'Mantle Cell Lymphoma Pathology Update in the 2016 WHO Classification'. *Annals of Lymphoma* 3 (0). <https://doi.org/10.21037/aol.2019.03.01>.
- Vilarrasa-Blasi, Roser, Paula Soler-Vila, Núria Verdaguer-Dot, Núria Russiñol, Marco Di Stefano, Vicente Chapaprieta, Guillem Clot, et al. 2021. 'Dynamics of Genome Architecture and Chromatin Function during Human B Cell Differentiation and Neoplastic Transformation'. *Nature Communications* 12 (1): 651. <https://doi.org/10.1038/s41467-020-20849-y>.
- Vilarrasa-Blasi, Roser, Núria Verdaguer-Dot, Laura Belver, Paula Soler-Vila, Renée Beekman, Vicente Chapaprieta, Marta Kulis, et al. 2022. 'Insights into the Mechanisms Underlying Aberrant SOX11 Oncogene Expression

- in Mantle Cell Lymphoma'. *Leukemia* 36 (2): 583–87.
<https://doi.org/10.1038/s41375-021-01389-w>.
- Vispé, Stéphane, Luc DeVries, Laurent Créancier, Jérôme Besse, Sophie Bréand, David J. Hobson, Jesper Q. Svejstrup, et al. 2009. 'Triptolide Is an Inhibitor of RNA Polymerase I and II-Dependent Transcription Leading Predominantly to down-Regulation of Short-Lived mRNA'. *Molecular Cancer Therapeutics* 8 (10): 2780–90.
<https://doi.org/10.1158/1535-7163.MCT-09-0549>.
- Visser, A. E., and J. A. Aten. 1999. 'Chromosomes as Well as Chromosomal Subdomains Constitute Distinct Units in Interphase Nuclei'. *Journal of Cell Science* 112 (Pt 19) (October):3353–60.
<https://doi.org/10.1242/jcs.112.19.3353>.
- Visser, H. P., M. J. Gunster, H. C. Kluin-Nelemans, E. M. Manders, F. M. Raaphorst, C. J. Meijer, R. Willemze, and A. P. Otte. 2001. 'The Polycomb Group Protein EZH2 Is Upregulated in Proliferating, Cultured Human Mantle Cell Lymphoma'. *British Journal of Haematology* 112 (4): 950–58.
<https://doi.org/10.1046/j.1365-2141.2001.02641.x>.
- Vogt, Niklas, Dmitriy Abramov, Karoline Koch, Neus Masqué-Soler, Monika Szczepanowski, and Wolfram Klapper. 2015. 'No Evidence of Cell Cycle Dysregulation in Mantle Cell Lymphoma in Vivo'. *Leukemia & Lymphoma* 56 (7): 2134–40. <https://doi.org/10.3109/10428194.2014.975700>.
- Wang, Chen, Wen Tian, Shou-Ye Hu, Chen-Xi Di, Chang-Yi He, Qi-Long Cao, Ruo-Han Hao, et al. 2022. 'Lineage-Selective Super Enhancers Mediate Core Regulatory Circuitry during Adipogenic and Osteogenic Differentiation of Human Mesenchymal Stem Cells'. *Cell Death & Disease* 13 (10): 866. <https://doi.org/10.1038/s41419-022-05309-3>.
- Wang, Michael, Wojciech Jurczak, Mats Jerkeman, Judith Trotman, Pier Luigi Zinzani, Jan Andrzej Walewski, Jun Zhu, et al. 2022. 'Primary Results from the Double-Blind, Placebo-Controlled, Phase III SHINE Study of Ibrutinib in Combination with Bendamustine-Rituximab (BR) and R Maintenance as a First-Line Treatment for Older Patients with Mantle Cell Lymphoma (MCL)'. *Journal of Clinical Oncology* 40 (17_suppl): LBA7502–LBA7502.
https://doi.org/10.1200/JCO.2022.40.17_suppl.LBA7502.
- Wang, Michael L., Jacqueline C. Barrientos, Richard R. Furman, Matthew Mei, Paul M. Barr, Michael Y. Choi, Sven de Vos, et al. 2022. 'Zilovertamab Vedotin Targeting of ROR1 as Therapy for Lymphoid Cancers'. *NEJM Evidence* 1 (1): EVIDoA2100001. <https://doi.org/10.1056/EVIDoA2100001>.
- Wang, Michael L., Wojciech Jurczak, Pier Luigi Zinzani, Toby A. Eyre, Chan Y. Cheah, Chaitra S. Ujjani, Youngil Koh, et al. 2023. 'Pirtobrutinib in Covalent Bruton Tyrosine Kinase Inhibitor Pretreated Mantle-Cell Lymphoma'. *Journal of Clinical Oncology* 41 (24): 3988–97.
<https://doi.org/10.1200/JCO.23.00562>.
- Wang, Michael L., Simon Rule, Peter Martin, Andre Goy, Rebecca Auer, Brad S. Kahl, Wojciech Jurczak, et al. 2013. 'Targeting BTK with Ibrutinib in

- Relapsed or Refractory Mantle-Cell Lymphoma'. *The New England Journal of Medicine* 369 (6): 507–16. <https://doi.org/10.1056/NEJMoa1306220>.
- Wang, Michael, Javier Munoz, Andre Goy, Frederick L. Locke, Caron A. Jacobson, Brian T. Hill, John M. Timmerman, et al. 2020. 'KTE-X19 CAR T-Cell Therapy in Relapsed or Refractory Mantle-Cell Lymphoma'. *The New England Journal of Medicine* 382 (14): 1331–42. <https://doi.org/10.1056/NEJMoa1914347>.
- Wang, Michael, Radhakrishnan Ramchandren, Robert Chen, Lionel Karlin, Geoffrey Chong, Wojciech Jurczak, Ka Lung Wu, et al. 2021. 'Concurrent Ibrutinib plus Venetoclax in Relapsed/Refractory Mantle Cell Lymphoma: The Safety Run-in of the Phase 3 SYMPATICO Study'. *Journal of Hematology & Oncology* 14 (1): 179. <https://doi.org/10.1186/s13045-021-01188-x>.
- Wang, Michael, Tanya Siddiqi, Leo I. Gordon, Manali Kamdar, Matthew Lunning, Alexandre V. Hirayama, Jeremy S. Abramson, et al. 2024. 'Lisocabtagene Maraleucel in Relapsed/Refractory Mantle Cell Lymphoma: Primary Analysis of the Mantle Cell Lymphoma Cohort From TRANSCEND NHL 001, a Phase I Multicenter Seamless Design Study'. *Journal of Clinical Oncology: Official Journal of the American Society of Clinical Oncology* 42 (10): 1146–57. <https://doi.org/10.1200/JCO.23.02214>.
- Wang, Siyuan, Jun-Han Su, Brian J. Beliveau, Bogdan Bintu, Jeffrey R. Moffitt, Chao-ting Wu, and Xiaowei Zhuang. 2016. 'Spatial Organization of Chromatin Domains and Compartments in Single Chromosomes'. *Science (New York, N.Y.)* 353 (6299): 598–602. <https://doi.org/10.1126/science.aaf8084>.
- Wang, Sophia S., Susan L. Slager, Paul Brennan, Elizabeth A. Holly, Silvia De Sanjose, Leslie Bernstein, Paolo Boffetta, et al. 2007. 'Family History of Hematopoietic Malignancies and Risk of Non-Hodgkin Lymphoma (NHL): A Pooled Analysis of 10 211 Cases and 11 905 Controls from the International Lymphoma Epidemiology Consortium (InterLymph)'. *Blood* 109 (8): 3479–88. <https://doi.org/10.1182/blood-2006-06-031948>.
- Wang, Xiao, A. Charlotta Asplund, Anna Porwit, Jenny Flygare, C. I. Edvard Smith, Birger Christensson, and Birgitta Sander. 2008. 'The Subcellular Sox11 Distribution Pattern Identifies Subsets of Mantle Cell Lymphoma: Correlation to Overall Survival'. *British Journal of Haematology* 143 (2): 248–52. <https://doi.org/10.1111/j.1365-2141.2008.07329.x>.
- Wang, Xiao, Stefan Björklund, Agata M. Wasik, Alf Grandien, Patrik Andersson, Eva Kimby, Karin Dahlman-Wright, Chunyan Zhao, Birger Christensson, and Birgitta Sander. 2010. 'Gene Expression Profiling and Chromatin Immunoprecipitation Identify DBN1, SETMAR and HIG2 as Direct Targets of SOX11 in Mantle Cell Lymphoma'. *PLOS ONE* 5 (11): e14085. <https://doi.org/10.1371/journal.pone.0014085>.
- Wang, Xiaofeng, Ryan S. Lee, Burak H. Alver, Jeffrey R. Haswell, Su Wang, Jakub Mieczkowski, Yotam Drier, et al. 2017. 'SMARCB1-Mediated SWI/SNF

- Complex Function Is Essential for Enhancer Regulation'. *Nature Genetics* 49 (2): 289–95. <https://doi.org/10.1038/ng.3746>.
- Wang, Yu, and Shuangge Ma. 2014a. 'Racial Differences in Mantle Cell Lymphoma in the United States'. *BMC Cancer* 14 (October):764. <https://doi.org/10.1186/1471-2407-14-764>.
- Wang, Zhongwang, Hui Zhou, Jing Xu, Jinjin Wang, and Ting Niu. 2023. 'Safety and Efficacy of Dual PI3K- δ , γ Inhibitor, Duvelisib in Patients with Relapsed or Refractory Lymphoid Neoplasms: A Systematic Review and Meta-Analysis of Prospective Clinical Trials'. *Frontiers in Immunology* 13 (January):1070660. <https://doi.org/10.3389/fimmu.2022.1070660>.
- Warburg, O., F. Wind, and E. Negelein. 1927. 'THE METABOLISM OF TUMORS IN THE BODY'. *The Journal of General Physiology* 8 (6): 519–30. <https://doi.org/10.1085/jgp.8.6.519>.
- Wasik, Agata Magdalena, Martin Lord, Xiao Wang, Fang Zong, Patrik Andersson, Eva Kimby, Birger Christensson, Mohsen Karimi, and Birgitta Sander. 2013. 'SOXC Transcription Factors in Mantle Cell Lymphoma: The Role of Promoter Methylation in SOX11 Expression'. *Scientific Reports* 3 (1): 1400. <https://doi.org/10.1038/srep01400>.
- Watt, April C., Paloma Cejas, Molly J. DeCristo, Otto Metzger-Filho, Enid Y. N. Lam, Xintao Qiu, Haley BrinJones, et al. 2021. 'CDK4/6 Inhibition Reprograms the Breast Cancer Enhancer Landscape by Stimulating AP-1 Transcriptional Activity'. *Nature Cancer* 2 (1): 34–48. <https://doi.org/10.1038/s43018-020-00135-y>.
- Weintraub, Abraham S., Charles H. Li, Alicia V. Zamudio, Alla A. Sigova, Nancy M. Hannett, Daniel S. Day, Brian J. Abraham, et al. 2017. 'YY1 Is a Structural Regulator of Enhancer-Promoter Loops'. *Cell* 171 (7): 1573-1588.e28. <https://doi.org/10.1016/j.cell.2017.11.008>.
- Weiwei, Zheng, Zhou Hui, Xi Zhang, Jing Hongmei, Zhou Dongmei, Zhou Fang, Gao Li, et al. 2022. 'An Open-Label, Multicenter, Single-Arm, Phase I Study to Evaluate the Safety, Pharmacokinetics, Pharmacodynamics and Efficacy of XNW5004 in Patients with Relapsed or Refractory Hematologic Malignancies'. *Blood* 140 (Supplement 1): 9353–55. <https://doi.org/10.1182/blood-2022-157853>.
- Weston, Victoria J., Ceri E. Oldreive, Anna Skowronska, David G. Oscier, Guy Pratt, Martin J. S. Dyer, Graeme Smith, et al. 2010. 'The PARP Inhibitor Olaparib Induces Significant Killing of ATM-Deficient Lymphoid Tumor Cells in Vitro and in Vivo'. *Blood* 116 (22): 4578–87. <https://doi.org/10.1182/blood-2010-01-265769>.
- Whyte, Warren A., David A. Orlando, Denes Hnisz, Brian J. Abraham, Charles Y. Lin, Michael H. Kagey, Peter B. Rahl, Tong Ihn Lee, and Richard A. Young. 2013. 'Master Transcription Factors and Mediator Establish Super-Enhancers at Key Cell Identity Genes'. *Cell* 153 (2): 307–19. <https://doi.org/10.1016/j.cell.2013.03.035>.
- Wiestner, Adrian, Mahsa Tehrani, Michael Chiorazzi, George Wright, Federica

- Gibellini, Kazutaka Nakayama, Hui Liu, et al. 2007. 'Point Mutations and Genomic Deletions in CCND1 Create Stable Truncated Cyclin D1 mRNAs That Are Associated with Increased Proliferation Rate and Shorter Survival'. *Blood* 109 (11): 4599–4606.
<https://doi.org/10.1182/blood-2006-08-039859>.
- Witzig, Thomas E., Susan M. Geyer, Irene Ghobrial, David J. Inwards, Rafael Fonseca, Paul Kurtin, Stephen M. Ansell, et al. 2005. 'Phase II Trial of Single-Agent Temsirolimus (CCI-779) for Relapsed Mantle Cell Lymphoma'. *Journal of Clinical Oncology: Official Journal of the American Society of Clinical Oncology* 23 (23): 5347–56.
<https://doi.org/10.1200/JCO.2005.13.466>.
- Wlodarska, I., S. Pittaluga, A. Hagemeyer, C. De Wolf-Peeters, and H. Van Den Berghe. 1999. 'Secondary Chromosome Changes in Mantle Cell Lymphoma'. *Haematologica* 84 (7): 594–99.
- Wolf, Natalie K., Djem U. Kissiov, and David H. Raulet. 2023. 'Roles of Natural Killer Cells in Immunity to Cancer, and Applications to Immunotherapy'. *Nature Reviews Immunology* 23 (2): 90–105.
<https://doi.org/10.1038/s41577-022-00732-1>.
- Wong, Regina Wan Ju, Phuong Cao Thi Ngoc, Wei Zhong Leong, Alice Wei Yee Yam, Tinghu Zhang, Kaori Asamitsu, Shinsuke Iida, et al. 2017. 'Enhancer Profiling Identifies Critical Cancer Genes and Characterizes Cell Identity in Adult T-Cell Leukemia'. *Blood* 130 (21): 2326–38.
<https://doi.org/10.1182/blood-2017-06-792184>.
- Wu, Tianzhi, Erqiang Hu, Shuangbin Xu, Meijun Chen, Pingfan Guo, Zehan Dai, Tingze Feng, et al. 2021. 'clusterProfiler 4.0: A Universal Enrichment Tool for Interpreting Omics Data'. *The Innovation* 2 (3): 100141.
<https://doi.org/10.1016/j.xinn.2021.100141>.
- Wu, Wenjun, Weige Wang, Carrie A. Franzen, Hui Guo, Jimmy Lee, Yan Li, Madina Sukhanova, et al. 2021. 'Inhibition of B-Cell Receptor Signaling Disrupts Cell Adhesion in Mantle Cell Lymphoma via RAC2'. *Blood Advances* 5 (1): 185–97.
<https://doi.org/10.1182/bloodadvances.2020001665>.
- Xing, Z., H. C. Chen, J. K. Nowlen, S. J. Taylor, D. Shalloway, and J. L. Guan. 1994. 'Direct Interaction of V-Src with the Focal Adhesion Kinase Mediated by the Src SH2 Domain'. *Molecular Biology of the Cell* 5 (4): 413–21.
<https://doi.org/10.1091/mbc.5.4.413>.
- Xu, Xiaoyang, Xiaojing Chang, Zhenhua Li, Jiang Wang, Peng Deng, Xinjiang Zhu, Jian Liu, Chundong Zhang, Shuchen Chen, and Dongqiu Dai. 2015. 'Aberrant SOX11 Promoter Methylation Is Associated with Poor Prognosis in Gastric Cancer'. *Cellular Oncology (Dordrecht)* 38 (3): 183–94.
<https://doi.org/10.1007/s13402-015-0219-7>.
- Xu, Y., T. Ashley, E. E. Brainerd, R. T. Bronson, M. S. Meyn, and D. Baltimore. 1996. 'Targeted Disruption of ATM Leads to Growth Retardation, Chromosomal Fragmentation during Meiosis, Immune Defects, and

- Thymic Lymphoma.' *Genes & Development* 10 (19): 2411–22.
<https://doi.org/10.1101/gad.10.19.2411>.
- Y, Chen, Zhang Y, Wang Y, Zhang L, Brinkman Ek, Adam Sa, Goldman R, van Steensel B, Ma J, and Belmont As. 2018. 'Mapping 3D Genome Organization Relative to Nuclear Compartments Using TSA-Seq as a Cytological Ruler'. *The Journal of Cell Biology* 217 (11).
<https://doi.org/10.1083/jcb.201807108>.
- Y, Drosos, Escobar D, Chiang My, Roys K, Valentine V, Valentine Mb, Rehg Je, et al. 2017. 'ATM-Deficiency Increases Genomic Instability and Metastatic Potential in a Mouse Model of Pancreatic Cancer'. *Scientific Reports* 7 (1).
<https://doi.org/10.1038/s41598-017-11661-8>.
- Yaffe, Eitan, and Amos Tanay. 2011. 'Probabilistic Modeling of Hi-C Contact Maps Eliminates Systematic Biases to Characterize Global Chromosomal Architecture'. *Nature Genetics* 43 (11): 1059–65.
<https://doi.org/10.1038/ng.947>.
- Yamamoto, Kenta, Yunyue Wang, Wenxia Jiang, Xiangyu Liu, Richard L. Dubois, Chyuan-Sheng Lin, Thomas Ludwig, Christopher J. Bakkenist, and Shan Zha. 2012. 'Kinase-Dead ATM Protein Causes Genomic Instability and Early Embryonic Lethality in Mice'. *Journal of Cell Biology* 198 (3): 305–13.
<https://doi.org/10.1083/jcb.201204098>.
- Yamanashi, Y., M. Miyasaka, M. Takeuchi, D. Ilic, J. Mizuguchi, and T. Yamamoto. 1991. 'Differential Responses of P56lyn and P53lyn, Products of Alternatively Spliced Lyn mRNA, on Stimulation of B-Cell Antigen Receptor'. *Cell Regulation* 2 (12): 979–87.
<https://doi.org/10.1091/mbc.2.12.979>.
- Yang, Keri Keri, Eleanor Lucas, Beth Leshner, Tony Caver, and Boxiong Tang. 2019. 'A Systematic Review of the Epidemiology and Economic Burden of Mantle Cell Lymphoma (MCL)'. *Blood* 134 (Supplement_1): 5831.
<https://doi.org/10.1182/blood-2019-129677>.
- Yang, Ping, Weilong Zhang, Jing Wang, Yuanyuan Liu, Ran An, and Hongmei Jing. 2018. 'Genomic Landscape and Prognostic Analysis of Mantle Cell Lymphoma'. *Cancer Gene Therapy* 25 (5–6): 129–40.
<https://doi.org/10.1038/s41417-018-0022-5>.
- Yang, Rumeng, Zitian Huo, Yaqi Duan, Weilin Tong, Yiyun Zheng, Yinxia Su, Liping Lou, et al. 2020. 'SOX11 Inhibits Tumor Proliferation and Promotes Cell Adhesion Mediated-Drug Resistance via a CD43 Dependent Manner in Mantle Cell Lymphoma'. *Leukemia & Lymphoma* 61 (9): 2068–81. <https://doi.org/10.1080/10428194.2020.1762877>.
- Yang, Xiaoyong, and Kevin Qian. 2017. 'Protein O-GlcNAcylation: Emerging Mechanisms and Functions'. *Nature Reviews Molecular Cell Biology* 18 (7): 452–65. <https://doi.org/10.1038/nrm.2017.22>.
- Yazbeck, Victor, Danielle Shafer, Edward B. Perkins, Domenico Coppola, Lubomir Sokol, Kristy L. Richards, Thomas Shea, et al. 2018. 'A Phase II Trial of Bortezomib and Vorinostat in Mantle Cell Lymphoma and

- Diffuse Large B-Cell Lymphoma'. *Clinical Lymphoma, Myeloma & Leukemia* 18 (9): 569-575.e1. <https://doi.org/10.1016/j.clml.2018.05.023>.
- Yi, Shuhua, Yuting Yan, Meiling Jin, Supriyo Bhattacharya, Yi Wang, Yiming Wu, Lu Yang, et al. 2022. 'Genomic and Transcriptomic Profiling Reveals Distinct Molecular Subsets Associated with Outcomes in Mantle Cell Lymphoma'. *The Journal of Clinical Investigation* 132 (3). <https://doi.org/10.1172/JCI153283>.
- Yi, Xuemei, Yajun Zhao, Li Xue, Jing Zhang, Yujie Qiao, Qianqian Jin, and Hongling Li. 2018. 'Expression of Keap1 and Nrf2 in Diffuse Large B-Cell Lymphoma and Its Clinical Significance'. *Experimental and Therapeutic Medicine* 16 (2): 573-78. <https://doi.org/10.3892/etm.2018.6208>.
- Yohe, Marielle E., Berkley E. Gryder, Jack F. Shern, Young K. Song, Hsien-Chao Chou, Sivasish Sindiri, Arnulfo Mendoza, et al. 2018. 'MEK Inhibition Induces MYOG and Remodels Super-Enhancers in RAS-Driven Rhabdomyosarcoma'. *Science Translational Medicine* 10 (448): ean4470. <https://doi.org/10.1126/scitranslmed.aan4470>.
- Yoon, Dok Hyun, Youngil Koh, Miyoung Jung, Jeong-Eun Kwak, Eui-Cheol Shin, Yu Kyeong Hwang, and Won Seog Kim. 2023. 'Phase I Study: Safety and Efficacy of an Ex Vivo-Expanded Allogeneic Natural Killer Cell (MG4101) with Rituximab for Relapsed/Refractory B Cell Non-Hodgkin Lymphoma'. *Transplantation and Cellular Therapy* 29 (4): 253.e1-253.e9. <https://doi.org/10.1016/j.jtct.2022.12.025>.
- Young, Ryan M., Tianyi Wu, Roland Schmitz, Moez Dawood, Wenming Xiao, James D. Phelan, Weihong Xu, et al. 2015. 'Survival of Human Lymphoma Cells Requires B-Cell Receptor Engagement by Self-Antigens'. *Proceedings of the National Academy of Sciences of the United States of America* 112 (44): 13447-54. <https://doi.org/10.1073/pnas.1514944112>.
- Yu, Guangchuang, Li-Gen Wang, and Qing-Yu He. 2015. 'ChIPseeker: An R/Bioconductor Package for ChIP Peak Annotation, Comparison and Visualization'. *Bioinformatics* 31 (14): 2382-83. <https://doi.org/10.1093/bioinformatics/btv145>.
- Zakharova, Vlada V., Mikhail D. Magnitov, Laurence Del Maestro, Sergey V. Ulianov, Alexandros Glentis, Burhan Uyanik, Alice Williart, et al. 2022. 'SETDB1 Fuels the Lung Cancer Phenotype by Modulating Epigenome, 3D Genome Organization and Chromatin Mechanical Properties'. *Nucleic Acids Research* 50 (8): 4389-4413. <https://doi.org/10.1093/nar/gkac234>.
- Zelenetz, Andrew D., Leo I. Gordon, Jeremy S. Abramson, Ranjana H. Advani, Babis Andreadis, Nancy L. Bartlett, L. Elizabeth Budde, et al. 2023. 'NCCN Guidelines® Insights: B-Cell Lymphomas, Version 6.2023: Featured Updates to the NCCN Guidelines'. *Journal of the National Comprehensive Cancer Network* 21 (11): 1118-31. <https://doi.org/10.6004/jnccn.2023.0057>.
- Zhang, Jenny, Dereje Jima, Andrea B. Moffitt, Qingquan Liu, Magdalena Czader,

- Eric D. Hsi, Yuri Fedoriw, et al. 2014. 'The Genomic Landscape of Mantle Cell Lymphoma Is Related to the Epigenetically Determined Chromatin State of Normal B Cells'. *Blood* 123 (19): 2988–96. <https://doi.org/10.1182/blood-2013-07-517177>.
- Zhang, Liang, Zhengzi Qian, Zhen Cai, Luhong Sun, Huaqing Wang, J. Blake Bartlett, Qing Yi, and Michael Wang. 2009. 'Synergistic Antitumor Effects of Lenalidomide and Rituximab on Mantle Cell Lymphoma in Vitro and in Vivo'. *American Journal of Hematology* 84 (9): 553–59. <https://doi.org/10.1002/ajh.21468>.
- Zhang, Liang, Yixin Yao, Shaojun Zhang, Yang Liu, Hui Guo, Makhdum Ahmed, Taylor Bell, et al. 2019. 'Metabolic Reprogramming toward Oxidative Phosphorylation Identifies a Therapeutic Target for Mantle Cell Lymphoma'. *Science Translational Medicine* 11 (491): eaau1167. <https://doi.org/10.1126/scitranslmed.aau1167>.
- Zhang, Shaojun, Vivian Changying Jiang, Guangchun Han, Dapeng Hao, Junwei Lian, Yang Liu, Rongjia Zhang, et al. 2021. 'Longitudinal Single-Cell Profiling Reveals Molecular Heterogeneity and Tumor-Immune Evolution in Refractory Mantle Cell Lymphoma'. *Nature Communications* 12 (1): 2877. <https://doi.org/10.1038/s41467-021-22872-z>.
- Zhang, Song, Shuo Li, and Jin-Liang Gao. 2013. 'Promoter Methylation Status of the Tumor Suppressor Gene SOX11 Is Associated with Cell Growth and Invasion in Nasopharyngeal Carcinoma'. *Cancer Cell International* 13 (1): 109. <https://doi.org/10.1186/1475-2867-13-109>.
- Zhang, Xin-Yu, Ji Xu, Hua-Yuan Zhu, Yan Wang, Li Wang, Lei Fan, Yu-Jie Wu, Jian-Yong Li, and Wei Xu. 2016. 'Negative Prognostic Impact of Low Absolute CD4+ T Cell Counts in Peripheral Blood in Mantle Cell Lymphoma'. *Cancer Science* 107 (10): 1471–76. <https://doi.org/10.1111/cas.13020>.
- Zhao, J., R. Pestell, and J. L. Guan. 2001. 'Transcriptional Activation of Cyclin D1 Promoter by FAK Contributes to Cell Cycle Progression'. *Molecular Biology of the Cell* 12 (12): 4066–77. <https://doi.org/10.1091/mbc.12.12.4066>.
- Zhou, Xiao-Hui, Xin-Yu Zhang, Jin-Hua Liang, Hua-Yuan Zhu, Li Wang, Yi Xia, Lei Cao, et al. 2019. 'Low Absolute NK Cell Counts in Peripheral Blood Are Associated with Inferior Survival in Patients with Mantle Cell Lymphoma'. *Cancer Biomarkers: Section A of Disease Markers* 24 (4): 439–47. <https://doi.org/10.3233/CBM-182193>.
- Zhu, Lihua J., Claude Gazin, Nathan D. Lawson, Hervé Pagès, Simon M. Lin, David S. Lapointe, and Michael R. Green. 2010. 'ChIPpeakAnno: A Bioconductor Package to Annotate ChIP-Seq and ChIP-Chip Data'. *BMC Bioinformatics* 11 (May):237. <https://doi.org/10.1186/1471-2105-11-237>.
- Zink, D., T. Cremer, Rainer Saffrich, Roger Fischer, Michael F. Trendelenburg, Wilhelm Ansorge, and Ernst H. K. Stelzer. 1998. 'Structure and Dynamics of Human Interphase Chromosome Territories in Vivo'. *Human Genetics*

102 (2): 241–51. <https://doi.org/10.1007/s004390050686>.

Zinzani, Pier Luigi, Marek Trněný, Vincent Ribrag, Vittorio Ruggero Zilioli, Jan Walewski, Jacob Haaber Christensen, Vincent Delwail, et al. 2023. 'Parsaclisib, a PI3K δ Inhibitor, in Relapsed and Refractory Mantle Cell Lymphoma (CITADEL-205): A Phase 2 Study'. *EClinicalMedicine* 62 (August):102131. <https://doi.org/10.1016/j.eclinm.2023.102131>.

Title: Epigenomic and 3D-genomic changes in Mantle Cell Lymphoma

Keywords: MCL, chromosomal translocations, 3D genome, epigenome.

Abstract: Mantle cell lymphoma is an aggressive B cell malignancy with poor prognosis. More than 90% of MCL cases are associated with a recurrent chromosomal translocation t(11;14) that results in the overexpression of cyclin D1 (CCND1), a potent cell-cycle regulator. Nevertheless, CCND1 overexpression alone does not lead to malignancies in animal models. Thus, the development of MCL should be triggered by additional factors, which may guide the development of new therapies once discovered.

A chromosomal translocation can trigger large-scale changes in the 3D genome organization, as well as the transcriptional and epigenetic changes in the translocated loci. Here we demonstrated that the translocated CCND1 locus on derivative chr14 is relocated to the nuclear center in MCL cells. This is accompanied by the appearance of a new super-enhancer (SE) inside this locus. Surprisingly, the region around the novel SE was not significantly enriched for the genes upregulated in MCL. Instead, most of the overexpressed genes were located on chr19 in both the MCL cell lines and the B cells from MCL patients.

Among these genes, there were many related to lymphoma or other cancers. Using HiC, we detected the presence of an interchromosomal contact between chr11 and chr19, which was further confirmed by 3D-FISH. The contact colocalized with the active RNAPolIII and formed predominantly with the derivative CCND1 locus.

We hypothesize that the deregulated chr19 genes contribute to the MCL oncogenesis, and their upregulation is at least partially explained by the action of an MCL-specific SE inside the CCND1 locus. Thus, inhibiting super-enhancer activity may represent a new treatment strategy for MCL. We tested two substances with such properties, Abemaciclib and Minnelide, in MCL cell lines and the B cells from MCL patients. Minnelide had a strong inhibitory effect on the chromatin landscape of MCL cells, including the novel SE, and was effective against mantle cell lymphoma cells in vitro and in vivo. Our results provide valuable preclinical data and novel insights into the mechanisms of MCL pathogenesis.

Title: Changements épigénomiques et 3D-génomiques dans le lymphome à cellules du manteau

Keywords: Lymphome à cellules du manteau, translocations chromosomiques, génome 3D, épigénome.

Abstract: Le lymphome à cellules du manteau (LM) est une tumeur maligne agressive à cellules B, caractérisée par un mauvais pronostic. Plus de 90 % des cas de LM sont associés à une translocation chromosomique récurrente t(11;14) qui entraîne la surexpression de la cycline D1 (CCND1), un puissant régulateur du cycle cellulaire. Néanmoins, la surexpression de la CCND1 seule ne suffit pas à provoquer des tumeurs malignes dans les modèles animaux. Par conséquent, le développement du LM doit être déclenché par d'autres facteurs, ce qui pourrait guider le développement de nouvelles thérapies une fois ces facteurs découverts.

Une translocation chromosomique peut entraîner des modifications à grande échelle dans l'organisation 3D du génome, ainsi que des changements transcriptionnels et épigénétiques dans les loci transloqués. Nous avons démontré que le locus CCND1 participant à la translocation est déplacé vers le centre nucléaire dans les cellules de LM. Cela s'accompagne de l'apparition d'un nouveau super-enhancer (SE) à l'intérieur de ce locus. De manière surprenante, la région autour du nouveau SE n'était pas enrichie avec des gènes surexprimés dans les cellules de LM.

En revanche, la plupart des gènes surexprimés dans les cellules de LM étaient situés sur chr19. Parmi ces gènes, beaucoup étaient liés au lymphome ou à d'autres cancers. En utilisant le Hi-C, nous avons détecté la présence d'un contact interchromosomique entre chr11 et chr19, confirmé par 3D-FISH. Ce contact se colocalise avec l'ARN polymérase II active et se forme principalement avec le locus CCND1 dérivé.

Nous émettons l'hypothèse que les gènes dérégulés sur chr19 contribuent à l'oncogenèse du LM et que leur régulation est influencée par l'action d'un SE spécifique au LM à l'intérieur du locus CCND1. Ainsi, l'inhibition de l'activité du super-enhancer pourrait représenter une nouvelle stratégie thérapeutique pour le LM. Nous avons testé deux substances possédant de telles propriétés, l'Abemaciclib et le Minnelide, sur des lignées cellulaires de LM et sur les cellules B de patients atteints de LM. Le Minnelide a eu un fort effet inhibiteur sur le chromatine des cellules de LM, y compris le nouveau SE, et a été efficace contre les cellules de lymphome à cellules du manteau in vitro et in vivo. Nos résultats fournissent des données précliniques précieuses et de nouvelles perspectives sur les mécanismes de la pathogenèse du LM.

